



Dipl. Ing. Peter Sommersacher

**Innovative characterisation techniques for solid biomass fuels
regarding their thermal utilisation in fixed-bed reactors**

DOCTORAL THESIS

to achieve the university degree of
Doktor der technischen Wissenschaften
submitted to

Graz University of Technology

Supervisor

Dipl.-Ing. Dr.techn. Univ.-Doz. Prof. Ingwald Obernberger

Institute of Process and Particle Engineering

Graz, April 2016

AFFIDAVIT

I declare that I have authored this thesis independently, that I have not used other than the declared sources/resources, and that I have explicitly marked all material which has been quoted either literally or by content from the sources used. The text document uploaded to TUGRAZonline is identical to the present doctoral thesis.

04/04/2016

Date

Pekir Sömer

Signature

Acknowledgements

At this point I would like to thank all people without whose professional as well as emotional support I would not have been able to complete the work in hand.

First and foremost, I would like to thank my supervisor Prof. Ingwald Obernberger for his support and guidance, which made my thesis possible. I am grateful for his patience, encouragement, enthusiasm and immense knowledge which, taken together, make him a great mentor.

I would also like to express my sincere appreciation of my assistant supervisor Thomas Brunner. He introduced me to the field of biomass combustion and I am deeply grateful for all those fruitful and spirited discussions. He also helped me with questions and problems along the way, and with occasional serious setbacks.

Special thanks to all colleagues at BIOENERGY 2020+ for their support over the past years. Specifically, I would like to thank Nicola Evic for initiating me into the workings of the lab-scale reactor and available gas measurement devices. His calm and scientific mode of operation was a great help, especially during the initial phase of my thesis. Special thanks also go to Michael Maier, who was mainly responsible for the construction of the single particle reactor. Further, I would like to thank Norbert Kienzl, head of the laboratory, and all the laboratory staff for carrying out countless fuel and ash analyses and for their unstinting support regarding the interpretation of the results. Special mention needs to be made of the fact that Norbert Kienzl was also in charge of successfully coupling the single particle reactor to the ICP-MS, providing valuable input into the operation of the system. I would, further, like to thank my loyal friend Stefan Retschitzegger, who supports me with regard to technical issues and who actively encouraged me to finish this thesis.

Heartfelt thanks to my family and friends for supporting me through an occasionally difficult period, and for encouraging me to carry on and finish the work started. Finally I want to thank my partner Magdalena for her infinite patience and for standing by me in good and in bad days.

Abstract

The increased utilisation of alternative biomass feedstocks (herbaceous biomass and agricultural residues) for combustion purposes can cause ash-related problems (ash melting on grates, deposit formation and corrosion) in furnaces and boilers, and it can lead to increased particulate, NO_x , SO_x and HCl emissions. One way to combat problematic combustion behaviours is the application of fuel additives and fuel blends. So far, the evaluation of fuels as well as the application of additives and fuel blends has been based on experimental investigations. In this thesis, new characterisation methods (fuel indexes, thermodynamic equilibrium calculations (TEC) and fixed-bed lab-scale reactor experiments) have been developed and used for the characterisation of pure fuels, fuel additive mixtures and biomass fuel blends. In addition, a new single particle reactor has been developed to determine relevant parameters during the thermal conversion process and to simultaneously record time resolved release profiles of relevant inorganic aerosol forming elements (S, Cl, K, Na, Zn and Pb).

An initial pre-evaluation of combustion-related problems that may arise can be performed by means of fuel indexes which are calculated on the basis of the results of chemical fuel analysis. Fuel indexes are checked and evaluated with regard to applicability by measurements performed at lab- and real-scale combustion plants for a large variety of fuels. They can directly be applied to pure fuels and biomass mixtures, whereby the application for biomass additive mixtures has to be checked. Since a meaningful prediction of the release of inorganic aerosol forming elements (especially for K) from the fuel to the gas phase is not possible with fuel indexes, a qualitative determination by TEC can be performed. TEC deliver qualitative information regarding ash transformation, the release behaviour of inorganic aerosol forming elements (S, Cl, K, Na, Zn, Pb) and ash melting behaviour. For a quantitative evaluation of the release of aerosol forming elements, fixed-bed lab-scale reactor experiments have been performed. The basic idea behind this reactor is to provide a tool which is capable of simulating the fuel decomposition behaviour in real-scale fixed-bed biomass combustion systems. The experiments deliver information regarding thermal decomposition behaviour, the release of NO_x precursor species, the release of inorganic aerosol forming elements and provide a first indication regarding ash melting behaviour. By means of these experiments, release ratios of inorganic aerosol forming elements for the entire combustion experiment are determined. For a time resolved determination of the release behaviour, a new single particle reactor connected to an inductively coupled plasma mass spectrometer (ICP-MS) has been developed. With this reactor it is possible to simultaneously determine the surface and centre temperatures of a biomass particle, the weight loss of the particle and the composition of gases released during thermal conversion. A series of validation tests, as well as tests with biomass fuels (softwood and straw) were performed which show that the simultaneous time resolved determination of the release of S, Cl, K, Na, Zn and Pb is possible, whereas the Cl signal can only be used with limitations. This reactor can be used for targeted experiments in a temperature range of 250°-1,050°C under inert, reducing and oxidising conditions, and especially the time resolved release data lead to a better understanding of the release of inorganic aerosol forming elements during thermal biomass conversion.

The new characterisation methods have been developed for fixed-bed combustion systems, where also the limitations of the application have to be considered. The applicability of fuel

indexes to biomass additive mixtures and biomass fuel blends has to be checked. Also for the fixed-bed lab-scale reactor and the single particle reactor it has to be ascertained whether the experimental conditions during the experiments are representative of the real-scale process.

The application of the methods presented allows the identification of problematic combustion behaviour of biomass fuels. Furthermore, an appropriate additive ratio or a fuel blend can be determined to improve the combustion behaviour. On the basis of the work performed, a general guideline for the characterisation of pure fuel, fuel additive mixtures and biomass blends can be suggested. These methods facilitate a newly developed fuel characterisation which reduces time-consuming and cost-intensive testing campaigns.

Kurzfassung

Der verstärkte Einsatz von alternativen Rohstoffen (halmgutartiger Biomasse und landwirtschaftliche Reststoffe) für Verbrennungszwecke kann ascherelevante Probleme (Ascheschmelzen am Rost, Bildung von Depositionen und Korrosion) in Öfen und Kessel verursachen, sowie zu erhöhten Partikel, NO_x , SO_x und HCl Emissionen führen. Eine Möglichkeit zur Minimierung des problematischen Verbrennungsverhaltens ist die Anwendung von Additiven und Brennstoffmischungen. Bisher wurden Brennstoffadditive und Brennstoffmischungen hinsichtlich ihres Einsatzes experimentell untersucht. In dieser Arbeit wurden neue Charakterisierungsmethoden (Brennstoffindexe, thermodynamische Gleichgewichtsberechnungen (GGB) und Festbett-Laborreaktorversuche) für die Charakterisierung von Biomasse Brennstoffen, Additivmischungen und Biomassemischungen entwickelt und verwendet. Darüber hinaus wurde ein neuer Einzelpartikelreaktor entwickelt um relevanten Parameter während des thermischen Konversationsprozesses zu bestimmen und die gleichzeitige Aufzeichnung von zeitaufgelösten Freisetzungprofile von relevanten anorganischen Aerosolbildnern (S, Cl, K, Na, Zn und Pb) zu gewährleisten.

Eine erste Vorevaluierung von verbrennungsrelevanten Problemen, die auftreten können, kann anhand von Brennstoffindexen erfolgen, welche auf Basis von chemischen Brennstoffanalysen berechnet werden. Brennstoffindexe wurden hinsichtlich ihrer Anwendbarkeit durch Messungen an Labor- und Realanlagen für eine große Vielzahl von Brennstoffen evaluiert. Sie können für Reinbrennstoffe und Biomassemischungen direkt angewendet werden, wobei die Anwendung für Additivmischungen überprüft werden muss. Da eine sinnvolle Vorhersage der Freisetzung von anorganischen Aerosolbildnern (insbesondere für K) vom Brennstoff in die Gasphase mit Brennstoffindexen nicht möglich ist, wurde eine qualitative Bestimmung anhand von GGB durchgeführt. GGB liefern qualitative Informationen hinsichtlich Aschetransformation, das Freisetzungsverhalten von anorganischen Aerosolbildnern (S, Cl, K, Na, Zn, Pb) und über das Ascheschmelzverhalten. Für eine quantitative Bestimmung der Freisetzung von anorganischen Aerosolbildnern wurden Festbett-Laborreaktorexperimente durchgeführt. Generell soll dieser Reaktor das Brennstoffabbauverhalten einer realen Festbett-Biomasseverbrennungsanlage simulieren. Die Versuche liefern Informationen über das thermische Zersetzungsverhalten, die Freisetzung von NO_x Vorläuferspezies, die Freisetzung von anorganischen Aerosolbildnern und erste Hinweise hinsichtlich des Ascheschmelzverhaltens. Anhand dieser Versuche werden die Freisetzungen von anorganischen Aerosolbildnern für den gesamten Verbrennungsexperiment bestimmt. Für eine zeitaufgelöste Bestimmung des Freisetzungsverhaltens wurde ein neuer Einzelpartikelreaktor, verbunden mit einem Massenspektrometer mit induktiv gekoppeltem Plasma (ICP-MS), entwickelt. Mit diesem Reaktor ist eine gleichzeitige Bestimmung der Oberfläche- und Zentrumstemperaturen eines Biomassepartikels, des Gewichtsverlustes des Partikels und der Zusammensetzung der freigesetzten Gase während der thermischen Konversation möglich. Eine Reihe von Validierungstests sowie Tests mit Biomasse Brennstoffen (Weichholz und Stroh) wurden durchgeführt, wobei gezeigt wurde, dass die gleichzeitige zeitaufgelöste Bestimmung von S, Cl, K, Na, Zn und Pb möglich ist und Cl-Signale nur mit Einschränkungen verwendet werden können. Dieser Reaktor kann für gezielte Versuche in einem Temperaturbereich von 250°-1.050°C unter inerten, reduzierenden und oxidierenden Atmosphären verwendet werden. Vor allem die zeitaufgelösten Freisetzungsdaten führen zu einem besseren Verständnis

hinsichtlich der Freisetzung anorganischen Aerosolbildnern während der thermischen Konversion von Biomasse.

Die neuen Methoden zur Brennstoffcharakterisierung wurden für Festbett-Verbrennungssysteme entwickelt, wo auch die Grenzen der Anwendung berücksichtigt werden müssen. Die Anwendbarkeit von Brennstoffindexen für Additivmischungen und Biomasseemischungen ist zu überprüfen. Auch für Experimente mit dem Festbett-Laborreaktor und dem Einzelpartikelreaktor muss geprüft werden, ob die Randbedingungen, die während der Experimente vorherrschen, den realen Prozess repräsentieren.

Durch die Anwendung der vorgestellten Methoden kann problematisches Verbrennungsverhalten für Biomasse Brennstoffe identifiziert werden. Zusätzlich kann ein geeignetes Additiv-Verhältnis oder eine Brennstoffmischung bestimmt werden, die das Verbrennungsverhalten verbessert. Auf Grundlage der durchgeführten Arbeiten kann eine allgemeine Empfehlung für die Charakterisierung von Biomasse Brennstoffen, Additivmischungen und Biomasseemischungen vorgeschlagen werden. Dieser Ansatz ermöglicht eine neu entwickelte Brennstoffcharakterisierung, die den Aufwand für die zeit- und kostenintensiven Testkampagnen reduziert.

Innovative characterisation techniques for solid biomass fuels regarding the thermal utilisation and their application

Peter Sommersacher

This thesis contains the following publications in its scope, referred to by the Roman numerals I-V:

- I Fuel indexes – a novel method for the evaluation of relevant combustion properties of new biomass fuels
Sommersacher P., Brunner T., Obernberger I.
Energy and Fuels 2012, 26, 380-390
- II Application of novel and advanced fuel characterization tools for the combustion related characterization of different wood/kaolin and straw/kaolin mixtures
Sommersacher P., Brunner T., Obernberger I., Kienzl N., Kanzian W.
Energy and Fuels 2013, 27 (9), 5192–5206
- III Combustion related characterisation of Miscanthus peat blends applying novel fuel characterisation tools
Sommersacher P., Brunner T., Obernberger I., Kienzl N., Kanzian W.
Fuel 2015, 158, 253–262
- IV Simultaneous online determination of S, Cl, K, Na, Zn and Pb release from a single particle during biomass combustion Part 1: Experimental setup-implementation and evaluation
Sommersacher P., Kienzl N., Brunner T., Obernberger I.
Energy and Fuels 2015, 29, 6734-6746
- V Simultaneous online determination of S, Cl, K, Na, Zn and Pb release from a single particle during biomass combustion Part 2: Results from test runs with spruce and straw pellets
Sommersacher P., Kienzl N., Brunner T., Obernberger I.
Accepted for publication in *Energy and Fuels*, DOI: 10.1021/acs.energyfuels.5b02766

Additional publications of relevance – not included in the thesis:

Conference proceedings

Brunner T., Sommersacher P., Obernberger I. Fuel indexes – a novel method for the evaluation of relevant combustion properties of new biomass fuels. - In: Proceedings of the 19th European Biomass Conference & Exhibition, 2011, 1351 – 1357; DOI: 10.5071/19thEUBCE2011-VP2.2.14

Sommersacher P., Brunner T., Obernberger I. 2012: Fuel indexes –a novel method for the evaluation of relevant combustion properties of new biomass fuels. - In: Proc. of the Conference Impacts of Fuel Quality on Power Production and Environment, 23rd-27th September 2012, Puchberg, Austria

Sommersacher P., Brunner T., Obernberger I. Neue Methoden zur Charakterisierung von Biomasse-Brennstoffen - In: Proc of the 4th Central European Biomass Conference 15th-18th January 2014, Graz, Austria

Sommersacher P., Kienzl N., Brunner T., Obernberger I. Online determination of the release of inorganic elements using a single particle reactor coupled with an ICP-MS - In: Oral presentation at 23rd European Biomass Conference and Exhibition, 01st-04th June, 2015, Vienna, Austria; ISBN: 978-88-89407-516

The author's contribution to this thesis

Paper I

The paper is based on a high number of test runs which were performed over several years before the author started to work on this topic. The author made the results accessible for evaluation, researched the literature and wrote the paper. The steps mentioned were performed in close cooperation with the co-authors.

Paper II

The planning as well as the major part of the experiments (preparation, fixed-bed lab-scale reactor combustion experiments) were performed by the author. The evaluation of the results as well as the thermodynamic equilibrium calculations (TEC) were done by the author in close cooperation with the co-authors. The author finally edited the results and wrote the paper.

Paper III

Identical contributions by the author as in **Paper II**.

Paper IV

The design of the reactor was devised in close cooperation with the co-authors. The author supervised a master's student (Michael Maier), who did most of the construction work. The author was mainly responsible for the set-up and for conducting first tests. The validation procedure was developed in close cooperation with the co-authors. Writing the paper also fell within the remit of the author.

Paper V

The author was ultimately in charge of the planning and implementation of the conducted test runs and then wrote the paper. Evaluation and interpretation were performed in close cooperation with the co-authors.

Contents

List of Figures	III
List of Tables	V
Nomenclature	VI
1 Introduction and objectives	1
1.1 Background	1
1.2 Characteristics of different biomass assortments	1
1.3 Biomass combustion in fixed-bed systems	3
1.4 Emissions and operational problems during biomass combustion	3
1.5 Evaluation of combustion-related properties based on fuel analysis	4
1.5.1 Fuel Indexes	4
1.6 Selected experimental lab-scale equipment and reactors for the determination of combustion-related properties of biomass	5
1.6.1 Thermogravimetric analysers	6
1.6.2 Single particle reactors	7
1.6.3 Fixed-bed reactors	8
1.7 Improvement of combustion-related properties by additive application	9
1.8 Biomass upgrading by preparation of fuel blends with peat	11
1.9 Objective of the work presented	12
2 Analytical, experimental and theoretical methods used	13
2.1 Fuel and ash analysis	13
2.2 Thermodynamic equilibrium calculations	14
2.3 Fixed-bed lab-scale reactor	16
3 Fuels used for the investigations	19
3.1 General information regarding biomass additive and Miscanthus peat blends investigations	20
4 Results	20
4.1 Pre-evaluation of combustion properties based on fuel indexes - Paper I	20
4.1.1 Fuel indexes defined	21
4.1.2 N-concentration in the fuel as an indicator of NO _x emissions	22
4.1.3 The molar 2S/Cl ratio for the prediction of the risk of high-temperature corrosion	22

4.1.4	Sum of K, Na, Zn and Pb as an indicator regarding aerosol emissions (fine particles smaller 1 μm) and deposit build-up-----	23
4.1.5	Molar Si/K ratio for an estimation of the K release from the fuel to the gas phase -----	25
4.1.6	Molar (K+Na)/[x*(2S+Cl)] ratio for the prediction of the gaseous emissions of SO _x and HCl.-----	26
4.1.7	The prediction of the ash melting temperatures with the molar Si/(Ca+Mg), the molar (Si+K+P)/(Ca+Mg) as well as the molar (Si+K+P)/(Ca+Mg+Al) ratio -----	28
4.1.8	Summary of the pre-evaluation of combustion properties based on fuel indexes -----	30
4.2	Prediction of the ash melting and release behaviour of different wood/kaolin and straw/kaolin mixtures as well as Miscanthus peat blends by TEC - Paper II and Paper III-----	30
4.2.1	Evaluation of the ash melting behaviour predicted by TEC in comparison to experimental results -	31
4.2.2	Evaluation of TEC in comparison with experimental results regarding the release behaviour of ash-forming elements-----	33
4.2.3	Summary of the predictions of the ash melting and release behaviour of different wood/kaolin and straw/kaolin mixtures as well as Miscanthus peat blends by TEC-----	37
4.3	Results of fixed-bed lab-scale reactor experiments performed with different wood/kaolin and straw/kaolin mixtures as well as Miscanthus peat blends – Paper II and Paper III-----	37
4.3.1	Prediction of aerosol emissions for pure biomass fuels, fuel/kaolin mixtures and Miscanthus peat blends-----	37
4.3.2	Prediction of HCl and SO ₂ emissions for pure biomass fuels, fuel/kaolin mixtures and Miscanthus peat blends-----	39
4.3.3	Optical evaluation of selected ashes after fixed-bed lab-scale reactor experiments -----	40
4.3.4	Summary of the results of lab-scale reactor experiments performed with different wood/kaolin and straw/kaolin mixtures as Miscanthus peat blends-----	41
4.4	Experimental setup implementation and evaluation for the online determination of S, Cl, K, Na Zn and Pb release from a single particle during biomass combustion – Paper IV-----	41
4.4.1	Motivation for the development of the single particle reactor -----	41
4.4.2	Description of the reactor-----	41
4.4.3	Launch of the reactor without ICP-MS coupling-----	44
4.4.4	Tests performed with pure salts as a functionality check of the ICP-MS coupling-----	46
4.4.5	In-depth validation of the S-signals-----	46
4.4.6	Quench tests with Miscanthus-----	47
4.5	Simultaneous online determination of S, Cl, K, Na, Zn and Pb release from a single particle during biomass combustion: Results from test runs with spruce and straw pellets – Paper V-----	51
4.5.1	Tests performed-----	51
4.5.2	Release behaviour of ash-forming elements-----	51
4.5.3	Time resolved release behaviour of ash-forming elements during combustion experiments-----	53
4.5.4	Results of targeted quench experiments-----	58
4.5.5	Summary of the benefits of the single particle reactor coupled to an ICP-MS for online determination of the S, Cl, K, Na, Zn and Pb release -----	59
5	Conclusions and recommendations -----	60
5.1	Conclusions -----	60
5.2	Recommendations for further work-----	63
6	Bibliography -----	64
7	Appendix-----	71
7.1	Scientific journal papers-----	71

List of Figures

Figure 1: Abo Akademi single particle reactor [26].....	7
Figure 2: Schematic drawing of the lab-scale tube reactor at Technical University of Denmark [29]	9
Figure 3: Scheme of the fixed-bed lab-scale reactor, including measurement setup (left), common test conditions prevailing for all experiments (middle), and projection of the fixed-bed lab-scale reactor to the fuel layer in a grate furnace (right) [50, 51, 52]	18
Figure 4: NO _x emissions and fuel-N converted to N in NO _x dependent on the N content	22
Figure 5: Dependence of the molar ratios of 2S/Cl in fuels versus aerosol particles.....	23
Figure 6: PM ₁ emissions in the flue gas downstream the boiler, and estimated aerosol emissions for pure spruce and straw, spruce/kaolin, straw/kaolin, pure Miscanthus and peat as well as for the blends versus concentrations of aerosol forming elements in the fuel	24
Figure 7: Molar Si/K ratio versus K release for different biomass fuels.....	25
Figure 8: Molar (K+Na)/[x*(2S+Cl)] ratio versus SO _x emissions and the conversion of fuel-S to SO _x	27
Figure 9: Molar (K+Na)/[x*(2S+Cl)] ratio versus HCl emissions and the conversion of fuel-Cl to HCl	28
Figure 10: Molar (Si+P+K)/(Ca+Mg) ratio versus shrinkage starting temperature for pure biomass fuels, spruce/kaolin mixtures, straw/kaolin mixtures and Miscanthus peat blends.....	29
Figure 11: Molar (Si+P+K)/(Ca+Mg+Al) ratio versus shrinkage starting temperature for pure spruce and spruce/kaolin mixtures as well as for pure straw and straw/kaolin mixtures in comparison with the results gained from thermodynamic equilibrium calculations	31
Figure 12: Molar (Si+P+K)/(Ca+Mg+Al) ratio versus shrinkage starting temperature for pure Miscanthus, peat, as well as for blends in comparison with thermodynamic equilibrium calculations	32
Figure 13: Experimentally determined element release from the fuel to the gas phase from fixed-bed lab-scale reactor experiments in comparison with thermodynamic equilibrium calculations for pure spruce and spruce/kaolin mixtures	33
Figure 14: Experimentally determined element release from the fuel to the gas phase from fixed-bed lab-scale reactor experiments in comparison with TEC for pure straw and straw/kaolin mixtures	35
Figure 15: Experimentally determined element release from the fuel to the gas phase from fixed-bed lab-scale reactor experiments in comparison with TEC results for pure Miscanthus and peat as well as blends.....	36
Figure 16: Estimated aerosol emissions for pure spruce and spruce/kaolin mixtures as well as for straw and straw/kaolin mixtures	38
Figure 17: Estimated gaseous SO ₂ and HCl emissions for pure spruce and spruce/kaolin mixtures as well as for straw and straw/kaolin mixtures	39
Figure 18: Estimated gaseous SO ₂ and HCl emissions for pure Miscanthus and peat as well as for the blends.....	40
Figure 19: Photos of the residual ash of M100 (left), P25 (middle) and P50 (right) gained from lab-scale tests.....	41

<i>Figure 20: Scheme of the single particle reactor including measurement set-up</i>	<i>42</i>
<i>Figure 21: Experimental data for Miscanthus at a temperature set at 850°C: gravimetric data and pressure trends (left-side up), temperature curves (right-side up), flue gas compositions (left-side down).....</i>	<i>45</i>
<i>Figure 22: S and C counts recorded by ICP-MS for an undoped straw pellets (left), for a straw pellet with 2-fold S doping (right)</i>	<i>47</i>
<i>Figure 23: ICP-MS signals for C, S, K, Na, Zn and Pb of the quenching experiments compared with an unquenched experiment for Miscanthus at 850°C.....</i>	<i>49</i>
<i>Figure 24: ICP-MS signals for Cl of the quenching experiments compared to an unquenched experiment for Miscanthus at 850°C.....</i>	<i>50</i>
<i>Figure 25: Release of inorganic elements from the fuel to the gas phase dependent on the respective temperature</i>	<i>52</i>
<i>Figure 26: Time dependent K release from straw for reactor a temperature of 850°C for the three replicated test runs.....</i>	<i>53</i>
<i>Figure 27: Time dependent release of S, Cl and K from softwood (left) and straw (right) at reactor temperatures of 700°, 850° and 1,000°C (from top to bottom)</i>	<i>54</i>
<i>Figure 28: Time dependent release of K and Na from softwood (left) and straw (right) at reactor temperatures of 700°, 850° and 1,000°C (from top to bottom)</i>	<i>55</i>
<i>Figure 29: Time dependent release of Zn and Pb from softwood (left) and straw (right) at reactor temperatures of 700°, 850° and 1,000°C (from top to bottom)</i>	<i>57</i>

List of Tables

<i>Table 1: Proximate and ultimate analyses of woody biomass and for herbaceous biomass; data from [10].....</i>	<i>2</i>
<i>Table 2: Elemental ash composition (mg/kg d.b.) for wood and woody biomass and for herbaceous biomass based on data from [10].....</i>	<i>3</i>
<i>Table 3: Experimentally determined K release rates for different biomass fuels as well as resulting factors x.....</i>	<i>26</i>
<i>Table 4: Release data for complete burnout in comparison with quench experiments for straw at reactor temperatures of 700°, 850° and 1,000°C.....</i>	<i>59</i>

Nomenclature

Abbreviations

a.c.	ash content
d.a.f.	dry ash free
d.b.	dry basis
f.c.	fixed carbon
FID	flame ionisation detector
FT-IR	fourier transform infrared spectroscopy
ICP-MS	inductively coupled plasma mass spectrometer
ICP-OES	inductively coupled plasma optical emission spectrometry
m.	moisture
M100	pure Miscanthus
OGC	organic gaseous hydrocarbons
P100	pure peat
P25 – P75	Miscanthus peat mixtures (wt.% of peat in the mixture)
PM	particulate matter
PM ₁	particles with a diameter smaller 1 µm
SEM/EDX	scanning electron microscopy and energy disperse x-ray spectrometry
SST	shrinkage starting temperature
SW	softwood
TEC	thermodynamic equilibrium calculations
TGA	thermogravimetric analysis
TIC	total inorganic carbon
v.m.	volatile matter
vol.%	volume percent
w.b.	wet basis

wt.% weight percent

λ excess air ratio

Chemical formulas

Al aluminium

Ar argon

C carbon

Ca calcium

Cl chlorine

Cr chromium

Fe iron

H hydrogen

He helium

K potassium

Mg magnesium

Mn manganese

N nitrogen

Na sodium

Ni nickel

O oxygen

P phosphorus

Pb lead

S sulphur

Si silicon

Ti titan

Xe xenon

Zn zinc

Chemical compounds

Al_2O_3	aluminium oxide
$\text{Al}_2\text{Si}_2\text{O}_5(\text{OH})_4$	kaolinite
CaCl	calcium chloride
CaO	calcium oxide
CaSO_4	calcium sulphate
CH_4	methane
CO	carbon monoxide
CO_2	carbon dioxide
C_xH_y	hydrocarbons
Fe_2O_3	iron(III) oxide
H_2O	water
H_3BO_3	boric acid
HCl	hydrogen chloride
HCN	hydrogen cyanide
HF	hydrofluoric acid
HNO_3	nitric acid
K_2CO_3	potassium carbonate
K_2O	potassium oxide
K_2SO_4	potassium sulphate
KCl	potassium chloride
KPO_3	monopotassium phosphate
MgO	magnesium oxide
N_2	nitrogen
N_2O	nitrous oxide
Na_2CO_3	sodium carbonate

Na_2O	sodium oxide
Na_2SO_4	sodium sulphate
NaCl	sodium chloride
NaOH	sodium hydroxide
NH_3	ammonia
$(\text{NH}_4)_2\text{SO}_4$	ammonium sulphate
NO	nitrogen oxide
NO_x	nitrogen oxides
O_2	oxygen
P_2O_5	phosphorus pentoxide
PbCl_2	lead(II) chloride
SiO_2	silicon dioxide
SO_2	sulphur dioxide
SO_x	sulphur oxides
TiO_2	titanium dioxide
ZnCl_2	zinc chloride
ZnO	zinc oxide

1 Introduction and objectives

1.1 Background

Renewable energy is generally defined as energy that comes from resources which are naturally regenerated. Their supply potentially exceeds the world's energy needs and will constitute a significant share in the global energy portfolio of the future. Renewable energy sources encompass biomass, geothermal, hydropower, solar and wind [1]. According to the World Bioenergy Association [2], the primary energy supply of renewables was 13.2% of the global energy supply by the end of 2012, with the biomass share alone amounting to 10%. The relatively high share of biomass in renewable energy production is mainly due to the fact that biomass is a carbon-based fuel and fits into the present mainly carbon-based fuel infrastructure.

There is broad agreement on the need to increase the worldwide share of renewable energy to slow down climate change, since climate change is considered to be one of the most urgent sustainability issues facing our planet [3]. The ongoing depletion of fossil fuels [4, 5], energy supply security issues and political conflicts [6, 7] as well as the opportunity for job creation [8] are further arguments for the increased use of sustainable energy.

A global estimate of biomass use is difficult since reliable data are lacking for developing countries. A prediction of future biomass use is even more difficult, since most important factors affecting biomass potentials cannot be predicted with certainty. However, a systematic summary of existing data has been performed by [9] and four possible scenarios for the biomass potential have been presented. The most optimistic scenario suggests it is possible to replace and exceed all fossil fuels today, whereas the least optimistic scenario suggests it is possible to double the supply of the bioenergy currently used. The large spread of these scenarios mainly results from the biomass potential gained from energy crops. These are intrinsically linked to the demand for food and the availability of land areas for energy crop production. Furthermore, production yield and scope of agricultural productivity increase are uncertain. In spite of all these uncertainties, the biomass potential in energy production is enormous and should be increased in the future.

1.2 Characteristics of different biomass assortments

Biomass is a complex biogenic organic-inorganic solid product generated by natural and anthropogenic processes. The general classification of biomass varieties as fuel resources can be divided roughly into several groups and sub-groups according to their distinct biological diversity, comparable source and origin. According to EN 17225, the main biomass groups consist of woody biomass (biomass from trees, bushes and shrubs), herbaceous biomass (biomass from plants that have a non-woody stem and which die back at the end of the growing season), fruit biomass (biomass from the parts of a plant

which hold seeds), and blends and mixtures (blends of biomass assortments mentioned above).

The listed biomass groups reflect the broad variety of possible/potential biomass fuels, with different physical behaviour as well as chemical compositions typical of different biomass groups. The prevailing differences necessitate a systematic characterisation for combustion purposes. Ref. [10] provides a summary of the most commonly used parameters for characterising biomass fuels, usually based on proximate and ultimate analysis as well as elemental ash composition of the fuel. The proximate analysis covers volatile matter, fixed carbon, moisture, and ash content. The ultimate analysis covers C, O, H, N, and S.

The proximate and ultimate analyses for woody biomass (28 different wood fuels) and herbaceous biomass (19 different fuels consisting of grasses and straws) are summarised in Table 1 [10]. This summary shows the heterogeneity of biomass as well as the broad variation of the parameters displayed. In the same study, the elements were ranked in accordance with the quantity in which they occur in biomass fuels, in decreasing order, valid for wood and woody biomass as follows: C, O, H, N, Ca, K, Si, Mg, Al, S, Fe, P, Cl, Na, Mn, and Ti. A comparison of biomass with coal showed that biomass is highly enriched in Mn > K > P > Cl > Ca > (Mg, Na) > O > moisture > volatile matter and depleted in total ash, Al, C, Fe, N, S, Si and Ti.

Table 1: Proximate and ultimate analyses of woody biomass and for herbaceous biomass; data from [10]

Explanation: d.b. ... dry basis, d.a.f. ... dry ash free, v.m. ... volatile matter, f.c. ... fixed carbon, m. ... moisture, a.c. ... ash content

	Proximate analysis (d.b.)				Ultimate analysis (d.a.f.)				
	v.m.	f.c.	m.	a.c.	C	O	H	N	S
Woody biomass									
Mean	78.0	18.5	19.3	3.5	52.1	41.2	6.2	0.40	0.08
Minimum	69.5	12.3	4.7	0.10	48.7	32.0	5.4	0.10	0.01
Maximum	86.3	26.3	62.9	16.5	57.0	45.3	10.2	0.70	0.42
Herbaceous biomass									
Mean	76.8	16.6	11.5	6.6	49.3	43.5	6.1	1.03	0.14
Minimum	64.3	13.6	4.5	0.90	46.1	40.1	5.1	0.30	0.04
Maximum	81.6	19.5	42.0	20.1	52.0	44.6	6.5	2.8	0.28

In Table 2, average values, minimum and maximum of the composition of the most important ash-forming elements for woody biomass and herbaceous biomass are summarised (the same fuels were used as for the comparison in Table 1). The values were derived from data presented in [10] and it becomes obvious that wood and woody biomass show higher Ca concentrations than herbaceous biomass. Furthermore, in herbaceous biomass, higher concentrations of Cl, S, Si, K, Na, and P prevail. The composition of ash-forming elements strongly influences thermal decomposition behaviour, whereby in [11] the most important ash-forming elements with respect to ash transformation reactions have also been determined to include Si, Ca, Mg, K, Na, P, S, Cl, and Al.

Table 2: Elemental ash composition (mg/kg d.b.) for wood and woody biomass and for herbaceous biomass based on data from [10]

	Cl	S	Si	Ca	Mg	K	Na	P	Al	Fe
	mg/kg d.b.									
Woody biomass										
Mean	267.9	314.3	4,639.2	10,101.7	1,114.3	2,144.8	544.6	409.3	1,193.1	834.2
Minimum	0.0	8.9	45.4	333.7	33.2	119.3	2.6	24.9	12.4	14.7
Maximum	2,600.0	2,381.5	50,772.8	48,322.1	5,410.1	6,681.5	3,304.9	1,501.5	12,971.1	6,080.8
Herbaceous biomass										
Mean	2,936.8	764.7	15,743.3	5,111.3	1,550.1	12,617.2	661.4	1,185.1	708.6	546.3
Minimum	0.0	132.6	417.4	286.9	356.6	2,164.1	20.7	455.4	28.1	42.2
Maximum	8,300.0	1,861.6	72,544.2	13,610.0	4,507.2	39,915.7	2,669.1	2,720.0	3,184.5	2,129.8

1.3 Biomass combustion in fixed-bed systems

The firing of biomass for cooking and heating goes back to pre-historic times and is still conducted in real-scale systems at the present time. There are different combustion systems like fixed-bed reactors, fluidised bed or entrained flow reactors. The most frequently used automated biomass conversion systems are fixed-bed reactors or so-called grate combustion systems. The big advantage of these systems is the simplicity and robustness of operation.

During biomass combustion, the chemically stored energy in the fuel is released by oxidation. Ideally, the carbon contained in the fuel is converted into CO₂, and the hydrogen into H₂O. In a real process this oxidation happens in several stages, whereby the biomass fuel undergoes three main combustion stages (drying of the fuel, pyrolysis/gasification and subsequent gas phase combustion of released reaction products and charcoal burnout). Not only carbon and hydrogen are oxidised but also other elements contained in the fuels (e.g. nitrogen). After char burnout, the non-volatile inorganic elements (ashes) contained in the fuel usually remain on the grate in oxidised form and are removed from the furnace. A part of these ashes is also entrained into the flue gas (coarse fly ash). Semi-volatile and volatile ash-forming elements are partly released from the fuel to the gas phase during biomass combustion and form aerosol as well as gaseous emissions (e.g. PM₁, SO_x and HCl). [12]

Grate combustion systems are available in a wide operation range (>15 kW up to around hundred MW). These systems are technically mature for the combustion of a broad range of biomass fuels. For so-called “difficult” biomass fuels (e.g. herbaceous biomass), the higher contents of ash-forming elements as well as N can cause operational and emission-related problems. Therefore, grate combustion systems designed for e.g. woody fuels can usually not directly be used for herbaceous and other difficult biomass fuels without modifications.

1.4 Emissions and operational problems during biomass combustion

Increased utilisation of biomass and increasing prices for wood fuels have led to increased usage of alternative feedstocks (herbaceous biomass and agricultural residues). Compared with wood fuels, these new alternative feedstocks usually show higher N contents (see Table 1) as well as higher amounts of ash-forming elements (see Table 2).

These elevated contents can cause a higher fouling probability due to aerosol and deposit formation, increased risk of high-temperature corrosion, higher emission tendencies (NO_x , SO_x , HCl, fine particulate matter) as well as higher ash melting tendencies and slagging risks. For the thermal utilisation of these alternative feedstocks, methods are needed which can predict emission and operational problems. A comprehensive characterisation as well as the application of additives or preparation of fuel blends can lead to better fuel properties and form the basis for an appropriate furnace and boiler design.

1.5 Evaluation of combustion-related properties based on fuel analysis

Chemical fuel analysis is the first step in fuel characterisation. Based on these results, so-called fuel indexes can be calculated. For this calculation, certain elements or element groups are correlated, taking into consideration chemical reaction and possible ash transformations. For coal fuels, there are several fuel indexes, and also for biomass fuel such indexes have been developed. This approach can deliver primary information regarding combustion-related issues and can lead a broader utilisation of difficult to use biomass fuels.

1.5.1 Fuel Indexes

Research on the fireside behaviour of minerals in coal started more than a hundred years ago. When high-sulphur coals rich in pyrites (FeS_2) were first burnt on grates, it was quickly recognised that pyrite was responsible for the formation of clinkers. This was the first time that a combustion-related problem was directly related to a specific mineral species [13].

One frequently used correlation for coal, considering the basic and acid ash-forming components, has been developed by [14] and is shown in Equation 1. The acidic oxide constituents (SiO_2 , Al_2O_3 and TiO_2) are generally considered to produce high melting temperatures, whereas ash melting temperatures will be lowered proportionally with relative amounts of basic oxides (Fe_2O_3 , CaO , MgO , Na_2O , K_2O and P_2O_5). For the calculation of the index, the oxides of coal, which has been ashed under laboratory conditions [15], have been considered.

$$\frac{\text{basic}}{\text{acid}} = \frac{(\text{Fe}_2\text{O}_3 + \text{CaO} + \text{MgO} + \text{Na}_2\text{O} + \text{K}_2\text{O} + \text{P}_2\text{O}_5)}{(\text{SiO}_2 + \text{Al}_2\text{O}_3 + \text{TiO}_2)} \quad \text{Eq. 1}$$

A range between <0.4 or >0.7 has been proposed for low or medium slagging or fouling propensity, whereby for values not in this range a high slagging propensity has been reported. There are several of such fusibility characteristics, which were slightly modified and adapted for each individual application. Some of these correlations are only valid for a special type of coal.

As already mentioned, for coal there are many empirical correlations or fuel indexes. For biomass fuels far fewer fuel indexes predicting combustion-related problems have so far been found in literature. For fluidised bed systems, the indexes $(K+Na)/(2S+Cl)$, $(K+Na+Si)/(Ca+P+Mg)$ and K/Si have been investigated [16]. The index $(Na+K)/(2S+Cl)$ is based on the general observation that the initial gas phase alkali concentration is attributable to the alkali concentration in the fuel. A molar $(Na+K)/(2S+Cl)$ ratio in the fuel >1 reflects/indicates the chance that the excess alkali over the sum of S and Cl will stay in the bed and may react with silicates. The formation of alkali-silicates is often observed, and it leads to sintering or de-fluidisation. The index $(K+Na+Si)/(Ca+P+Mg)$ is applied to describe the probability of the formation of a non-sticky outer coating on a bed material particle. For a ratio smaller than 1, the refractory outer coating is likely to form and prevent the sintering of coatings. Also a third agglomeration indicator, the molar K/Si ratio, was introduced where values >1 indicate that the occurrence of agglomeration is more probably a result of melt-induced sintering than the sintering of coating.

Based on results of combustion test runs with twelve different biomass fuels in a residential biomass pellet boiler, slagging tendencies and K retention were investigated. The molar amounts of $Si-(Cl+Ca+Mg)$ in the fuel indicate the K retention in residual ash (slag and bottom ash). The second correlation, the molar amounts of $Si-(Cl+Ca+Mg)$ in the residual ash, indicate the K retention in the slag and the slagging tendency. There is a trend reported towards the latter relation where, with increasing value of this index, the K retention in the slag and the slagging tendency increases. [17] It is assumed that the elements Cl, Ca and Mg may increase the K release, whereby higher Si contents in the fuel favour the K retention in the ash and slag.

The molar $Si/(Ca+Mg)$ ratio has been reported to predict the slagging tendency for residential heating appliances, where slagging increases with rising values. [18]

1.6 Selected experimental lab-scale equipment and reactors for the determination of combustion-related properties of biomass

A considerable variety of laboratory devices are available for the experimental investigation of combustion-related properties. These laboratory devices are characterised by a broad variation concerning sample mass, heating rates and prevailing atmosphere. The experimental boundary conditions are responsible for the type of combustion-related parameters to be determined.

Thermogravimetric analysers (TGA), for instance, are characterised by low sample masses and usually low heating rates operating in inert atmospheres. These experiments are used to describe the thermal decomposition behaviour of the sample, and since the experiments are conducted under a kinetically limited regime, the derivation of kinetic parameters regarding thermal decomposition is possible. TGA is a standard method, and such devices are commercially available on the market.

To additionally gain combustion-related parameters under strictly defined lab-scale conditions, different reactor types have been developed. The design and concept of the

reactors strongly depends on the kind of information to be gained from such experiments. These reactors are usually not commercially available and are mainly individual/customised developments by research institutes. The most relevant reactor systems, which are strongly related to the reactors used and developed in this thesis, are single particle reactors or macro-TGAs and fixed-bed reactors (see sections 1.6.1 to 1.6.3). The sample mass applied in single particle reactors ranges from 10 mg to 1 g, whereby in fixed-bed reactors sample masses of several g up to 400 g are applied. Since higher sample masses than in TGAs are applied, these reactors are not working in a kinetically controlled regime. The reactors are used to describe the thermal decomposition behaviour, where parameters like the mass loss during conversion or char formation can be of interest. The experiments are usually conducted in oxidising atmospheres, and combustion-related parameters like NO_x emission or the release of inorganic elements during the conversion process are determined. In general, the reactors are adjusted to allow a comparison with real-scale processes.

1.6.1 Thermogravimetric analysers

In thermogravimetric analysis (TGA), mass loss and thermal history of a sample exposed to a heating program are determined simultaneously, whereby mass changes in relation to changes in temperature are studied. The data provided by this technique deliver information concerning the partial degradation processes of the sample. A kinetically controlled regime can be assured by the application of very small samples and moderate heating rates <40 K/min [19]. Relevant parameters, such as the moisture, volatile and char content of the samples investigated, can directly be derived from TGA experiments. By means of model application, reaction rates and kinetic parameters for biomass decomposition can be established. [20]

A great variety of standard TGA devices is available on the market. In general, they are all equipped with a small sample holder connected to a highly sensitive microbalance, which is inserted into an electrically heated oven. In the oven, controlled heating of the sample in accordance with a desired heating ramp/or temperature program is ensured. A controlled gas flow is supplied to the oven. The TGA can also be connected to different analysers (e.g. mass spectrometer, FT-IR) for online analysis of the gases released during heating.

Thermogravimetric measurements are influenced by factors such as sample preparation, sample pre-treatment, particle size, sample mass, crucible, atmosphere, flow rate and heating rate. Sample preparation should change the sample properties as little as possible and it has to be noted that sample pre-treatment (e.g. washing of inorganic salts) has a strong influence on pyrolytic behaviour [20]. The particle size should be such as to avoid a temperature gradient from the surface to the core of the particle, with a size range of 120 µm – 1 mm prevailing. The sample mass which is usually used in a kinetically controlled regime is between 3 mg and 50 mg, which also influences the results obtained [21].

In pyrolysis tests, N₂, He, Ar, and in combustion tests, mixtures of N₂, O₂ or air are supplied to the electrically heated oven. The flow rate strongly depends on the device,

sample mass and the experiment conducted. Typical heating rates during TGA experiments are from 5° to 40°C/min, where usually the char yield decreases with increasing heating rates [22, 23]. Generally, TGA experiments deliver decomposition data which can be used as input parameters for modelling and simulation.

However, also macro TGAs operating with higher sample masses >100 mg up to ~1 g (biomass particles or pellets) and also packed biomass bed reactors with sample masses <500 g are in operation. Since these macro TGAs do not operate in a kinetically controlled regime, they are more frequently used as reactors for the determination of the combustion behaviour (see sections 1.6.2 and 1.6.3).

1.6.2 Single particle reactors

1.6.2.1 Single particle reactor at Abo Akademi

At Abo Akademi, a single particle reactor for the investigation of solid biomass fuels is used. The general setup of the reactor can be seen in Figure 1.

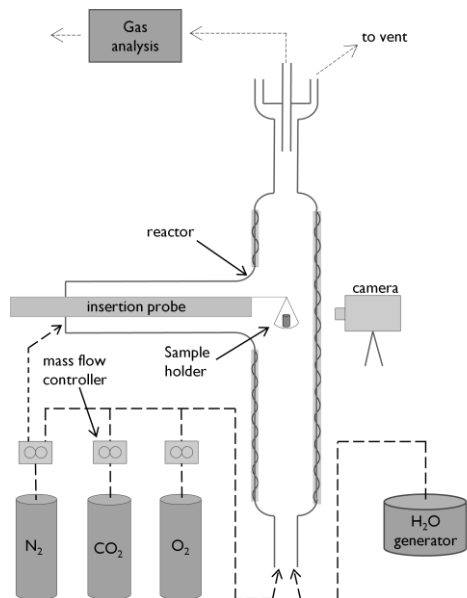


Figure 1: Abo Akademi single particle reactor [26]

The setup consists of a quartz tube reactor inserted into an electrically heated ceramic furnace. Reactant gases are fed from the bottom and middle of the reactor. The main reaction gas is fed from the bottom, whereby a part of the reaction gas (N₂) is introduced through the sample insertion port to cool the sample and to ensure that no unwanted reactions are taking place before and after insertion of the sample. The gas flow exiting from the top is directed to gas analysers. The temperature in the reactor is measured with a thermocouple inserted into the ceramic wall of the furnace, close to the surface of the quartz reactor in the proximity of the sample placement point. [24, 25, 26]

The sample is inserted into the reactor using a movable probe that can be inserted from room temperature into the hot reactor within a fraction of a second. The sample holder

for pulverised fuels is made of quartz, with a porous bottom, where sample masses of 10-15 mg are placed [24]. For the investigation of biomass pellets [25, 26], the sample holder consists of a thin net on which a single fuel pellet (~200 mg) is placed. The reactor can operate in a temperature range from ambient temperature up to a temperature of 1,050°C in variable atmospheres. During the experiments, the gas produced is analysed with regard to O₂, CO, CO₂, NO and SO₂. Moreover, optical observation via an optical board and a camera is possible. [24, 25, 26]

In [24] the combustion characteristics of biomass residues were studied, and special emphasis was put on the N to NO conversion. In [25] the release of NO during the combustion of single char particles of spruce bark was investigated. The data were used for NO formation model development. In [26] the char gasification of raw and torrefied pine shell, olive stones and straw was investigated, to determine char conversion. Based on these experiments, kinetic parameters for the experimentally determined char conversions were derived.

1.6.2.2 Macro TGA at Umea University

The macro TGA at Umea University consists of an electrically heated furnace connected to an analytical balance from where a sample basket of platinum is hung. Pre-heated air is continuously supplied to the furnace from the bottom through a distribution plate. A pneumatic device is used to move the furnace up and down to enable inserting the sample and quenching during combustion. A window on the front panel facilitates visual inspection of the combustion process. [27]

The setup was used to investigate the effects of pelletising conditions on combustion behaviour of single pellets [27]. Furthermore in [28] a tuneable diode laser absorption spectroscopy was used for the detection of gaseous elemental K, which is released from a single pellet. Additionally, tests were performed where the combustion process was stopped at different times (mainly during char burnout). The residues after the stop of the combustion process were chemically analysed and the release of ash-forming elements was determined.

1.6.3 Fixed-bed reactors

1.6.3.1 Lab-scale tube reactor at Technical University of Denmark

The setup includes a gas mixing system, a reactor unit, a gas conditioning system containing cooling and filtration stages, gas analysers (O₂, CO, CO₂, NO and SO_x), a thermocouple, and a data acquisition system.

The laboratory-scale fixed-bed reactor consists of a two-zone electrically heated oven in which a cylindrical alumina tube is mounted horizontally, with water-cooled flanges at both ends (cooling zone). Inside the tube, a removable alumina tube is placed, in which a sample boat can be inserted. The configuration and dimensions of the reactor tubes are shown in Figure 2. [29]

The setup is used for the investigation of the conversion (pyrolysis and combustion) of solid fuel samples under controlled conditions. The temperature, gas flow rate and composition simulate the conditions on the grate of a real-scale boiler. The release of inorganic elements can be quantified by weight measurements and chemical analyses of the fuel and the ash residues. The release is of special relevance regarding aerosol emissions and deposit build-up and can lead to an improved understanding of ash transformation process during combustion in grate-fired boilers.

Several studies regarding the release of inorganic elements have been performed with the fixed-bed reactor, where sample masses between 3 g to 30 g were used. In [30, 31] the release behaviour of agricultural residues (barley, rice, wheat, oat, rape and carinata), in [29, 32] spruce bark and beech, in [33] corn stover and in [34] poplar and brassica energy crops were investigated. Furthermore, relevant ash transformation processes and possible release mechanisms are discussed in these studies.

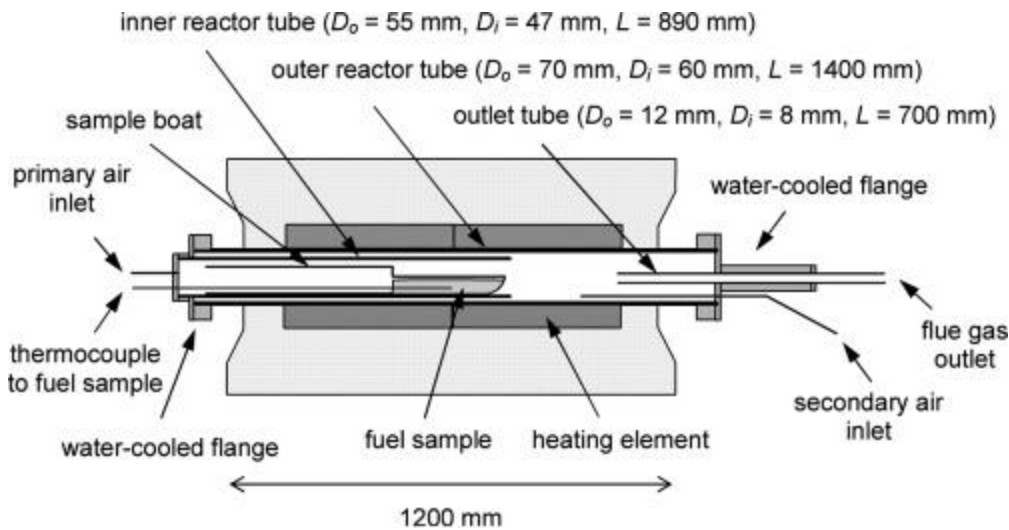


Figure 2: Schematic drawing of the lab-scale tube reactor at Technical University of Denmark [29]

1.7 Improvement of combustion-related properties by additive application

An interesting option to reduce combustion-related problems associated with challenging biomass fuels is the application of additives. Fuel additives may be mixed and fed into the furnace together with the biomass fuel, or mixed with the raw material before pellet production. The latter has the advantage that the additive can be homogeneously distributed in the fuel, and separation of the fuel and the additive during fuel feeding and in the fuel bed is avoided. In larger heating and CHP plants, the main objectives for using fuel additives are to reduce bed agglomeration, sintering/slagging, deposit formation and corrosion. In smaller (residential and medium-sized) grate-fired appliances, the main objectives for using fuel additives are to lower slagging problems and to reduce fine particle emissions.

Feasible options are calcium-based and aluminosilicate-based additives. They can generally be applied to reduce ash-related problems and for SO_x , HCl and PM emission

reduction. It has to be noted that they do not influence NO_x emissions. Certain additives are able to reduce only one combustion-related issue, whereas some additives can reduce more than one combustion-related problem. Ca-based additives, for instance, are used for reactions of HCl and SO_2 to CaCl and CaSO_4 and have also been used for reducing the slagging tendency in grate-fired systems by the formation of high-melting Ca/Mg/(K)-silicates and oxides. They usually show no influence on alkali release. The second and, so far, most thoroughly studied additive is kaolin, which is composed mainly of the mineral kaolinite ($\text{Al}_2\text{Si}_2\text{O}_5(\text{OH})_4$). This mineral captures alkali compounds. By this mechanism K-Al-silicates are formed, which have higher melting temperatures than the pure K-silicates. This effect allows slagging prevention and the reduction of aerosol emissions in parallel. However, due to reduced alkali release, higher SO_x and HCl emissions have to be expected. [35]

Several studies have been presented regarding the application of additives in small-scale combustion systems for various biomass fuels. A decreasing potential of fine particulate emissions as well as an improvement of the slagging tendency by addition of kaolin to straw have been reported [35]. The same trend concerning decreasing aerosol emissions has been reported with regard to kaolin addition to woody biomass fuels (bark from pine and cleaning assortments) [36]. Another study reported decreased slag formation as a result of the addition of kaolin and limestone during combustion of wood fuels [37]. A further study investigated the slagging characteristics of corn stover mixtures with kaolin and calcite and showed an improvement of the slagging tendency by additive utilisation [38]. In [39] and [40] also P-rich fuels were investigated. Fine particulate emission reductions of 31% and 57% have been reported for kaolin additions of 2% and 4% respectively to oat grains, whereas kaolin addition increased the gaseous emissions of HCl and SO_2 [39] as a side effect. A further study [40] investigated the influence of kaolin and calcite additives on ash transformation during small-scale combustion of oat. By means of kaolin addition, the formation of slag in the bottom ash could be totally avoided. Moreover, the addition of kaolin effected the formation of fine particulate emissions, where an increased share of condensed K-phosphates at the expense of K-sulphates and KCl (was almost completely absent in the particulate matter) was established. However, due to reduced formation of KCl and K_2SO_4 , increased gaseous HCl and SO_2 emissions were measured. Just one study [41] has been found dealing with additive application in large-scale combustion systems, where the positive influence of increased sintering temperatures was investigated in a 35 MW circulating fluidised bed boiler. It has been reported that fine kaolin powder captures K vapours which get incorporated in the fly ash. Therefore, less K is available in the furnace, which decreases the risk of bed agglomeration.

It has to be noted that fuel additives have not been broadly applied by the industry so far. This might be because of a lack of detailed analyses of their functionality and the fact that their application has not been optimised with regard to economic and technical issues.

1.8 Biomass upgrading by preparation of fuel blends with peat

Peat is an accumulation of partially decayed vegetation. One of the most common components is Sphagnum moss, although many other plants can contribute. Soils that contain mostly peat are known as a histosol. Peat forms in wetland conditions, where flooding obstructs flows of O₂ from the atmosphere, which reduces rates of decomposition. [42]

The composition of peat [43] depends on the geological surroundings, historical topography as well as hydrology and meteorology. That is why peat lands offer differing peat compositions. For this reason it is important to consider the elemental composition, since it has a strong influence on the application of fuel blending.

From [43] it can be concluded that peat usually contains higher amounts of N, S, Al and Ca and lower concentrations of K compared to virgin wood fuels without chemical treatment or coatings and paint. The Si concentration in peat may vary, depending on the type of peat; average values of 0.55±1.3 wt.% d.b. have been reported. Typically, Si concentrations are considerably higher than in wood fuels. For blending peat with alternative feedstocks (herbaceous biomass and agricultural residues), higher ash melting temperatures are expected, since peat typically elevates the Ca and Al concentration of the blend, whereby Si in combination with K decreases the ash melting temperatures. A reduced K release may result from better embedding of K in the ash due to K-alumino-silicate formation. In cases of an elevated Si content in the peat, a lower K release can also result from the formation of Si melts. The increasing S content in the blend may lead to decreased high-temperature chlorine corrosion problems. On the other hand, gaseous NO_x and SO_x emissions may increase due to the increasing concentrations of S and N in the blend.

A few studies regarding biomass/peat blends have already been published. In [44] the effect of peat addition to wood pellets on slagging characteristics during combustion in residential pellet burners was investigated. It was reported that the addition of a Si rich peat increased the slagging tendency, whereas the slagging tendency was significantly lower when adding ash poor peat with a relatively high Ca/Si ratio. In [45], forest residues and wheat straw were co-combusted with peat (15 or 40 wt.% d.b.) in a small-scale (15kW) grate-fired boiler. Peat addition led to a reduction of the release of fine particle and deposit forming alkali metals of up to 74% for forest residues and up to 45% for wheat straw. In [46] it is reported that the addition of peat prevented agglomeration in a fluidised bed, where bark from pine and spruce were used as fuels. This study reports that even 5% peat was found to have a significant effect on preventing bed agglomeration. Another study [47] investigated the combustion of mixtures of forest residues and peat in controlled experiments in a bench-scale fluidised bed reactor. The main results were an increased bed agglomeration temperature, a decreased concentration of K and an increased concentration of Ca in the inner bed particle layers, a reduced amount of fine particle but an increased amount of coarse particle emissions. The mechanisms underpinning the positive effects were the transfer and/or removal of K in the gas phase to a less reactive solid form via sorption and/or the reaction with the

reactive peat ash (SiO_2 and CaO), which in most cases formed larger particles ($>1 \mu\text{m}$) containing Ca, Si and K.

1.9 Objective of the work presented

Wider utilisation of alternative feedstocks (herbaceous biomass and agricultural residues) for combustion processes can cause increased emissions (NO_x , SO_x , HCl, fine particulate matter) as well as operational problems (higher ash melting tendencies and slagging risks as well as corrosion) (see section 1.4). To anticipate these problems and to characterise alternative feedstocks, appropriate characterisation methods are needed. Furthermore, strategies to minimise emissions and operational problems by utilisation of additives and preparation of fuel blends will have to be developed.

The main objective of the work covered by this thesis was the development of characterisation methods for solid biomass to predict combustion-related properties, based on laboratory methods and appropriate calculation procedures. The methods developed and applied focus on fixed-bed biomass combustion regarding the temperature ranges investigated as well as the tests performed. These methods should help to minimise the need for time-consuming and expensive real-scale combustion tests. Furthermore, these methods should facilitate a targeted selection of biomass mixtures and biomass additives.

For a pre-evaluation of combustion-related properties of biomass fuels, biomass mixtures and biomass additive mixtures, special fuel indexes had to be developed. A first prediction of combustion- and emission-related properties should be based on fuel indexes. Thermodynamic equilibrium calculations (TEC) should be performed for a qualitative determination of the release of inorganic elements and to gain a deeper insight into ash transformation processes. TEC also deliver first indications of the ash melting temperatures. To verify the quantitative release prediction, fixed-bed lab-scale reactor experiments should be performed. The characterisation methods mentioned so far should be applied to the characterisation of different wood/kaolin and straw/kaolin mixtures as well as to Miscanthus peat blends. Fixed-bed lab-scale reactor experiments make the determination of the release of inorganic elements for the entire combustion experiment possible. To gain a more detailed insight into the release behaviour, a reactor for the time resolved release determination of single particles should be developed. The time resolved release data should be validated and results from tests with biomass fuels should be presented.

The work includes five separate papers in which the detailed objectives were:

- I. The development of fuel indexes for biomass for a quick pre-evaluation of combustion-related properties. **(Paper I)**
- II. To show how fuel indexes, TEC and fixed-bed lab-scale reactor experiments can support the evaluation of the combustion-related properties of biomass/kaolin mixtures. Based on laboratory methods, optimum mixing ratios should be identified without the need for time-consuming and expensive real-scale combustion tests. **(Paper II)**

III. To investigate the influence of peat addition to Miscanthus (as a case study of fuel blending) and to identify a meaningful blending ratio by the application of fuel indexes, TEC and fixed-bed lab-scale reactor experiments. **(Paper III)**

IV. To develop a single particle reactor connected to an inductively coupled plasma mass spectrometer (ICP-MS) in order to be able to investigate biomass decomposition and the release of inorganic aerosol forming elements of single biomass particles. Furthermore, a validation of the determined release data was to be performed. **(Paper IV)**

V. To investigate whether the time resolved release data for inorganic elements gained from single particle reactor tests can support proposed release mechanisms in the literature. Also transport-limited release processes should be revealed by the experiments conducted. Furthermore, the time dependent release profiles should be validated by additional quench experiments. These experiments should also reveal further insights regarding ongoing release processes. **(Paper V)**

2 Analytical, experimental and theoretical methods used

2.1 Fuel and ash analysis

Wet chemical fuel analyses, which were generally used in **Papers I-V**, form the basis for a comprehensive fuel characterisation. It is strongly recommended to generally follow the best practice guidelines worked out within the EU FP6 project BIONORM [48] and subsequently implemented in various CEN/EN standards for biomass fuels.

The moisture content of fuel samples has been determined according to EN 14774 (determination of the weight loss during drying at 105°C until a constant weight is reached).

Fuel and ash sample preparations were carried out in accordance with EN 14780, which includes (i) drying of the sample at 105°C, (ii) milling of the whole sample in a cutting mill to a particle size <4 mm, (iii) sample division, (iv) milling of the final analyses sample in an ultracentrifugal mill equipped with a titanium rotor and screen to a particle size <0.2 mm.

The ash content was determined in accordance with EN 14775 by determination of the loss of ignition at 550°C. Additionally the TIC (total inorganic carbon) content of the ashed fuel was analysed to calculate a carbonate-free (only oxide based) ash content.

C, H, N and Cl content: The determination of C, H and N contents was carried out in accordance with EN 15104 by combustion and subsequent gas-phase chromatographical separation and measurement in an elemental analyser (Vario EL 3, Elementar). The determination of Cl was carried out in accordance with EN 15289, applying a digestion step based on bomb combustion in O₂ and absorption in NaOH (0.05 molar), followed by an ion chromatographic detection (ISC 90, Dionex).

The concentrations of major and minor elements as well as of S in the fuel and ash samples were determined by multi-step pressurised digestion of the fuel with HNO₃

(65%)/HF (40%)/H₃BO₃ (Multiwave 3000, Anton Paar), followed by detection applying inductively coupled plasma optical emission spectrometry (ICP-OES) (Arcos, Spectro) or inductively coupled plasma mass spectrometry (ICP-MS) (Agilent 7500x, Agilent), depending on detection limits. The digestion method applied is of great importance to ensure a complete dissolution of the ash matrix, which is a basic requirement for correct element detection.

The determination of the ash melting behaviour was done in accordance with CEN/TS 15370-1. The fuel samples are ashed at a temperature of 550°C and the remaining ash is pressed into cylindrical moulds. These samples are then heated in an oven under oxidising conditions. The characteristic temperatures (shrinkage starting temperature, deformation temperature, hemisphere temperature, flow temperature) are determined. It has to be taken into consideration that the characteristic ash melting temperatures are valid for the total ash (fuel ash). In real-scale applications, the distribution of certain elements in different ash fractions may influence the melting temperatures of the individual fractions.

2.2 Thermodynamic equilibrium calculations

Thermodynamic equilibrium calculations (TEC) were used to support the interpretation of the experiments conducted especially for **Paper II** and **Paper III**. For the interpretation of TEC results it has to be remembered that kinetically limited processes and imperfect mixing are not taken into account in the calculation. Furthermore, the selection of databases as well as the thermodynamic data themselves strongly influence the results. However, TEC give an idea which components are commonly formed in equilibrium conditions.

TEC provide the possibility to predict multi-phase equilibria, where gaseous, liquid and solid phases of interest can be identified and quantified. These calculations are conducted for a multi-component thermodynamic system in a pre-determined gas atmosphere, on the assumption that chemical equilibrium can be achieved for the system investigated. TEC were used to qualitatively investigate the release behaviour of inorganic compounds (K, Na, S, Cl, Zn, Pb) and the ash melting behaviour. The thermochemical software packages FactSage 6.2 and 6.3 were applied, which use the image component method in Gibbs free energy minimisation concerning thermodynamic equilibrium. In FactSage, a series of calculation modules as well as databases are included. The currently accessed databases are "solution databases" including the optimised parameters for a wide range of solution phases and "pure compound" databases containing the data for over 4,500 stoichiometric compounds. For the work presented, the component database Fact 53, the solution databases FToxid (slags and other oxide mixtures) and FTsalt (liquid and solid salt phases) were used. More than 1,000 components and 9 solutions (which were shown to be stable and thermodynamically relevant) were considered. The selection was application-oriented for biomass fuels, biomass/kaolin mixtures, peat and biomass/peat blends as well as their ashes.

Previous work showed that a realistic prediction of the characteristic ash melting temperatures and the release behaviour primarily depends on a reliable quantification of

the molten solution phases SLAGH and SALTf over the temperature range of interest. Experience has shown that the assessment of these two phases is strongly influenced by the amounts of Al, Si and K. Therefore, based on empirically estimated limits for the characteristic molar ratios of $(\text{Si}+\text{K}+\text{P})/(\text{Ca}+\text{Mg})$, $\text{K}/(\text{Si}+\text{P})$ and Al/Si , an optimisation method [49] for TEC was developed which is briefly discussed below.

(1) The fraction of reactive Si considered in the calculation is related to the molar ratio of $(\text{Si}+\text{K}+\text{P})/(\text{Ca}+\text{Mg})$, whereby for fuels with a value lower than 0.94 a Si-reactivity of only 10% is assumed. Especially for pure wood ashes, the inclusion of typically sand-like contaminants combined with the low ash content of the corresponding fuels causes a significant share of Si to be less, or almost not, reactive. It can be assumed that this inert Si-fraction (approx. 90%) does not take place in the ash melting processes and thus, by limiting the reactive fraction, an overestimation of slag formation can be avoided. For non-wood ashes, Si-reactivity is defined to be 100%, because the corresponding fuels usually contain high Si amounts, making the Si fraction stemming from external contaminants (e.g. sand, stones) less relevant.

(2) To avoid an unrealistic prediction of slag formation, Al_2O_3 is excluded from SLAGH in calculation cases with a molar Al/Si ratio <0.2 . Al_2O_3 has a strong influence on slag formation, and the currently available thermodynamic data for Al in slag solutions seem inaccurate. Therefore, this exclusion was defined.

(3) The molar ratio $\text{K}/(\text{Si}+\text{P})$ determines whether the molten salt solution SALTf is used in the TEC model. SALTf is eliminated from the TEC model for molar ratios larger than 1, otherwise SALTf phases (mainly composed of K-carbonates/sulphates) are over-predicted, which results in an unrealistic drop of the melting temperatures estimated.

To achieve a more accurate prediction of inorganic element release from the fuel to the gas phase (especially regarding K and Na), the calculations were performed following a 2-step procedure which separately considers the devolatilisation and charcoal combustion phases. For step 1 of the calculation, the input data consist of the complete elemental fuel composition, under consideration of a sub-stoichiometric combustion air ratio (λ typically 0.7) and atmospheric pressure. The evaluation of step 1 was performed for a temperature of 700°C , which is assumed to be a realistic fuel bed temperature during volatilisation. For step 2 of the calculation, which simulates the charcoal combustion phase, the input consists of the solid residues from step 1 (ash-forming matter and charcoal), whereby the charcoal is assumed to consist of pure C and amounts to 15 wt.% of the initial organic dry matter. In this step, an oxidising atmosphere ($\lambda >1$) and atmospheric pressure are applied, and the calculations are carried out in a temperature range from 700°C - $1,500^\circ\text{C}$. The release resulting from this calculation stage was evaluated for a temperature of $1,250^\circ\text{C}$, since this is a typical charcoal bed temperature for fixed-bed combustion systems. The total release of the elements considered was calculated as the sum of the release in step 1 and step 2. The calculated release ratios are compared with experimentally determined release ratios from lab-scale experiments (see section 4.2).

The calculations of the ash melting temperatures were performed in a 1-step approach using the results of chemical analysis of the laboratory ashed fuel (ashed at 550°C) as input data. The composition of the ashed fuel was used to gain better comparability with the standard ash melting test in accordance with CEN/TS 15370-1. The calculations were performed in oxidising gas atmospheres as well as at atmospheric pressure in a temperature range of 500°-1,600°C. The calculated ash melting temperatures were compared with the results of the standard ash melting test (see section 4.2).

In [49] additional information regarding the software, the applied models and the evaluation procedure can be found.

2.3 Fixed-bed lab-scale reactor

For the investigations presented in **Papers I-III** a fixed-bed lab-scale batch reactor, especially designed for the investigation of the thermal decomposition behaviour of biomass fuels, was used. The reactor was developed at the Institute for Process and Particle Engineering, Graz University of Technology [50].

The basic idea of the lab-scale batch reactor was to simulate the fuel decomposition behaviour in real-scale grate combustion systems as closely as possible. Therefore, the following constraints were set out:

- Reasonable sample intake to consider secondary reactions in the fuel bed appropriately.
- Heating rates of the fuel comparable to real-scale grate furnaces.
- Inert reactor material to avoid reactions of the fuel, ashes and flue gases with the reactor.
- High flexibility regarding analytical equipment connected with the reactor.
- Online recording of relevant operation data and emissions as well as mass loss.

The fixed-bed lab-scale reactor consists of a cylindrical retort (height 35 cm, inner diameter 12 cm) which is heated electrically and controlled by two separate proportional-integral-derivative PID-controllers, as can be seen in Figure 3. The fuel is inserted in a cylindrical sample holder of 100 mm height and 95 mm inner diameter. The reactor wall and sample holder are made of reinforced silicon carbide. This material is inert under reducing and oxidising conditions, which ensures that the wall does not react with the fuel, ash and flue gas. The sample holder is placed on the plate of a scale. The scale, which is used to determine the weight loss of the sample, is mechanically separated from the retort by a liquid sealing (synthetic thermal oil: Therminol 66). This setup ensures the possibility to continuously determine the weight loss of the sample during drying, pyrolysis, gasification and charcoal combustion. The sample is introduced into the pre-heated reactor and rapid heating is achieved, which compares well with conditions in real-scale fixed-bed thermal conversion processes. The test conditions for all test runs performed with the fixed-bed lab-scale reactor are defined in Figure 3.

The following measurements/analyses were performed during each of the combustion test runs:

- Mass decrease of the fuel over time (balance).
- Concentrations of flue gas species over time:
 - CO₂, H₂O, CO, CH₄, NH₃, HCN, N₂O and basic hydrocarbons were determined with a multi-component Fourier transform infrared (FT-IR) spectroscopy device (Ansyco Series DX 4000).
 - The O₂, H₂ concentrations were measured with a multi-component gas analyser (Rosemount NGA 2000). This device uses paramagnetism as a measurement principle for O₂ detection and a thermal conductivity detector for H₂ detection.
 - C in organic gaseous hydrocarbons (OGC) was determined with a flame ionisation detector (FID) (Bernath Atomic 3005) which detects organic compounds by ionisation in a burning H₂ flame.
 - Wide band lambda sensor (O₂).
 - A nitric oxide analyser (ECO Physis CLD 700 El ht), which employs the principle of chemiluminescence, was used for NO and NO_x detection.
- Temperature measurements over time.
 - 5 thermo-couples in the fuel bed (3 different heights NiCr-Ni).
 - Thermo-couples in the gas phase (NiCr-Ni).
- Analysis of the biomass fuel used and residual ash produced.

The testing protocol was defined as follows:

- At first the fuel is pre-dried to 10 wt.% moisture content and a sub-sample of the fuel is forwarded to wet chemical analyses.
- First, the fuel is filled into the sample holder.
- The reactor is pre-heated, applying 750° and 450°C as pre-settings for the upper and lower heating element. These settings are kept constant during the whole test run.
- Subsequently, the reaction gas flow through the grate and the fuel bed is activated and the sample holder with the fuel is introduced into the reactor. All experiments documented in this thesis were performed with dry air (21 vol.% O₂ and 79 vol.% N₂) as the reaction agent and a gas flow of 30 l/min at 0°C and 101,325 Pa. This gas flow is kept constant during the whole test run.
- All parameters mentioned above, with the exception of the FT-IR (5 s interval) are continuously recorded at 2 s intervals over the whole test run. The test usually lasts about 60 min, depending on the fuel.
- At the end of the test run, the residues (ashes) are first visually evaluated regarding ash sintering and slag formation and then removed and forwarded to chemical analyses.

More detailed information about the test procedure and the evaluation of the fixed-bed lab-scale reactor experiments can be found in [50]. The specific design of the reactor ensures that the burning conditions of a biomass fuel layer on a grate are simulated as

closely as possible (Figure 3, right). It reproduces the behaviour of a fuel segment moving along the grate. This segment first passes through the drying zone, then through the devolatilisation and charcoal gasification zone and finally, through the char burnout zone. Since a constant air flow through the fuel bed is applied throughout the whole experiment, the excess air ratios vary depending upon the stage of combustion. High λ values (during drying) over understoichiometric conditions (usually a λ between 0.6 and 0.9) during the devolatilisation phase, back to λ values above 1 during charcoal burnout prevail. This corresponds to the different air ratios prevailing in the different zones of a real-scale moving grate. This approach is valid if diffusional transport and mixing effects on the grate can be neglected. Validation was achieved in previous research, which showed that the fuel transport along the grate can be fluidically characterised by a plug flow in good approximation [51, 52]. Therefore, tests within this reactor can be used to evaluate and validate the predictions gained from TEC for fixed-bed combustion conditions.

Consequently, with this setup, comprehensive information on the thermal decomposition process of biomass on a grate can be gained. This information can be transferred to real-scale systems. It includes mass losses during drying, pyrolysis, and charcoal combustion, the compositions of the gases produced, and comprehensive information about the formation of NO_x precursors. Moreover, the data gained from the fuel analysis and the residual ash analysis as well as the weight measurements of the fuel sample and the ash sample can be used to calculate the elemental release to the gas phase. This is done by calculating the mass balance for every relevant element, as well as for the total ash.

Furthermore, fixed-bed lab-scale reactor experiments can give preliminary information about the ash sintering tendency. According to visual evaluations of the ash residues after a test run, the ash may be described as: loose ash residue, slightly sintered ash with a brittle structure, hard sintered ash residue with partial melting, very hard sintered ash residue with slag formation and completely molten ash residues.

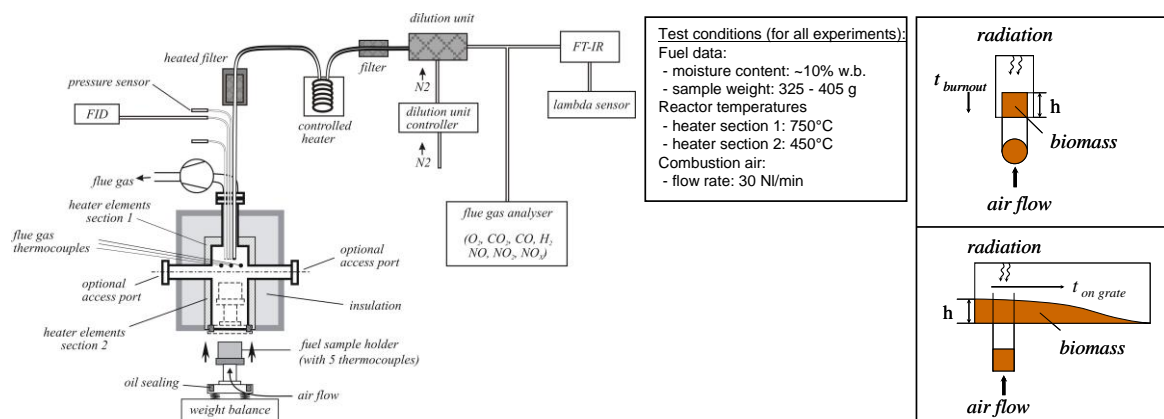


Figure 3: Scheme of the fixed-bed lab-scale reactor, including measurement setup (left), common test conditions prevailing for all experiments (middle), and projection of the fixed-bed lab-scale reactor to the fuel layer in a grate furnace (right) [50, 51, 52]

3 Fuels used for the investigations

Experimental data gained in previous projects, which were performed by employees of BIOS BIOENERGIESYSTEME GmbH, the Institute for Process and Particle Engineering, Graz University of Technology as well as BIOENERGY 2020+ GmbH were used for this thesis. In prior projects, especially pure biomass fuels were investigated. Fuels from five different biomass categories which are typical of different climate zones were used. In addition, biomass/kaolin mixtures as well as biomass blends (see sections 4.2 and 4.3) were explored within this thesis. The biomass fuels, biomass additive mixtures as well as fuel blends investigated can be summarised as follows:

- wood and woody biomass
 - beech woodchips from Austria
 - spruce woodchips from Austria
 - spruce pellets from Austria
 - bark of softwood
 - waste wood
 - torrefied softwood
- short rotation coppice
 - poplar from Austria
- herbaceous and agricultural biomass
 - Miscanthus pellets from Germany
 - wheat straw from Austria
 - olive kernels from Greece
 - maize spindle pellets (maize residues) from Austria
 - grass pellets
- others
 - sewage sludge from Austria
- industrial biomass residues
 - decanter and rapeseed press cake
 - residues of starch production
- biomass and additive mixtures
 - spruce softwood from Sweden and wheat straw from Denmark mixed with kaolin delivered from the company Thiele Nordic AB (Sweden)
 - spruce with 0, 0.2, 1 and 3 wt.% kaolin
 - straw 0, 1, 4 and 7 wt.% kaolin
- biomass mixtures
 - Miscanthus peat blends
 - 75 wt.% Miscanthus with 25 wt.% peat (P25), 50/50 (P50) and 25/75 (P75) related to dry basis
 - A pure Miscanthus sample (M100) and a pure peat sample (P100) were used as reference points.

3.1 General information regarding biomass additive and Miscanthus peat blends investigations

Previously, the kind of additive and its dosing, which influence the combustion/emission behaviour, as well as the influence of biomass mixtures were mainly experimentally evaluated. **Paper II** presents an approach how fuel indexes, TEC and fixed-bed lab-scale reactor experiments can support the evaluation of the combustion-related properties of biomass/kaolin mixtures as a case study of fuel/additive mixtures. With their help, optimum mixing ratios were identified without the need for time-consuming and expensive real-scale combustion tests. In **Paper III** the same methods were applied to investigate different Miscanthus peat blends as a case study of fuel blending.

For the kaolin investigations performed in **Paper II**, softwood and straw were chosen as biomass fuels. Pure softwood, straw and kaolin were chemically analysed, and theoretical mixing calculations of promising kaolin ratios were performed. Fuel indexes and TEC were used for the evaluation of appropriate kaolin addition ratios, which were later prepared. Based on these investigations, for spruce 0, 0.2, 1 and 3 wt.% kaolin (related to dry basis), whereas for straw 0, 1, 4 and 7 wt.% kaolin (related to dry basis), were selected and for spruce 1 wt.% kaolin and for straw 4 wt.% kaolin were evaluated as an optimum kaolin addition ratio.

For the investigations of Miscanthus peat blends presented in **Paper III**, three different blends of Miscanthus and peat were prepared: 75 wt.% Miscanthus with 25 wt.% peat (P25), 50/50 (P50) and 25/75 (P75) related to dry basis. A pure Miscanthus sample (M100) and a pure peat sample (P100) were used as reference points.

4 Results

4.1 Pre-evaluation of combustion properties based on fuel indexes - Paper I

There is growing interest in the utilisation of non-wood feedstocks (herbaceous biomass and agricultural residues) to increase biomass utilisation in the energy sector. However, since these non-wood feedstocks are not sufficiently defined yet with regard to their combustion behaviour, fuel characterisation with a special focus on combustion-related fuel properties represents a first important step towards their introduction. In this, possible ash-related problems (ash melting on grates, deposit formation and corrosion, particulate emissions) as well as problems regarding NO_x, SO_x and HCl emissions are the main focal points. One option to gain quick first indications regarding the problems mentioned is the development, evaluation and application of fuel indexes.

As mentioned in section 1.2, in herbaceous biomass, usually higher N, Cl, S, Si, K, Na and P concentrations prevail compared to woody biomass. During the combustion process, a part of the semi-volatile and volatile ash-forming elements such as S, Cl, K, Na, Zn and Pb is released from the fuel to the gas phase. In the gas phase they undergo homogenous gas-phase reactions and later, due to supersaturation in the gas phase, they start to nucleate or condense on the surfaces of existing particles or of heat exchanger tubes

[12, 53]. Since in most biomass fuels the concentrations of K are significantly higher than other aerosol forming elements (e.g. Na, Zn and Pb), the release of K is most relevant to the formation of aerosol emissions. These aerosols, as well as entrained fly ash particles, are responsible for deposit formation on heat exchanger surfaces which can cause fouling and slagging. Furthermore, these deposits can cause corrosion. A comprehensive study has shown that with rising Cl concentrations in tube-near deposit layers an increased risk regarding high-temperature chlorine corrosion prevails [54]. Furthermore, the concentration of S and Cl mainly influences the gaseous SO_x and HCl emissions. The increased N-content in the fuel can cause increased NO_x emissions, since [55, 56, 57] report that in biomass combustion processes NO_x emissions mainly result from the fuel-N, while their formation from the combustion air (prompt and thermal NO_x formation) play only a minor role. Ash melting on grates can cause operational problems and can lead to unexpected plant shutdowns. It is a generally known fact that Ca and Mg increase, whereas Si in combination with K decreases the ash melting temperature [58, 59, 60]. On consideration of low melting phases for P [61], e.g. KPO₃, a further element can be identified which leads to low ash melting temperatures.

4.1.1 Fuel indexes defined

Fuel indexes are calculated on the basis of results of fuel analyses. They are defined by considering the physical behaviour and chemical reactions of dedicated elements during biomass combustion, known interactions of different ash-forming elements during thermal biomass conversion, and correlations and experience gained from pilot and real-scale combustion as well as lab-scale combustion tests for a broad spectrum of biomass fuels.

A quick estimation of combustion-related problems is possible, but the boundary conditions for the application of these indexes have to be considered. Since the data for the definition of a fuel index in this work are based on test runs in fixed-bed lab-, pilot- and real-scale combustion systems, the indexes derived in this work (especially **Paper I**) are applicable to grate combustion plants only. The indexes are calculated on the basis of results of chemical analysis and therefore, special effort has been taken with regard to fuel sampling. A representative fuel sample without contaminations (e.g. sand, stones) is essential for a proper fuel index evaluation.

Based on the evaluation of the fuel analysis and test runs as well as on a theoretical evaluation, the following fuel indexes were investigated (**Paper I and Paper II**):

- N-concentration in the fuel as an indicator of NO_x emissions.
- Sum of K, Na, Zn and Pb as an indicator regarding aerosol emissions (fine particles smaller 1 µm) and deposit build-up.
- Molar Si/K ratio for an estimation of the K release from the fuel to the gas phase.
- The molar 2S/Cl ratio for the prediction of the risk of high-temperature corrosion.
- Molar (K+ Na)/[x*(2S+Cl)] ratio for the prediction of the gaseous emissions of SO_x and HCl.

- The prediction of the ash melting temperatures with the molar $\text{Si}/(\text{Ca}+\text{Mg})$, the molar $(\text{Si}+\text{K}+\text{P})/(\text{Ca}+\text{Mg})$ ratio as well as the molar $(\text{Si}+\text{K}+\text{P})/(\text{Ca}+\text{Mg}+\text{Al})$ ratio

4.1.2 N-concentration in the fuel as an indicator of NO_x emissions

As mentioned in section 1.4, the N-content of the fuel can cause increased NO_x emissions, which is taken into consideration in the fuel index.

To correlate the fuel N-concentration with NO_x emissions (see Figure 4), the results of test runs at modern state-of-the-art grate combustion plants equipped with air staging technology were used. Therefore, the correlation is only valid for state-of-the-art grate-fired combustion units with air staging technology.

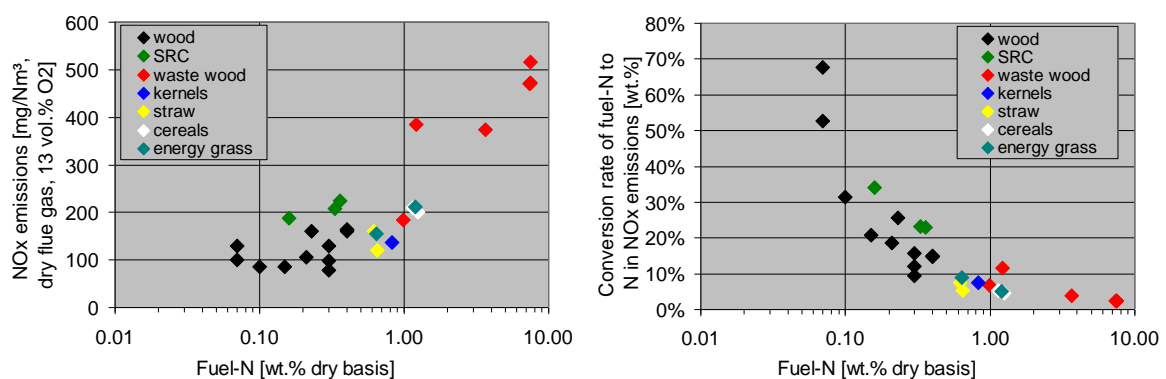


Figure 4: NO_x emissions and fuel-N converted to N in NO_x dependent on the N content

Explanation: Both correlations are statistically significant ($p < 0.05$)

NO_x emissions increase with the N-content of the fuel (see Figure 4). No linear correlation exists since with increasing N-content of the fuel the conversion of fuel-N to NO_x decreases (see Figure 4).

The index is applicable to fuel mixtures. Only the N content of the mixture changes and the conversion of fuel-N to NO_x is similar to that of a pure biomass fuel. Such behaviour has been observed for the fuel blends investigated in **Paper III**. The application of additives usually also does not influence NO_x emissions, provided the additive contains no N and the conversion from fuel N to N in NO_x is not influenced.

4.1.3 The molar 2S/Cl ratio for the prediction of the risk of high-temperature corrosion

A comprehensive study [54] has shown that with rising Cl concentrations in tube-near deposit layers an increased risk regarding high-temperature chlorine corrosion prevails. Moreover, it has been observed (see Figure 5) that there is a correlation between the 2S/Cl ratio in the fuel and in fine particulate matter emissions, which are mainly responsible for S- and Cl-rich deposit build-up. Guiding values to predict high-temperature corrosion risk, using the molar 2S/Cl ratios of the fuel, have been presented [54]. A high corrosion risk for values < 1 prevails, minor corrosion risks have to be expected for values > 4 , and for values over 8 negligible Cl levels in the boiler deposits can be achieved which eliminate corrosion from this source.

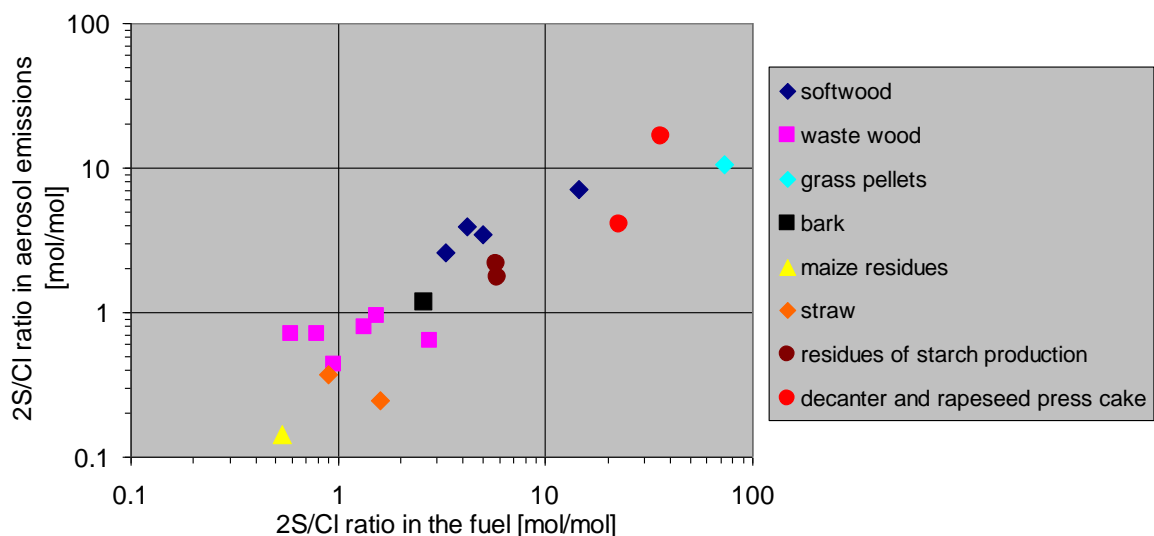


Figure 5: Dependence of the molar ratios of 2S/Cl in fuels versus aerosol particles

Explanation: The correlation is statistically significant ($p < 0.05$)

According to Figure 5, Cl concentrations in aerosols increase with decreasing 2S/Cl ratios in the fuel, while sulphate concentrations decrease. For 2S/Cl ratios in the fuel < 2 , even a Cl surplus in aerosols prevails, indicating that severe corrosion risks have to be taken into account. Accordingly, corrosion risks increase from bark over waste wood and straw to maize residues.

The index is applicable to fuel mixtures, since the release behaviour of S and Cl is not influenced by the mixing of pure fuels. This index is not directly applicable to the application of biomass additive mixtures. Additives can influence the S and Cl release behaviour and may also lead to increased SO_x and HCl concentrations in the flue gas which have to be considered.

4.1.4 Sum of K, Na, Zn and Pb as an indicator regarding aerosol emissions (fine particles smaller $1 \mu\text{m}$) and deposit build-up

As mentioned in the introduction to this section, the elements S, Cl, K, Na, Zn and Pb are partly released from the fuel to the gas phase, and they are mainly responsible for aerosol formation. It was also noticed that high K concentrations prevail in most biomass fuels and the K release from the fuel to the gas phase is of relevance to aerosol emissions. Since the K release strongly depends on the ash chemistry and varies for different biomass assortments, the application of this index has to be handled with care.

As presented in Figure 6, the sum of K, Na, Zn and Pb in the fuel can be applied as an indicator regarding the potential for PM_{10} emissions. The fuel and PM_{10} emission data presented are taken from a considerable number of pilot- and real-scale test runs at grate-fired combustion plants with nominal thermal boiler capacities between 0.5 and 110 MW. Additionally, data of estimated aerosol emissions for pure spruce softwood and straw and mixtures of straw with kaolin, pure Miscanthus, peat and different Miscanthus peat blends were added. These aerosol emissions were calculated on the basis of the

determined release ratios of K, Na, Zn and Pb with fixed-bed lab-scale reactor experiments. The aerosol forming elements K, Na, Zn and P were considered as K_2SO_4 , KCl, Na_2SO_4 , NaCl and ZnO. These estimations do not consider particle losses caused by condensation of ash-forming vapours on walls and deposit formation in the furnace and the boiler sections, particle losses caused by reactions of ash-forming vapours with coarse fly ash particles or condensation on coarse fly ash particles as well as gaseous emissions of S (i.e. SO_x) and Cl (i.e. HCl). More detailed information regarding the estimation of aerosol emissions can be found in section 4.3.1.

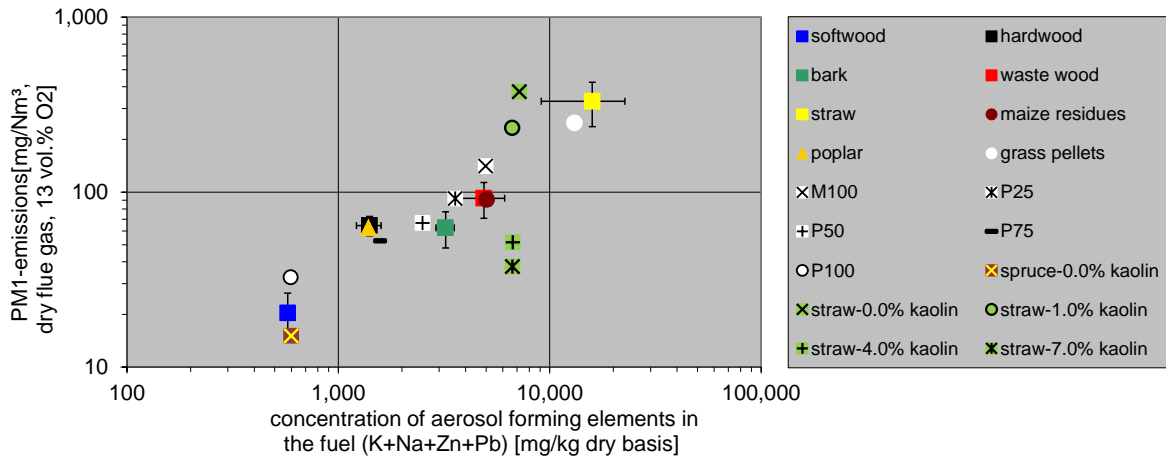


Figure 6: PM_{10} emissions in the flue gas downstream the boiler, and estimated aerosol emissions for pure spruce and straw, spruce/kaolin, straw/kaolin, pure Miscanthus and peat as well as for the blends versus concentrations of aerosol forming elements in the fuel

Explanations: Data for softwood, hardwood, bark and straw taken from [12]; M100 ... pure Miscanthus, P100 ... pure peat, P25 – P75 ... Miscanthus peat mixtures according to **Paper III**; The correlation is statistically significant ($p < 0.05$) if the straw kaolin mixtures are not considered

Aerosol emissions rise with higher values of the sum of K, Na, Zn and Pb in the fuel. (see Figure 6). Based on the data, direct applicability of the index to pure biomass fuels as well as to mixtures of biomass fuels can be deduced. It can also be seen in the case of straw/kaolin mixtures that the index is not applicable. Aerosol emissions decrease with kaolin addition, with the sum of K, Na, Zn and Pb remaining constant. A similar trend has been determined for softwood/kaolin mixtures, with the aerosol emissions for the softwood/kaolin mixtures not displayed in the diagram to ensure proper readability.

Since increasing aerosol emissions are usually associated with increased deposit formation on heat exchanger tubes (due to the fact that aerosol formation is always accompanied by direct condensation of ash vapours on cold heat exchanger surfaces), also deposit build-up usually increases with increased values of this index.

4.1.5 Molar Si/K ratio for an estimation of the K release from the fuel to the gas phase

A high molar Si/K ratio generally leads to the formation of potassium silicates, [30, 62, 63] which are bound in the bottom ash. Therefore, the K release is reduced, which is of relevance since, for instance, aerosol formation strongly depends on the amount of K released from the fuel. Moreover, if less K is available in the gas phase for reactions with S and Cl, the gaseous SO_x and HCl emissions may increase.

In Figure 7 data regarding the correlation between the molar Si/K ratio and K release, gained from lab-scale test runs, are presented.

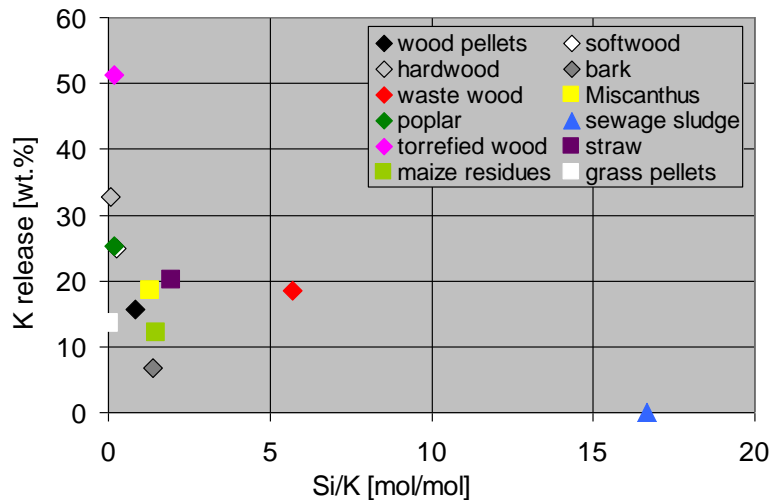


Figure 7: Molar Si/K ratio versus K release for different biomass fuels

Explanations: No statistically significance

For very high Si/K ratios, a good embedding of K in the bottom ash and consequently a very low K release prevails (see Figure 7). However, for low Si/K ratios (<2.5) no clear conclusion can be drawn concerning the dependency of the K release on the Si/K ratio.

Also other elements, such as P, may influence the K release. P is able to bind K in the residual ash as potassium phosphates [64]. The formation of melted K-P-phases can also be explained with the ternary phase diagrams $\text{CaO-K}_2\text{O-P}_2\text{O}_5$ and $\text{MgO-K}_2\text{O-P}_2\text{O}_5$ [61]. From these phase diagrams, possible low melting molecules e.g. KPO_3 can be determined. Also Ca and Mg may influence the K release. A possible explanation for this behaviour is that Ca primarily binds Si as calcium silicates, and not as potassium calcium silicates, therefore Ca may increase the K release as well [65].

Since K release strongly depends on various parameters, an accurate prediction is not possible at the moment. Therefore, an experimental determination of the K release for biomass fuels which have not been investigated so far is necessary.

4.1.6 Molar $(K+Na)/[x*(2S+Cl)]$ ratio for the prediction of the gaseous emissions of SO_x and HCl.

This index can be used to predict the gaseous SO_x and HCl emissions. As can be seen from **Paper I**, S and Cl show almost constant release ratios of 80% to 90% or >90% for biomass fuels. During combustion, S and Cl preferably form alkaline (K and Na) sulphates and chlorides. S also forms Ca and Mg sulphate, and to a smaller extent Ca and Mg chlorides can be formed. Cl and S, which are not bound by these elements to the solid phase, form gaseous emissions, namely HCl and SO_x . Due to the fact that in biomass fuels usually the K concentration is much higher than the Na concentration, the K release to the gas phase is of great relevance to the reaction schemes explained above.

The factor x in the molar $(K+Na)/[x*(2S+Cl)]$ ratio describes the average release rates of K and Na in relation to the average release rates of S and Cl. When considering the reaction schemes mentioned above, this index can be defined in order to predict the potential for SO_x and HCl emissions associated with the combustion of a specific fuel.

A molar ratio $(K+Na)/[x*(2S+Cl)] >1$ indicates a surplus of released alkaline metals. Therefore, for a value clearly >1, very low HCl and SO_x emissions are to be expected, since most of the S and Cl will be bound in the ash. If the value of the index is clearly <1, elevated HCl and SO_x emissions are to be expected.

Based on the results of pilot- real- and lab-scale combustion tests with different biomass fuels, the K release ratios from the fuel to the gas phase were calculated. For a broad variety of biomass fuels, K release and respective values for the factor x are summarised in Table 3. An averaged release of S and Cl (90 wt.%) is divided by the average K release to obtain the factor x. These values can be used for the calculation of the index $(K+Na)/[x*(2S+Cl)]$.

Table 3: Experimentally determined K release rates for different biomass fuels as well as resulting factors x

	average value K [wt.%]	standard deviation K [wt.%]	factor x [-]
hardwood chips	32.8	12.0	2.7
softwood chips	24.9	8.1	3.6
waste wood	18.5	3.2	4.9
bark	6.8	1.3	13.2
Arundo Donax	18.5	4.6	4.9
straw	20.1	2.6	4.5
maize residues	12.1	1.7	7.4
grass pellets	13.5	1.3	6.7
decanter and rapeseed press cake	8.6	1.6	10.5
residues of starch production	10.8	2.5	8.4

Figure 8 shows the correlation of the molar $(K+Na)/[x*(2S+Cl)]$ ratio versus SO_x emissions and the conversion of fuel-S to S in SO_x .

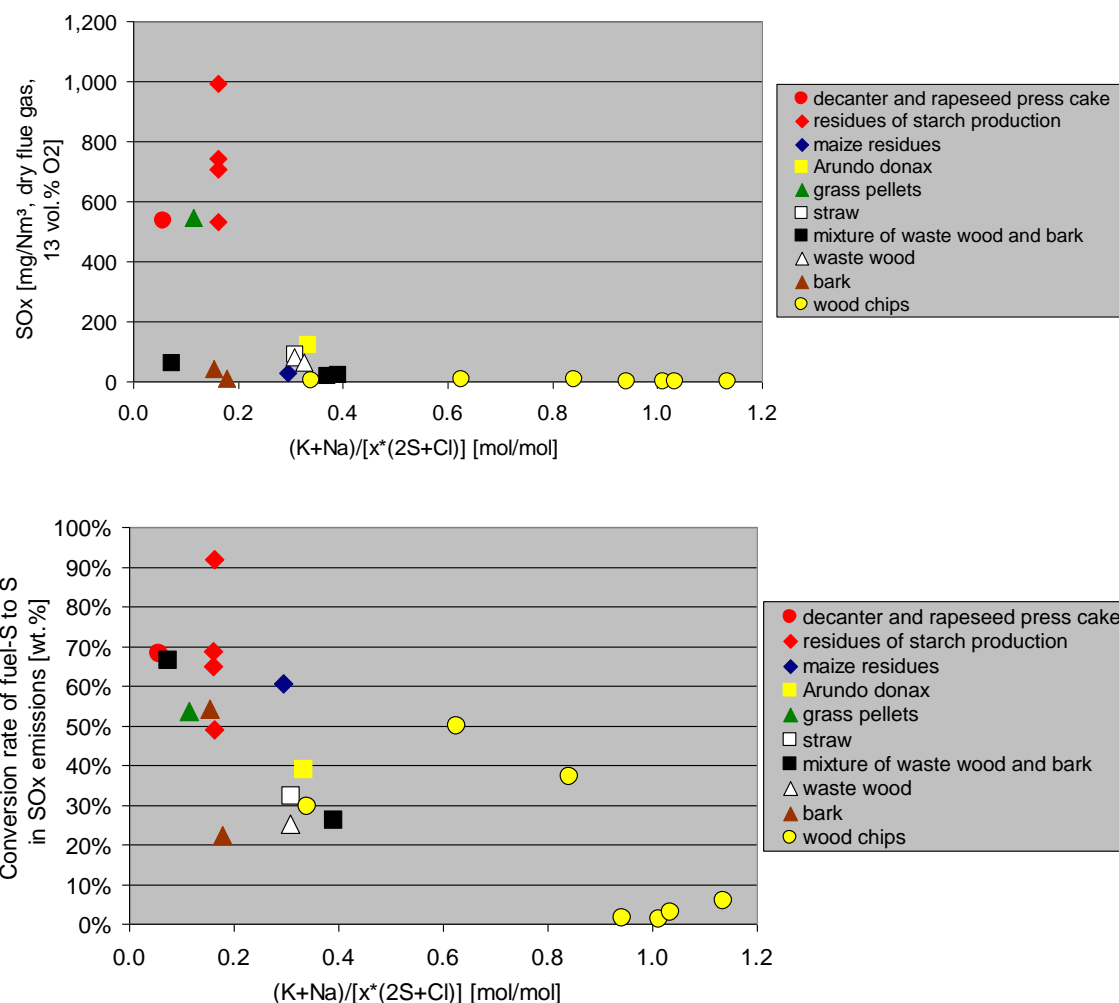


Figure 8: Molar $(K+Na)/[x^*(2S+Cl)]$ ratio versus SO_x emissions and the conversion of fuel-S to SO_x

Explanations: Both correlations are statistically significant ($p < 0.05$)

From Figure 8 it can be seen that with a decreasing molar $(K+Na)/[x^*(2S+Cl)]$ ratio SO_x emissions are increasing. In the second diagram of Figure 8, the molar $(K+Na)/[x^*(2S+Cl)]$ ratio is plotted against the conversion of fuel-S to S in SO_x . The same trend can be observed with regard to the molar $(K+Na)/[x^*(2S+Cl)]$ ratio and the conversion of fuel-S to SO_x . Hence, SO_x emissions are negligible for a fuel molar $(K+Na)/[x^*(2S+Cl)]$ ratio higher than, or close to, 0.5. Therefore, this index is suitable for estimating the SO_x emission range to be expected.

Figure 9 shows the correlation between the molar $(K+Na)/[x^*(2S+Cl)]$ ratio and HCl emissions and the conversion of fuel-Cl to Cl in HCl.

No clear correlation between the molar $(K+Na)/[x^*(2S+Cl)]$ ratio and the HCl emissions can be seen. For a molar ratio of $(K+Na)/[x^*(2S+Cl)] < 0.5$, HCl emissions vary from 0 – 110 mg/Nm^3 dry flue gas at 13 vol.% O_2 . The reason for this strong scattering in comparison with S is not yet understood; further investigations are needed. In our case, it can be seen from Figure 9 that with a molar ratio of $(K+Na)/[x^*(2S+Cl)]$ higher, or close to, 0.5 the HCl

emissions are very low. Therefore, this index can also be used to make a first estimation of the gaseous HCl emissions to be expected.

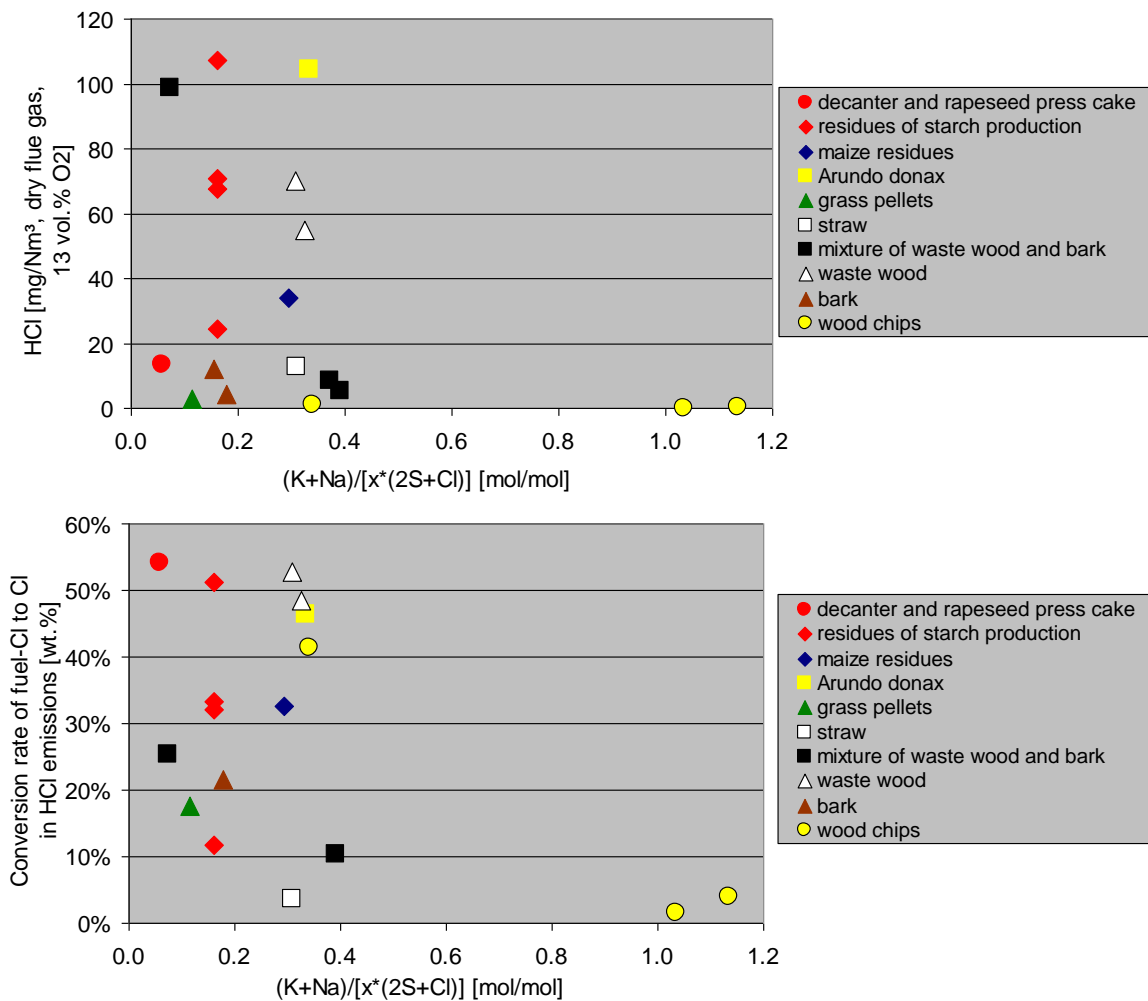


Figure 9: Molar $(K+Na)/[x*(2S+Cl)]$ ratio versus HCl emissions and the conversion of fuel-Cl to HCl

Explanations: both correlations are statistically not significant

When the index was defined, low SO_x and HCl emissions were expected for values lower than 1. Figure 8 and Figure 9 clearly show that SO_x and HCl emissions are negligible for fuels with a molar $(K+Na)/[x*(2S+Cl)]$ ratio higher than 0.5. It seems that Cl and S compounds are also bound to Ca and Mg, which also decrease SO_x and HCl emissions.

4.1.7 The prediction of the ash melting temperatures with the molar $Si/(Ca+Mg)$, the molar $(Si+K+P)/(Ca+Mg)$ as well as the molar $(Si+K+P)/(Ca+Mg+Al)$ ratio

It has already been mentioned in section 4.1 that the elements Ca and Mg increase, whereas Si, K and P decrease, the ash melting temperatures. The molar $Si/(Ca+Mg)$ ratio can therefore provide first information about ash melting tendencies in ash systems dominated by Si, Ca, Mg and K. However, for P-rich systems, this correlation is not valid.

In **Paper I**, a linear increase of the ash melting temperature with a decreasing molar $\text{Si}/(\text{Ca}+\text{Mg})$ ratio is reported, which is not valid for P-rich fuels (e.g. grass pellets).

Taking into consideration all elements showing a potential for decreasing the ash melting temperatures, an index for pure fuels and fuel mixtures $(\text{Si}+\text{P}+\text{K})/(\text{Ca}+\text{Mg})$ can be derived.

Biomass fuels usually contain low amounts of Al; therefore Al has not been considered for the indexes predicting ash melting tendencies. For biomass/kaolin mixtures, Al concentrations are significantly higher compared to untreated biomass fuels. From the ternary phase diagram [66] for $\text{CaO}-\text{SiO}_2-\text{Al}_2\text{O}_3$, melting temperatures higher than $1,300^\circ\text{C}$ can be determined. For the $\text{K}_2\text{O}-\text{SiO}_2-\text{Al}_2\text{O}_3$ system [66] it can be specified that for pure $\text{K}_2\text{O}-\text{SiO}_2$ phases for SiO_2 concentrations $<80\text{wt.}\%$ low melting temperatures prevail ($\sim 800^\circ\text{C}$). With increasing Al_2O_3 concentrations, the melting temperatures rise, and at an Al_2O_3 concentration $>20\text{ wt.}\%$ melting temperatures higher than $1,300^\circ\text{C}$ are reached. It can be concluded that melting temperatures increase with increasing Al_2O_3 concentrations. Thus, Al was also considered in the fuel index applied for ash melting evaluations, and the molar $(\text{Si}+\text{P}+\text{K})/(\text{Ca}+\text{Mg}+\text{Al})$ ratio was used.

To show the applicability of this fuel index, the data for pure biomass fuels (**Paper I**), biomass kaolin mixtures (**Paper II**) and for biomass mixtures (Miscanthus peat blends **Paper III**) are summarised in Figure 10.

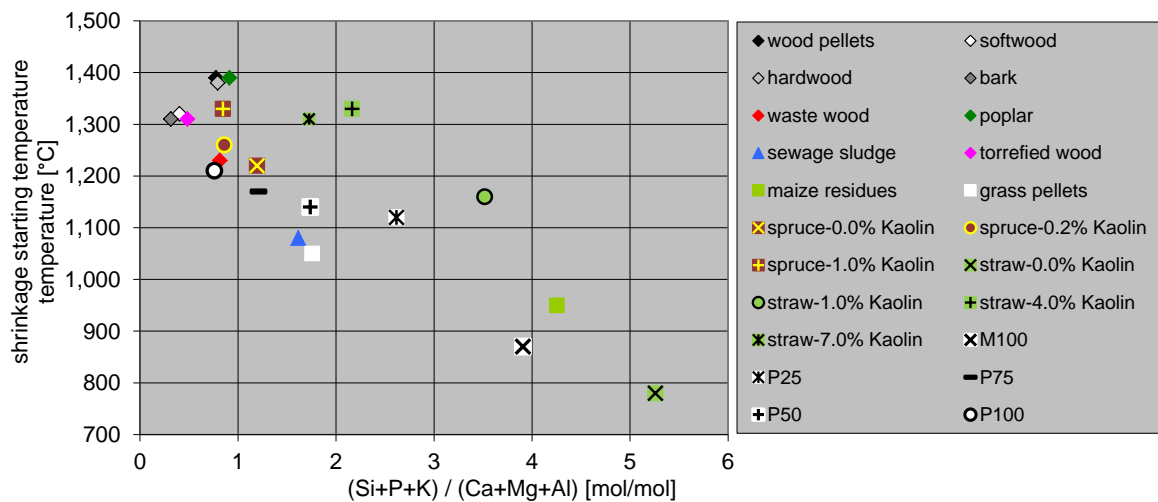


Figure 10: Molar $(\text{Si}+\text{P}+\text{K})/(\text{Ca}+\text{Mg})$ ratio versus shrinkage starting temperature for pure biomass fuels, spruce/kaolin mixtures, straw/kaolin mixtures and Miscanthus peat blends *Explanations:* shrinkage starting temperature according to standard ash melting test (CEN/TS 15370-1); M100 ... pure Miscanthus, P100 ... pure peat, P25 – P75 ... Miscanthus peat mixtures according to **Paper III**. The correlation is statistically significant ($p < 0.05$)

There is an almost linear correlation between the molar $(\text{Si}+\text{P}+\text{K})/(\text{Ca}+\text{Mg}+\text{Al})$ ratio and the SSTs for the fuels investigated. It can also be seen that with increasing kaolin addition the ash melting temperatures increase for straw and spruce. The SST of pure straw was determined at 780°C . With increasing kaolin addition the SSTs increase and show a maximum value ($1,330^\circ\text{C}$) for a kaolin addition ratio of 4 wt.%. As was to be expected from the low values of the molar $(\text{Si}+\text{P}+\text{K})/(\text{Ca}+\text{Mg}+\text{Al})$ ratios for spruce and the

spruce/kaolin mixtures, the SSTs for these mixtures are on a high level. For pure spruce, the SST exceeds 1,200°C. Kaolin addition to spruce further raises the SSTs, and for a kaolin addition of 3 wt.% a SST >1,480°C has been determined. In the case of the Miscanthus peat blends, an index of 3.9 for M100 indicates a very low SST. With increasing amount of peat the index decreases and the SST rises.

4.1.8 Summary of the pre-evaluation of combustion properties based on fuel indexes

The application of fuel indexes provides a good basis for a quick pre-evaluation of combustion-related problems that may arise. This approach can therefore be applied to support decision-making concerning the application of non-wood feedstocks (herbaceous biomass and agricultural residues) or fuel blends in existing combustion plants as well as the preliminary design and engineering of new combustion plants.

Among the fuel indexes which allow accurate qualitative predictions are N-content, the molar 2S/Cl ratio and the molar ratio of (Si+P+K)/(Ca+Mg+Al). The N-content of the fuel determines the potential for NO_x emission formation. The molar 2S/Cl ratio gives a first indication regarding high-temperature corrosion risk. Indications of the ash melting tendency can be gained from the molar (Si+P+K)/(Ca+Mg+Al), which is also applicable to biomass/kaolin mixtures.

Indexes which can be applied with some restrictions regarding other constraints: the sum of K, Na, Zn and Pb, the molar ratios of (K+Na)/[x*(2S+Cl)], Si/(Ca+Mg) as well as (Si+P+K)/(Ca+Mg). The sum of K, Na, Zn and Pb (as an indicator of aerosol emissions) and the molar ratio of (K+Na)/[x*(2S+Cl)] (indicator of SO_x and HCl emissions) strongly depend on the K released to the gas phase, which crucially depends on the ash chemistry and varies with different biomass assortments as well as with additive application. Therefore, the application of these indexes has to be handled with care. For the indexes of the molar Si/(Ca+Mg) and (Si+P+K)/(Ca+Mg) ratio, which can give an indication of the ash melting tendency, applicability has to be checked. Both indexes are applicable to chemically untreated biomass fuels without the supplement of an additive. The molar Si/(Ca+Mg) can be applied to systems dominated by Si, Ca, Mg and K, with the molar (Si+P+K)/(Ca+Mg) ratio also being valid for P-rich systems.

4.2 Prediction of the ash melting and release behaviour of different wood/kaolin and straw/kaolin mixtures as well as Miscanthus peat blends by TEC - Paper II and Paper III

General information about the fuels and the fuel additive mixtures as well as the fuel blends used in the investigations is provided in section 3.1. TEC were used to determine the trend regarding ash melting and release behaviour of inorganic elements. For validation of the TEC predictions, the experimental ash melting temperatures in accordance with CEN/TS 15370-1 were determined. The determination of the release ratios of inorganic elements was done by fixed-bed lab-scale reactor experiments.

4.2.1 Evaluation of the ash melting behaviour predicted by TEC in comparison to experimental results

The ash melting behaviour was investigated by means of the standard ash melting test (CEN/TS 15370-1) and TEC. Based on TEC, the amount of molten fractions can be calculated, whereby T_{30} is defined as the temperature at which 30 wt.% liquid phases occur. Previous work [49] has shown that this temperature is an appropriate indicator of the shrinkage starting temperature (SST) (in accordance with CEN/TS 15370-1).

The ash melting index (molar $(\text{Si}+\text{P}+\text{K})/(\text{Ca}+\text{Mg}+\text{Al})$ ratio) has already been discussed in section 4.1.7. In Figure 11, the molar $(\text{Si}+\text{P}+\text{K})/(\text{Ca}+\text{Mg}+\text{Al})$ ratio is plotted versus the SST for biomass/kaolin mixtures. In addition, also the results from TEC are displayed in the same diagram.

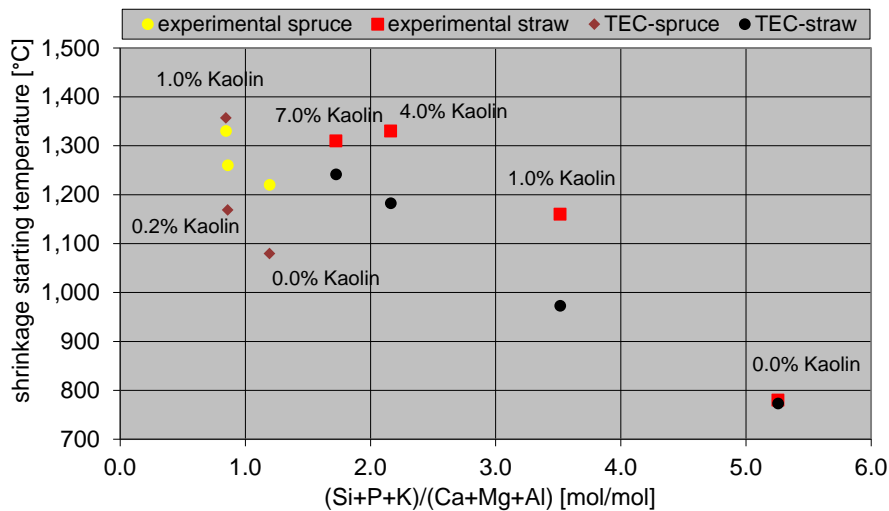


Figure 11: Molar $(\text{Si}+\text{P}+\text{K})/(\text{Ca}+\text{Mg}+\text{Al})$ ratio versus shrinkage starting temperature for pure spruce and spruce/kaolin mixtures as well as for pure straw and straw/kaolin mixtures in comparison with the results gained from thermodynamic equilibrium calculations

Explanations: experimental ... shrinkage starting temperature according to the standard ash-melting test (CEN/TS 15370-1); TEC ... thermodynamic equilibrium calculations (temperature at which 30 wt.% liquid phase occurs)

For straw as well as for spruce, TEC predict lower ash SSTs compared to the experimental data, with the exception of spruce with 1 wt.% kaolin. The differences decrease with rising kaolin content. Quantitative differences can most probably be explained by the fact that TEC were developed for pure biomass fuels. Especially for pure straw, there is close agreement between TEC and the experimental determination, with differences for the straw/kaolin mixtures occurring. Although quantitative differences between TEC and the experimentally determined melting temperature exist, TEC can predict the melting temperature qualitatively. In addition, possible ash transformation processes can be derived, based on TEC.

For pure straw, it can be demonstrated by TEC that a significant transformation of solid K-Si-phases into slags at temperatures above 750°C takes place. With increasing temperatures, the amount of molten slag phases rises. In cases of kaolin addition, mainly solid K-Al-Si phases are formed, which remain almost stable up to calculation temperatures of 1,600°C. For kaolin addition, no distinct phase can be identified which is clearly transformed to liquid phases since many solid phases are gradually transformed to slags. For pure softwood, TEC indicate an enhanced amount of solid Ca-Mg-Si and Ca-Si phases which are transformed into slags at temperatures above 1,050°C. For softwood with 0.2 wt.% kaolin, solid Ca-Mg-Si, Ca-Al-Si and K-Al-Si phases are transformed into slags at temperatures above 1,150°C. Higher amounts of kaolin (1 and 3 wt.%) form solid Ca-Al-Si phases which remain in the solid phase up to temperatures of 1,200°C, which are gradually transformed into liquid slags at higher temperatures.

For both fuels and kaolin mixtures, the phases mainly responsible for slag formation can be identified. Furthermore, the temperature at which a significant ash transformation of solid phases into liquid slags takes place, can be revealed by TEC.

In Figure 12, by comparison, the SST and the T_{30} values (temperature where 30 wt.% liquid phase occurs) are plotted against the molar $(\text{Si}+\text{P}+\text{K})/(\text{Ca}+\text{Mg}+\text{Al})$ ratio for the Miscanthus peat blends as well as for pure fuels.

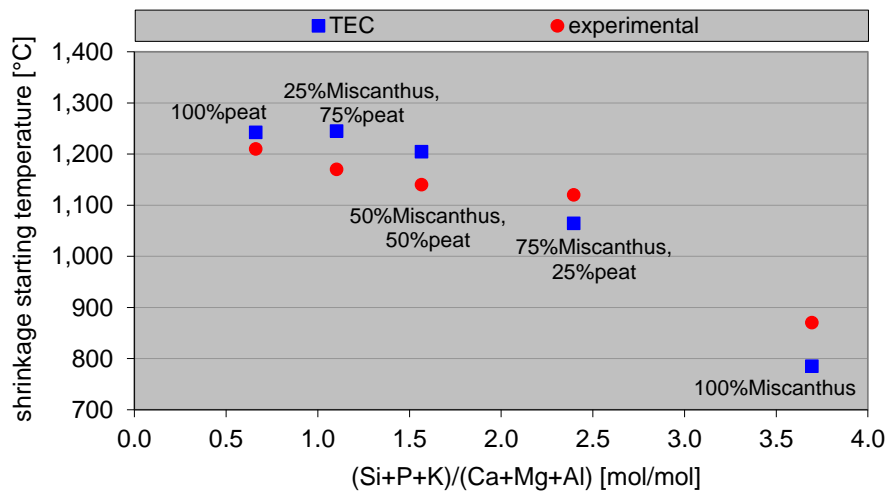


Figure 12: Molar $(\text{Si}+\text{P}+\text{K})/(\text{Ca}+\text{Mg}+\text{Al})$ ratio versus shrinkage starting temperature for pure Miscanthus, peat, as well as for blends in comparison with thermodynamic equilibrium calculations

Explanations: experimental ... shrinkage starting temperature according to standard ash melting test (CEN/TS 15370-1); TEC ... results of thermodynamic equilibrium calculations (temperature where 30 wt.% liquid phase occur)

The results of the experimentally determined SST and TEC largely agree. The trend of the melting temperature for the fuels and the mixtures is well predicted by TEC, with only slight quantitative differences between the experimental results and TEC.

Detailed evaluation of TEC for Miscanthus reveals behaviour similar to that of pure straw. For temperatures above 750°C, a clear transformation of solid K-Si phases into slags can be identified. For the Miscanthus peat blends a solid K-Al-Si phase can be identified, which remains stable throughout the temperature range investigated. For P75 and P100, solid Ca-Mg-Si phases can be identified, which are transformed into slags at temperatures above 1,200°C. Thus, possible ash transformations which are responsible for ash melting can be identified by TEC.

4.2.2 Evaluation of TEC in comparison with experimental results regarding the release behaviour of ash-forming elements

TEC were also used to predict the release ratios of inorganic elements. A 2-step approach (see section 2.2) was applied to simulate the devolatilisation and the charcoal combustion phases. The determined release ratios of inorganic elements by fixed-bed lab-scale reactor experiments were used for validation. As already mentioned, the release behaviour is essential for aerosol, SO_x and HCl emissions (see section 4.1.6).

In Figure 13, the experimentally determined inorganic element release ratios from the fuel to the gas phase from fixed-bed lab-scale reactor experiments in comparison with results from TEC for pure spruce and spruce/kaolin mixtures are presented.

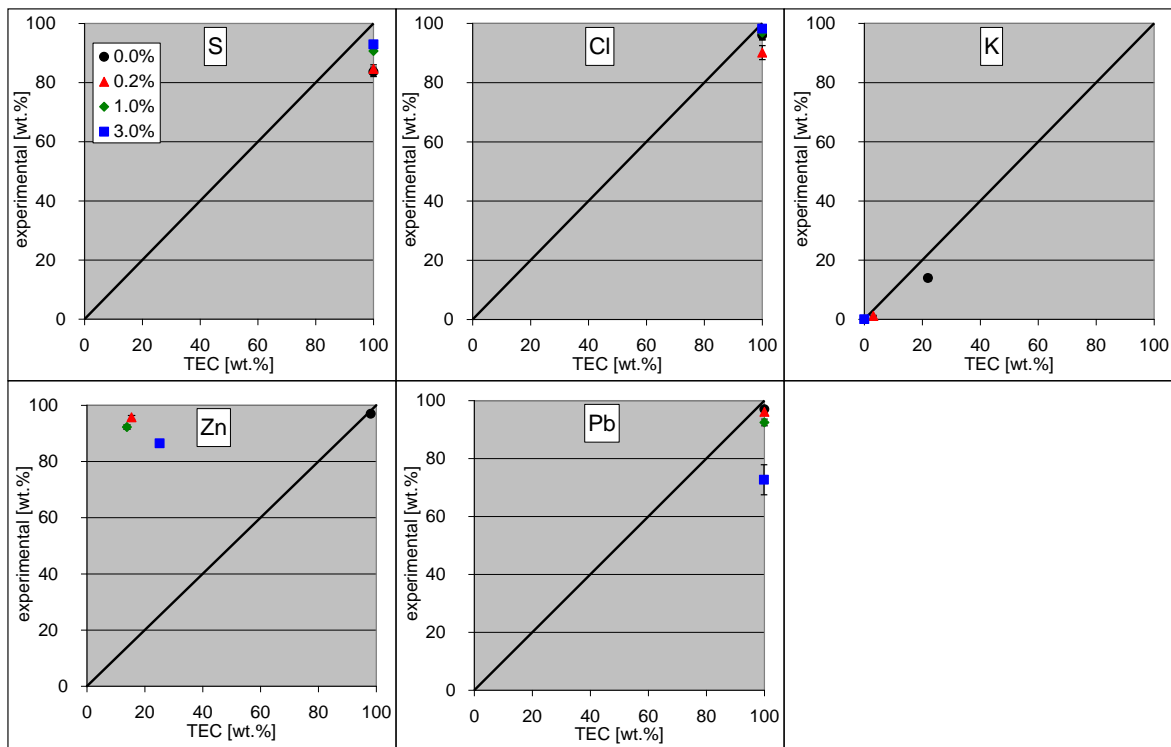


Figure 13: Experimentally determined element release from the fuel to the gas phase from fixed-bed lab-scale reactor experiments in comparison with thermodynamic equilibrium calculations for pure spruce and spruce/kaolin mixtures

Explanation: TEC ... thermodynamic equilibrium calculations (TEC release estimated at 1,250°C)

From Figure 13 it can be deduced that TEC point to slightly higher S, Cl and Pb release ratios compared to the experimentally determined release. A complete release of these elements is predicted from TEC, whereas from fixed-bed lab-scale reactor experiments, release ratios of 84–93 wt.% for S, of 90–98 wt.% for Cl and of 73–97 wt.% for Pb were determined. In **Paper I**, release ratios for spruce wood chips were determined for S of 82 wt.%, and for Cl of 99 wt.%. It can be concluded that the addition of kaolin does not influence the release ratios of S and Cl to the gas phase. The low Pb release for the 3 wt.% kaolin ratio might be explained with the low concentrations in the fuel sample (close to the detection limit), which increases the unreliability of results. For the remaining fuels, the Pb released from the fuel to the gas phase is on an almost constant level and thus it can be stated that the addition of kaolin does not appear to influence Pb release.

Concerning K, it can be seen that, with increasing kaolin addition ratio, K release to the gas phase decreases. The K release predicted by TEC closely agrees with the release determined by fixed-bed lab-scale reactor experiments.

For Zn, a close agreement between TEC and lab-scale experiments for pure spruce can be observed, whereas for spruce/kaolin mixtures a strong deviation between TEC and the experimental determinations is obvious. For spruce/kaolin mixtures below 700°C, TEC predict the formation of solid zinc aluminate spinel, which is most likely overestimated and leads to a low Zn release during the first calculation step. According to TEC, this spinel is stable for the second calculation step, which results in low overall release ratios. Therefore, TEC-based release predictions for Zn have to be viewed as problematic.

In Figure 14, a comparison between the experimentally determined element release from the fuel to the gas phase from fixed-bed lab-scale reactor experiments and TEC for pure straw and straw/kaolin mixtures is outlined.

From Figure 14, it can be noted that TEC point to S, Cl and Pb release ratios of 100% for pure straw and straw/kaolin mixtures. The experimentally determined release ratios for S (89–95 wt.%), Cl (98–100 wt.%) and Pb (82–92 wt.%) closely agree with the results of TEC.

It can also be concluded that the addition of kaolin has no influence on the release ratios of S, Cl and Pb. Concerning K release, the same trend (as for spruce) of decreasing K-release with increasing kaolin addition can be observed.

The Zn release predicted by TEC for pure straw and straw with 1wt.% kaolin is in close agreement with the experimental evaluation. For higher kaolin addition ratios similar to softwood, an overestimation of solid zinc aluminate spinel leads to low release ratios.

It has to be noted that TEC greatly underestimate the K release in comparison with the fixed-bed lab-scale reactor experiments, especially for straw and for straw with 1 wt.% kaolin addition. For TEC, the results of the wet chemical fuel analyses were used as input data and the calculations were evaluated at the maximum bed temperature occurring during the char combustion phase. The K release during the devolatilisation phase is considered in calculation step 1 of TEC. During fixed-bed lab-scale reactor experiments it is possible for part of K already to be released to the gas phase during the start of the

char combustion phase. This part of K is not available for a possible inclusion in solid K-Al-Si phases. This behaviour is a possible explanation of the over-predicted K release from TEC. In ref. [67] a similar behaviour was found. This study reports an experimentally determined K release of 40.7 wt.% for straw. The test runs were also performed in a lab-reactor [31, 68] and also TEC were performed, with a K release of 28.5 wt.% predicted for a temperature of 1,000°C. This shows that process factors like the temperature gradient inside the particle or a packed bed as well as diffusion most likely influence the K release.

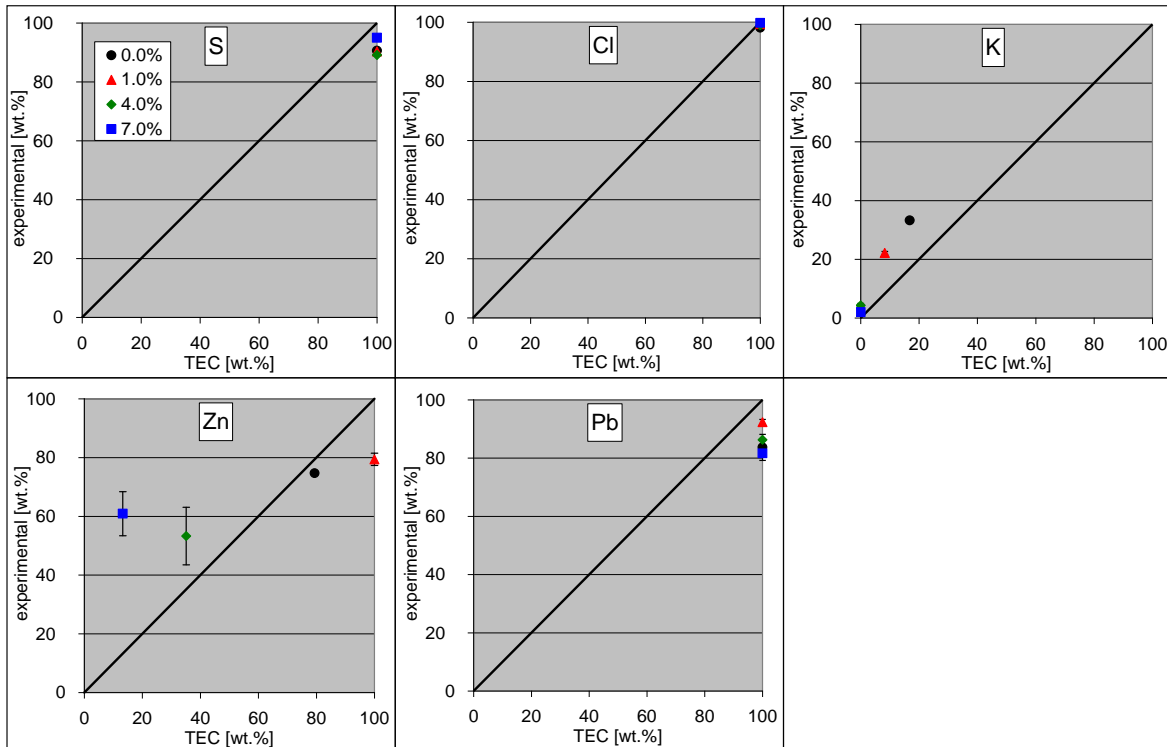


Figure 14: Experimentally determined element release from the fuel to the gas phase from fixed-bed lab-scale reactor experiments in comparison with TEC for pure straw and straw/kaolin mixtures

Explanation: TEC ... thermodynamic equilibrium calculations (TEC release estimated at 1,250°C)

In Figure 15, the experimentally determined inorganic element release ratios from the fuel to the gas phase from fixed-bed lab-scale reactor experiments are compared with results from TEC for Miscanthus peat blends as well as for the pure fuels.

The release behaviour of S and Cl is fairly accurately predicted by TEC (see Figure 15). For S, TEC slightly overestimates the release ratios compared with fixed-bed lab-scale reactor experiments (84-89 wt.%).

K release is the most relevant parameter regarding fine particulate matter emissions as well as deposit build-up. The tendency of increasing K release with increasing peat shares, identified during the fixed-bed lab-scale reactor tests, is also predicted by TEC. TEC underestimate the K release for M100, whereas for P100 TEC overestimate it, with a good agreement for the blends in comparison with experimental results. A detailed evaluation

of TEC showed that almost the complete release takes place during the devolatilisation phase (calculation step 1). Therefore, the evaluation temperature of this step influences the results of the release prediction. Furthermore, it was shown that the gas atmosphere has a strong influence on K release behaviour. In a fuel bed, conditions can switch between reducing and oxidising zones and thus equilibrium might not be reached. This, and the definition of the evaluation temperature in step 1, can be the reason for the quantitative differences observed regarding K release.

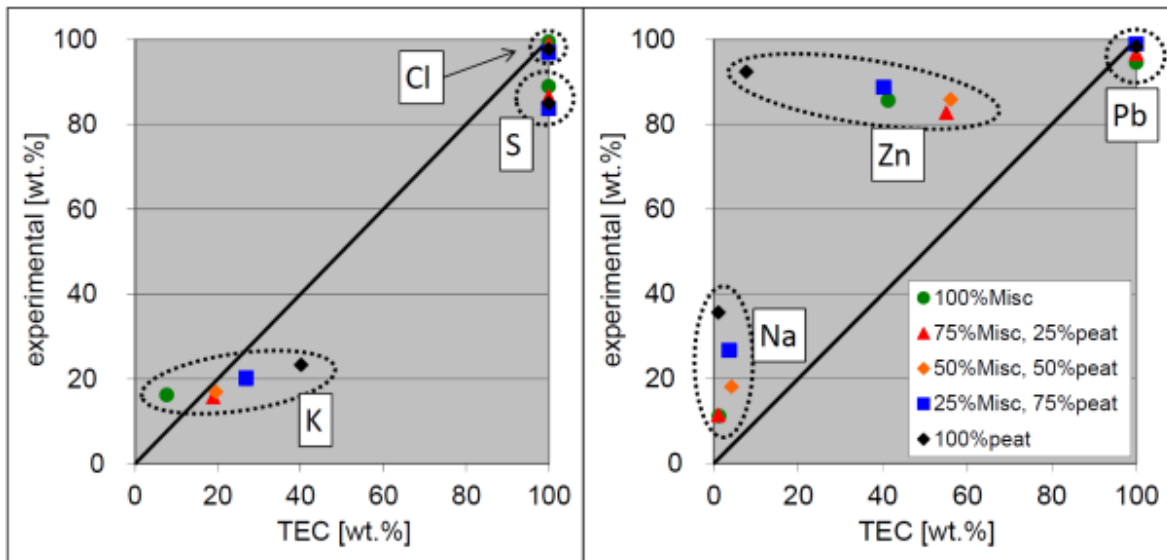


Figure 15: Experimentally determined element release from the fuel to the gas phase from fixed-bed lab-scale reactor experiments in comparison with TEC results for pure Miscanthus and peat as well as blends

Explanation: TEC ... thermodynamic equilibrium calculation, TEC release estimated at 1,250°C

The release prediction for Pb agrees closely with experimental results. For Na and Zn, strong deviations between TEC and experimental results can be observed. While the fixed-bed lab-scale reactor experiments indicate an increased Na release with increasing peat content of the blend, TEC predicts a Na release <5%, which results from an almost complete embedding in solid phases (Na-Ca-Si phases for M100 to P75; Na-Al-Si phases for P100) for calculation step 1 (devolatilisation phase) at 700°C. Also the second calculation step predicts small amounts (<5%) of Na to be stable in the gas phase. Generally, for Na, the formation of solid phases is overestimated by TEC.

For Zn, TEC predict a non-systematic variation of the release between 7–55 wt.% while the experimental results show release ratios of about 80-90 wt.%. Zn shows strongly differing release behaviours under oxidising and reducing conditions. Generally, TEC reveal that the main part of Zn is released during calculation step 1, where reducing conditions prevail. A steep increase of the Zn release can be observed for calculation step 1 in the temperature window between 700°-900°C, whereas the release ratios for the remaining ash-forming elements (S, Cl, K, Na, Pb) stay rather constant. Reducing atmospheres inside char particles, which are not considered by TEC, are most probably

responsible for the high Zn release ratios. Therefore, TEC-based release predictions for Zn have to be viewed as problematic.

4.2.3 Summary of the predictions of the ash melting and release behaviour of different wood/kaolin and straw/kaolin mixtures as well as Miscanthus peat blends by TEC

In sum, TEC are a useful tool to predict the tendency of the ash melting temperatures for the fuel/kaolin mixtures and Miscanthus peat blends evaluated. Especially the influence of kaolin addition and peat addendum is predicted quite accurately, although quantitative differences between the experimental determinations exist. By detailed evaluation of TEC, possible phase transformation processes can be identified which lead to a better understanding of ongoing melting processes.

TEC have proven to be a valuable tool to predict the trend of volatile and semi-volatile element release from the fuel to the gas phase for the fuel/kaolin mixtures and Miscanthus peat blends evaluated, except for Zn. The TEC-based release predictions for Zn have to be viewed as problematic. Furthermore, TEC support the interpretation of the experimentally determined release ratios. For validation of the predicted release ratios by TEC, as well as to gain quantitative values, fixed-bed lab-scale reactor experiments have to be conducted.

4.3 Results of fixed-bed lab-scale reactor experiments performed with different wood/kaolin and straw/kaolin mixtures as well as Miscanthus peat blends – Paper II and Paper III

To gain quantitative data regarding the release behaviour of volatile and semi-volatile ash-forming elements, fixed-bed lab-scale reactor experiments were conducted. The experiments also give a first indication regarding the ash melting potential by means of optical evaluation.

4.3.1 Prediction of aerosol emissions for pure biomass fuels, fuel/kaolin mixtures and Miscanthus peat blends

Based on the release data gained from the fixed-bed lab-scale reactor experiments for pure spruce and spruce/kaolin mixtures as well as for straw and straw/kaolin mixtures, an estimation of the potential for fine particulate emissions can be made. The aerosol forming elements K, Na, Zn and P were considered as K_2SO_4 , KCl, Na_2SO_4 , NaCl, ZnO and P_2O_5 . In addition, the formation of carbonates (K_2CO_3 and Na_2CO_3) is probable if there is not enough S and Cl available in order to completely bind K and Na as chlorides and sulphates. For the calculation, the logarithmic correlation between the 2S/Cl ratio in biomass fuels and the 2S/Cl ratio found in aerosols sampled downstream, the boiler (see Figure 5) was used to estimate the S and Cl distribution in the aerosols. These estimations do not consider particle losses caused by condensation of ash-forming vapours on walls and deposit formation in the furnace and the boiler sections, particle losses caused by reactions of ash-forming vapours with coarse fly ash particles or condensation on coarse fly ash particles as well as gaseous emissions of S (i.e. SO_x) and Cl (i.e. HCl).

The decreasing aerosol emission potential with increasing amounts of kaolin added can clearly be seen in Figure 16. It is also obvious that the main influence on aerosol emissions is indicated by the amount of K released from the fuel to the gas phase. For spruce, already a ratio of 0.2 wt.% kaolin can significantly reduce aerosol emissions. An increase in the kaolin addition ratio to 1 and 3 wt.% leads to a further slight decrease.

Concerning straw, a kaolin addition of 1 wt.% reduces the estimated aerosol emissions from 416 to 264 mg/Nm³. Up to 4 wt.% kaolin addition, a strong decrease in aerosol emissions can be seen; further kaolin addition then produces only minor additional effects.

The results of the determined aerosol emission potential for the biomass kaolin investigations, with the exception of the spruce/kaolin mixtures, were already implemented in Figure 6. It was shown in section 4.1.4 that the index (sum of K, Na, Zn and Pb) cannot be used to predict the aerosol emissions for biomass kaolin mixtures. The sum of the index remains constant for the biomass kaolin mixtures, with aerosol emissions clearly decreasing with kaolin addition (see Figure 6 and Figure 16).

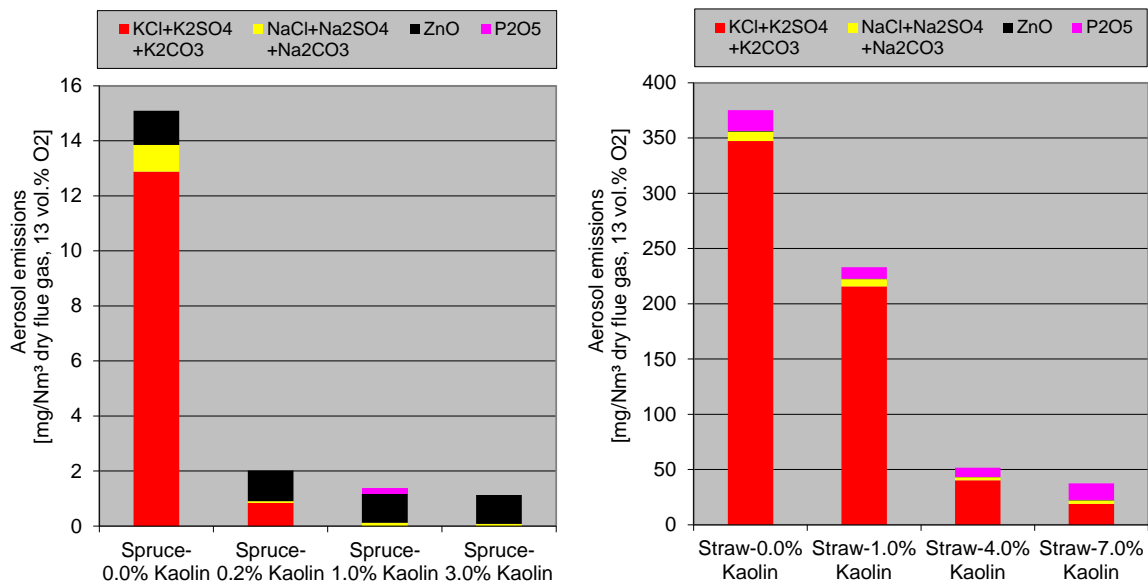


Figure 16: Estimated aerosol emissions for pure spruce and spruce/kaolin mixtures as well as for straw and straw/kaolin mixtures

Also for pure Miscanthus and peat as well as for the blends, the potential for aerosol formation have been estimated, based on the release data gained from the fixed-bed lab-scale reactor experiments. The same approach as for the biomass/kaolin investigations was used to estimate the aerosol emissions.

The results of this evaluation were already implemented in Figure 6, where the fuel index (sum of K, Na, Zn and Pb) vs. the measured aerosol emissions downstream the boiler is discussed. It can clearly be seen (Figure 6) that with an increasing amount of the sum of K, Na, Zn and Pb the estimated aerosol emissions increase. There is close agreement between the sum of K, Na, Zn and Pb and the estimated aerosol emissions based on

release data determined in fixed-bed lab-scale reactor experiments (**Paper III**) and the trend which was determined from pilot- and real-scale combustion tests (**Paper I**). This shows that the determination of the aerosol emissions based on determined release data from fixed-bed lab-scale reactor experiments is meaningful.

4.3.2 Prediction of HCl and SO₂ emissions for pure biomass fuels, fuel/kaolin mixtures and Miscanthus peat blends

Based on the release data, also an estimation of the potential of gaseous SO₂ and HCl emissions can be made. The logarithmic correlation between the 2S/Cl ratio in biomass fuels versus the 2S/Cl ratio found in aerosols (see Figure 5) was used to estimate the S and Cl distribution in the aerosols. With the release data for K, Na, S and Cl and the distribution of S and Cl in the aerosols, the gaseous emissions of SO₂ and HCl can be estimated (S and Cl which are not bound by K and Na). This estimation does not consider particle losses in boilers nor S and Cl bound by Ca and Mg. In Figure 17, the results of the estimation of gaseous SO₂ and HCl are displayed.

In Figure 17, it can be seen that for both fuels SO₂ and HCl emissions increase with increasing kaolin addition. This is due to the fact that with increasing kaolin addition less K is released to the gas phase which is available for binding S and Cl to solid aerosol particles. Low SO₂ and HCl emissions have to be expected for pure spruce and for the spruce/kaolin mixtures. Regarding straw, kaolin addition may lead to problems with emission limits which have to be checked with regard to individual cases.

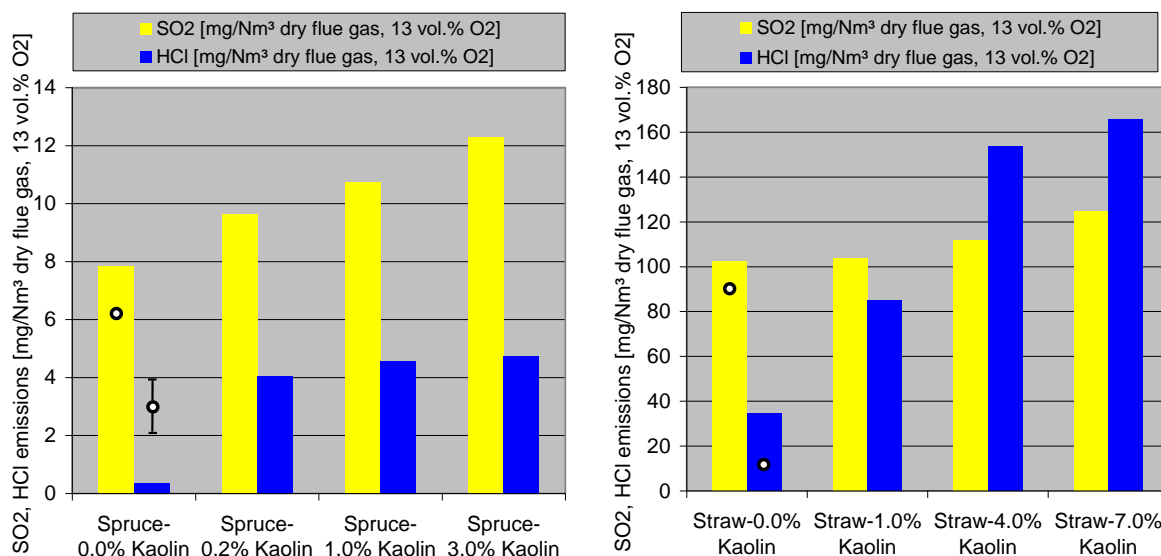


Figure 17: Estimated gaseous SO₂ and HCl emissions for pure spruce and spruce/kaolin mixtures as well as for straw and straw/kaolin mixtures

Explanations: The black dots indicate SO_x as well as HCl emissions of comparable fuels taken from **Paper I** as a basis for a validation of the calculated SO₂ and HCl emissions

Also for the Miscanthus peat blends, the potential of gaseous SO₂ and HCl emissions was established. In Figure 18, results of the estimation of gaseous SO₂ and HCl are displayed.

It can be seen (Figure 18) that SO₂ emissions strongly increase with rising amounts of peat. The explanation lies in the increasing S content and the decreasing K content in the fuel with rising peat shares. HCl emissions slightly increase with increasing amount of peat in the blend and remain almost constant for >P50. This is due to the fact that the Cl concentrations in both fuels are almost the same, but with increasing amounts of peat the K content in the blend decreases. Even if, at the same time, the K release ratio increases, the absolute K release (in mg/kg fuel) decreases. Therefore, less K is available in the gas phase to bind S and Cl, which leads to increased SO₂ and HCl emissions. Consequently, the blending of peat with Miscanthus may lead to strongly increased SO₂ emissions, which has to be considered with regard to emission limits.

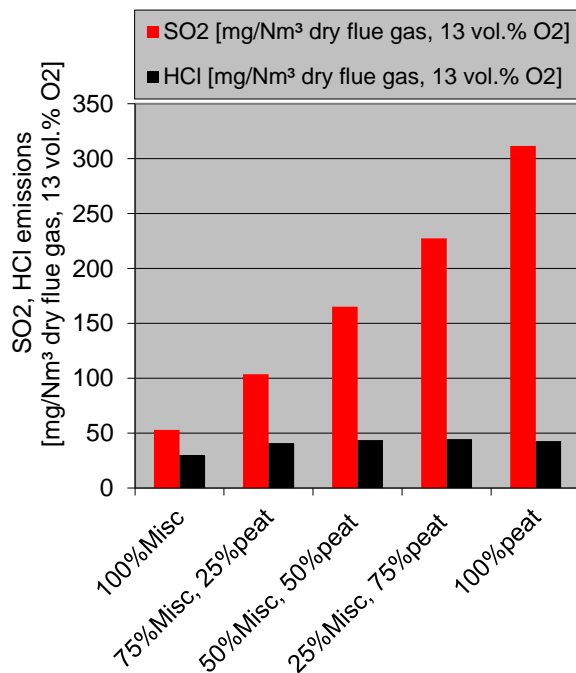


Figure 18: Estimated gaseous SO₂ and HCl emissions for pure Miscanthus and peat as well as for the blends

4.3.3 Optical evaluation of selected ashes after fixed-bed lab-scale reactor experiments

Fixed-bed lab-scale reactor experiments were also used for an optical evaluation of the ash sintering tendencies. Here, the ash sintering tendency is discussed in connection with the tests with pure Miscanthus and peat as well as with the blends. From the residual ashes of tests with M100 and P25 (see Figure 19 middle) slightly sintered ash particles with a brittle structure were obtained, with a decreasing amount of sintered particles compared to M100 observed for P25. This is also in agreement with the SST determined for M100 (870 °C) and for P25 (1,120 °C). For higher amounts of peat, P50 (see Figure 19 right), P75 as well as for P100 loose ash residues were noticed. This optical evaluation shows that the fixed-bed lab-scale reactor experiments can be viewed as a first indication regarding the ash melting tendency.



Figure 19: Photos of the residual ash of M100 (left), P25 (middle) and P50 (right) gained from lab-scale tests

4.3.4 Summary of the results of lab-scale reactor experiments performed with different wood/kaolin and straw/kaolin mixtures as Miscanthus peat blends

The lab-scale reactor experiments were performed to determine the inorganic element release. These data can be used to estimate the aerosol and gaseous SO_x and HCl emissions. The estimated parameters were compared with data obtained from real-scale combustion tests, where a comparable fuel was used. The close agreement indicated that these estimations seem to be meaningful. In addition, fixed-bed lab-scale reactor experiments provide a first indication regarding the ash melting tendency.

4.4 Experimental setup implementation and evaluation for the online determination of S, Cl, K, Na Zn and Pb release from a single particle during biomass combustion – Paper IV

4.4.1 Motivation for the development of the single particle reactor

In the previous sections (4.1- 4.3), the strong influence of the inorganic element release behaviour regarding aerosol, SO_x and HCl emissions was discussed. It was shown that especially K release is of major relevance, which cannot be predicted with sufficient accuracy by means of fuel indexes or TEC. This necessitates an experimental determination by fixed-bed lab-scale reactor experiments. In fixed-bed lab-scale reactor experiments, such as those described in section 2.3, the determination of the inorganic element release is only possible for the entire combustion experiment. Presently, almost no data regarding the time resolved release of ash-forming elements from single particles exist. Such data may provide valuable information regarding different release mechanisms which form a relevant basis for release model development. Furthermore, such data can lead to a better understanding of the ongoing chemical reactions and release processes. From this perspective, the experimental setup (see **Paper IV**) was developed which was to facilitate a simultaneous online investigation of biomass decomposition and inorganic element release. In order to simulate the conversion behaviour in real-scale applications, the setup was to be designed as a single particle reactor with high heating rates and variable atmospheres.

4.4.2 Description of the reactor

In Figure 20, the setup of the reactor and the ICP-MS coupling is presented.

The design of the reactor (see Figure 20) is based on a macro TGA. The main part is an electrically heated oven, with a reaction gas (variable N₂ and air mixtures) supplied from below. The biomass particle is placed on a sample holder which is connected to a scale for the determination of the mass loss during thermal decomposition. The flue gases released during the experiment are diluted at the top of the reactor in a porous tube diluter. A part of the flue gas is extracted by an ejector diluter and is delivered, after a further dilution step, to an inductively coupled plasma mass spectrometer (ICP-MS).

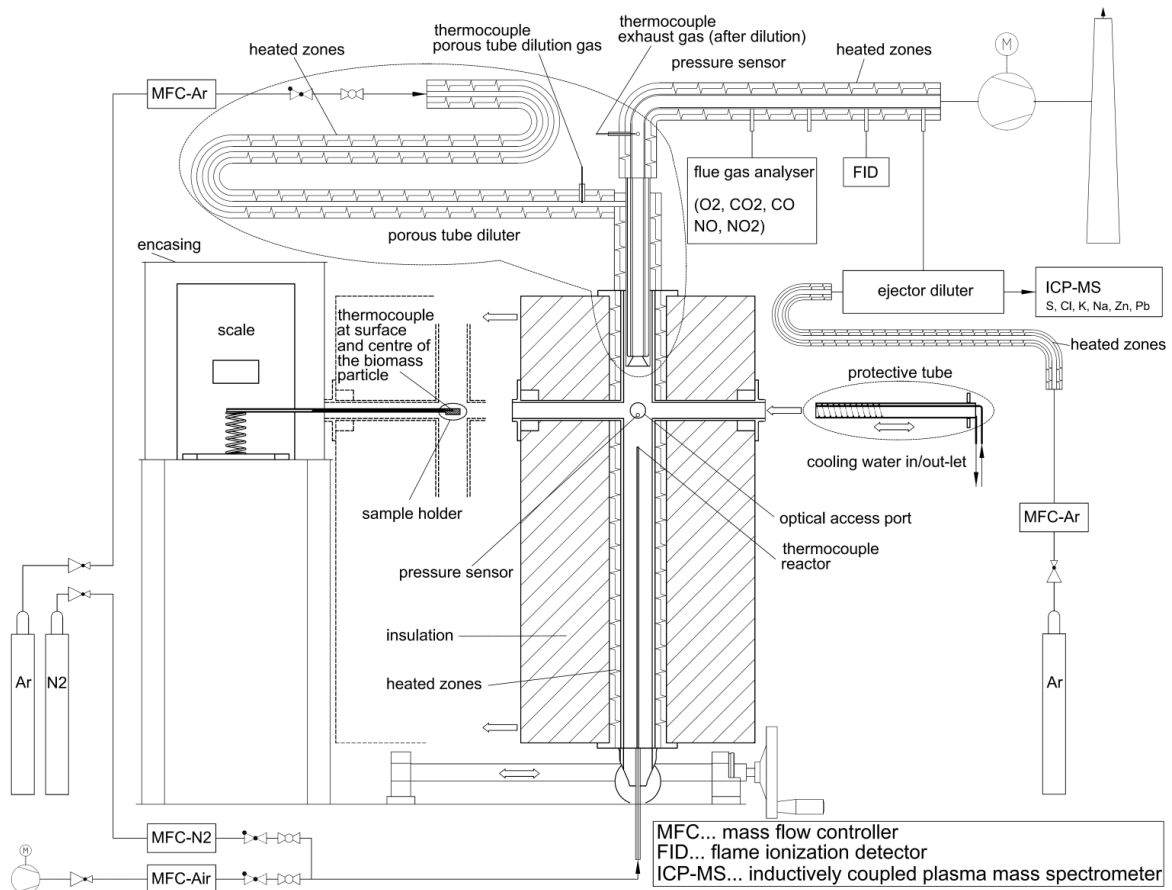


Figure 20: Scheme of the single particle reactor including measurement set-up

The reactor unit consists of an electrically heated (250°-1,050°C) vertical main tube (height 755 mm, inner diameter 50 mm) and four horizontal side tubes (length 177 mm, inner diameter 28 mm) of which one port (two axial tubes on opposite sides) provides an optical access, the other ports are used for sample introduction and sample cooling. The material of the ceramic tubes is Alsint, a ceramic material mainly composed of Al₂O₃ (99.7%), which contains traces of MgO and SiO₂. According to the manufacturer, diffusion of alkali metals into the material is negligible under reducing and oxidising conditions. Comprehensive measuring and control devices are applied in order to control and monitor the conditions during the experiment. The reaction gas (N₂/air mixtures), which is controlled by means of mass flow controllers (Sierra Smart Trak 2, Series 100), flows through the reactor from below and is heated up to a defined set-temperature until it reaches the position of the sample holder. The sample (~1 g biomass particle) is placed on a grid which is mounted on a horizontal sample holder. This sample holder is directly

connected to a scale (Mettler Toledo XS105DU) for the determination of the mass loss during thermal decomposition. With the sample, two thermocouples Type N (NiCrSi-NiSiMg) are placed to measure the temperatures in the centre and on the surface of the particle. The released flue gases (containing also inorganic vapours) enter a porous tube diluter at the top of the reactor, where Ar is used as dilution gas which is pre-heated to 500°C. Pre-calculations were performed in which the concentrations of inorganic vapours in the flue gas were estimated based on TEC. The dilution ratio as well as the temperature of the diluted gas were adjusted to avoid nucleation or condensation of these inorganic vapours. However, the formation of solid particles should only negligibly influence the ICP-MS measurement, provided that solid particles are transported to the device and are not deposited in sampling lines. A check of possible deposit formation was performed for the heated sample line between the ejector diluter and the entrance of the ICP-MS, which indicated that deposit formation in this location is negligibly low (additional information see **Paper IV**). Dilution (in the porous tube diluter) further ensures that during pyrolysis CO-concentrations do not exceed the measurement range of the flue gas analyser. A constant dilution ratio of 1:3 is provided with a mass flow controller (Sierra Smart Trak 2, Series 100). The diluted flue gas passes to a stainless steel tube, to which different gas analysers can be connected. A side stream is extracted, further diluted with Ar in an ejector diluter prior to the entrance of the ICP-MS (ejector diluter: gas temperature 500°C, dilution ratio 1:10; dilution prior to the ICP-MS: gas temperature 25°C, dilution ratio 1:5) and supplied to an ICP-MS. Further information concerning the dilution strategy can be found in **Paper IV**. Generally, the flue gases are drawn through the reactor, with constant under-pressure in the reactor provided by a suction fan. The pressures close to the sample holder and in the flue gas tube after the ejector diluter are recorded using Kalinsky pressure transmitters (DS1-420).

The experiments were generally performed in accordance with the following procedure. Before the experiment the reactor is pre-heated to the desired temperature. The reaction gas (typically 15 l/min; N₂/air mixtures) is supplied to the reactor and an under-pressure of 5 Pa (at the position of the sample holder) is set. A reaction prevention tube is inserted in the reactor from the opposite side of the sample holder. The tube is water-cooled and can be flushed with N₂. A hole is drilled to the centre of the fuel particle in axial direction. A thermocouple is inserted in the fuel particle, which measures the centre temperature during the experiment. A second thermocouple to measure the surface temperature is positioned between the sample holder grid and the particle. In a next step, the reactor is moved until the sample holder reaches the centre of the reactor. During this movement the sample is cooled and flushed with N₂ via the protection tube. When the reactor reaches the encasing of the scale and is sealed against the environment, the valve of the N₂ supply for flushing the sample is closed. After the pressure in the reactor is stable (~20 s) the protection tube is removed and the experiment starts immediately. After the experiment the ash residues are collected from the sample holder, whereby the main part of the ashes typically remains on the thermocouple determining the centre temperature. This is an indication that the gas flow applied in the reactor (0.5 m/s at 1,000°C) is low enough so that almost no entrainment of ash particles takes place.

4.4.3 Launch of the reactor without ICP-MS coupling

In a first phase, the reactor was tested without the ICP-MS coupling. The recorded parameters as well as the definition of prevailing combustion phases (release of volatiles and char burnout) will be discussed based on a test run with a Miscanthus pellet. Generally, one single pellet with a particle diameter of ~8 mm and a length of ~20 mm was used per test run (sample mass ~1g). The same Miscanthus pellets were used as in the investigations in **Paper III**. The sample mass was 1,142 mg fresh substance (f.s.) with a corresponding ash-free mass of 1,113 mg f.s.. The test run was performed at a reactor temperature of 850°C, with an O₂ content in the carrier gas of 5.6 vol.% at a flow rate of 15 l/min. This O₂ content was selected to achieve pyrolysis/gasification conditions during the devolatilisation phase (as is typical in real-scale combustion processes).

To define the prevailing combustion phase, increased CO₂ concentration above 0.1 vol.% was used. It can be seen in Figure 21 (left-side down) that in this case the release of volatiles starts after 16 s. The CO₂ concentration increases and reaches a plateau, afterwards the concentration decreases again. When the CO₂ trend reaches an inflection point, it is assumed that charcoal combustion starts to be the dominating process step. It is worth noting that devolatilisation and charcoal combustion overlap during particle conversion, therefore these processes cannot be exactly separated, but the phases when a certain process dominates can be defined. In this case, the inflection point occurs after 64 s. To identify the end of the char combustion phase and the end of the experiment, the drop in CO concentration to the initial value before the start of the experiment was used. The end of the experiment occurs after 1,071 s, which is not displayed.

In Figure 21 (left-side up), the gravimetric data as well as the pressure trends for the reactor and the flue gas are shown. To start the experiment, the protective tube is removed and the sample is exposed to the hot carrier gas. It is obvious that after 5 s the mass starts to decrease, and after 10 s a steep decrease of the mass during the release of volatile compounds occurs, which is followed by a slower mass decrease during char burnout. It can be seen that about 78% of the mass is decomposed during the release of volatile compounds. The pressure in the reactor is set at 5 Pa before the experiment. After 27 s the pressure drops to zero, due to released gases from the pellet. After the release of volatile compounds the pressure in the reactor increases and again reaches the initial value.

The temperature curves are displayed in Figure 21 (right-side up). After the protective tube is removed, a steep increase of the surface temperature takes place and after 95 s a temperature of 900°C is reached, which stays rather constant until the end of the test run (after 1,071 s). The slope of the centre temperature is characterised by a slow initial increase to 100°C attributed to the drying phase, followed by a quick increase up to 70 s (pyrolysis) and a steeper increase to 850°C during char burnout. After 100 s the temperature in the core of the pellet reaches 900°C and then stays rather constant up to the end of the experiment. The differences between surface and centre temperatures, especially during the devolatilisation phase, indicate that conversion takes place in different layers of the particle. It can also be seen that the flue gas temperature, which is

measured after the porous tube diluter, increases during the devolatilisation phase and reaches its initial value during the charcoal combustion phase.

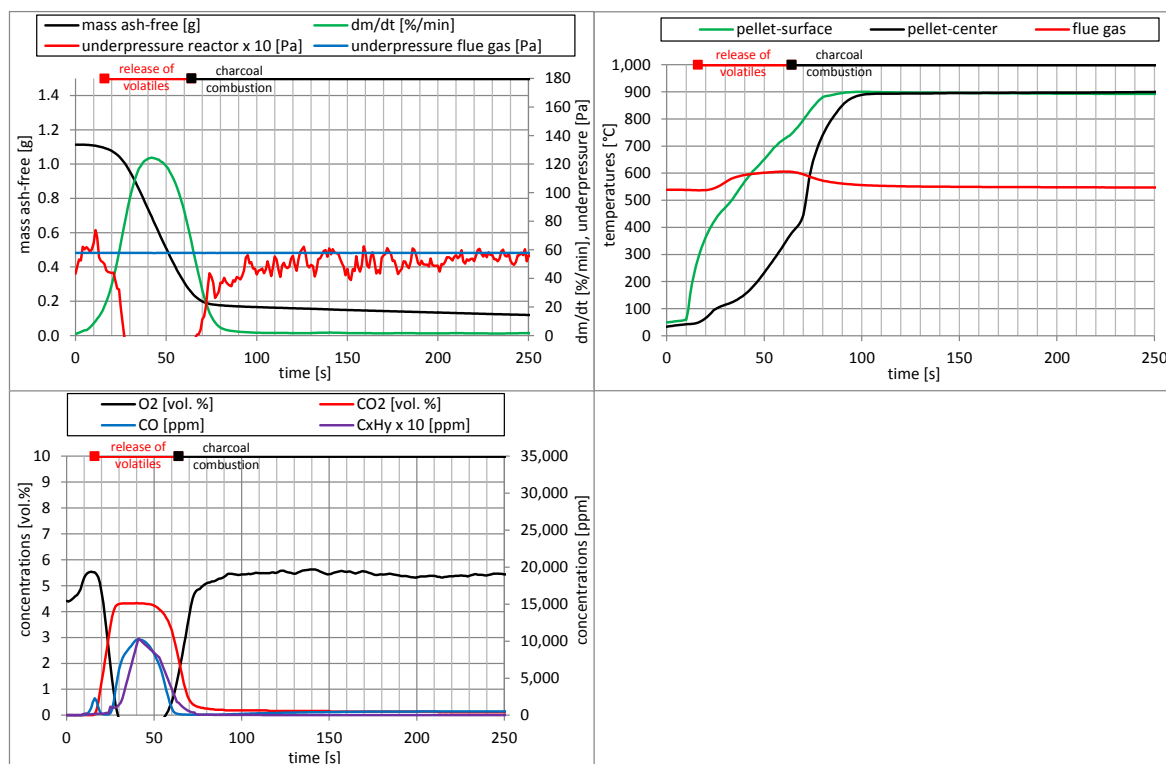


Figure 21: Experimental data for Miscanthus at a temperature set at 850°C: gravimetric data and pressure trends (left-side up), temperature curves (right-side up), flue gas compositions (left-side down)

The flue gas concentrations are displayed in Figure 21 (left-side down). Analogous to the surface temperature increase, CO₂ and CO concentrations as well as OGC increase and O₂ concentrations decrease. During char burnout, CO₂ concentrations decrease and O₂ concentrations reach the initial value of 5.6 vol.%. For the first 15 s of the test run, most probably the N₂ used for cooling the sample dilutes the carrier gas and, therefore, a lower concentration than 5.6 vol.% is measured. Also CO and OGC concentration decrease at the end of the devolatilisation phase. During char combustion, CO₂ and CO concentrations continuously decrease until the end of the experiment. For a validation of the test run, mass balances for C and the ashes were calculated. For the calculation of the balance, the amount of C, released to the gas phase, and the C in the ashes was taken into consideration. The amount of C in the gas phase was determined on the basis of the measured CO, CO₂ concentrations (gas analyser) and the OGC (FID). Furthermore, the amount of C in the ash was determined on the basis of analysis data of the total organic carbon (TOC) and the total inorganic carbon (TIC). For the test run described, a balance closure of 93% was determined. For the calculation of the ash mass balance, the expected ash according to fuel analysis was compared with the ash left after the experiment, with a balance closure of 88% determined for this test run. Only test runs which showed reasonable C and ash balance closures in a range between 80% and 120% were further evaluated. Experience has shown that possible ash losses mostly occur during ash

sampling from the sample holder. To quantify these losses, the balance closure regarding refractory (non-volatile) elements (e.g. Si, Ca, Mg) was also checked for each test run.

4.4.4 Tests performed with pure salts as a functionality check of the ICP-MS coupling

At first, several tests without ICP-MS coupling were performed to check the functionality of the reactor. In a next step, the reactor was coupled to the ICP-MS, and pure salts [KCl, NaCl, $(\text{NH}_4)_2\text{SO}_4$, ZnCl_2 and PbCl_2] were evaporated in the reactor and the signals provided by the ICP-MS were interpreted. The masses of pure salts were adjusted in order to simulate the expected element release from a straw pellet and to simulate the gas concentrations of inorganic vapours occurring during such experiments. The tests were carried out at 850°C with a carrier gas flowrate of 10 l/min of air. For the tests performed, clear signals were detected for S, K, Na, Zn and Pb. Only for the test where the amount of Cl was approximately equal to the amount of Cl which is expected to be released from a straw pellet, a clear signal was measured. For significantly lower amounts of Cl contained in the salt, no satisfying Cl signals were obtained. This behaviour can be explained on account of a low ionisation rate of Cl compounds in the ICP-MS [69]. This already shows that detection of Cl appears to be difficult with an ICP-MS.

4.4.5 In-depth validation of the S-signals

In a next step, tests with biomass pellets were performed. In **Paper IV**, the interpretation of the signals measured by the ICP-MS, the time synchronisation procedure as well as the calibration of the signals are discussed. For the first tests with *Miscanthus* and straw pellets, similar S and C ICP-MS trends were obtained. This may mean that the S release is coupled to the degradation of the organic matrix, but it is also possible that this is an indifference of the ICP-MS. It is possible that the mass spectrometric separation of C and S is reaching its limit. An initial S release related to the degradation of organic sulphur compounds (proteins) has been proposed in the literature [70]. To verify whether an indifference during ICP-MS measurements exists, experiments were carried out with straw pellets doped with $(\text{NH}_4)_2\text{SO}_4$.

For these tests, the same wheat straw pellets were used, as in **Paper II**, which contained an S amount of about 1 mg. Using an aqueous solution of 371 g/l $(\text{NH}_4)_2\text{SO}_4$, which was pipetted onto the straw pellets, the S amount of the pellets was increased to 2 and 4 mg respectively.

The test runs were performed at a reactor temperature of 850°C, an O_2 content of 5.6 vol.% and a carrier gas flowrate of 15 l/min.

To characterise the combustion behaviour, only a gas analyser was used. From the data of the flue gas analyser, the temperature profiles as well as the data of the mass loss curves similar conditions for all experiments can be assumed. Regarding the ICP-MS signals, similar results were obtained for the replications; therefore, only one test run for undoped straw and for the 2-fold amount of S is displayed in the following discussion.

In Figure 22, the counts for the ^{34}S and ^{13}C isotopes are displayed for an undoped straw pellet, with both signals showing one plateau. For the S signal after 70 s, a drop to zero is obvious, whereas the C release after 70 s is still ongoing. It can also be seen that the shape of the curve for the plateau of both signals is similar.

The counts of the ^{34}S and ^{13}C isotopes of the ICP-MS for the doped straw pellets with a 2-fold S amount are displayed in Figure 22. From the tests it can clearly be seen that the trend of the curve for C is the same for doped and undoped pellets. Regarding the experiments with doped pellets for the S signal, a higher peak is clearly visible at the beginning of the main release. This higher peak corresponds to the evaporation of the $(\text{NH}_4)_2\text{SO}_4$ salt. When the evaporation of the salt is completed, the counts of the S signal reach about the same quantity as measured for undoped pellets. Also tests with a 4-fold S amount were performed, which showed (see **Paper IV**) a more distinct first S release peak than in the test run with a 2-fold S amount. These experiments show that no differences between the S and C signals prevail and that the S signal can be interpreted as such. Furthermore, these experiments prove that the S release is coupled to the degradation of the organic matrix, which can be derived from the S and C signals of the ICP-MS.

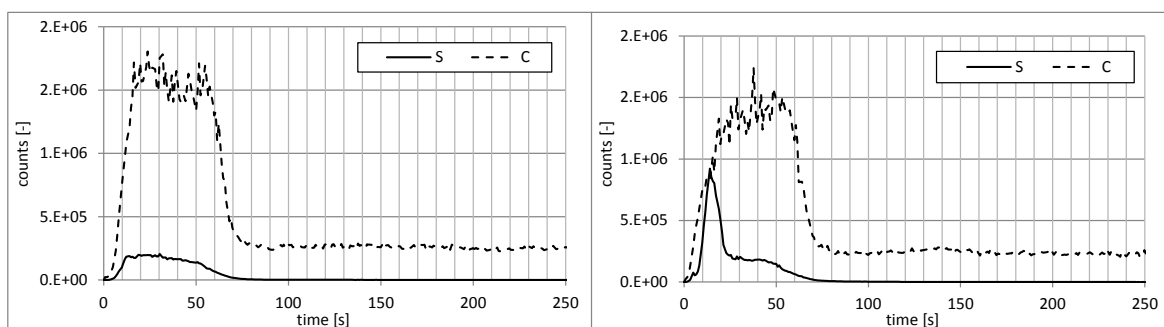


Figure 22: S and C counts recorded by ICP-MS for an undoped straw pellets (left), for a straw pellet with 2-fold S doping (right)

4.4.6 Quench tests with Miscanthus

In a quench test the ongoing combustion reactions are abruptly stopped at a certain time. These tests were used for a further validation of the ICP-MS signals obtained. When the experiment is stopped during the release of ash-forming elements, the signals immediately drop to 0, provided that care is taken that the flue gas still being released (containing inorganic vapours) does not enter the sample line. This is realised by channelling these released flue gases and quench gases leaving the reactor into an exhaust pipe and thus avoiding their entering the sampling line to the ICP-MS. If condensation and deposit formation of ash-forming vapours occur, this is likely to take place in the section of the unheated sample line prior to the ionisation in the ICP-MS. Condensates and deposits can be re-evaporated from the sample tube or the sample cone, which can cause release signals of ash-forming elements, not resulting from the momentary release of inorganic vapours from the pellet. This seems likely for Cl.

The quench experiments were carried out with Miscanthus pellets, which were also used in **Paper III** at a reactor temperature of 850°C and an O_2 content of 5.6 vol.% (carrier gas

flowrate 15 l/min). Quenching was set to take place after the release of volatile compounds, so that the quench time did not match with the maximum release of ash-forming elements. Quench times of 70 s and 100 s after the start were defined. In this thesis only the quench test after 70 s will be discussed, the discussion of the quench test after 100 s can be found in **Paper IV**.

To start the experiment, the protective tube is removed and the sample holder is exposed to the hot carrier gas. For quenching the sample, the protective tube must be moved back over the sample holder and the N₂ purge gas is activated for quenching the sample. Simultaneously with the activation of the N₂ purge gas, two valves are opened at the enclosure of the balance. This ensures that the sample is cooled and that the majority of the still arising combustion gases flow towards the scale enclosure and subsequently reach the laboratory.

After the N₂ purge gas activation, the sample was cooled for about 5 minutes and the ICP-MS signals were recorded for the experiment as well as for the cooling period.

To compare the quenching experiments, also test runs with unquenched Miscanthus pellets were performed. Generally, the experiments were performed in triplicate, with similar results obtained. Therefore only one experiment is presented for the unquenched as well as for each quenched sample.

The influence of the quenching procedure on the gravimetric data, the pressure trend, the temperature curves as well as the flue gas composition is described in detail in **Paper IV**. Here, only the most relevant effects of the quench procedure on the above-mentioned parameters will be given.

After the quench, a clear pressure drop in the exhaust gas and the reactor was observed. This was because the sample was flushed with N₂ and the valves at the enclosure of the scale were opened. Regarding the temperature trend, a steep drop in temperature after quenching occurred, with the temperature in the centre of the pellet lower than 500°C after 10 s. Concerning the flue gas concentration after the quench no CO₂ was measured, and after the quench a lower O₂ concentration than at the beginning of the experiment was reached. This is an indication that a small fraction of N₂, which was needed to quench the sample, was sucked in the direction of the porous tube diluter. However, it can be assumed that the small amounts of flue gas entering the direction of the porous tube diluter after the quench do not affect the results of the quenching experiments, since no concentrations of flue gas compounds were measured.

In Figure 23 and Figure 24, signals from the ICP-MS for C, S, K, Na, Zn, Pb and Cl for the quenching experiments are shown in comparison with an unquenched experiment. The comparison illustrates the influence of quenching with regard to each recorded isotope.

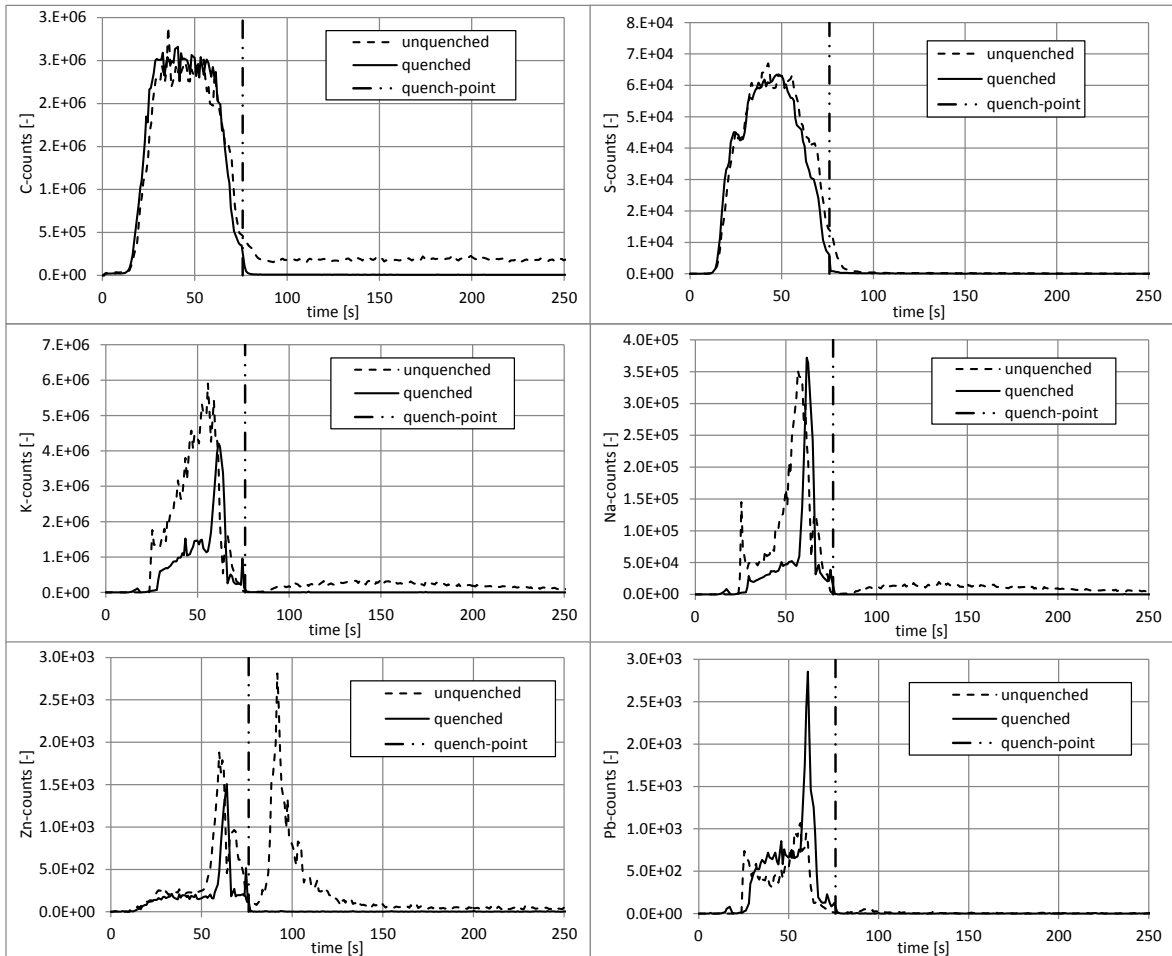


Figure 23: ICP-MS signals for C, S, K, Na, Zn and Pb of the quenching experiments compared with an unquenched experiment for Miscanthus at 850°C

In Figure 23, a clear drop of the C, S, K, Na, Zn and Pb signals to 0 after the quench-point can be observed. This is an indication of proper dilution of the sample gas and of minimising possible interactions (condensation and/or deposition of inorganic vapours as well as interactions on or close to the sample cone) prior to the ionisation of the gas in the ICP-MS. For K and Na, the release during the unquenched experiments occurs in two stages. The main release takes place during devolatilisation, whereas the remaining K is released during char burnout. Although Zn and Pb are trace elements in biomass fuels, usable signals on the ICP-MS can be obtained. For Zn and Pb two release peaks were measured during the unquenched experiments. For Pb only one clear peak can be seen during the quench experiments compared to the unquenched test run. Although these differences between unquenched and quenched experiments are evident, it can clearly be seen that after the quench the release of Zn and Pb drops to zero. The drop of the ICP-MS signals after the quench for C, S, K, Na, Zn and Pb indicates that the ICP-MS signals are not influenced by possible interactions of the gas prior to the ionisation in the ICP-MS. Therefore, the signals obtained can be interpreted as resulting from the release of inorganic compounds from the biomass pellet. For the signals obtained, the parts before the quench point for both tests are slightly different. There is a good agreement of the start of the release and the occurrence of the maximum release for the unquenched and

quenched experiments. A slight variation can be observed for K and Na regarding the release curves between the start and the maximum release. During this phase, different processes (pyrolysis, gasification and char combustion) occur in parallel which can also influence the release of inorganic compounds. Furthermore, the temperature development of the particle during the unquenched and quenched experiment is slightly different (see **Paper IV**), which also influences the release profiles.

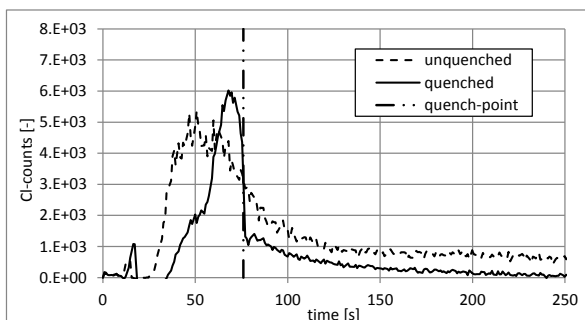


Figure 24: ICP-MS signals for Cl of the quenching experiments compared to an unquenched experiment for Miscanthus at 850°C

Regarding Cl (Figure 24), it can be seen from the unquenched experiment, that the main release takes place during the release of volatile compounds. In contrast to K (Figure 23), only a continuous decrease of the signal with ongoing test duration is determined. This long tail off may originate from a Cl release of the pellet, but can also result from deposition and release processes in the ICP-MS prior to the ionisation of the gas. Judging by the Cl signals of the quenching experiments, a drop of the Cl signals after the quench occurs, whereas after the drop a continuously tailing Cl signal was measured. Hence, deposition and release processes (interactions) of Cl compounds, most likely located in the unheated zone (between the entrance of the ICP-MS and the sample cone), cause this behaviour. Reference [71] reports that chlorine is released in the shape of $\text{CH}_3\text{Cl}(\text{g})$ at a temperature range of 250°-350°C during torrefaction of wood and straw. Condensation of this component in the sample line prior to the ionisation in the ICP-MS can be excluded due to the low boiling point (-23,8 °C at 101,300 Pa) as well as the high dilution (dilution ratio 1:150) of the sample gas. But interactions of Cl compounds can possibly also occur at the sample cone caused by possible deposition and re-evaporation processes which cannot be avoided. However, this inexplicable behaviour of the Cl signals means that only strong changes of the Cl signals may be qualitatively evaluated, whereas continuously decreasing Cl signals most likely result from interactions in the ICP-MS. It must also be noted that the probability of ionisation of Cl in an ICP-MS is at about 1% [69]. The low ionisability and possible interactions of Cl compounds indicate that the Cl signal can only be evaluated with restrictions.

The quench tests also proved that the time synchronisation regarding the recorded data works well, which can clearly be seen since the quench point occurs at the same time for the gravimetric data, the temperature profiles, the measured flue gas compounds and the ICP-MS data (see **Paper IV**).

4.5 Simultaneous online determination of S, Cl, K, Na, Zn and Pb release from a single particle during biomass combustion: Results from test runs with spruce and straw pellets – Paper V

The setup presented in **Paper IV** and section 4.4.2 was used to perform test runs with spruce and straw pellets.

4.5.1 Tests performed

Test runs were performed with softwood (spruce SW) and wheat straw at reactor temperatures of 700°, 850° and 1,000°C (in the following referred to as SW700, SW850, SW1000 and straw700, straw850, straw1000). Single biomass pellets were used, which were 8 mm in diameter and about 20 mm in length, resulting in a sample mass of about 1 g. The tests were performed in oxidising atmospheres (5.6 vol.% O₂ in the reaction gas) at a total flow-rate of the reaction gas of 15 l/min at 0°C and 101,325 Pa. The O₂ content was selected to achieve gasification or pyrolysis conditions during the devolatilisation phase comparable with real-scale combustion processes. For the SW700 experiments, the O₂ content was decreased to 4.2 vol.% to gain better stability of the decomposition process. The tests were generally performed in triplicate to check whether they could be replicated.

Quench tests were performed as a validity check for the online release profiles and to gain further information about ash transformation and inorganic release processes. The same procedure for the quench tests like already described in section 4.4.6 was applied.

The quench tests (conducted for straw) were performed in triplicate under the same boundary conditions as was the case with complete burnout. After quenching, the residues were removed and chemically analysed. Based on these data, the release ratios for the relevant inorganic ash-forming elements at the quench point were calculated.

4.5.2 Release behaviour of ash-forming elements

The overall release ratios of volatile and semi-volatile ash-forming elements from the fuel to the gas phase for the entire combustion experiment were calculated by element balances, based on analysis data of the fuel and the ash residues. The results of the calculations are summarised in Figure 25.

Generally, the release of inorganic elements increases with higher temperatures, which is in agreement with literature data [30, 32].

In the case of S, the release of mainly organically bound S can be assumed for temperatures of 700° and 850°C. Typically, 75% S is organically bound, and the remaining part is inorganically associated [72], which explains the high release rates (50%-60%) seen as early as at 700°C. High Cl release ratios are also obtained for 700°C, and, especially in the case of straw, the remaining Cl is most likely bound in alkali salts (e.g. KCl). Higher K release ratios were determined for straw700 and straw850 than for SW at these temperatures. The higher K release for straw may result from the significantly higher Cl

content in the fuel and therefore in an increased KCl(s) evaporation [30, 31, 68]. For straw1000, an inclusion of K in molten K-Si phases is most likely and reduces the K release, since the molar K/Si ratio amounts to 0.45 and 0.96 for straw and the SW used at this temperature. Furthermore, a rather low shrinkage starting temperature of 780°C was determined for straw, and at reactor temperatures of 1,000°C the ash was completely fused after the experiment.

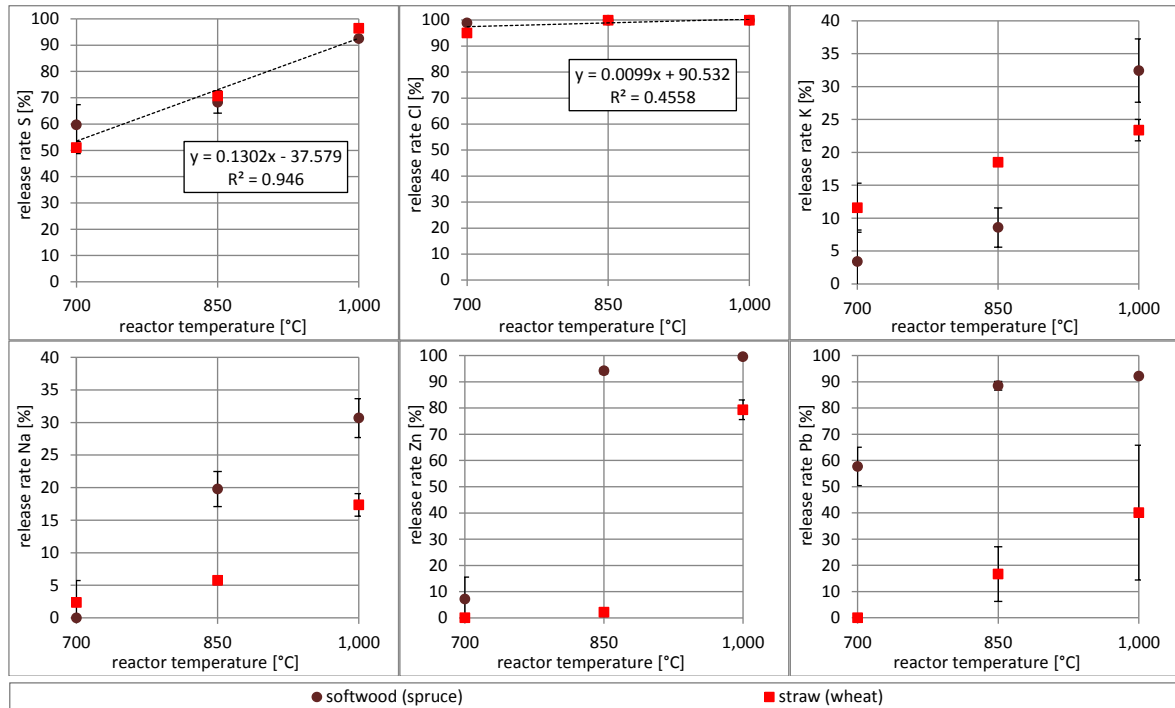


Figure 25: Release of inorganic elements from the fuel to the gas phase dependent on the respective temperature

Explanation: Only for S a statistically significance ($p < 0.05$) can be identified

Lower Na release rates were determined for SW700 than for K and, in the case of straw, lower Na release rates were obtained for all temperatures. A low Na release below 800°C was also reported in [73, 74], which is in line with results at 700°C. In the case of higher reactor temperatures, sublimation of NaCl and Na-carbonate decomposition [32] can cause higher release ratios.

For Zn, a steep increase of the release ratios can be observed between 700° and 850°C in the case of wood, whereas for straw the steep increase is shifted to temperatures between 850° and 1,000°C. Lower release ratios of straw in comparison to SW can be explained by a possible interaction of Zn with Si and Al [32]. TEC performed in **Paper II**, also showed the formation of solid Si-Zn phases below 500°C.

For Pb, lower release ratios were determined for straw than for SW. Straw shows higher concentrations of Si and Al than SW, which indicates that interactions of these elements with Pb [32] can reduce the Pb release. Furthermore, Pb compounds can be included in molten phases, which can reduce the Pb release. The occurrence of these inclusions can

vary for each experiment and therefore higher standard deviations prevail for straw (for reactor temperatures above 700°C) than for SW.

4.5.3 Time resolved release behaviour of ash-forming elements during combustion experiments

In general, three replications of the tests were performed. To show the reproducibility of the method, the results of the K release trends for all 3 replications for straw850 are shown (see Figure 26).

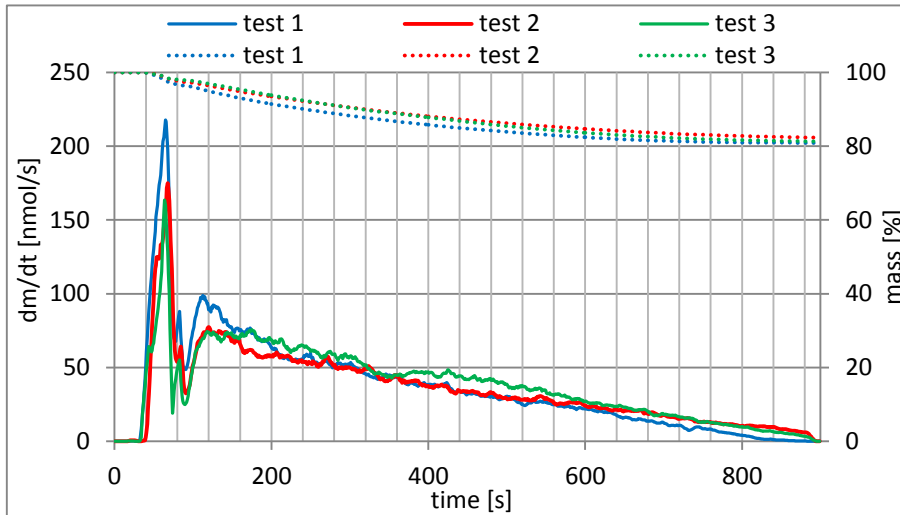


Figure 26: Time dependent K release from straw for reactor a temperature of 850°C for the three replicated test runs

For all three replications (see Figure 26), a main release for the first 40 s after the release starts can be identified, where devolatilisation is the dominating combustion phase. A second release peak occurs during the char combustion phase. For all three replications a similar release trend can be identified. This indicates that the method applied is reproducible. Therefore, only one representative test runs is displayed and discussed per temperature and fuel in the further discussion.

Trends regarding the release of S and Cl over time as well as the development of the particle temperatures (surface and centre) during the experiments are displayed in Figure 27. In the time resolved release figures (see Figure 27-Figure 29) also the dominating combustion phase is specified. The procedure for identifying the dominating combustion process (e.g. release of volatiles and charcoal combustion) has already been described in section 4.4.3.

In the case of reactor temperatures of 700° and 850°C, mainly organically bound S is released, as already mentioned in section 4.5.2. Furthermore, in [29, 30, 32], it has been proposed that the release of inorganic S begins at temperatures above 900°C. Based on the release curves (see Figure 27), the release of S usually starts at surface temperatures of between 300°-400°C for both fuels. At a reactor temperature of 850°C, a release of mainly organically associated S is most likely, but inorganically associated S (e.g. alkali

sulphate) can also contribute to the S release. For SW1000, the bimodal release profile might consist of an organic and inorganic part, which is supported by the temperature development of the particle. Straw1000 is seen to exhibit different behaviour than SW1000. For straw, one release peak is clearly pronounced, whereas the remaining S is continuously released during char burnout. The low release during char burnout is most likely caused by transport limitation due to the occurrence of molten phases.

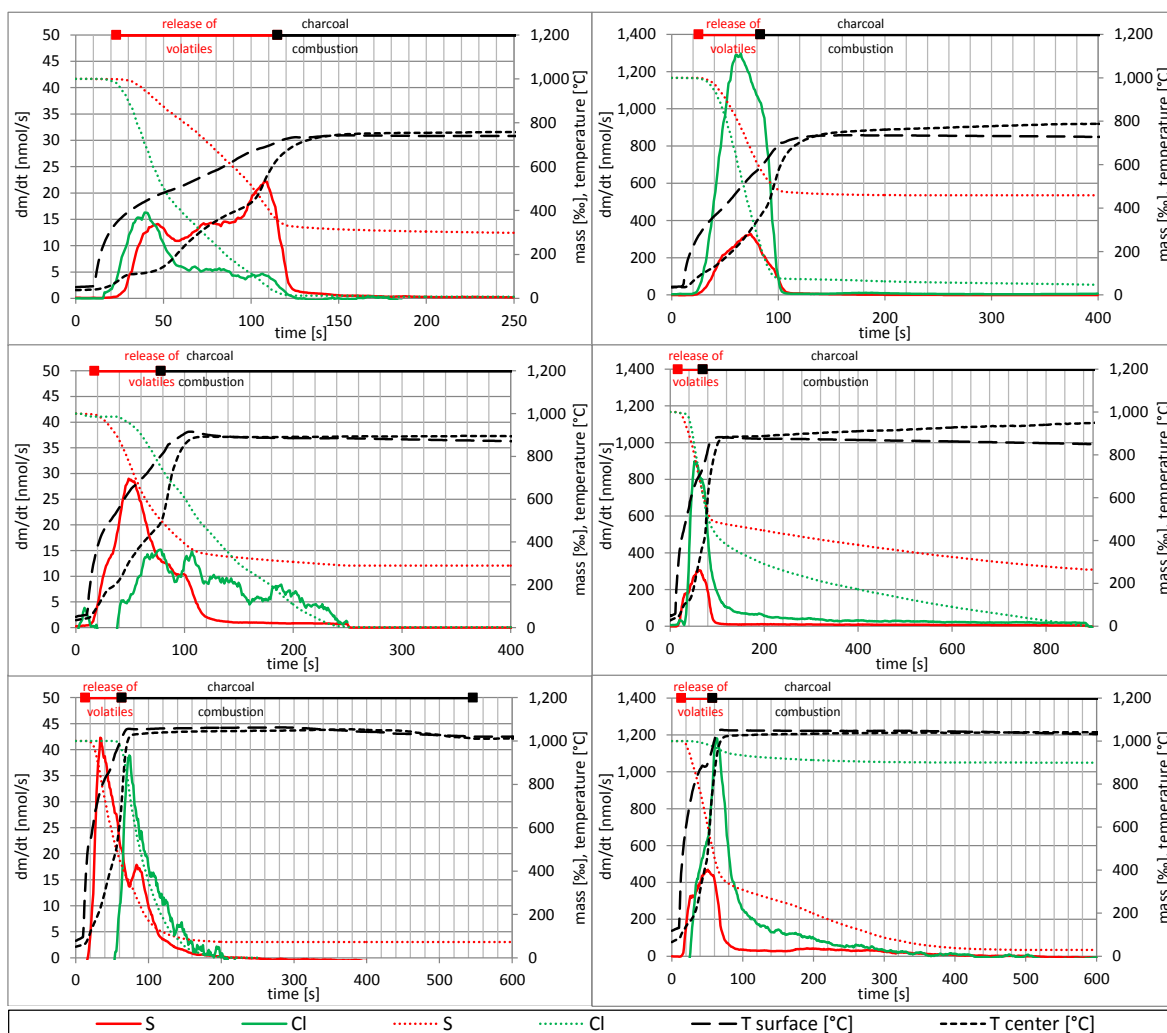


Figure 27: Time dependent release of S, Cl and K from softwood (left) and straw (right) at reactor temperatures of 700°, 850° and 1,000°C (from top to bottom)

In section 4.4.6 it was concluded that the ICP-MS determined Cl release can only be interpreted to a limited degree. Possible deposition and release processes of Cl compounds, most likely located in the unheated zone of the sample line, can influence the Cl signals. Marked changes to the Cl release profiles may be qualitatively evaluated, whereas continuously decreasing Cl release most likely results from condensation or deposition and release processes in the unheated part of the sample line and the ICP-MS. However, the release trends determined are displayed in the diagrams and were validated for straw by additional quench experiments (see section 4.5.4).

For SW700 and straw700, the Cl release starts at surface temperatures of about 300°C and the main release takes place during devolatilisation, which most likely results from the release of CH₃Cl [71]. During experiments with higher reactor set-temperatures (850° and 1,000°C), the main release starts at higher surface temperatures, which may result from transport limitations when the particle is being heated up. The section of the Cl trends after the release peak should, as already mentioned, not be evaluated.

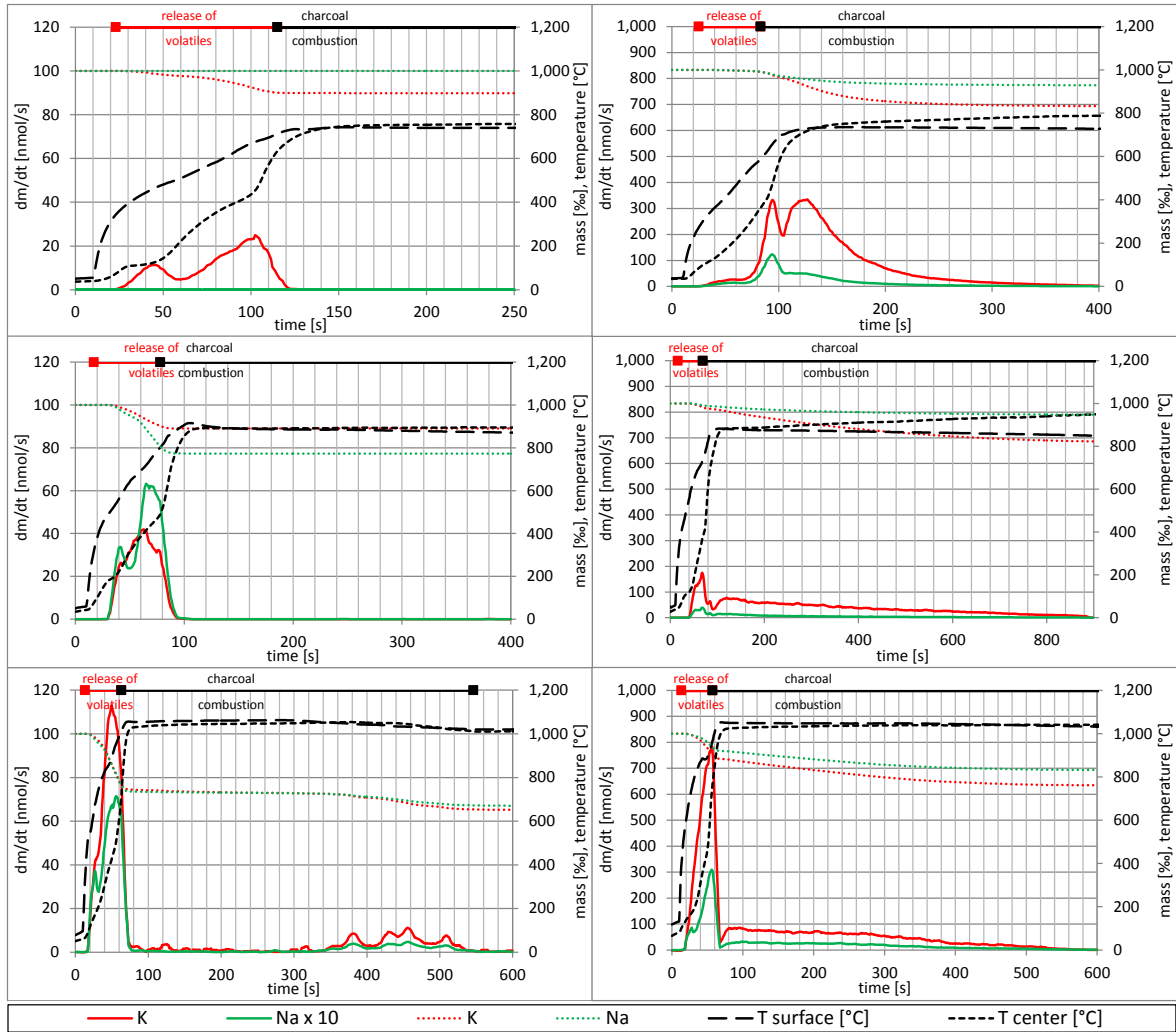


Figure 28: Time dependent release of K and Na from softwood (left) and straw (right) at reactor temperatures of 700°, 850° and 1,000°C (from top to bottom)

In general, the release processes in the literature are in close agreement with time resolved release profiles. In the case of K, the release starts in the temperature range of 500°C, independent of the fuel and heating rate, which can be explained by the release of alkaline carboxylates and phenol-associated K [32]. At temperatures above 700°C KCl(s), sublimation and K₂CO₃(s) decomposition take place [32]. The main release (see Figure 28) takes place during devolatilisation, and a lower K release occurs during char burnout. For SW700, low shares of K release as KCl(g) are probable, since the K release is almost finished when surface temperatures above 700°C are reached. For reactor temperatures of 850° and 1,000°C, particle temperatures clearly above 700°C are reached, and the

evaporation of KCl(s) and a dissociation of K_2CO_3 take place. For SW1000, a release can be identified during the later stages of char combustion, which may result from the K_2CO_3 dissociation. Such behaviour was identified for straw (see **Paper V** and section 4.5.4) and a similar behaviour for SW can be assumed. For straw, a bimodal K release trend (especially for straw700) was determined. The first release peak (occurring during devolatilisation and early stages of char combustion) may result from organically associated K as well as a possible sublimation of KCl. Quench experiments with subsequent chemical analysis (see **Paper V** and section 4.5.4) were performed, which revealed that the second release peak mainly results from K_2CO_3 decomposition. For straw850 and straw1000, the occurrences of molten phases (mainly K-Si, further information also supported by TEC can be found in **Paper II**) can cause the continuously decreasing K release during char burnout.

Since significantly fewer literature data are available for Na than for K, similar release behaviour was proposed taking into consideration different characteristic temperatures regarding Na release (melting points: NaCl 801°C, carbonate decomposition above 850°C).

The release starts at a surface temperature of about 500°C (see Figure 28), which is in good agreement with [73, 74] where the start of the release was proposed to be at around 400°C during pyrolysis. This low temperature release can be observed for reactor temperatures of 700 and 850°C and also partly for reactor temperatures of 1,000°C. Similar release trends can be observed for Na and K (see Figure 28) for straw850 and straw1000. The bimodal release profile in the case of SW850 most likely originates from the dissociation of organically associated Na (first peak) and the second release peak results from NaCl evaporation and possible Na_2CO_3 decomposition, since surface temperatures around 800°C prevail. For straw700, a different release profile to that of K can be observed at that temperature. Since a relatively high Na release ratio (7%) was determined for the presented test, and the particle surface temperatures in particular are close to 800°C, evaporation of NaCl or carbonate decomposition can already take place at that reactor temperature.

It has already been mentioned in **Paper IV** that Zn release starts at temperatures above 500°C and that particle temperatures above 700°C are necessary for a distinct Zn release. In the conducted experiments (see Figure 29), Zn release starts at surface temperatures of between 500°C (SW850, straw850 and straw1000) and 700°C (SW700 and SW1000). For SW, the main Zn release finishes when the maximum surface temperature is reached. Especially in the case of straw1000, a low and continuously decreasing release trend can be observed during char burnout. The occurrence of molten phases most likely hinders Zn release during char burnout. For SW850, a bimodal release trend was obtained. The release maxima can be explained by reaching a sufficient temperature at the surface and at the centre of the particle for a distinct Zn release, where the minimum between the two release maxima may result from a possible capture of Zn compounds in the char matrix. A possible retention of Zn compounds in ashes by Si and Al is very improbable for SW due to the low concentrations of these elements in the fuel (see **Paper V**). During the second release peak, surface temperatures above 900°C prevail, where Zn compounds previously captured in the char are released. For SW1000, one single release peak was

obtained, with the maximum at centre temperatures about 900°C. The higher reactor temperatures cause a faster decomposition of the particle, and a possible capture of Zn compounds in the char is not visible in the release profile. For straw, different Zn release profiles have been determined than for SW, most likely caused by interactions of Zn compounds in the ashes by Si and Al. For straw850, only a single Zn release peak occurs, with an unclear maximum at surface temperatures between 700° and 800°C. In the case of straw1000, a bimodal Zn release trend prevails, where maximum release peaks occur at surface and centre temperatures of 1,000°C. It seems that at temperatures below 1,000°C, Zn compounds are retained in the ashes, and a sudden release takes place when 1,000°C is reached. Generally, the peaks of the release profiles are shifted to higher particle temperatures with rising reactor temperatures (or heating rates of the particle) (see **Paper V**), which are caused by transport limitations when the particle is heated up. This shift can be observed for Zn and Pb for both fuels.

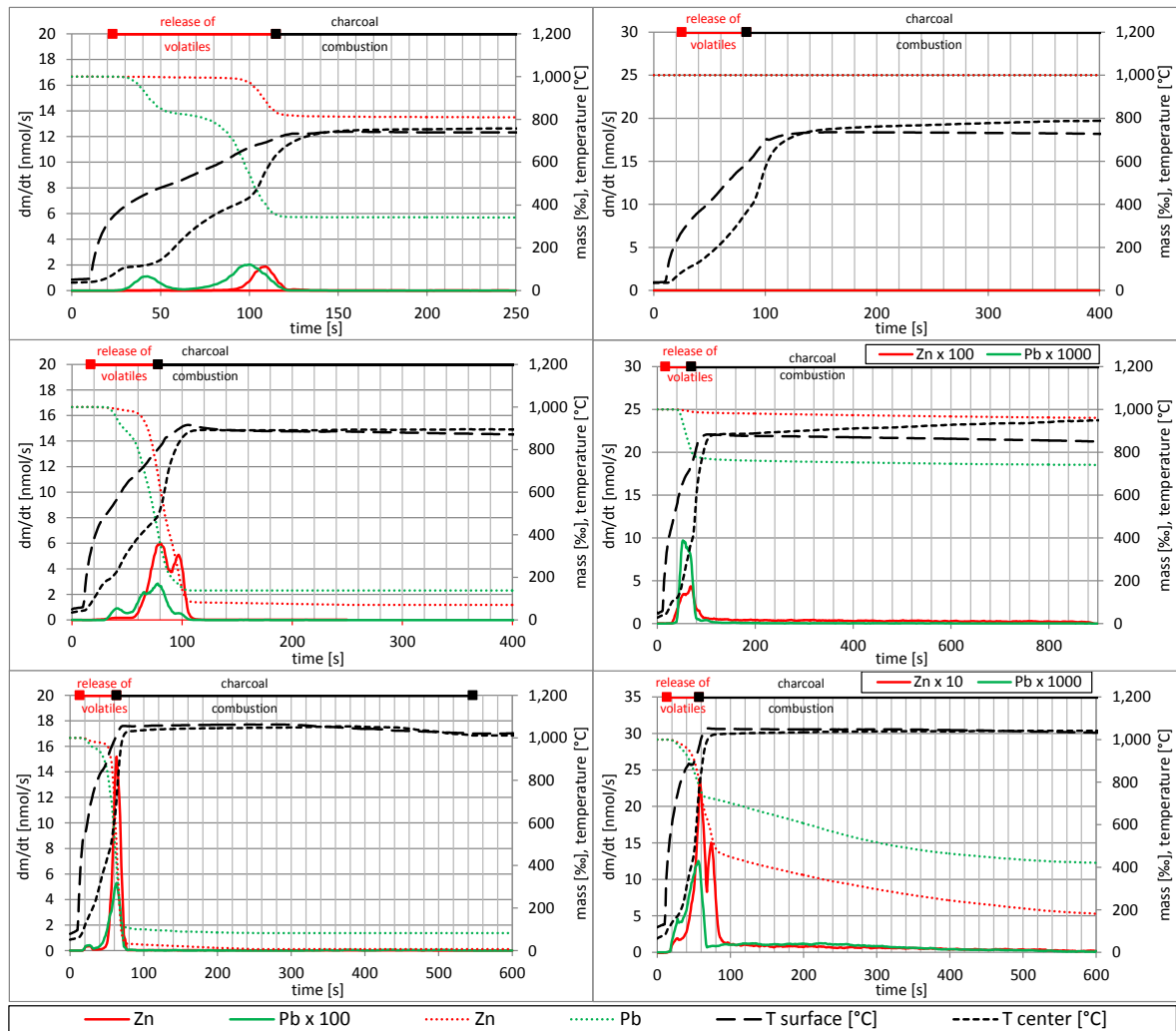


Figure 29: Time dependent release of Zn and Pb from softwood (left) and straw (right) at reactor temperatures of 700°, 850° and 1,000°C (from top to bottom)

Pb release starts at surface temperatures of around 500°C (see Figure 29), independent of the reactor temperature and the fuel. For SW, a bimodal release trend (SW700 and

SW1000) and a multimodal release (SW850) can be observed. The minima of these release trends can be caused by Pb compounds being captured in the char. The captured Pb compounds are later released at higher particle temperatures. For SW, a low release takes place at surface temperatures above 500°C. A second release peak occurs during the switch between devolatilisation and char burnout, which is more pronounced at higher reactor temperatures. In contrast to SW, straw shows one distinct release peak during devolatilisation and a continuously decreasing release trend during char burnout (transport limitations caused by ash melting). Straw has a significantly higher ash content than SW as well as a different ash composition (interactions of Pb with Si and Al – see also section 4.5.2), factors which explain the different release profiles for both fuels.

4.5.4 Results of targeted quench experiments

The quench points were adjusted to the K release profiles determined (see Figure 28). For straw700, the quench point was defined with the minimum between the peaks of the bimodal K release profile (105 s). For straw850 and straw1000, the quench was chosen to occur after devolatilisation and to start at char burnout, which is after 90 and 70 s respectively. The release ratios at the reference point were derived from the time resolved release profiles at complete burnout (Figure 28) determined at the averaged centre temperature which were measured at the quench points. The averaged centre temperature at the quench point was selected since the determined centre temperatures at the quench point are in a narrow range (Table 4) in the replications, and by choosing this approach only one reference point is obtained. These data were compared with the data gained from the quench experiments. Based on these framework conditions, quench tests as presented in **Paper V** were performed with straw.

In Table 4, the results of the quench experiments with straw as well as the results from the reference point at complete burnout are summarised.

With the exception of Cl, a very good agreement between the reference point and the averaged release ratios for the quench tests prevails (see Table 4). Consequently, meaningful time resolved release profiles were obtained for S, K, Na, Zn and Pb.

For straw850, slightly lower Na and Zn release and a higher Pb release ratio were determined for the reference point in comparison with the quench test. The deviations regarding Na and Zn are most probably due to their low concentrations and an inhomogeneous distribution in the fuel. The deviations of Pb can be explained by the high standard deviation of the release ratios determined at complete burnout.

The results of the quench tests can also provide a rough estimation regarding the K release that may result from KCl evaporation and K_2CO_3 decomposition. The K release is not completed at the quench point in any quench experiments. Organically associated K is released before the quench point. Additionally, the high Cl release ratios at the quench points indicate (78% – 90%) that a part of K is released in the form of KCl. A decomposition of K_2CO_3 before the quench is only probable for straw1000, since the average centre temperature of 947°C at the quench point was above the temperature

when K_2CO_3 decomposition starts (800°C [32]). After the quench, the remaining KCl(s) is evaporated and K_2CO_3 (s) decomposition mainly takes place.

Table 4: Release data for complete burnout in comparison with quench experiments for straw at reactor temperatures of 700°, 850° and 1,000°C

Explanation: T-quench ... centre temperature at the quench point; reference point ... released amount derived from the time resolved release profiles at complete burnout determined at the averaged centre temperature measured at the quench points

reactor temperature [°C]		complete burnout	reference point	quench tests			average	std. dev.	
T-quench °C				1	2	3			
700	S	wt.%	54.1	51.5	574	612	564	46.6	0.7
	Cl	wt.%	95.3	93.4	47.6	46.3	45.8	90.0	3.1
	K	wt.%	16.7	3.3	89.1	94.1	86.7	3.2	0.9
	Na	wt.%	7.1	2.8	4.2	3.5	2.0	2.4	0.9
	Zn	wt.%	0.00	2.0	1.4	3.6	2.2	3.3	2.7
	Pb	wt.%	0.00	0.00	0.00	0.00	0.00	0.00	0.00
850	S	wt.%	73.5	64.9	757	753	750	52.5	1.0
	Cl	wt.%	99.9	54.0	53.9	51.8	51.9	77.8	7.6
	K	wt.%	17.7	2.6	88.3	70.7	74.3	5.3	0.9
	Na	wt.%	5.2	1.3	4.0	6.2	5.8	6.5	1.5
	Zn	wt.%	4.0	1.5	5.8	8.6	5.1	4.6	1.5
	Pb	wt.%	25.9	24.2	6.0	5.5	2.5	9.4	4.7
1000	S	wt.%	97.1	66.8	967	936	938	59.1	1.4
	Cl	wt.%	100.0	34.3	60.4	59.6	57.2	79.8	1.6
	K	wt.%	23.8	11.4	81.8	79.7	78.0	11.6	2.3
	Na	wt.%	16.8	8.3	14.9	9.9	10.0	10.0	3.2
	Zn	wt.%	81.9	39.9	53.3	46.8	33.7	44.6	8.2
	Pb	wt.%	57.9	57.1	66.3	64.7	60.6	63.8	2.4

In the case of Cl, an acceptable agreement between the reference point and the quench point only exists for straw700. For reactor temperatures of between 850° and 1,000°C, the calculated reference point shows a significantly lower release than the quench test. This again confirms that the Cl release during charcoal combustion is overestimated during the tests at complete burnout.

4.5.5 Summary of the benefits of the single particle reactor coupled to an ICP-MS for online determination of the S, Cl, K, Na, Zn and Pb release

The single particle reactor device can be used for targeted combustion experiments in a temperature range of 250°–1,050°C under reducing and oxidising conditions. During the experiments, relevant parameters such as mass loss during thermal decomposition, the temperature development of particles (surface and centre), flue gas composition and the S, Cl, K, Na, Zn and Pb release trends were recorded online. A validation of the time resolved inorganic element release profiles was performed by a targeted and controlled interruption (or quench experiment) of the ongoing decomposition process, which also supported the interpretation of the release data. Test runs with softwood and straw were performed at reactor temperatures of 700°, 850° and 1,000°C under oxidising conditions (5.6 or 4.2 vol.% O₂). The results clearly indicate that the inorganic element release increases with rising reactor temperatures. The time resolved release profiles can be used

to validate existing release mechanisms proposed in the literature. The quench experiments are a valuable method to validate the inorganic element release profiles. The experiments are also very useful regarding the interpretation of the inorganic element release profiles. The online release data can also be used for the development of inorganic element release models in the future.

5 Conclusions and recommendations

5.1 Conclusions

The utilisation of non-wood feedstocks (herbaceous biomass and agricultural residues) is of increasing interest to enhance biomass utilisation in the energy sector. However, since these non-wood feedstocks have not been sufficiently analysed with regard to their combustion behaviour, fuel characterisation with a special focus on combustion-related fuel properties constitutes a first important step towards their introduction. In this context, possible ash-related problems (ash melting on grates, deposit formation and corrosion) as well as problems regarding particulate, NO_x , SO_x and HCl emissions are the main focal points. One way to combat problematic combustion behaviours is the application of fuel additives and fuel blends. The common method for evaluating additives and fuel blends is based on experimental investigation. In this thesis, characterisation methods (fuel indexes, thermodynamic equilibrium calculations (TEC) and fixed-bed lab-scale reactor experiments) were used to determine appropriate biomass/kaolin mixtures and *Miscanthus* peat blends as relevant case studies of these applications. Based on the work performed, an effective approach to the characterisation of pure fuels, fuel additive mixtures and biomass fuel blends is suggested. In addition, a new single particle reactor was developed to determine relevant parameters during the thermal conversion process and to simultaneously record time resolved release profiles of relevant aerosol forming elements (S, Cl, K, Na, Zn and Pb).

For an initial pre-evaluation of combustion-related problems that may arise, fuel indexes were developed. They were calculated on the basis of the results of chemical fuel analyses. The data for the investigation were derived from test runs using fixed-bed lab-, pilot- and real-scale combustion systems. Hence, the indexes derived in this thesis are applicable to grate combustion plants. They are directly applicable to pure biomass fuels and fuel mixtures where, for biomass fuels upgraded with minerals (e.g. kaolin), the applicability of a fuel index has to be checked. Among the fuel indexes which allow for accurate qualitative predictions are the N-content for the prediction of the NO_x emission range, the molar 2S/Cl ratio as an indicator of high-temperature corrosion risk and the molar ratio of $(\text{Si}+\text{P}+\text{K})/(\text{Ca}+\text{Mg}+\text{Al})$ to predict the ash melting tendency. Indexes which can be applied with some restrictions regarding other constraints are the sums of K, Na, Zn and Pb as indicators of the aerosol emissions range, the molar ratios of $(\text{K}+\text{Na})/[\text{x}*(2\text{S}+\text{Cl})]$ to estimate the SO_x and HCl emission to be expected, $(\text{Si}+\text{P}+\text{K})/(\text{Ca}+\text{Mg})$ as well as $\text{Si}/(\text{Ca}+\text{Mg})$ as indicators of the ash melting tendency. The prediction accuracy of the indexes regarding aerosol and gaseous SO_x and HCl is strongly influenced by the release behaviour of inorganic elements during the combustion process. While high and relatively constant release rates for S and Cl were determined for

different biomass fuels, the K release strongly depends on the ash composition. Since a meaningful prediction of the K release from the fuel to the gas phase is not feasible with fuel indexes, a qualitative determination by TEC can be performed.

TEC constitute a method to predict multi-phase equilibria, where gaseous, liquid and solid phases of interest can be identified and quantified. These calculations are conducted for a multi-component thermodynamic system in a pre-determined gas atmosphere, on the assumption that a chemical equilibrium can be achieved for the system investigated. TEC deliver qualitative information about the release behaviour of inorganic compounds (S, Cl, K, Na, Zn, Pb) and the ash melting behaviour. Especially with regard to the ash melting behaviour, relevant ash transformation processes can be identified. For a quantitative evaluation of the release of ash-forming elements fixed-bed lab-scale reactor experiments were performed.

The basic idea behind the fixed-bed lab-scale reactor is to provide a tool which is capable of the simulation of the fuel decomposition behaviour in real-scale fixed-bed biomass combustion systems. The experiment delivers information regarding thermal decomposition behaviour, the release of NO_x precursor species, the release of ash-forming elements and a first indication regarding ash melting behaviour. The results of the release of ash-forming elements can be used to estimate aerosol and gaseous SO_x and HCl emissions.

Based on combustion experiments with fixed-bed lab-scale reactors and single particle reactors, integral release data regarding ash-forming vapours can be obtained. At the moment, almost no data regarding time resolved release of ash-forming elements from single particles are available. In order to make a time resolved determination of the release behaviour possible, a new single particle reactor was developed, which was connected to an inductively coupled plasma mass spectrometer (ICP-MS). During the experiments, the temperatures at the surface and the centre of the particle, the weight loss of the particle, the pressures as well as the resulting flue gases were recorded. To couple the reactor to an ICP-MS, a part of the flue gas stream has to be delivered to the ICP-MS. This gas stream needs to be sufficiently diluted with Ar to ensure that the gas as well as the molecules it contains can be ionised in the Ar plasma. The ionised isotopes are subsequently detected by a mass spectrometer, where intensities or counts are recorded for the respective isotopes. A series of performance and validation tests were performed. The tests showed that simultaneous time resolved determination of S, Cl, K, Na, Zn and Pb is possible, in which the Cl signal is only of limited use. Based on element balances, the release ratios of ash-forming elements through the entire combustion experiments can be calculated. These release data can be used for quantification/calibration of the measured intensities of S, Cl, K, Na, Zn and Pb.

Test runs with softwood and straw were performed at reactor temperatures of 700°, 850° and 1,000°C under oxidising conditions (5.6 or 4.2 vol.% O₂). A validation of the time resolved release profiles for straw was performed by targeted interruption (quench) experiments, which also supported the interpretation of the release data. The surface and centre temperature developments of the particles clearly indicate overlapping processes

(drying, devolatilisation and char combustion) in different layers of the particle. Increasing reactor temperatures led to higher heat-up rates of the particle, higher thermal degradation rates and shorter test durations being needed to achieve complete particle burnout. Furthermore, as reactor temperatures rise, the release ratios of inorganic elements from fuel to gas phase increase. Results show S release ratios between 50%-93%, an almost complete release of Cl, even at 700°C, and K and Na release ratios below 33%. The Zn and Pb release ratios strongly depend on the reactor temperatures prevailing and on interactions with the ash matrix, where, in general, higher release ratios were obtained for softwood than for straw.

The time resolved release profiles of inorganic elements indicate that S release is mainly coupled with the decomposition of the organic matrix and that, in the case of softwood, a distinction between the release of organically and inorganically associated S is possible. In the case of K, release mechanisms proposed by [32] (decomposition of organically dissociated K for T below 500°C, KCl and K₂CO₃ decomposition above 700°C) were confirmed by the tests performed. The same mechanism can also be applied to Na. For Zn and Pb, the release strongly depends on the particle temperature development during the thermal conversion process, where a particle temperature above 700°C is necessary for a distinct release. The maximum peaks of the Zn and Pb release profiles are shifted to higher particle temperatures with rising reactor temperatures (higher heating rates), most probably triggered by transport limitations while the particle is being heated up. A clear indication of transport limitations due to the occurrence of molten phases was obvious for straw at 850° and 1,000°C. The quench tests performed are an effective method for validating the time resolved release profiles. Such tests can be used to validate the results regarding element release. They also show that the Cl release trends need to be interpreted with caution since they are overestimated during char burnout. The quench tests additionally supported the interpretation of the time resolved K release profiles with respect to KCl sublimation.

To sum up, regarding alternative non-wood feedstocks which have not been characterised with regard to their combustion behaviour in a comprehensive way so far, the following strategy for a comprehensive characterisation can be suggested, which also includes the preparation of biomass additive mixtures and biomass fuel blends. In a first step, fuel indexes calculated on the basis of results of chemical analysis, deliver a pre-evaluation of combustion-related properties that may arise. By means of TEC, a qualitative investigation of the ash melting and release behaviour is possible. In addition, information about possible ash transformation processes can be gained. With the help of fixed-bed lab-scale reactor experiments a quantitative evaluation of the release behaviour is possible. Further, a single particle reactor coupled to an ICP-MS can be used for quick and targeted experiments in a temperature range of 250°-1,050°C under inert, reducing and oxidising conditions. Moreover, with the single particle reactor, time resolved determination of inorganic element release is possible. Such data strongly support the knowledge regarding elemental release during thermal biomass conversion. The new fuel characterisation methods were developed for fixed-bed combustion systems, where also the limitations of the application have to be considered. The applicability of fuel indexes to biomass additive mixtures and biomass fuel blends has to

be checked. Also for the fixed-bed lab-scale reactor and the single particle reactor it has to be checked whether the experimental conditions during the experiments are representative of the real-scale process. Bearing in mind these limitations, the approach presented facilitates the characterisation of alternative biomass fuels, meaningful biomass additive mixtures and fuel blends, and thus minimises the need for time-consuming and expensive pilot- and full-scale tests.

5.2 Recommendations for further work

The application of additives and fuel mixtures should be investigated in more detail in single particle reactor experiments. Here, especially the online release of inorganic ash-forming elements and quench experiments with subsequent SEM/EDX analysis can lead to a better understanding regarding ash transformation processes for biomass additive mixtures or fuel blends.

At the moment, S, Cl, K, Na, Zn and Pb are determined by the single particle reactor coupled to an ICP-MS. Also an online determination of P should be performed in parallel. Presently, no online release data for P from single biomass fuel particles are available. Furthermore, these investigations can lead to a better understanding of P ash transformation and release processes. In general, extensive investigations of a broad spectrum of biomass fuels (including P-rich fuels) should be performed since up to now only two biomass fuels have been evaluated by means of the single particle reactor.

So far, only models are available for the description of the thermal decomposition behaviour of the organic matrix of single biomass particles [75, 76]. These models have already been successfully applied within computational fluid dynamics (CFD) simulations. By this approach the accuracy of the CFD simulations was significantly increased, compared with empirical models used earlier on [77]. The recorded online release data of inorganic elements provided by the single particle reactor coupled to an ICP-MS led to a better understanding of release processes. These data also represent a basis for the development of inorganic release models which can be used within CFD simulations. A combination of the existing model with release models regarding inorganic elements would provide the possibility to simulate also subsequent processes, such as particle and deposit formation, more precisely.

The characterisation methods presented were developed for fixed-bed combustion processes. The application range of these methods should be extended to other thermal decomposition processes. Here, gasification, torrefaction and pyrolysis are of major interest.

6 Bibliography

- [1] Ellabjana O., Rubb H., Blaabjergc F. Renewable energy resources: Current status, future prospects and their enabling technology. *Renewable and Sustainable Energy Reviews* 2014, 39, 748–764
- [2] WBA GLOBAL BIOENERGY STATISTICS 2015 <http://www.worldbioenergy.org/content/wba-global-bioenergy-statistics-2015-report> |Accessed Aug. 2015
- [3] Rockström J. and colleagues. A safe operating space for humanity. *Nature* 2009, 461 (24), 472-475
- [4] Hoel M., Kvemdokk S. Depletion of fossil fuels and the impacts of global warming. *Resource and Energy Economics* 1996, 18, 115-136
- [5] Höök M., Tang X. Depletion of fossil fuels and anthropogenic climate change—A review. *Energy Policy* 2013, 52, 797–809
- [6] Correlje A., Van der Linde C. Energy supply security and geopolitics A European perspective. *Energy Policy* 2006, 34, 532–543
- [7] Umbach F. Global energy security and the implications for the EU. *Energy Policy*, 2010, 38, 1229–1240
- [8] <http://www.irena.org/Publications/rejobs-annual-review-2014.pdf> |Accessed Aug. 2015
- [9] Slade R., Saunders R., Gross R., Bauen A. Energy from biomass: the size of the global resource. 2011 Imperial College Centre for Energy Policy and Technology and UK Energy Research Centre, London, 2001, ISBN: 1 903144 108
- [10] Vassilev S. V., Baxter D., Andersen L. K., Vassileva C. G. An overview of the chemical composition of biomass. *Fuel* 2010, 89, 913–933
- [11] Boström D., Skoglund N., Grimm A., Boman C., Öhman M., Broström M., Backman R. Ash Transformation Chemistry during Combustion of Biomass. *Energy and Fuels* 2012, 26, 85–93
- [12] Brunner T. Aerosols and coarse fly ashes in fixed-bed biomass combustion. PhD-Thesis 2006, Graz University of Technology, Austria, ISBN 3-9501980-3-2
- [13] Bryers R.W. Fireside slagging, fouling, and high-temperature corrosion of heat-transfer surfaces due to impurities in steam-raising fuels. *Progress in Energy and Combustion Science* 1996, 22, pp. 29-120
- [14] Winegartner, E. C. (ed.). Coal Fouling and Slagging Parameters. ASME research Committee on Corrosion and Deposits from Combustion Gases, ASME pub.,1974.

- [15] Karr C. Analytical Method for Coal and Coal Products. Academic Press, 1978, ISBN: 978-0-12-399901-6
- [16] Visser H. J. M. The influence of fuel composition on agglomeration behaviour in fluidised-bed combustion. 2004, ECN-C—04-054, <https://www.ecn.nl/docs/library/report/2004/c04054.pdf>
- [17] Gilbe C., Öhman M., Lindström E., Boström D., Backman R., Samuelsson R., Burval J., Slagging Characteristics during Residential Combustion of Biomass pellets. Energy and Fuels 2008, 22, 3536-3543
- [18] Lindström E., Öhman M., Backman R., Boström D. Influence of Sand Contamination on Slag Formation during Combustion of Wood Derived Fuels. Energy and Fuels 2008, 22, 2216-2220
- [19] Gómez Díaz C. J. 2006. Understanding biomass pyrolysis kinetics: improved modeling based on comprehensive thermokinetic analysis. PhD-Thesis 2006, Universitat Politècnica de Catalunya, Spain, ISBN: 9788469055588
- [20] Gabbott P. 2008. Principles and Applications of Thermal Analysis. ISBN-13: 978-1-4051-3171-1
- [21] Blasi C.D. Modeling chemical and physical processes of wood and biomass pyrolysis. Progress in Energy and Combustion Science 2008, 34, 47–90
- [22] Vamvukaa D., Kakaras E., Kastanakis E., Grammelis P. Pyrolysis characteristics and kinetics of biomass residuals mixtures with lignite. Fuel 2003, 82, 1949–1960
- [23] Demirbas A. Biomass resource facilities and biomass conversion processing for fuels and chemicals. Energy Conversion and Management 2004, 45 (5), 651–671
- [24] Giuntoli J., de Jong W., Verkooijen A. H. M., Piotrowska P., Zevenhoven M., Hupa M. Combustion Characteristics of Biomass Residues and Biowastes: Fate of Fuel Nitrogen. Energy and Fuels 2010, 24, 5309–5319
- [25] Karlström O., Brink A., Hupa M. Biomass Char Nitrogen Oxidation-Single Particle Model. Energy and Fuels 2013, 27, 1410–1418
- [26] Karlström O., Costa M., Brink A., Hupa M. CO₂ gasification rates of char particles from torrefied pine shell, olive stones and straw. Fuel 2015, 158, 753–763
- [27] Biswas A. K., Rudolfsson M., Broström M., Umeki K. Effect of pelletizing conditions on combustion behaviour of single wood pellet. Applied Energy 2014, 119, 79-84

- [28] Qu Z., Fagerström J., Steinvall E., Broström M., Boman C., Schmidt F. Real-time in-situ detection of potassium release during combustion of pelletized biomass using tunable diode laser absorption spectroscopy. Proceedings of the Conference Impacts of Fuel Quality on Power Production and Environment 2014, 26-31 October 2014, Snowbird, Utah, USA, EPRI (Ed.), Palo Alto, CA, USA
- [29] Van Lith S., Alonso-Ramirez V., Jensen P. A., Frandsen F. J., Glarborg P. Release to the Gas Phase of Inorganic Elements during Wood Combustion. Part 1: Development and Evaluation of Quantification Methods. Energy and Fuels 2006, 20, 964-978
- [30] Knudsen J.N., Jensen P.A., Dam-Johansen K. Transformation and release to the gas phase of Cl, K, and S during combustion of annual biomass. Energy and Fuels 2004, 18 (5), 1385–1399
- [31] Knudsen J.N. Volatilization of inorganic matter during combustion of annual biomass. PhD-Thesis, Technical University of Denmark; 2004, ISBN: 8791435110, 9788791435119
- [32] van Lith S., Jensen P.A., Frandsen F.J., Glarborg P. Release to the gas phase of inorganic elements during wood combustion. Part 2: influence of fuel composition. Energy and Fuels 2008, 22 (3), 1598–1609
- [33] Johansen J. M., Jakobsen J. G. Frandsen F.J., Glarborg P. Release of K, Cl, and S during Pyrolysis and Combustion of High-Chlorine Biomass. Energy and Fuels, 2011, 25 (11), 4961–4971
- [34] Díaz-Ramírez M., Frandsen F. J., Glarborg, P. Sebastián F., Royo J. Partitioning of K, Cl, S and P during combustion of poplar and brassica energy crops. Fuel 2014, 134, 209–219
- [35] Bäfver L., Boman C., Rönnbäck M. Reduction of particle emissions by using additives. Proceedings of the Central European Biomass Conference, 2011, 26-29 January 2011, Graz, Austria
- [36] Boman C., Böström D., Öhman M., Effect of fuel additive sorbent (Kaolin and Calcite) on aerosol particle emission and characteristics during combustion of pelletized woody biomass. Proceedings of the 16th European Biomass Conference & Exhibition 2008 June 2008, Valencia, Spain, 1514-1517, ISBN-10: 8889407581, ISBN-13: 978-8889407585
- [37] Öhman M., Boström D., Nordin A., Effect of Kaolin and Limestone Addition on Slag Formation during Combustion of Wood Fuels. Energy and Fuels 2004, 18, 1370-1376
- [38] Xiong S., Burvall J., Örberg H., Kalen G., Thyrel M., Öhman M., Boström D., Slagging Characteristics during Combustion of Corn Stovers with and without Kaolin and Calcite. Energy and Fuels 2008, 22, 3465-3470

- [39] Bäfver L., Rönnbäck M., Leckner B., Claesson F., Tullin C., Particle emission from combustion of oat grain and its potential reduction by addition of limestone or Kaolin. *Fuel Processing Technology* 2009, 90 (3), 353-359
- [40] Boström D., Grimm A., Boman C., Björnbom E., Öhman M., Influence of Kaolin and Calcite additives on ash transformations in small-scale combustion of oat. *Energy and Fuels* 2009, 23, 5184-5190
- [41] Davidsson K. O., Steenari B.-M., Eskilsson D. Kaolin Addition during Biomass Combustion in a 35 MW Circulating Fluidized-Bed Boiler. *Energy and Fuels* 2007, 21 (4), 1959-1966
- [42] Keddy P A. 2010 *Wetland Ecology: Principles and Conservation* (2nd edition). Cambridge University Press, Cambridge, UK, ISBN: 9780521519403, 9780521739672
- [43] Nordin A. Chemical elemental characteristics of biomass fuels. *Biomass and Bioenergy* 1994, 6, 339-347
- [44] Nyström I., Boström D., Boman C., Öhman M. Effect of peat addition to woody biomass pellets on slagging characteristics during combustion in residential pellet burners. In: *Proceedings 17th European Biomass Conference & Exhibition 2009 June 2009, Hamburg, Germany, ETA-Renewable Energies (Ed.), Italy, 1400-1405, ISBN-10: 8889407573, ISBN-13: 978-8889407578*
- [45] Fangerström J., Näzelius I., Boström D., Öhman M., Boman C. Reduction of fine particle- and deposit forming alkali by co-combustion of peat with wheat straw and forest residues. *Proceedings of the Conference Impacts of Fuel Quality on Power Production and Environment 2010, August 2010, Saariselkä, Finland, EPRI (Ed.), Palo Alto, CA, USA*
- [46] Lundholm K., Nordin A., Öhman M., Boström D. Reduced bed agglomeration by co-combustion biomass with peat fuels in a fluidized bed. *Energy and Fuels* 2005, 19, 2273-2278
- [47] Pommer L., Ohman M., Bostrom D., Burvall J., Backman R., Olofsson I., et.al. Mechanisms Behind the Positive Effects on Bed Agglomeration and Deposit Formation Combusting Forest Residue with Peat Additives in Fluidized Beds. *Energy and Fuels* 2009, 23, 4245-4253
- [48] Bärenthaler G., Zischka M., Hanraldsson C., Obernberger I. Determination of major and minor ash- forming elements in solid biofuels. *Biomass and Bioenergy* 2006, 30(11), 983-997

- [49] Evic N, Brunner T, Obernberger I. Prediction of biomass ash-melting behaviour – correlation between the data obtained from thermodynamic equilibrium calculations and simultaneous thermal analysis (STA). In: Proceedings 20th European Biomass Conference & Exhibition 2012 June 2012, Milano, Italy, ETA-Renewable Energies (Ed.), Italy, 807-813, ISBN 978-88-89407-54-7
- [50] Brunner T., Biedermann F., Kanzian W., Evic N., Obernberger I. Advanced biomass fuel characterization based on tests with a specially designed lab-scale reactor. *Energy and Fuels* 2013, 27, 5691-5698
- [51] Weissinger A., Fleckl T., Obernberger I. Application of FT-IR in-situ absorption spectroscopy for the investigation of the release of gaseous compounds from biomass fuels in a laboratory scale reactor - Part II: Evaluation of the N-release as functions of combustion specific parameters. *Combustion and Flame* 2004, 137, 403-417, ISSN 0010-2180
- [52] Stubenberger G., Scharler R., Obernberger I. Nitrogen release behaviour of different biomass fuels under lab-scale and pilot-scale conditions. Proceedings of the 15th European Biomass Conference & Exhibition 2007 May 2007, Berlin, Germany, 1412-1420, ISBN 978-88-89407-59-X, ISBN 3-936338-21-3
- [53] Christensen K. The Formation of Submicron Particles from the Combustion of Straw. PhD-Thesis 1995, Department of Chemical Engineering (ed), Technical University of Denmark, Lyngby, Denmark, ISBN 87-90142-04-7
- [54] Salmenoja K. Field and laboratory studies on chlorine-induced superheater corrosion in boilers fired with Biofuels. PhD-Thesis 2000, Abo Akademi, Faculty of Chemical Engineering, Abo/Turku, Finland, ISBN: 9521206195, 9789521206191
- [55] Keller R. Primärmaßnahmen zur NO_x-Minderung bei der Holzverbrennung mit dem Schwerpunkt der Luftstufung. Forschungsbericht Nr. 18. Laboratory for Energy Systems (Ed.), ETH Zürich, Switzerland 1994
- [56] Glarborg P., Jensen A. D., Johnsson J. E. Fuel nitrogen conversion in solid fuel fired systems. *Progress in Energy and Combustion Science* 2003, 29, 89–113
- [57] Weissinger A. Experimentelle Untersuchungen und reaktionskinetische Simulationen zur NO_x-Reduktion durch Primärmaßnahmen bei Biomasse-Rostfeuerungen. PhD-Thesis 2002, Graz University of Technology, Graz, Austria
- [58] Lindström E., Öhman M., Backman R., Boström D. Influence of Sand Contamination on Slag Formation during Combustion of Wood Derived Fuels. *Energy and Fuels* 2008, 22, 2216-2220

- [59] Öhman M., Boman C., Hedman H., Nordin A., Boström D. Slagging tendencies of wood pellet ash during combustion in residential pellet burners. *Biomass and Bioenergy* 2003, 27, 585–596
- [60] Baxter L., Miles T., Miles T. Jr., Jenkins B., Milne T., Dayton D., Bryers R., Oden L. The behavior of inorganic material in biomass-fired power boilers: field and laboratory experiences. *Fuel Processing Technology* 1998, 54, 47–78
- [61] Sandström M. Structural and Solid State EMF Studies of Phases in the CaO–K₂O–P₂O₅ System with Relevance for Biomass Combustion. PhD-Thesis 2006, Luleå University of Technology, Sweden, ISSN 1653-0551, ISBN 91-7264-149-5
- [62] Novakovic A., Van Lith S., Frandsen F., Jensen P., Holgersen L. Release of Potassium from the Systems K–Ca–Si and K–Ca–P. *Energy and Fuels* 2009, 23, 3423-3428
- [63] Müller M., Wolf K.J., Smeda A., Hilpert K. Release of K, Cl and S Species during Co-combustion of Coal and Straw. *Energy and Fuels* 2006, 20, 1444-1449
- [64] Boström D., Broström M., Skoglund N., Boman C., Backman R., Öhman M., Grimm A. Ash transformation chemistry during energy conversion of Biomass. *Proceedings of the Conference Impact of Fuel Quality on power production & Environment* 2010, 1-20
- [65] Risnesa H., Fjellerupb J., Henriksenc U., Moilanend A., Norbye P., Papadakisb K., Posseltf D., Sorensenb L.H., Calcium addition in straw gasification. *Fuel* 2003, 82, 641–651
- [66] Osborn E.F.; Muan A.; *Phase Equilibrium Diagrams of Oxide Systems*. American Ceramic Society and the Edward Orton Jr. Ceramic Foundation, 1960, OCLC: 223365250
- [67] Flemming F., van Lith S. Quantification of the Release of Inorganic Elements during Combustion of Biofuels and Coals – Comparison and Evaluation of Results from Different Techniques. Final report for SES6-CT-2003-50267: Ash and Aerosol Related Problems in Biomass Combustion and Co-Firing (BIOASH), Task 1.4 2007
- [68] van Lith S. Release of Inorganic Elements during Wood-Firing on a Grate. PhD-Thesis 2005, Technical University of Denmark, Lyngby, Denmark, ISBN: 87-91435-29-3
- [69] Monatser, A. *Inductively coupled plasma mass spectrometry*. Wiley-VCH, 1998, pp. 811, ISBN 978-0-471-18620-5
- [70] Knudsen, N. J.; Jensen, A. P.; Lin, W.; Frandsen, J. F.; Dam-Johansen, K. Sulfur Transformations during Thermal Conversion of Herbaceous Biomass. *Energy Fuels* 2004, 18, pp 810-819
- [71] Saleh S. B., Flensburg J. P., Shoulaifar T. K., Sárossy Z., Hansen B. B., Egsgaard H., DeMartini N., Jensen P. A., Glarborg P., Dam-Johansen K. Release of Chlorine and Sulfur during Biomass Torrefaction and Pyrolysis. *Energy and Fuels* 2014, 28 (6), 3738–3746

- [72] Werkelin J. Ash forming matter and their chemical forms in woody biomass fuels. PhD-Thesis, Abo Akademi University 2008, Finland
- [73] Quyn D. M., Wu H., Li C.-Z. Volatilization and catalytic effects of alkali and alkaline earth metallic species during the pyrolysis and gasification of Victorian brown coal. Part I. Volatilization of Na and Cl from a set of NaCl-loaded sample. *Fuel* 2002, 81 (2), 143-149
- [74] Quyn D. M., Wu H., Bhattacharya S. P., Li, C.-Z. Volatilization and catalytic effects of alkali and alkaline earth metallic species during the pyrolysis and gasification of Victorian brown coal. Part II. Effects of chemical form and valence. *Fuel* 2002, 81 (2), 151-158
- [75] Mehrabian R., Zahirovic S., Scharler R., Obernberger I., Kleditzsch S., Wirtz S., Scherer V., Lu H., Baxter L. A CFD model for thermal conversion of thermally thick biomass particles. *Fuel Processing Technology* 2012, 95, 96–108
- [76] Lu H. Experimental and modeling investigations of biomass particle combustion. PhD-Thesis 2006, Brigham Young University (Department Chemical Engineering), USA, <http://scholarsarchive.byu.edu/cgi/viewcontent.cgi?article=1777&context=etd>
- [77] Mehrabian R., Shiehnejadhesar A., Scharler R., Obernberger I. Multi-physics modelling of packed bed biomass combustion. *Fuel*, 2014, 122, 164–178

7 Appendix

7.1 Scientific journal papers

Paper I

Fuel Indexes: A Novel Method for the Evaluation of Relevant Combustion Properties of New Biomass Fuels

Peter Sommersacher,^{*,†} Thomas Brunner,^{†,‡,§} and Ingwald Obernberger^{†,‡,§}

[†]BIOENERGY 2020+ GmbH, Inffeldgasse 21b, A-8010 Graz, Austria

[‡]Institute for Process and Particle Engineering, Graz University of Technology, Inffeldgasse 21a, A-8010 Graz, Austria

[§]BIOS BIOENERGIESYSTEME GmbH, Inffeldgasse 21b, A-8010 Graz, Austria

ABSTRACT: The increasing demand for biomass fuels leads to the introduction of new biomass fuels into the market. These new biomass fuels (e.g., wastes and residues from agriculture and the food industry, short rotation coppices, and energy crops) are usually not well-defined regarding their combustion behavior. Therefore, fuel characterization methods with a special focus on combustion-related problems (gaseous NO_x, HCl, and SO_x emissions, ash-melting behavior, and PM emissions) have to be developed. For this purpose, fuel indexes are an interesting option. Fuel indexes are derived from chemical fuel analyses and are checked and evaluated regarding their applicability by measurements performed at lab- and real-scale combustion plants for a large variety of fuels. They provide the possibilities for a pre-evaluation of combustion-relevant problems that may arise from the use of a new biomass fuel. A possible relation to describe the corrosion risk is, for instance, the molar 2S/Cl ratio. The N content in the fuel is an indicator for NO_x emissions, and the sum of the concentrations of K, Na, Zn, and Pb in the fuel can give a prediction of the aerosol emissions, whereas the molar (K + Na)/[x(2S + Cl)] ratio provides a first indication regarding the potential for gaseous HCl and SO_x emissions. The molar Si/K ratio can supply information about the K release from the fuel to the gas phase. The molar Si/(Ca + Mg) ratio can give indications regarding the ash-melting temperatures for P-poor fuels. For P-rich fuels, the (Si + P + K)/(Ca + Mg) ratio can be used for the same purpose. The fuel indexes mentioned can provide a first pre-evaluation of combustion-relevant properties of biomass fuels. Therefore, time-consuming and expensive combustion tests can partly be saved. The indexes mentioned are especially developed for grate combustion plants, because interactions of the bed material possible in fluidized-bed combustion systems are not considered.

1. INTRODUCTION, BACKGROUND, AND SCOPE

The general increase in energy demand, higher costs, and oncoming depletion of fossil fuels are reasons for considerable research on renewable energies and raw material resources. Biomass energy can be an important factor in reducing greenhouse gas emissions and energy source independence.¹

To increase the biomass use in the energy sector, products such as wastes and residues from agriculture and the food industry, as well as short-rotation plants, such as poplar, and energy crops, such as *Miscanthus*, *Arundo donax*, and grasses, can be used. These new biomass fuels gain rising interest for use in biomass combustion systems. As a result, new biomass fuels are of relevance for furnace and boiler manufacturers as well as utilities. According to the increasing prices for conventional biomass fuels (e.g., wood), new options for heat and power generation from cheap feedstocks have to be identified to increase the economic efficiency of biomass heating and combined heat and power (CHP) plants. The introduction of new biomass fuels may also create new employment opportunities in rural areas and, therefore, also contribute to the social aspect of sustainability.^{2,3}

For the past decade, agricultural studies throughout Europe have been focusing on introducing new nonfeed crops with a perspective for industrial applications. Perennial rhizomatous grasses, such as switchgrass (*Panicum virgatum*), *Miscanthus* spp., giant reed (*A. donax*), and red canarygrass (*Phalaris arundinacea*), have been considered as the most promising energy crops for Europe. The employment of such raw

materials contributes to reduce anthropogenic CO₂ emissions. Also, the situation of the agricultural sector in the European Union (EU) can be improved. This sector is characterized by food surplus, which has led to a policy of setting land aside. Therefore, introducing alternative nonfood crops as energy crops can represent a new opportunity for the population of rural areas. Perennial grasses, such as *Miscanthus* and giant reed, show some ecological advantages. They require limited soil management and a low demand for nutrient inputs. Also, further restoration of degraded land may be possible.⁴

Short-rotation coppices (SRCs) are fast-growing tree species, which are used to produce biomass as a renewable energy source. The most common SRCs are willow and poplar, which have been shown to be viable alternatives to fossil fuels.²

Agricultural residues, such as olive stones, are already used as fuels for combustion processes; however, a great further potential of these fuels exist, which is presently not used but disposed.⁵

However, because new biomass fuels are not well-defined yet regarding their combustion behavior, fuel characterization with a special focus on combustion-related fuel properties is a first important step for their introduction. Possible ash-related problems (ash melting on grates, bed agglomeration in fluidized-bed combustion systems, deposit formation and

Received: August 29, 2011

Revised: November 25, 2011

Published: November 30, 2011



corrosion, and particulate emissions) as well as problems regarding NO_x , SO_x , and HCl emissions are thereby the main focus points. With state-of-the-art fuel characterization methods, these issues cannot be sufficiently covered, and therefore, new and advanced fuel characterization methods are needed. One option to gain quick first indications regarding the problems mentioned is the development, evaluation, and application of fuel indexes as one advanced biomass fuel characterization tool.

1.1. Background and Scope. The fireside behavior of minerals in coal was first investigated more than 100 years ago. After the beginning of burning high-sulfur coals rich in pyrites (FeS_2) on grates, it was quickly recognized that pyrite was responsible for the formation of clinkers. For the first time, a combustion-related problem was directly related to a specific mineral species. It was understood that iron occurring in high-sulfur coals acted as a fluxing agent, lowering the melting temperature of quartz and clays found in coal. These early problems associated with slagging were the trigger for the development of empirical correlations for the prediction of slagging tendencies. The correlations describe the relationship between the melting temperature of slag and the proportional distribution between basic and acidic constituents.⁶

Afterward, the increasing electricity demand since the 1950s as well as the ambition to increase the electric efficiency resulted in continuously increasing steam temperatures. Also, the use of more problematic coals resulted in further fireside problems, such as ash sintering or slagging, fouling of convective heat recovery surfaces, and high-temperature corrosion. Therefore, various empirical correlations especially to predict the ash-sintering behavior of coal have been developed.⁶

In a pre-evaluation step of this work, existing empirical correlations for coals were tested regarding their applicability for biomass fuels. It was seen that indexes developed for coal cannot be applied for biomass. Because coal is a type of sedimentary rock, minerals can occur disposed as tiny inclusions within macerals, layers, nodules, fissures, and rock fragments. Thick layers and abundant nodules are removed by standard preparation facilities. The thinner layers and nodules stay in the coal and typically consist of aluminum silicates (clay, illite, kaolinite, feldspar) and silicon oxide (quartz). The alkali metals (typically Na) are bound in this aluminum silicate structure and occur in minor concentrations. In biomass fuels, in contrast, K exists in high concentrations, and its chemical binding in the fuel matrix is different from coal. K occurs as highly mobile ion in biomass fuels. Si as a further example is introduced in the plants by absorption of silicate acid from the soil. Si is deposited as a hydrated oxide usually in an amorphous form but occasionally in crystalline form. Dependent upon the biomass species, the major elements responsible for the ash chemistry can roughly be categorized in low-Si/high-Ca-containing fuels, e.g., wood and woody biomass and high-Si/low-Ca-containing fuels, e.g., herbaceous biomass. It can generally be said that coals contain higher amounts of S mostly in the form of FeS_2 . In biomass plants, S exists as sulfates or organic sulfur. The amount of Cl in coal depends upon the coal type and exists predominantly as inorganic alkali chlorides and a smaller amount of unspecific organic chlorides. In biomass, Cl appears as a chloride ion, where its concentration is closely related to the nutrient composition of the soil.⁶ The difference in occurrence and in chemical binding of certain elements explains the non-applicability of empirical coal correlations for

sintering or slagging, fouling, and high-temperature corrosion on biomass fuels.

Far less empirical correlations or fuel indexes predicting combustion-related problems have thus far been found in the literature for biomass. For fluidized-bed systems, the indexes $(\text{K} + \text{Na})/(2\text{S} + \text{Cl})$, $(\text{K} + \text{Na} + \text{Si})/(\text{Ca} + \text{P} + \text{Mg})$, and K/Si have been investigated.⁷ The index $(\text{Na} + \text{K})/(2\text{S} + \text{Cl})$ is based on the general observation that the initial gas-phase alkali concentration is attributable to the alkali concentration in the fuel. A molar $(\text{Na} + \text{K})/(2\text{S} + \text{Cl})$ ratio in the fuel >1 reflects the chance that the excess alkali over the sum of S and Cl would stay in the bed and may react with silicates. The formation of alkali silicates is often observed and leads to sintering or defluidization. The index $(\text{K} + \text{Na} + \text{Si})/(\text{Ca} + \text{P} + \text{Mg})$ is applied to describe the probability of the formation of a non-sticky outer coating on a bed material particle. For a ratio smaller than 1, the refractory outer coating is likely to form and prevent the sintering of coatings. Also, a third agglomeration indicator, the molar K/Si ratio, was introduced, where values >1 indicate that the occurrence of agglomeration is more likely a result of melt-induced sintering than the sintering of coating.

On the basis of results of test runs in a residential biomass pellet boiler with 12 different fuels, which were combusted, the slagging tendencies and the K retention have been investigated. The molar amounts of $\text{Si}/(\text{Cl} + \text{Ca} + \text{Mg})$ in the fuel should describe the K retention in residual ash (slag and bottom ash). The second correlation, the molar amounts of $\text{Si}/(\text{Cl} + \text{Ca} + \text{Mg})$ in the residual ash, should describe the K retention in the slag and the slagging tendency. There is a trend reported for the second correlation, where with increasing value of this index, the K retention in the slag and the slagging tendency increase.⁸ It is assumed that the elements Cl, Ca, and Mg may increase the K release, whereby higher Si contents in the fuel favor the K retention in the ash and slag.

The molar $\text{Si}/(\text{Ca} + \text{Mg})$ ratio has been reported to predict the slagging tendency for residential heating appliances, where with rising value, slagging increases.⁹

Although the indexes of $(\text{K} + \text{Na})/(2\text{S} + \text{Cl})$, $(\text{K} + \text{Na} + \text{Si})/(\text{Ca} + \text{P} + \text{Mg})$, and K/Si were developed for fluidized-bed systems, where interactions of the bed material influence the combustion behavior, some fundamental considerations may also be used within this work focusing on fixed-bed systems.

The aim of this work was the evaluation of the applicability of already defined fuel indexes as well as the development of new fuel indexes, which can be applied to predict combustion-related problems. This work is based on data from lab, pilot, and field tests performed with a broad spectrum of biomass fuels at fixed-bed combustion systems.

2. METHODOLOGICAL APPROACH

2.1. Fuels Investigated. Biomass fuels from five different biomass categories, which are typical for different climate zones, were used within this study: (1) wood and woody biomass (WWB): (i) beech woodchips from Austria, (ii) spruce wood chips from Austria, (iii) spruce pellets from Austria, (iv) bark of softwood, (v) waste wood, and (vi) torrefied softwood; (2) SRC: (i) poplar from Austria; (3) herbaceous and agricultural biomass (HAB): (i) *Miscanthus* pellets from Germany, (ii) wheat straw from Austria, (iii) olive kernels from Greece, (iv) maize spindle pellets (maize residues) from Austria, and (v) grass pellets; (4) others: (i) sewage sludge from Austria; and (5) industrial biomass residues: (i) decanter and rapeseed press cake and (ii) residues of starch production.

The group WWB represents the conventional biomass fuels, whereas the remaining groups represent new biomass fuels.

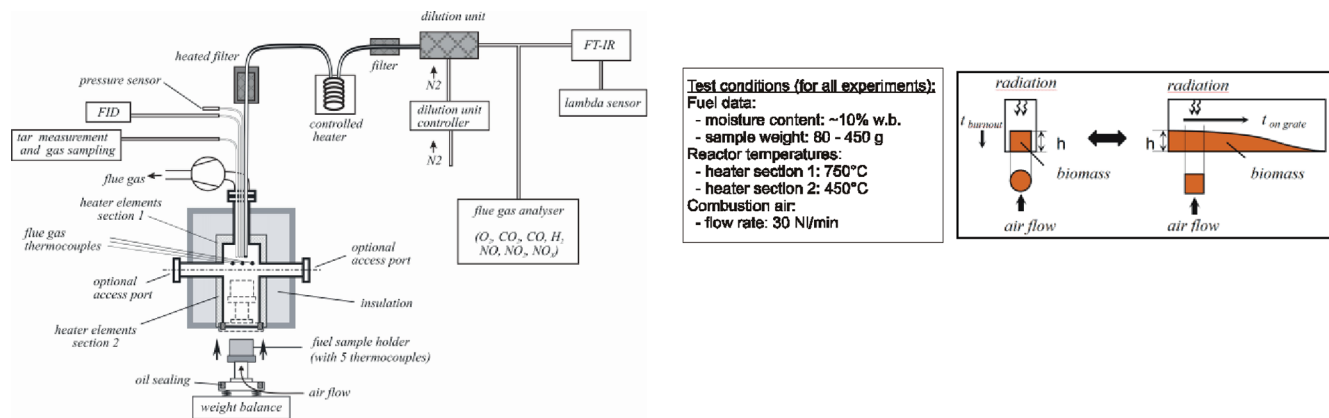


Figure 1. Scheme of the lab-scale reactor, including measurement setup (left), definition of common test conditions for all experiments (middle), and projection of the lab-scale reactor fuel bed to the fuel layer in a grate furnace (right).^{10,11}

2.2. Methodology. Proximate and ultimate analyses of the fuels investigated (ash content, contents of N, S, Cl, and major and minor ash-forming elements) are applied as the basis for the work presented. The analytical methods are described in section 3. From the results of these analyses, fuel indexes are calculated and evaluated. They are defined by considering the physical behavior and chemical reactions of dedicated elements during biomass combustion, known interactions of different ash-forming elements during thermal biomass conversion, and correlations and experiences gained from pilot- and real-scale combustion as well as lab-scale combustion tests with conventional and new biomass fuels. Data derived from combustion tests performed at BIOENERGY 2020+, the Institute for Process and Particle Engineering, Graz University of Technology, and BIOS BIOENERGIESYSTEME GmbH, Graz, Austria, were considered.

2.3. Pilot- and Real-Scale Combustion Tests. All combustion plants have geometrically separated primary and secondary combustion zones and, thus, enable an efficient air staging. The primary air ratio (amount of primary air/stoichiometric amount of air) is typically below 1 (0.6–0.9), and the overall air ratio applied is between 1.4 and 1.6. The plants are also equipped with flue gas recirculation, which ensures that the bed temperature is kept in a range of 900–1100 °C.

The real-scale combustion plants investigated are also grate-fired combustion systems with nominal thermal boiler capacities between 0.5 and 110 MW. Also, these boilers are equipped with air-staging technology, and most of them are equipped with flue gas recirculation. Grate combustion plants representing the present state-of-the-art were chosen, and only comparable combustion setups were considered within the evaluation.

During the pilot- and real-scale combustion tests, the following data were collected: (1) Fuel sampling and subsequent analyses: (i) moisture content, ash content, and chemical composition. (2) Aerosol and fly ash sampling: (i) For aerosol emissions, low-pressure-cascade impactors (Berner-type low-pressure impactors) were used. (ii) For total fly ash emissions, the gravimetric method according to VDI 2066 was used. (3) Deposit sampling with deposit probes. (4) Emission measurements concerning CO, CO₂, NO, NO_x, O₂, SO_x, and HCl: (i) CO, CO₂, and O₂ were measured with a multi-component gas analyzer (Rosemount NGA 2000). This device uses non-dispersive infrared measurement technique (NDIR) for CO and CO₂ analyses and paramagnetism as a measurement principle for O₂ detection. (ii) A nitric oxide analyzer (ECO Physis CLD 700 El ht), which uses the principle of chemiluminescence, has been used for NO and NO_x detection. (iii) The SO_x and HCl emissions were performed by discontinuous measurements according to VDI 3480, Sheet 1. (5) Determination of the furnace temperatures. (6) Sampling of all relevant ash fractions (bottom ash, furnace ash, cyclone ash, filter fly ash, and aerosols) and subsequent analyses: (i) chemical composition. (7) Recording of all relevant operating parameters (O₂ content in the flue gas, furnace temperature, load, combustion air supply, etc.)

The methods used for fuel and ash analyses are described in section 3. On the basis of the analysis results and measurement data, energy, mass, and element balances over the plant were calculated. Moreover, recovery rates for all ash-forming elements considered were evaluated to ensure the quality of the data. Only test runs with recovery rates >90% were used for further evaluation.

2.4. Lab-Scale Reactor Tests. In addition, results from test runs with a lab-scale reactor especially designed for the investigation of the thermal decomposition behavior of biomass fuels have been considered.

This lab-scale reactor consists of a cylindrical retort (height, 35 cm; inner diameter, 12 cm), which is heated electrically and controlled by two separated proportional–integral–derivative (PID) controllers (see Figure 1, left). The fuel is put in a cylindrical holder of 100 mm height and 95 mm inner diameter. The material of the reactor wall and sample holder is silicon carbide, which is inert under reducing and oxidizing conditions; therefore, the wall does not react with the fuel, ash, and flue gas. The mounting and vessel for the fuel bed are placed on the plate of a scale. The scale is mechanically separated from the retort by a liquid sealing (synthetic thermal oil: Therminol 66). The scale is used to determine the weight loss of the sample.

With this setup, it is possible to continuously measure the mass reduction of the sample during drying, pyrolysis, gasification, and charcoal combustion. The sample is introduced into the preheated reactor, and therefore, a rapid heating, which is well-comparable to the heating in real thermal conversion processes, can be achieved. The test conditions for all test runs performed with the lab-scale reactor are defined in Figure 1.

The following measurements/analyses were performed during each of the combustion test runs: (1) Mass decrease of the fuel over time (balance). (2) Concentrations of flue gas species over time: (i) Determination of CO₂, H₂O, CO, CH₄, NH₃, HCN, N₂O, and basic hydrocarbons was performed with a multi-component Fourier transform infrared (FTIR) spectroscopy device (Ansyco Series 447). (ii) The O₂ and H₂ concentrations were measured with a multi-component gas analyzer (Rosemount NGA 2000). This device uses paramagnetism as a measurement principle for O₂ detection and a thermal conductivity detector (TCD) for H₂ detection. (iii) The amount of total hydrocarbons (C_xH_y) was determined with a flame ionization detector (FID, Bernath Atomic 3005), which detects organic compounds by ionization in a burning H₂ flame. (iv) Wide-band λ sensor (O₂). (v) A nitric oxide analyzer (ECO Physis CLD 700 El ht), which uses the principle of chemiluminescence, has been used for NO and NO₂ detection. (3) Temperature measurements over time: (i) Five thermocouples in the fuel bed (three different heights NiCr–Ni). (ii) Thermocouples in the gas phase (NiCr–Ni). (4) Analysis of the biomass fuel used and residual ash produced (see section 3).

The data of the fuel analysis and the residual ash analysis as well as the weight measurements of the fuel sample and the ash sample can be

used to calculate the elemental release to the gas phase. This is performed by calculating the mass balance for every relevant element as well as the total ash.

The lab-scale reactor has been designed to represent the burning conditions of a biomass fuel layer on a grate as well as possible (Figure 1, right). This approach is valid if diffusional transport and mixing effects on the grate can be neglected in comparison to the transport of the fuel along the grate. The validation has been achieved in previous research, which has shown that the fuel transport along the grate can be fluidically characterized by a plug flow in good approximation.^{10,11}

2.5. Definition of Fuel Indexes. On the basis of the evaluation of the fuel analysis and test runs as well as a theoretical evaluation, the following fuel indexes have been investigated and are presented in the following: (1) N concentration in the fuel as an indicator for NO_x emissions, (2) sum of K, Na, Zn, and Pb as an indicator regarding aerosol emissions (fine particles smaller than 1 μm) and deposit buildup, (3) molar Si/K ratio for an estimation of the K release from the fuel to the gas phase, (4) molar 2S/Cl ratio for the prediction of the risk of high-temperature corrosion, (5) molar (K + Na)/[x(2S + Cl)] ratio for the prediction of the gaseous emissions of SO_x and HCl, and (6) the prediction of the ash-melting temperatures with the molar Si/(Ca + Mg) and molar (Si + K + P)/(Ca + Mg) ratios.

The definitions of the above-mentioned indexes are based on theoretical considerations. With the exception of the molar Si/K ratio and the factor *x* occurring in the index (K + Na)/[x(2S + Cl)], all indexes were validated using results of pilot- and real-scale combustion tests. The factor *x* is a function of the release of K, Na, S, and Cl from the fuel to the gas phase, which has been derived from lab-scale reactor tests (see Figure 1), because of the well-defined conditions provided by this unit. To evaluate the index of the molar Si/K ratio, data from the lab-scale reactor have also been used.

3. CHEMICAL FUEL ANALYSES: THE BASIS FOR THE CALCULATION OF FUEL INDEXES

3.1. General Aspects. Because the quality of the fuel analyses applied forms the most important basis for the evaluation of fuel indexes, only highly accurate methods, which have already proven their applicability for biomass fuels, should be applied. Moreover, it has to be taken into consideration that the fuel sample investigated is representative for the biomass fuel of interest. Especially when new agricultural biomass fuels are evaluated, it must always be clearly defined if the fuel contains, for instance, leaves, stalks, grains, whole fruits, etc., because usually different parts of a plant show strongly deviating chemical compositions. The application of the following analysis methods, which have also been used by the authors, is strongly recommended. The recommendation of the methods is a result of the FP6 project BioNorm,¹² which among other aspects also dealt with the definition of standards and best practice guidelines for biomass fuel analyses. Recommendations of this project also resulted in new European standards implemented by CEN/TC 335.

3.2. Moisture Content. The moisture content of fuel samples has been determined according to ÖNORM CEN/TS 14774 (determination of the weight loss during drying at 105 °C until a constant weight is reached).

3.3. Fuel Sample Preparation. Sample preparation has been carried out according to CEN/TS 14780: the samples are homogenized, and a cone is formed and subsequently divided into four portions. The two opposing portions are mixed to receive two sub-samples. One of the two sub-samples is stored as a retain sample. The other sub-sample is handled as follows: (1) drying of the sample at 105 °C, (2) milling of the whole sample in a cutting mill to a particle size <4 mm, (3) sample division, and (4) milling of the final analysis sample in an

ultracentrifugal mill equipped with a titanium rotor and screen to a particle size <0.2 mm.

3.4. Determination of the Ash Content. The ash content has been determined according to CEN/TS 14775 by determination of the loss of ignition at 550 °C. With this method, it has to be taken into account that especially Ca-rich fuels form considerable amounts of carbonates at the proposed treatment temperature. In real-scale systems, on the other side, almost no carbonates and preferably oxides are formed because of the significantly higher combustion temperatures. Consequently, the ash content is overestimated in comparison to the amount of ashes formed in a real process. Therefore, in deviation from CEN/TS 14775, it is recommended to determine the inorganic carbon content of the ashed fuel sample additionally and to correct the ash content by subtracting the CO₂ bound in carbonates.

3.5. Determination of C, H, N, and Cl Contents. The determination of C, H, and N contents of biomass fuels has been carried out according to ÖNORM CEN/TS 15104 by combustion and subsequent gas-phase chromatographical separation and measurement in an elemental analyzer (Vario EL 3, Elementar). The determination of chlorine should be carried out according to ÖNORM CEN/TS 15289, applying a digestion step based on bomb combustion in oxygen and absorption in NaOH (0.05 molar), followed by a measurement by ion chromatography (ISC 90, Dionex).

3.6. Major and Minor Elements and S Concentrations. Major and minor elements in fuels have been determined by multi-step pressurized digestion of the fuel with HNO₃ (65%)/HF (40%)/H₃BO₃ (Multiwave 3000, Anton Paar), followed by measurement by inductively coupled plasma–optical emission spectroscopy (ICP–OES, Arcos, Spectro) or inductively coupled plasma–mass emission spectroscopy (ICP–MS, Argiland 7500, Agilent), depending upon detection limits. This digestion method is of great importance to ensure a complete dissolution of the ash matrix, which is a basic requirement for correct element detection.

3.7. Ash Sample Preparation. The same sample preparation steps that are applied for the fuel sample are necessary for the bottom, furnace, and boiler ash (see section 3.3).

For fly ash samples, a vaporization of the silica wool used for sampling is necessary with HF (40%).

The aerosol samples are dissolved from the impactor foils in the respective fluid, which is used for digestion.

3.8. Determination of the Concentrations of Major and Minor Elements in the Ash. For the determination of major and minor elements, except Cl, the same methods as described for the fuel analysis have been applied (see section 3.6).

The Cl content was measured by ion chromatography (ISC 90, Dionex) after elution for 24 h with deionized water.

3.9. Determination of the Ash-Melting Behavior. The determination of the ash-melting behavior has been performed according to prCEN/TS 15370-1. The fuel samples are ashed at a temperature of 550 °C, and the remaining ash is pressed into cylindrical molds. These samples are then heated in an oven under oxidizing conditions. The following temperatures are determined: (1) sintering temperature, corners of the mold first become round; (2) sphere temperature, top of the mold takes a spherical shape; (3) hemisphere temperature, entire mold takes a hemispherical shape; and (4) melting temperature, molten ash collapses to a flattened button.

For the evaluation of the ash-melting behavior, primarily the sintering temperature (start of ash melting) and the temperature window between the sintering and melting temperatures are of relevance. It has to be considered that the characteristic ash-melting temperatures are valid for the total ash (fuel ash). In real-scale applications, the distribution of certain elements in different ash fractions may influence the melting temperatures of the individual fractions.

4. SELECTED RELEVANT FUEL INDEXES AND THEIR APPLICATION

4.1. N Content as an Indicator for the NO_x Emission Potential. In biomass combustion processes, NO_x emissions mainly result from the fuel N, while their formation from the combustion air (prompt and thermal NO_x formation) plays only a minor role.^{13–15} For the pre-evaluation of a new biomass fuel, it is important to know if problems with NO_x emissions exceeding the emission limits have to be expected, which cannot be overcome by primary measures and make secondary measures for NO_x emission control [e.g., selective non-catalytic reduction (SNCR)] affordable.

On the basis of results of test runs at modern state-of-the-art grate combustion plants (see section 2.3) equipped with air-staging technology, a correlation between the conversion rate of fuel N to N in NO_x emissions has been derived (see Figure 2),

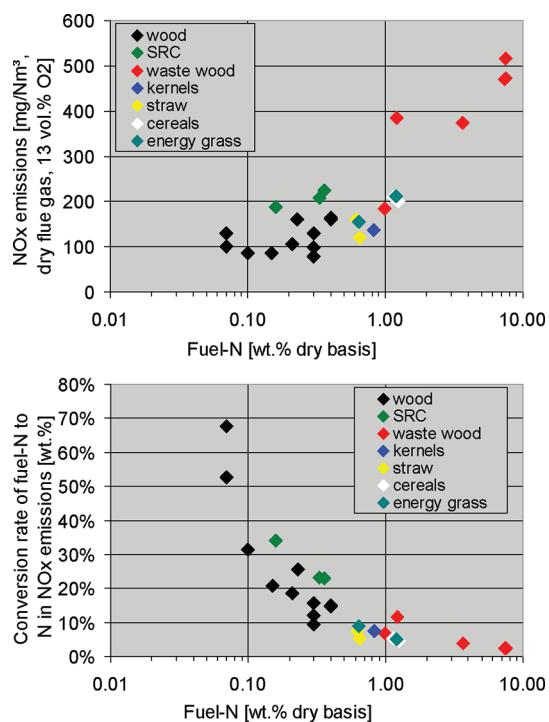


Figure 2. NO_x emissions and fuel N converted to N in NO_x dependent upon the N content. Explanation: both correlations are statically significant ($p < 0.05$).

which can be applied to estimate the NO_x emissions formed during the combustion of a certain fuel in grate combustion systems. Because combustion plants investigated are equipped with air-staging technology, the index is only valid for state-of-the-art grate-fired combustion units with air-staging technology.

As seen in Figure 2, the NO_x emissions increase with the N content of the fuel. However, there is no linear correlation

because, as the second diagram shows, with an increasing N content of the fuel, the conversion of fuel N to NO_x decreases.

The N concentrations in the biomass fuels can be categorized into (1) low-N fuels (<0.4 wt %, db), e.g., wood fuels; (2) medium-N fuels (0.4–1 wt %, db), e.g., SRCs, kernels, and straw; and (3) high-N fuels (1–10 wt %, db), e.g., cereals and waste wood.

Experience shows that many new biomass fuels are medium- or high-N fuels (e.g., SRCs, cereals, energy grass); thus, NO_x emissions >200 mg N⁻¹ m⁻³ (related to dry flue gas and 13 vol % O₂) have to be expected.

4.2. Sum of K, Na, Zn, and Pb as an Indicator Regarding Aerosol Emissions (Fine Particles Smaller than 1 μm) and Deposit Buildup. This indicator can be used to evaluate if highly efficient dust precipitators [electrostatic precipitators (ESPs) and baghouse filter] will be needed to keep the particulate matter (PM) emission limits for a plant using a specific fuel. It is also an indicator for the deposit buildup on heat-exchanger surfaces. This index is related to the formation of aerosols (particles with a diameter smaller than 1 μm = PM₁) during the combustion process and does not include coarse fly ashes.

A part of the semi-volatile and volatile ash-forming elements, such as K, Na, S, Cl, Zn, and Pb, is released from the fuel to the gas phase during combustion. In the gas phase, these elements undergo homogeneous gas-phase reactions, and later, because of supersaturation in the gas phase, these ash-forming vapors start to nucleate or condense on the surfaces of existing particles or heat-exchanger tubes.^{16,17}

Because for most biomass fuels K usually shows significantly higher concentrations than other aerosol-forming elements (e.g., Na, Zn, and Pb), the release of K is most relevant for the formation of aerosol emissions.

It is reported in previous studies^{18,19} that the main part of K released to the gas phase consists of KOH and KCl in the entire temperature range of 500–1150 °C. Smaller amounts of K are released as K₂SO₄ and K₂CO₃ in this temperature range. It is evident that there is a number of parameters influencing the K release.

It has also been reported²⁰ that ash-forming elements, such as Ca, Si, and P, may influence the K release to the gas phase to a certain degree. Therefore, well-defined mixtures of K, Ca, and Si (or P) species were heat-treated in a reactor at a constant temperature (900 and 1000 °C). The main findings of these experiments are summarized as follows. The presence of water in the gas flow was found to significantly enhance the K-release rate in both the K–Ca–Si and K–Ca–P systems. The K–Ca–Si system shows higher release rates at 1000 °C than at 900 °C. Doubling of the molar Ca/Si ratio in K₂CO₃–CaO–SiO₂ mixtures increased the K-release rate about 2 times. This suggests that it is more likely that SiO₂ reacts with CaO and K is being released to the gas phase instead of being incorporated into silicate structures. For the K–Ca–P system, where K₂CO₃ was used as the K source, it has been observed that, with a decreasing molar Ca/P ratio, the K-release rate significantly decreases. In the case of K–Ca–P mixtures, with KCl as the K source, the Ca/P ratio had no effect on the K-release rate. It has been proven that the sublimation of KCl is less influenced by other elements, whereas the release of K₂CO₃ is enhanced in the presence of water vapor because of the reaction to KOH.

Straw, *Miscanthus*, and maize residues are typical fuels with increased Si and slightly increased P concentrations. Because of still existing uncertainties regarding the K release, the

indications made by this index must be handled with care for Si- and P-rich fuels (see also section 4.3).

As presented in Figure 3, the sum of K, Na, Zn and Pb in the fuel can be applied as an indicator regarding the potential for

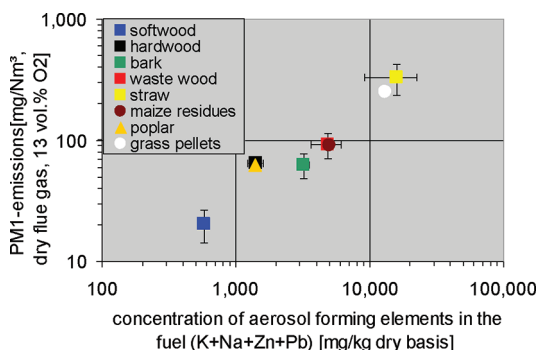


Figure 3. PM₁ emissions in the flue gas downstream of the boiler versus concentrations of aerosol-forming elements in the fuel. Explanation: the correlation is statistically significant ($p < 0.05$).

PM₁ emissions. The fuel and PM₁ emission data presented are taken from a considerable number of pilot- and real-scale test runs at grate-fired combustion plants (see also section 2).

It can be seen in Figure 3 that, with an increasing sum of K, Na, Zn, and Pb in the fuel, the aerosol emissions increase. According to this index regarding aerosol emissions, biomass fuels may be categorized in (1) low PM₁ emission range, index < 1000 mg/kg dry basis (db) for softwood; (2) medium PM₁ emission range, index 1000 – $10\,000$ mg/kg db for poplar, hardwood, bark, waste wood, and maize residues; and a (3) high PM₁ emission range, index $> 10\,000$ mg/kg db for grass pellets and straw.

New biomass fuel assortments (e.g., poplar, *Miscanthus*, and maize residues) are most commonly located in the medium to high PM₁ emission range.

Because increasing aerosol emissions are usually associated with increased deposit formation on heat-exchanger tubes (because of the fact that aerosol formation is always accompanied by direct condensation of ash vapors on cold heat-exchanger surfaces), with increased values of this index, also, deposit buildup usually increases. In future work, the influence of Si and P on the K release and, thus, aerosol formation will be investigated in more detail, especially for new biomass fuels.

4.3. Molar Si/K Ratio as an Indicator for the K Release.

A high molar Si/K ratio leads to a preferred formation of potassium silicates,^{19–21} which are bound in the bottom ash. Therefore, the K release is reduced. This is of relevance because, for instance, aerosol formation strongly depends upon the amount of K released from the fuel. Moreover, if less K is available in the gas phase for reactions with S and Cl, the gaseous SO_x and HCl emissions may increase.

In Figure 4, data regarding the correlation between the molar Si/K ratio and the K release, gained from lab-scale test runs, are presented.

For very high Si/K ratios (i.e., for sewage sludge), a good embedding of K in the bottom ash and, consequently, a very low K release prevails. However, for low Si/K ratios (< 2.5), no clear conclusion can be made concerning the dependency of the K release upon the Si/K ratio. Other parameters, such as

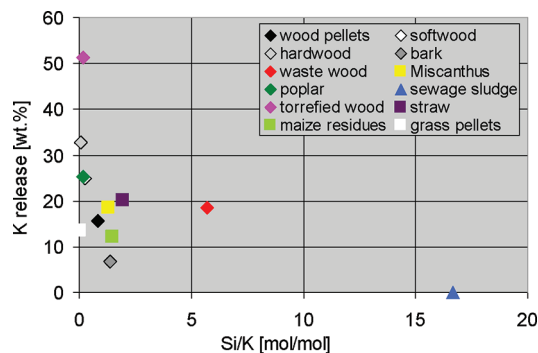


Figure 4. Molar Si/K ratio versus K release for different biomass fuels. Explanations: no statistical significance.

the fuel bed temperatures, as well as the association of K in the fuel, seem to have a strong influence on the K release.

As already mentioned in section 4.2, also, P may influence the K release. P is able to bind K in the residual ash as potassium phosphates.²² The formation of melted K–P phases can also be explained with the ternary-phase diagrams CaO–K₂O–P₂O₅ and MgO–K₂O–P₂O₅.²³ From these phase diagrams, possible low melting molecules, e.g., KPO₃, can be determined. Also, Ca and Mg may influence the K release. A possible explanation for this behavior is that Ca primarily binds Si as calcium silicates and not as potassium calcium silicates; therefore, Ca may increase the K release as well.²⁴

This complex system as well as its influencing parameters still have to be investigated further.

4.4. Release of S to the Gas Phase. During combustion, S forms mainly gaseous SO₂ (to a certain extent, also SO₃) and alkali and alkaline earth sulfates.^{16,17,19,21} Therefore, the knowledge about the release of S is relevant for the gaseous SO_x emissions as well as aerosol emissions and deposit formation.

In Figure 5, the absolute S release is plotted over the S content of the fuel (results from lab-scale reactor tests). As

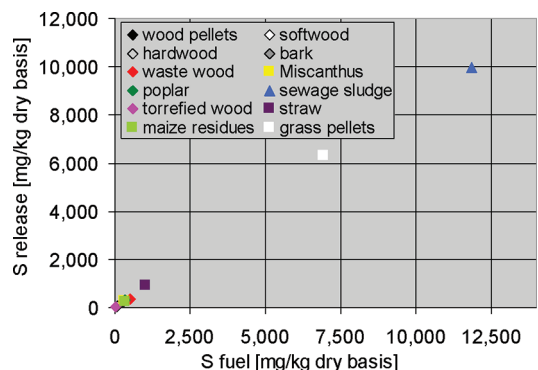


Figure 5. S concentration of the fuel versus S release to the gas phase. Explanation: the trend is statistically significant ($p < 0.05$).

seen, an almost linear correlation exists, which indicates that the S release is almost constant (around 80–90 wt %) and does not depend upon the remaining fuel composition or the ash matrix.

4.5. Release of Cl to the Gas Phase. Similar to S, Cl contained in the biomass during combustion mainly forms gaseous HCl, Cl₂, or alkali chlorides, such as KCl and NaCl.^{16,17,19,21} The Cl release is therefore of great relevance

for aerosol and deposit formation, gaseous HCl emissions, and regarding corrosion risks.

In Figure 6, data from lab-scale reactor tests are presented that clearly show that there is an almost linear increase of the

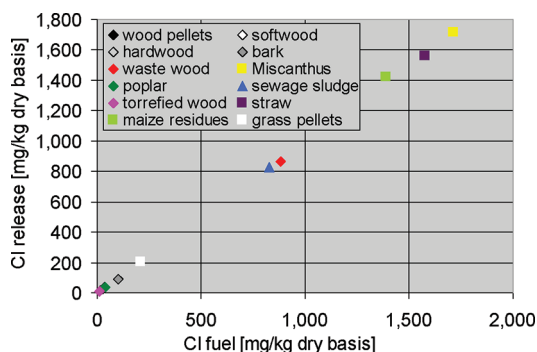


Figure 6. Cl concentration of the fuel versus Cl release to the gas phase. Explanation: the trend is statistically significant ($p < 0.05$).

amount of Cl released from the fuel to the gas phase and the Cl concentration in the fuel. As for S, this indicates that the Cl release does not strongly depend upon other fuel properties and is usually in the range of >90 wt %.

4.6. Molar 2S/Cl Ratio as an Indicator for High-Temperature Corrosion Risks. With regard to corrosion in biomass-fired boilers, in particular, three mechanisms are relevant:^{25,26} (1) the direct attack of gaseous HCl or Cl₂ to heat-exchanger surfaces, (2) the formation of alkali sulfate and/or alkali chloride melts, which dissolve the protective oxide layer of the heat-exchanger surface, and (3) the sulfation of alkali metal or heavy metal chlorides in the tube near the deposition layer. From this mechanism, Cl is released, which subsequently attacks the tube surface (so-called active oxidation).

Among the three mechanisms mentioned, active oxidation is the most relevant mechanism regarding high-temperature corrosion in boilers.²⁵

As already explained in sections 4.4 and 4.5, S and Cl show almost constant release ratios for different biomass fuels. Both elements are relevant for aerosol and deposit formation because, in the gas phase, they form alkaline sulfates and alkaline chlorides, which subsequently form particles or condense on heat-exchanger surfaces. Therefore, a link between the 2S/Cl ratio in the fuel and the respective aerosol deposits formed prevails. In Figure 7, data regarding the 2S/Cl ratio in

aerosol emissions are plotted over the respective index related to the fuel. A clear correlation can be derived. For fuels with high 2S/Cl ratios, a protective sulfate layer is formed at the tube surfaces. According to the literature,²⁵ therefore, only minor corrosion risks have to be expected for 2S/Cl ratios in the fuel of >4. It is additionally suggested that the molar 2S/Cl ratio in the fuel should be at least 8 to achieve negligible chlorine levels in boiler deposits and thereby eliminate corrosion from this source. Figure 7 shows that softwood and grass pellets show only minor corrosion risks.

According to Figure 7, the Cl concentrations in aerosols increase with decreasing 2S/Cl ratios in the fuel, while the sulfate concentrations decrease. For 2S/Cl ratios in the fuel <2, even a Cl surplus in aerosols prevails, indicating that severe corrosion risks have to be taken into account. Accordingly, corrosion risks increase from bark over waste wood and straw to maize residues.

The corrosion risk is additionally enforced by the fact that, with increasing concentrations of chlorides, also, the melting temperatures of deposits decrease.

4.7. Molar (K + Na)/[x(2S + Cl)] Ratio. This index can be used to predict the gaseous emissions of SO_x and HCl. As seen from the previous sections, the S and Cl release show an almost constant ratio of 80–90% and >90%, respectively. During combustion, S and Cl preferably form alkaline (K and Na) sulfates and chlorides. S also forms Ca and Mg sulfate, and to a smaller extent, Ca and Mg chlorides can be formed. Cl and S, which are not bound by these elements to the solid phase, form gaseous emissions, namely, HCl and SO_x. Because of the fact that in biomass fuels usually the K concentration is much higher than the Na concentration, the K release to the gas phase is of great relevance for the reaction schemes explained above.

The factor x in the molar $(K + Na)/[x(2S + Cl)]$ ratio describes the average release rates of K and Na in relation to the average release rates of S and Cl. When considering the reaction schemes mentioned above, this index can be defined to predict the potential for SO_x and HCl emissions associated with the combustion of a specific fuel.

A molar ratio $(K + Na)/[x(2S + Cl)] > 1$ indicates a surplus of released alkaline metals. Therefore, for a value clearly >1, very small HCl and SO_x emissions have to be expected, because most S and Cl will be bound in the ash. If the value of the index is clearly <1, elevated HCl and SO_x emissions are to be expected.

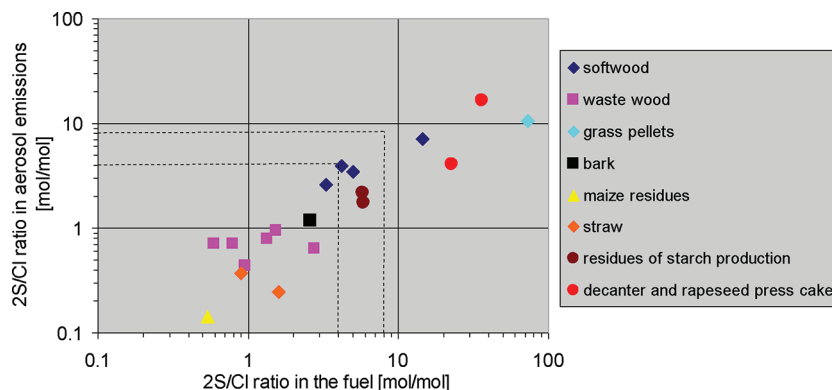


Figure 7. Dependency between the molar ratios of 2S/Cl in fuels and aerosol particles. Explanations: no statistical significance.

On the basis of the results from pilot, real, and lab reactor combustion tests with different biomass fuels, the release rates for K were calculated. The release was quantified by a mass balance based on weight measurements and chemical analysis of the fuel and ash obtained. The formula of the release rate for pilot- and real-scale combustion tests is shown in eq 1, and the formula of the release rate for lab-scale combustion tests is shown in eq 2.

$$\text{release}_{K,\text{wt}\%} = \left(1 - (c_{K,\text{bottom ash}(\text{db})} (m_{\text{bottom ash}(\text{db})} + m_{\text{furnace ash}(\text{db})} + m_{\text{boiler ash}(\text{db})}) / (c_{K,\text{fuel}(\text{db})} m_{\text{fuel}(\text{db})})\right) \times 100 \quad (1)$$

The incoming mass flow of fuel is $m_{\text{fuel}(\text{db})}$. The mass flow that is not released to the gas phase is the sum of the remaining ash fraction on the grate $m_{\text{bottom ash}(\text{db})}$ (kg/h, db) and the mass of entrained particles from the fuel bed. The mass flows (kg/h, db) that are entrained from the fuel bed and separated in the boiler are $m_{\text{furnace ash}(\text{db})}$ and $m_{\text{boiler ash}(\text{db})}$. The chemical composition of the fuel is $c_{K,\text{fuel}(\text{db})}$ (mg/kg, db), and the chemical composition for the ash sample is $c_{K,\text{bottom ash}(\text{db})}$. It is assumed that the entrained ash particles [$m_{\text{furnace ash}(\text{db})}$ and $m_{\text{boiler ash}(\text{db})}$] have the same composition as the bottom ash. This of course neglects the mass of ash-forming vapors, which end up on the surface of coarse fly ash particles (e.g., by condensation or surface reactions) in the boiler (e.g., K_2SO_4 and KCl). However, these processes have only a minor influence on the total mass of entrained particles.

$$\text{release}_{K,\text{wt}\%} = \left(1 - (c_{K,\text{output}(\text{db})} m_{\text{output}(\text{db})} / (c_{K,\text{input}(\text{db})} m_{\text{input}(\text{db})})\right) \times 100 \quad (2)$$

In equation (2) $m_{\text{input}(\text{db})}$ is the mass (g, db) of the sample fed to the reactor, $c_{K,\text{input}(\text{db})}$ is the concentration of K in the fuel (mg/kg, db), $m_{\text{output}(\text{db})}$ is the mass (g, db) of the ash residual after the experiment in the reactor and $c_{K,\text{output}(\text{db})}$ is the concentration of K in the ash residual (mg/kg, db). The mass of entrained fly ash particle is negligible because of the much lower air velocities in the fuel bed compared to pilot- or real-scale applications.

The determined release rates are shown in Figure 8.

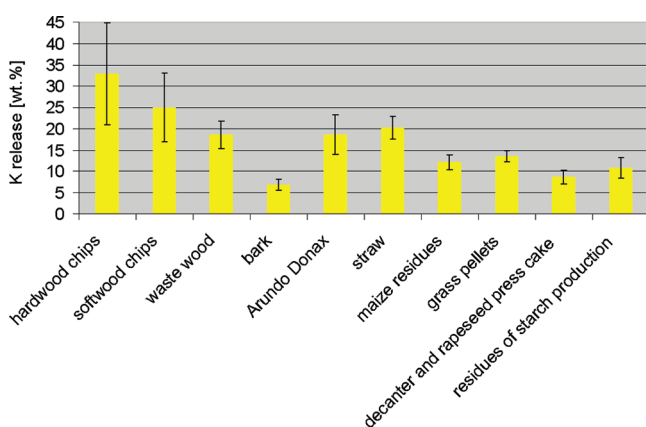


Figure 8. K release for different biomass fuels during combustion.

It can be assumed that Na shows a comparable release behavior to the gas phase as K. Therefore, the values of K release can be used for calculating the factor x of the molar $(K + Na)/[x(2S + Cl)]$ ratio. An averaged release for S and Cl (90 wt %) is divided by the average K release to obtain the factor x . The calculated values are summarized in Table 1.

Table 1. Experimentally Determined K-Release Rates for Different Biomass Fuels and the Resulting Factor x

	average K release (wt %)	standard deviation (wt %)	factor x
hardwood chips	32.8	12.0	2.7
softwood chips	24.9	8.1	3.6
waste wood	18.5	3.2	4.9
bark	6.8	1.3	13.2
<i>A. donax</i>	18.5	4.6	4.9
straw	20.1	2.6	4.5
maize residues	12.1	1.7	7.4
grass pellets	13.5	1.3	6.7
decanter and rapeseed press cake	8.6	1.6	10.5
residues of starch production	10.8	2.5	8.4

For biomass fuels for which the release behavior has not been investigated thus far, the release can be determined with a lab-scale reactor experiment, such as, for instance, described in section 2.4. On the basis of the results of such an experiment, a meaningful assumption for the K release can be made and, thus, the factor x can be calculated.

The estimated values from Table 1 can be used for the calculation of the index $(K + Na)/[x(2S + Cl)]$. Figure 9 shows the correlation of the molar $(K + Na)/[x(2S + Cl)]$ ratio versus the SO_x emissions and the conversion of fuel S to S in SO_x .

From Figure 9, it can be seen that, with a decreasing molar $(K + Na)/[x(2S + Cl)]$ ratio, SO_x emissions are increasing.

The SO_x emissions of the different fuels can be categorized into (1) a low SO_x emission range (<50 mg of $\text{SO}_x \text{ N}^{-1} \text{ m}^{-3}$, with dry flue gas, at 13 vol % O_2), e.g., wood chips, bark, mixtures of waste wood and bark, as well as maize residues; (2) a medium SO_x emission range (50–200 mg of $\text{SO}_x \text{ N}^{-1} \text{ m}^{-3}$, with dry flue gas, at 13 vol % O_2), e.g., waste wood, *A. donax*, and straw; and (3) a high SO_x emission range (>500 mg of $\text{SO}_x \text{ N}^{-1} \text{ m}^{-3}$, with dry flue gas, at 13 vol % O_2), e.g., grass pellets, a mixture of decanter and rapeseed press cake, and residues of starch production with high S content.

In the second diagram of Figure 9, the molar $(K + Na)/[x(2S + Cl)]$ ratio is plotted against the conversion of fuel S to S in SO_x . The same trend of the molar $(K + Na)/[x(2S + Cl)]$ ratio and the conversion of fuel S to SO_x can be observed. SO_x emissions are negligible for a fuel molar $(K + Na)/[x(2S + Cl)]$ ratio bigger or close to 0.5. This index is suitable to estimate the SO_x emission range to be expected.

Figure 10 shows the correlation of the molar $(K + Na)/[x(2S + Cl)]$ ratio versus HCl emissions and the conversion of fuel Cl to Cl in HCl.

No clear correlation between the molar $(K + Na)/[x(2S + Cl)]$ ratio and the HCl emissions can be seen. For a molar ratio of $(K + Na)/[x(2S + Cl)] < 0.5$, the HCl emissions are varied from 0 to 110 mg $\text{N}^{-1} \text{ m}^{-3}$, with dry flue gas, at 13 vol % O_2 . The reason for this strong scattering in comparison to S is not yet understood. Further investigations are needed. In our case, it can be seen from Figure 10 that, with a molar ratio of $(K +$

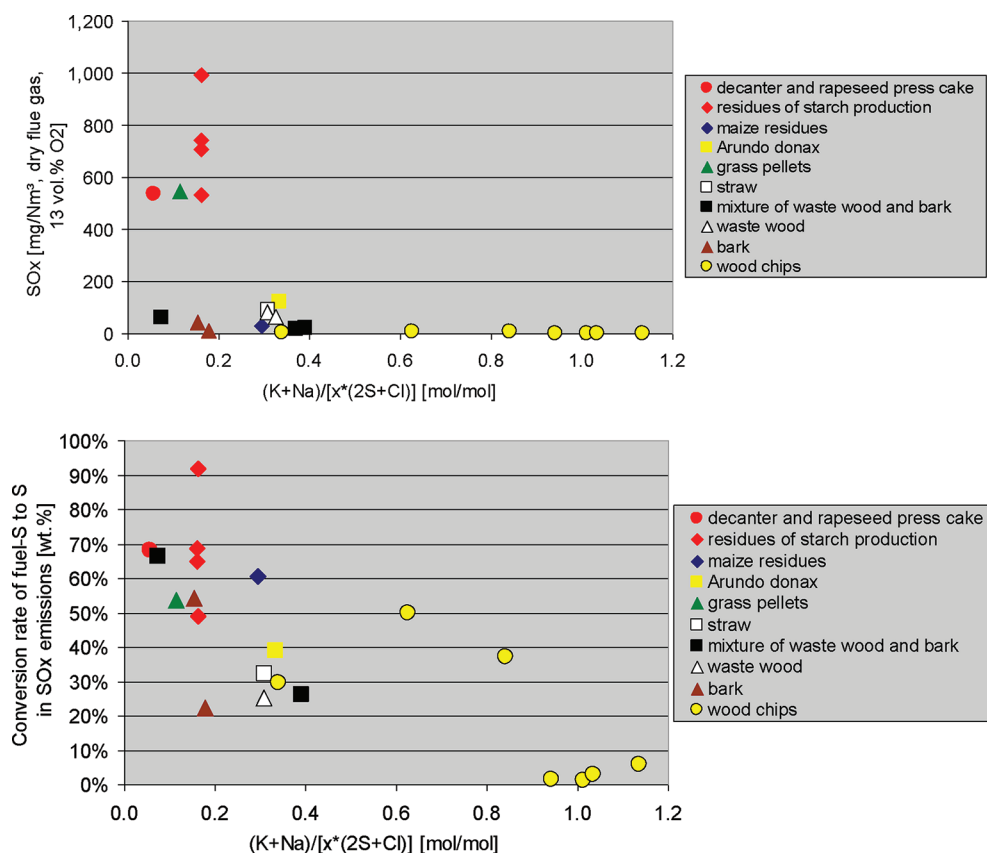


Figure 9. Molar $(K + Na)/[x(2S + Cl)]$ ratio versus SO_x emissions and the conversion of fuel S to SO_x . Explanation: both correlations are statistically significant ($p < 0.05$).

$(Na)/[x(2S + Cl)]$ bigger or close to 0.5, the HCl emissions are very low. Therefore, this index can also be used to make a first estimation of the gaseous HCl emissions to be expected.

When using this index, it has to be noted that the factor x is based on first estimations regarding the release of K and Na. Further investigations are recommended to ensure the alkali metal release described.

4.9. Indicators for Ash-Melting Problems. It is generally well known that Ca and Mg increases the ash-melting temperature, while Si in combination with K decreases the ash-melting temperature.^{9,27,28} The molar $Si/(Ca + Mg)$ ratio⁹ can therefore provide first information about ash-melting tendencies in ash systems dominated by Si, Ca, Mg, and K. However, for P-rich systems (e.g., grass pellets), this correlation is not valid (see Figure 11).

As seen in Figure 11, the ash-sintering temperature drops below 1100 °C as soon as the $Si/(Ca + Mg)$ ratio exceeds 1. It can also be seen that there is a linear correlation of the molar $Si/(Ca + Mg)$ ratio with the ash-sintering temperature, except for grass pellets that show a low ash-sintering temperature because of the high P concentration.

From the ternary-phase diagrams for $CaO-K_2O-P_2O_5$ and $MgO-K_2O-P_2O_5$,²³ it can be derived that, at constant K_2O/P_2O_5 ratios, the melting point increases with increasing CaO and MgO concentrations. It can be concluded that CaO and MgO increase the ash-sintering temperature, whereas K_2O and P_2O_5 decrease the sintering temperature. In combination with Si, a modified index $(Si + P + K)/(Ca + Mg)$ can be introduced (see Figure 12). With this index, also for P-rich fuels, a prediction regarding the ash-melting behavior is possible. There

is a linear correlation given between the molar $(Si + P + K)/(Ca + Mg)$ ratio and the ash-sintering temperature.

5. SUMMARY AND CONCLUSION

The application of fuel indexes as a characterization tool provides a good basis for a quick pre-evaluation of combustion-related problems that may arise. This new and advanced fuel characterization method can therefore be applied to support decision making concerning the application of new biomass fuels or fuel blends in existing combustion plants, as well as for the preliminary design and engineering of new combustion plants, which should be tailored to the needs of a specific fuel or fuel mixture. During this first decision phase regarding the applicability of a certain fuel, time-consuming and expensive combustion tests can therefore be saved.

The investigation of the fuel indexes has been performed for a broad spectrum of biomass fuels ranging from different types of wood to herbaceous and agricultural biomass, as well as industrial biomass residues. The data for the investigation are based on test runs from fixed-bed lab-, pilot-, and real-scale combustion systems, and therefore, the indexes derived in this work are applicable for grate combustion plants.

Fuel indexes, which allow for accurate qualitative predictions, are the N content, the molar $2S/Cl$ ratio, and the molar ratio of $(Si + P + K)/(Ca + Mg)$. Indexes that can be applied with some restrictions regarding other constraints are the sum of K, Na, Zn, and Pb and the molar ratios of $(K + Na)/[x(2S + Cl)]$ and $Si/(Ca + Mg)$.

The N content generally determines the potential for NO_x emission formation. A correlation between the conversion rates

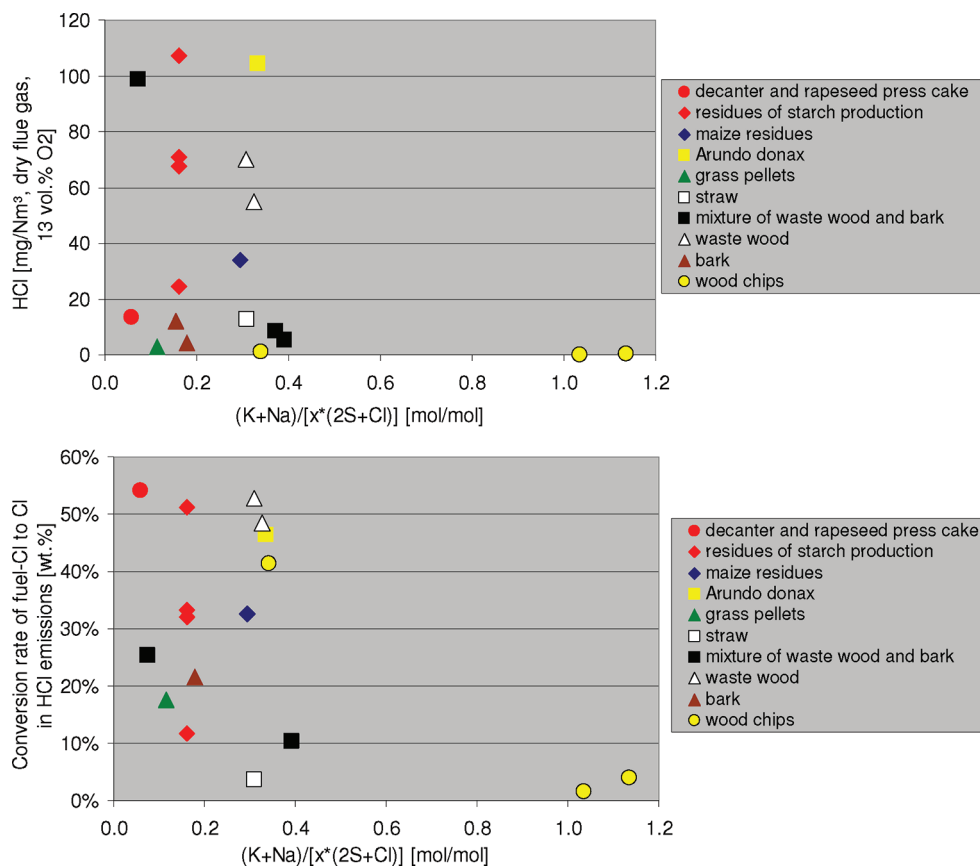


Figure 10. Molar $(K + Na)/[x(2S + Cl)]$ ratio versus HCl emissions and the conversion of fuel Cl to HCl. Explanation: both correlations are not statistically significant.

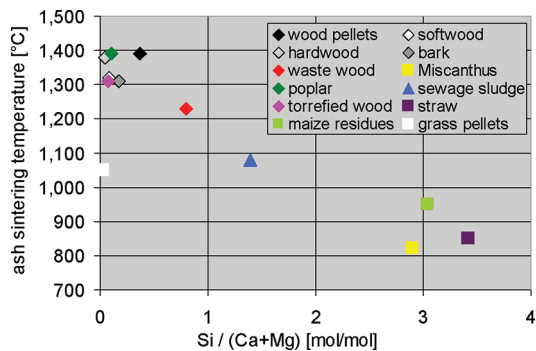


Figure 11. Molar $Si/(Ca + Mg)$ ratio versus ash-sintering temperature for different biomass fuels. Explanation: if grass pellets are excluded, the correlation is statistically significant ($p < 0.05$); ash-sintering temperature according to prCEN/TS 15370-1.

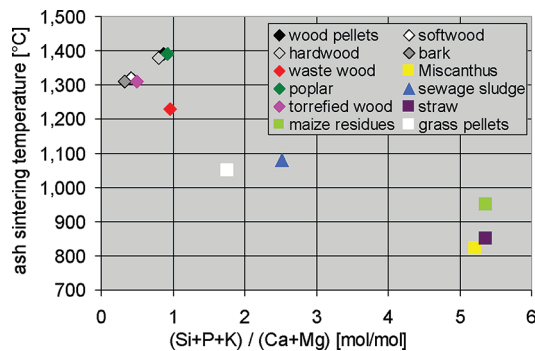


Figure 12. Molar $(Si + P + K)/(Ca + Mg)$ ratio versus ash-sintering temperature for different biomass fuels. Explanation: the correlation is statistically significant ($p < 0.05$).

of fuel N to NO_x emissions has been derived, showing a nonlinear correlation of the NO_x emissions with rising fuel N content. When this correlation is applied, a first estimation of the NO_x emissions can be made. During combustion, easily volatile and semi-volatile elements (K, Na, S, Cl, Zn, and Pb) are partly released from the fuel to the gas phase, where they undergo chemical reactions and finally contribute to problems concerning emissions, deposit formation, and corrosion. With a decreasing molar $2S/Cl$ ratio, for instance, the amount of alkaline chlorides in ash deposits on heat-exchanger surfaces increases. According to the literature,²⁵ a molar ratio of $2S/Cl < 8$ increases the risk of high-temperature Cl corrosion. The sum of K, Na, Zn, and Pb (in mg/kg of dry fuel) describes the

potential for aerosol and deposit formation, which increases with rising values of this index. Moreover, the molar ratio of $(K + Na)/[x(2S + Cl)]$, where x represents the ratio of the average K and Na release in relation to the average S and Cl release from the fuel to the gas phase, provides a first prediction concerning the expected HCl and SO_x emissions. For values >0.5 , it is very likely that most S and Cl will be embedded in the ashes. The molar ratio of $Si/(Ca + Mg)$ can provide first information about ash-melting tendencies in systems dominated by Si, Ca, Mg, and K (decreasing melting temperatures with an increasing value). The molar ratio of $(Si + P + K)/(Ca + Mg)$ is also valid for P-rich fuels and is therefore an index that can generally be applied regarding the pre-evaluation of ash-melting tendencies.

Presently, ongoing work is focusing on the further improvement of existing fuel indexes. For the prediction of HCl and SO_x emissions, a more detailed investigation of the K release to the gas phase and also possible Ca interactions is necessary. To investigate the K release from biomass fuels in more detail, interactions of Si and P with K as well as the combustion temperature need to be considered. However, more research on this special issue is needed.

AUTHOR INFORMATION

Corresponding Author

*Telephone: +43-(0)-316-481300-73. Fax: +43-(0)-316-481300-4. E-mail: peter.sommersacher@bioenergy2020.eu.

ACKNOWLEDGMENTS

This paper is the result of a project carried out in cooperation with BIOENERGY 2020+ (a research center within the framework of the Austrian COMET program), which is funded by the Republic of Austria as well as the federal provinces of Styria, Lower Austria, and Burgenland.

REFERENCES

- Gustavson, L.; Holmberg, J.; Dornburg, V.; Sathre, R.; Eggers, T.; Mahapatra, K.; Marland, G. Using biomass for climate change mitigation and oil use reduction. *Energy Policy* **2007**, *35*, S671–S691.
- McKendry, P. Energy production from biomass (Part 1): Overview of biomass. *Bioresour. Technol.* **2002**, *83*, 37–46.
- Hoogwijk, M.; Faaij, A.; van den Broek, R.; Berndes, G.; Gielen, D.; Turkenburg, W. Exploration of the ranges of the global potential of biomass for energy. *Biomass Bioenergy* **2003**, *25*, 119–133.
- Lewandowski, I.; Scurlock, J. M. O.; Lindvall, E.; Christou, M. The development and current status of perennial rhizomatous grasses as energy crops in the U.S. and Europe. *Biomass Bioenergy* **2002**, *25*, 335–361.
- Chouchene, A.; Jeguirim, M.; Khiari, B.; Zagrouba, F.; Trouvé, G. Thermal degradation of olive solid waste: Influence of particle size and oxygen concentration. *Resour., Conserv. Recycl.* **2010**, *54*, 271–277.
- Bryers, R. W. Fireside slagging, fouling, and high-temperature corrosion of heat-transfer surfaces due to impurities in steam-raising fuels. *Prog. Energy Combust. Sci.* **1996**, *22*, 29–120.
- Visser, H. J. M. *The Influence of Fuel Composition on Agglomeration Behaviour in Fluidised-Bed Combustion*; Energy Research Centre of the Netherlands (ECN): Petten, The Netherlands, 2004; ECN-C-04-054.
- Gilbe, C.; Öhman, M.; Lindström, E.; Boström, D.; Backman, R.; Samuelsson, R.; Burval, J. Slagging characteristics during residential combustion of biomass pellets. *Energy Fuels* **2008**, *22*, 3536–3543.
- Lindström, E.; Öhman, M.; Backman, R.; Boström, D. Influence of sand contamination on slag formation during combustion of wood derived fuels. *Energy Fuels* **2008**, *22*, 2216–2220.
- Weissingner, A.; Fleckl, T.; Obernberger, I. Application of FT-IR in-situ absorption spectroscopy for the investigation of the release of gaseous compounds from biomass fuels in a laboratory scale reactor—Part II: Evaluation of the N-release as functions of combustion specific parameters. *Combust. Flame* **2004**, *137*, 403–417.
- Stubenberger, G.; Scharler, R.; Obernberger, I. Nitrogen release behaviour of different biomass fuels under lab-scale and pilot-scale conditions. *Proceedings of the 15th European Biomass Conference and Exhibition*; Berlin, Germany, May 7–11, 2007; ISBN: 978-88-89407-59-X, ISBN: 3-936338-21-3, pp 1412–14120.
- Bärenthaler, G.; Zischka, M.; Hanraldsson, C.; Obernberger, I. Determination of major and minor ash-forming elements in solid biofuels. *Biomass Bioenergy* **2006**, 983–997.
- Keller, R. Primärmaßnahmen zur NO_x-Minderung bei der Holzverbrennung mit dem Schwerpunkt der Luftstufung. *Forschungsbericht 18: Laboratory for Energy Systems*; ETH Zürich: Zürich, Switzerland, 1994.
- Glarborg, P.; Jensen, A. D.; Johnsson, J. E. Fuel nitrogen conversion in solid fuel fired systems. *Prog. Energy Combust. Sci.* **2003**, *29*, 89–113.
- Weissingner, A. Experimentelle Untersuchungen und reaktionskinetische Simulationen zur NO_x-Reduktion durch Primärmaßnahmen bei Biomasse-Rostfeuerungen. Ph.D. Thesis, Graz University of Technology, Graz, Austria, 2002.
- Brunner, T. Aerosols and coarse fly ashes in fixed-bed biomass combustion. Ph.D. Thesis, Graz University of Technology, Graz, Austria, 2006.
- Christensen, K. The formation of submicron particles from the combustion of straw. Ph.D. Thesis, Department of Chemical Engineering, Technical University of Denmark, Lyngby, Denmark, 1995; ISBN: 87-90142-04-7.
- Jöller, M. Modelling of aerosol formation and behaviour in fixed-bed biomass combustion systems—Influencing aerosol formation and behaviour in furnaces and boilers. Ph.D. Thesis, Graz University of Technology, Graz, Austria, 2008.
- Knudsen, J.; Jensen, P.; Dam-Johansen, K. Transformation and release to the gas phase of Cl, K, and S during combustion of annual biomass. *Energy Fuels* **2004**, *18*, 1385–1399.
- Novaković, A.; Van Lith, S.; Frandsen, F.; Jensen, P.; Holgersen, L. Release of potassium from the systems K–Ca–Si and K–Ca–P. *Energy Fuels* **2009**, *23*, 3423–3428.
- Müller, M.; Wolf, K. J.; Smeda, A.; Hilpert, K. Release of K, Cl and S species during co-combustion of coal and straw. *Energy Fuels* **2006**, *20*, 1444–1449.
- Boström, D.; Broström, M.; Skoglund, N.; Boman, C.; Backman, R.; Öhman, M.; Grimm, A. Ash transformation chemistry during energy conversion of biomass. *Proceedings of the Impact of Fuel Quality on Power Production and Environment*; Puchberg, Austria, Sept 23–27, 2010; pp 1–20.
- Sandström, M. Structural and solid state EMF studies of phases in the CaO–K₂O–P₂O₅ system with relevance for biomass combustion. Ph.D. Thesis, Luleå University of Technology, Luleå, Sweden, 2006; ETPC Report 06-06, ISSN: 1653-0551, ISBN: 91-7264-149-5.
- Risnesa, H.; Fjellerup, J.; Henriksenc, U.; Moilanend, A.; Norbye, P.; Papadakisb, K.; Posseltf, D.; Sorensenb, L. H. Calcium addition in straw gasification. *Fuel* **2003**, *82*, 641–651.
- Salmenoja, K. Field and laboratory studies on chlorine-induced superheater corrosion in boilers fired with biofuels. Ph.D. Thesis, Faculty of Chemical Engineering, Abo Akademi, Abo/Turku, Finland, 2000.
- Obernberger, I.; Brunner, T. Depositionen und Korrosion in Biomassefeuerungen. *Tagungsband zum VDI-Seminar 430504 "Beläge und Korrosion in Großfeuerungsanlagen"*; Göttingen, Germany, 2004.
- Öhman, M.; Boman, C.; Hedman, H.; Nordin, A.; Boström, D. Slagging tendencies of wood pellet ash during combustion in residential pellet burners. *Biomass Bioenergy* **2003**, *27*, 585–596.
- Baxter, L.; Miles, T.; Miles, T. Jr.; Jenkins, B.; Milne, T.; Dayton, D.; Bryers, R.; Oden, L. The behavior of inorganic material in biomass-fired power boilers: Field and laboratory experiences. *Fuel Process. Technol.* **1998**, *54*, 47–78.

NOTE ADDED AFTER ASAP PUBLICATION

An addition sign was added between Ca and Mg in the fourth to last paragraph of the Background and Scope section of the version of this paper published December 16, 2011. The correct version published December 20, 2011.

Paper II

Application of Novel and Advanced Fuel Characterization Tools for the Combustion Related Characterization of Different Wood/Kaolin and Straw/Kaolin Mixtures

Peter Sommersacher,^{*,†} Thomas Brunner,^{†,‡,§} Ingwald Obernberger,^{†,‡,§} Norbert Kienzl,[†] and Werner Kanzian^{‡,§}

[†]BIOENERGY 2020+ GmbH, Inffeldgasse 21b, A-8010 Graz, Austria

[‡]Institute for Process and Particle Engineering, Graz University of Technology, Inffeldgasse 13, A-8010 Graz, Austria,

[§]BIOS BIOENERGIESYSTEME GmbH, Inffeldgasse 21b, A-8010 Graz, Austria

Supporting Information

ABSTRACT: The increased demand for energy from biomass enforces the utilization of new biomass fuels (e.g., energy crops, short-rotation coppices, as well as wastes and residues from agriculture and the food industry). Compared to conventional wood fuels, these new biomass fuels usually show considerably higher ash contents and lower ash sintering temperatures, which leads to increased problems concerning slagging, ash deposit formation, and particulate matter emissions. One possibility to combat these problematic behaviors is the application of fuel additives such as kaolin. In contrast to the usual approach for the application of additives based on an experimental determination of an appropriate additive ratio, this study applies novel and advanced fuel characterization tools for the characterization of biomass/kaolin mixtures. In the first step the pure biomass fuels (softwood from spruce and straw) and the additive were chemically analyzed. On the basis of the analysis theoretical mixing calculations of promising kaolin ratios were conducted. These theoretical mixtures were evaluated with fuel indexes and thermodynamic equilibrium calculations (TEC). Fuel indexes provide the first information regarding high temperature corrosion (2S/Cl) and ash melting tendency $(Si + P + K)/(Ca + Mg + Al)$. TEC can be used for a qualitative prediction of the release of volatile and semivolatile elements (K, Na, S, Cl, Zn, Pb) and the ash melting behavior. Moreover, selected mixtures of spruce and straw with kaolin were prepared for an evaluation and validation of the release behavior of volatile and semivolatile ash forming elements with lab-scale reactor experiments. The validation of the ash melting behavior was conducted by applying the standard ash melting test. It could be shown that the new approach to apply novel and advanced fuel characterization tools to determine the optimum kaolin ratio for a certain biomass fuel works well and thus opens a new and targeted method for additive evaluation and application. In addition, it helps to significantly reduce time-consuming and expensive testing campaigns.

1. INTRODUCTION

The utilization of biomass fuels in heat and power production plants is an important approach to gain independence from fossil fuels and to reduce CO₂ emissions. This leads to an increasing demand for biomass fuels and consequently to the introduction of so-called new biomass fuels. The most promising are fast-growing nonfood crops like perennial grasses such as Miscanthus and giant reed¹ and fast-growing wood species (so-called short-rotation coppices (SRC) such as willow and poplar²), as well as herbaceous and agricultural residues (e.g., straw, press cake from oil production, kernels). These fuels usually show considerably higher N, S, Cl, and ash contents as well as lower ash sintering temperatures in comparison with conventional wood fuels (wood pellets, wood chips, bark). This leads during combustion to increased problems regarding gaseous HCl, SO_x, NO_x emissions, and fine particle emissions as well as slagging and ash deposit formation. For these new biomass fuels characterization tools which can estimate emission and ash related problems are of major relevance for their market introduction, as presented in a previous study.³

An interesting option to reduce combustion related problems associated with challenging biomass fuels is the application of

additives. Several studies have been presented regarding the application of additives for small-scale combustion systems for different biomass fuels. A decreasing potential of fine particulate emissions and an improvement of the slagging tendency by addition of kaolin to straw have been reported.⁴ The same trend concerning decreasing aerosol emissions has been reported by kaolin addition to woody biomass fuels (bark from pine and cleaning assortments).⁵ Another study reported a decreased slag formation by the addition of kaolin and limestone during combustion of wood fuels.⁶ A further study investigated the slagging characteristics of corn stover mixtures with kaolin and calcite and showed an improvement of the slagging tendency by additive utilization.⁷ Also, P-rich fuels have been investigated. Fine particulate emission reductions of 31 and 57% have been reported for kaolin additions of 2 and 4% respectively to oat grains, whereas as a side effect the kaolin addition increased the gaseous emissions of HCl and SO₂.⁸ A further study⁹ investigated the influence of kaolin and calcite additives on ash transformation during the small-scale

Received: March 7, 2013

Revised: July 11, 2013

Published: July 12, 2013

combustion of oat. For kaolin addition the formation of slag in the bottom ash could be totally avoided. Moreover, the addition of kaolin affected the formation of fine particulate emissions where an increased share of condensed potassium phosphates at the expense of potassium sulfates and KCl (was almost completely absent in the particulate matter) has been determined. However, due to reduced formation of KCl and K_2SO_4 , increased gaseous HCl and SO_2 emissions were measured. Just one study has been found for additive application in large-scale combustion systems, where the positive influence of increased sintering temperatures has been investigated in a 35 MW circulating fluidized bed boiler. It has been reported that fine kaolin powder captures K vapors which get incorporated in the fly ash. Therefore, less potassium is available in the furnace, which decreases the risk of bed agglomeration.¹⁰

It has to be noted that fuel additives are not broadly industrially applied so far with the exception of sorbent application for SO_x and HCl reduction in flue gas cleaning systems. This might be because the detailed background of their functionality and an economic and technical optimization of their application have not been conducted yet.

Fuel additives may be mixed and fed to the furnace together with the biomass fuel, or mixed with the raw material before pellet production. The latter implies the advantage that the additive can be homogeneously distributed in the fuel and separation of the fuel and the additive during fuel feeding and in the fuel bed is avoided. In larger heating and combined heat and power plants the main objective for the use of fuel additives is to reduce bed agglomeration, sintering/slagging, deposit formation, and corrosion. In smaller (residential and medium sized) grate fired appliances the main objectives for the use of fuel additives are to lower slagging problems and to reduce fine particle emissions.

Feasible options are calcium based and aluminosilicate based additives. They can generally be applied for the reduction of ash related problems and for SO_x , HCl, and particulate matter (PM) emission reduction. It has to be noted that they do not influence NO_x emissions. Certain additives are able to reduce one combustion related issue, whereas some additives can reduce more than one combustion related problem. Ca based additives for instance are used for reactions with HCl and SO_2 to CaCl and $CaSO_4$ and have also been used for reducing the slagging tendency in grate fired systems by formation of high melting Ca/Mg/(K) silicates and oxides. They usually show no influence on the alkali release. The second and so far well-studied additive is kaolin, which is composed mainly of the mineral kaolinite ($Al_2Si_2O_5(OH)_4$). This mineral has the property that it captures alkali compounds whereby potassium is bound to the mineral. By this mechanism potassium–aluminum silicates are formed, which have higher melting temperatures than the pure potassium silicates. By this effect slagging prevention and the reduction of aerosol emissions is possible in parallel.⁴

Until now the kind of additive and its dosing which influence the combustion/emission behavior have been mainly experimentally evaluated. The aim of this work is to show how advanced fuel characterization tools can support the evaluation of the combustion related properties of biomass/kaolin mixtures. Thereby, optimum mixing ratios should be identified without the need for time-consuming and expensive real-scale combustion tests.

2. METHODS

For the estimation of an appropriate kaolin addition ratio which positively influences the ash melting and aerosol emissions, the following methods have been used. Wet chemical fuel analyses deliver the chemical composition of the pure fuels and the additive. On the basis of these data theoretical mixing calculations of promising kaolin ratios were conducted. Fuel indexes and thermodynamic equilibrium calculations (TEC) have been used for the evaluation of appropriate kaolin addition ratios, which have later been prepared. Fuel indexes were calculated which provide the first information about the high temperature corrosion risk (by using the molar $2S/Cl$ ratio) and the ash melting tendency (by using the molar $[Si + P + K]/[Ca + Mg + Al]$ ratio). TEC were used for the qualitative estimation of the release of volatile and semivolatile elements (K, Na, S, Cl, Zn, Pb) as well as for the prediction of the ash melting behavior. For an evaluation and validation of this new approach, lab-scale reactor combustion tests and ash melting analysis according to CEN/TS 15370-1 have been conducted with selected fuel/kaolin mixtures.

2.1. Wet Chemical Analysis. Wet chemical fuel analyses form the basis for the fuel characterization methods applied within this study. It is strongly recommended to generally follow the best practice guidelines worked out within the FP6 project BIONORM¹¹ and subsequently implemented in various CEN standards for biomass fuels.

The moisture content of fuel samples has been determined according to ÖNORM EN 14774 (determination of the weight loss during drying at 105 °C until a constant weight is reached).

Fuel sample preparation has been carried out according to ÖNORM EN 14780 which includes (i) drying of the sample at 105 °C, (ii) milling of the whole sample in a cutting mill to a particle size of <4 mm, (iii) sample division, and (iv) milling of the final analysis sample in an ultracentrifugal mill equipped with a titanium rotor and screen to a particle size of <0.2 mm.

The ash content has been determined according to ÖNORM EN 14775 by determination of the loss of ignition at 550 °C. With this method, it has to be taken into account that especially Ca-rich fuels form considerable amounts of carbonates at the proposed treatment temperature. In real-scale systems, on the other hand, almost no carbonates and preferably oxides are formed due to the high combustion temperatures prevailing. Consequently, the ash content is overestimated compared with the amount of ashes formed in a real process. Therefore, in deviation from ÖNORM EN 14775, the inorganic carbon content of the ashed fuel sample is determined additionally and used to correct the ash content by subtracting the CO_2 bound in carbonates to gain an oxide based ash content.

The determination of C, H, and N contents of biomass fuels has been carried out according to ÖNORM CEN/TS 15104 by combustion and subsequent gas-phase chromatographic separation and measurement in an elemental analyzer (Vario EL 3, Elementar). The determination of Cl has been carried out according to ÖNORM CEN/TS 15289, applying a digestion step based on bomb combustion in oxygen and absorption in NaOH (0.05 M), followed by ion chromatographic detection (ISC 90, Dionex).

The concentrations of major and minor elements as well as of S have been determined by multistep pressurized digestion of the fuel with HNO_3 (65%)/HF (40%)/ H_3BO_3 (Multiwave 3000, Anton Paar), followed by detection applying inductively coupled plasma optical emission spectroscopy (ICP-OES) (Arcos, Spectro) or inductively coupled plasma mass spectroscopy (ICP-MS) (Agilad 7500, Agilent), depending on detection limits. The digestion method applied is of great importance to ensure a complete dissolution of the ash matrix, which is a basic requirement for correct element detection.

The determination of the ash-melting behavior has been done according to CEN/TS 15370-1. The fuel samples are ashed at a temperature of 550 °C, and the remaining ash is pressed into cylindrical molds. These samples are then heated in an oven under oxidizing conditions. The following temperatures (shrinkage starting temperature, deformation temperature, hemisphere temperature, flow temperature) are determined.

For the evaluation of the ash-melting behavior, the shrinkage starting temperature (start of ash melting) and the temperature window between the shrinkage starting temperature (SST) and the flow temperature (FT) are of special relevance. It has to be considered that the characteristic ash-melting temperatures are determined for the total ash (fuel ash). In real-scale applications, the fractionation of certain elements in the different ash fractions influences the melting temperatures of the individual ash fractions.

For ash samples (from lab-scale reactor tests) the same sample preparation steps which are applied for fuel samples are needed.

For the determination of major and minor elements in the ash, except for Cl, the same methods as described for the fuel analysis are applied. The Cl content is measured by ion chromatography (ISC 90, Dionex) after elution for 24 h with deionized water.

For the determination of total inorganic carbon (TIC) and the determination of total organic carbon (TOC), the total carbon according to ÖNORM EN 13137 has been determined (using the element analyzer Leco RC-612). For the determination of TIC an aliquot amount of ash is heat treated and the generated CO₂ is measured by infrared spectroscopy (Leco RC-612). The measurement instrument is calibrated with CaCO₃. The TOC is determined by the amount of total carbon minus TIC.

2.2. Fuel Indexes. Fuel indexes can be used to provide indications regarding relevant combustion related properties of biomass fuels, for instance, the potential for gaseous NO_x, SO_x, and HCl emissions, the potential for fine particulate emissions and deposit formation, high temperature corrosion risks, and ash melting behavior.

They are calculated based on results of wet chemical fuel analysis. For the definition of a fuel index, the physical behavior, chemical reactions of ash forming elements, and interactions between different elements and groups of elements, respectively, during combustion are considered. For the validation of a defined index, correlations and experiences gained from pilot-scale and real-scale combustion tests have been used.

Fuel indexes which were used within this study are the molar (Si + P + K)/(Ca + Mg) ratio as an indicator for the ash melting tendency and the molar 2S/Cl ratio as an indicator for the high temperature corrosion risk. A detailed description of the definition and the evaluation procedure of the indexes introduced can be found in ref 3.

For the prediction of the ash melting tendency, not the molar (Si + P + K)/(Ca + Mg) ratio but the molar (Si + P + K)/(Ca + Mg + Al) ratio has been used. This approach has been chosen because, due to the addition of kaolin, the Al concentrations are higher compared to pure biomass fuels. From the ternary phase diagram¹² for CaO–SiO₂–Al₂O₃ melting temperatures higher than 1300 °C can be determined. For the K₂O–SiO₂–Al₂O₃ system¹² it can be specified that for pure K₂O–SiO₂ phases for SiO₂ concentrations of <80 wt % low melting temperatures prevail (~800 °C). With increasing Al₂O₃ concentrations the melting temperatures rise, and for an Al₂O₃ concentration of >20 wt % melting temperatures higher than 1300 °C are reached. It can be concluded that with increasing Al₂O₃ concentrations the melting temperatures increase; thus Al has also been considered in the fuel index applied for ash melting evaluations.

2.3. Thermodynamic Equilibrium Calculations. Thermodynamic equilibrium calculations (TEC) can be applied for the prediction of multiphase equilibria and for the identification and quantification of the liquid and solid phases of interest. These calculations are conducted for a multicomponent thermodynamic system in a predetermined gas atmosphere. Under the assumption that chemical equilibrium can be achieved for the system investigated, TEC provide the opportunity to qualitatively investigate the release behavior of inorganic compounds and the ash melting behavior in biomass combustion/gasification processes. For this study the thermochemical software package FactSage 6.2 has been applied. A series of calculation modules and databases are included in this package, which uses the image component method in Gibbs free energy minimization concerning thermodynamic equilibrium. The currently accessed databases are “solution databases” containing the optimized parameters for a wide range of solution phases and “pure compound” databases containing the data for over 4500 stoichiometric

compounds. For the work presented the component database Fact 53 as well as the solution databases FToxid (slags and other oxide mixtures) and FTsalt (liquid and solid salt phases) has been applied. More than 1000 components and nine solutions (which have been shown to be stable and thermodynamically relevant) have been considered—the selection has been done application oriented for biomass fuels and ashes. More detailed information on the model applied is given elsewhere.^{13,14}

A realistic prediction of the characteristic melting temperatures (T_{30} and T_{70}) and the release behavior primarily depends on a reliable quantification of the molten solution phases SLAGH and SALTF over the temperature range of interest. Previous work showed that the assessment of these two phases was strongly influenced by the amounts of Al, Si, and K. By means of empirically estimated limits for the characteristic molar ratios of (Si + K + P)/(Ca + Mg), K/(Si + P), and Al/Si, an optimization method for TEC has been developed which is briefly discussed in the following. More detailed information can be found in ref 14.

1. The Si reactivity (i.e., fraction of initial Si amount entering the calculation) was related to the molar ratio (Si + K + P)/(Ca + Mg), whereby for ashes with a value lower than 0.94 a Si reactivity of 10% was assumed. This primarily applies for pure wood ashes where the inclusion of typically sandlike contaminants combined with the low ash content of the corresponding fuels causes a significant share of the Si to be less reactive. This inert Si fraction (approximately 90%) is supposed not to take place in the ash melting processes, and thus an overestimation of slag formation can be avoided. For all other nonwood ashes the Si reactivity was defined to be 100%, because the corresponding fuels exhibited high Si concentrations in the ash, making the Si fraction coming from external contaminants (e.g., sand, stones) of minor relevance.

2. Al₂O₃ was excluded from SLAGH in calculation cases with a molar Al/Si ratio of <0.2 in order to avoid unrealistic slag formation prediction which is attributed to a strong influence of Al₂O₃ on slag formation and may be explained with the current inaccuracy of the thermodynamic data for Al in slag solutions.

3. The molar ratio K/(Si + P) was the determining criterion if the molten salt solution SALTF was used in the TEC model. For molar ratios larger than 1, SALTF was eliminated from the TEC model; otherwise it caused an overprediction of the SALTF phase (mainly composed of potassium carbonates/sulfates) connected with an unrealistic drop of the melting temperatures estimated. In ref 14 a more detailed description is given.

For the prediction of the inorganic element release, the calculations have been done following a two-step calculation. This approach has been developed for a better prediction of the K and Na released from the fuel to the gas phase. Step 1 simulates the devolatilization phase. The input data consist of the complete elemental fuel composition under consideration of a substoichiometric combustion air ratio ($\lambda < 1$) and atmospheric pressure. The results of step 1 are evaluated for a temperature of 700 °C, which is assumed to be a realistic fuel bed temperature during volatilization. For calculation step 2, which simulates the charcoal combustion phase, the input consists of the solid residues from step 1 (ash forming matter and charcoal), whereby the charcoal is assumed to consist of pure C and amounts to 15 wt % of the initial organic dry matter. Moreover, an oxidizing gas atmosphere ($\lambda > 1$) and atmospheric pressure are applied. The total release of the elements considered is calculated as the sum of the release during step 1 and step 2.

The calculations concerning step 2 are carried out in a temperature range from 700 to 1600 °C. The evaluation of the element release ratios for step 2 have been conducted at a typical charcoal bed temperature for fixed bed combustion systems, which is usually around 1250 °C (this value has been derived from various lab-scale combustion tests and does not vary strongly for different biomass fuels). The calculated release ratios are compared with experimentally determined release ratios from lab-scale reactor experiments (see section 4.5).

For the prediction of the ash melting behavior, as input data the results of chemical analyses of the laboratory ashed fuels are applied.

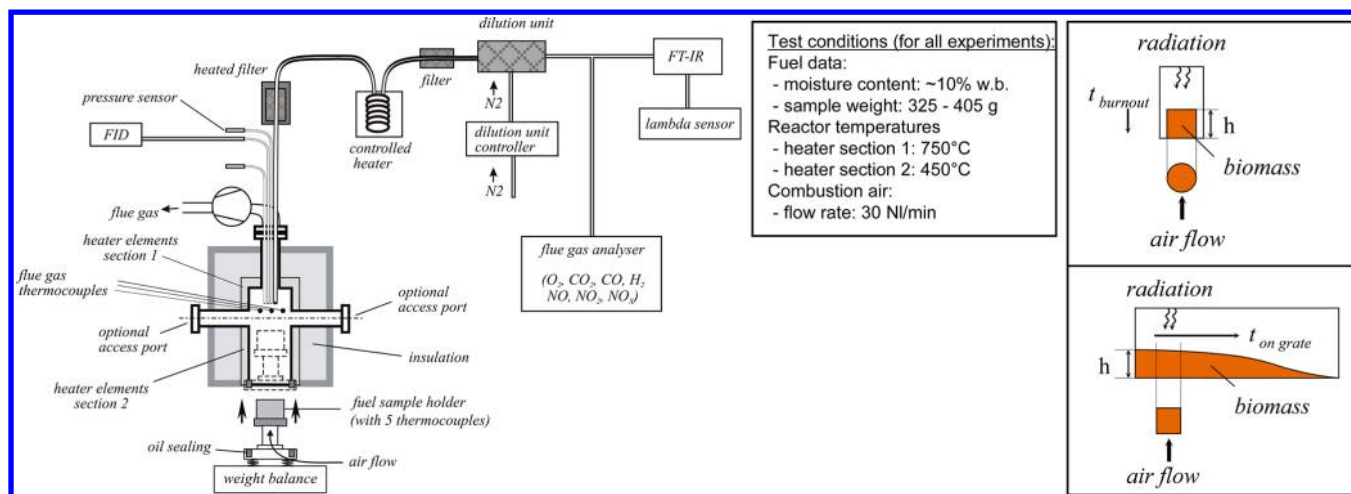


Figure 1. Scheme of the lab-scale reactor, including measurement setup (left), common test conditions prevailing for all experiments (middle), and projection of the lab-scale reactor to the fuel layer in a grate furnace (right).^{16,17}

The index regarding the Al₂O₃ exclusion and the selection of the SALT phase as well as the index of the molar (Si + K + P)/(Ca + Mg) ratio to consider the Si reactivity are considered. The calculations are performed for an oxidizing gas atmosphere as well as atmospheric pressure. The temperature range investigated has been 500–1600 °C, and these calculations have been performed in a one-step approach. The results of the calculations have been compared with the standard ash melting test according to CEN/TS 15370-1 (see section 4.2).

2.4. Lab-Scale Reactor Experiments. Test runs with a lab-scale reactor especially designed for the investigation of the thermal decomposition behavior of biomass fuels have been performed for selected biomass/kaolin mixtures. The results regarding inorganic element release gained from these lab-scale reactor experiments have been used to evaluate and validate the new approach concerning additive evaluation.

This lab-scale reactor consists of a cylindrical retort (height 35 cm, inner diameter 12 cm) which is heated electrically and controlled by two separated proportional-integral-derivative (PID) controllers, as can be seen in Figure 1. The fuel is inserted in a cylindrical sample holder of 100 mm height and 95 mm inner diameter. The reactor wall and sample holder are made of reinforced silicon carbide. This material is inert under reducing and oxidizing conditions, which ensures that the wall does not react with the fuel, ash, and flue gas. The sample holder is placed on the plate of a scale. The scale, which is used to determine the weight loss of the sample, is mechanically separated from the retort by a liquid seal (synthetic thermal oil, Therminol 66). This setup ensures the possibility of continuously determining the weight loss of the sample during drying, pyrolysis, gasification, and charcoal combustion. The sample is introduced into the preheated reactor, and therefore a rapid heating, which is well comparable with the one in real-scale fixed-bed thermal conversion processes, can be achieved. The test conditions for all test runs performed with the lab-scale reactor are defined in Figure 1. For the experiments conducted in this study, only pelletized fuels have been used. In ref 15 a more detailed description of the test procedure and the evaluation of the lab-scale reactor experiments can be found.

The following measurements/analyses were performed during each of the combustion test runs:

1. The mass decrease of the fuel over time (balance) was measured.
2. Concentrations of flue gas species over time were determined: (i) Determination of CO₂, H₂O, CO, CH₄, NH₃, HCN, N₂O, and basic hydrocarbons was done with a multicomponent Fourier transform infrared (FTIR) spectroscopy device (Ansyco Series DX 4000). (ii) The O₂ and H₂ concentrations were measured with a multicomponent gas analyzer (Rosemount NGA 2000). This device uses paramagnetism as a measurement principle for O₂ detection and a thermal conductivity detector (TCD) for H₂ detection. (iii) The amounts of total hydrocarbons (C_xH_y) were determined with a flame ionization

detector (FID) (Bernath Atomic 3005) which detects organic compounds by ionization in a burning H₂ flame. (iv) A wide band lambda sensor was used for O₂ detection. (v) A nitric oxide analyzer (ECO Physis CLD 700 El ht), which uses the principle of chemiluminescence, has been used for NO and NO₂ detection.

3. The temperature was measured over time with (i) five thermocouples in the fuel bed (three different heights, NiCr–Ni) and (ii) thermocouples in the gas phase (NiCr–Ni).

4. The biomass fuel used and residual ash produced were analyzed (see section 2.1).

The data gained from the fuel analysis and the residual ash analysis as well as the weight measurements of the fuel sample and the ash sample can be used to calculate the elemental release to the gas phase. This is done by calculating the mass balance for every relevant element, as well as for the total ash.

The special design of the lab-scale reactor ensures that the burning conditions of a biomass fuel layer on a grate are represented as good as possible (Figure 1, right). This approach is valid if diffusional transport and mixing effects on the grate can be neglected compared to the transport of the fuel along the grate. The validation has been achieved in previous research which has shown that the fuel transport along the grate can be fluidically characterized by a plug flow to a good approximation.^{16,17} Therefore, tests within this reactor can be applied to evaluate and validate the predictions gained from the advanced fuel characterization tools for fixed bed combustion conditions.

Furthermore, lab-scale reactor experiments can give the first information about the ash sintering tendency. According to visual evaluation of the ash residues after a test run, the ash may be described as loose ash residue, slightly sintered ash with a brittle structure, hard sintered ash residue with partial melting, very hard sintered ash residue with slag formation, and completely molten ash residue.

3. MATERIALS

3.1. Fuels Investigated. Softwood and straw have been chosen as biomass fuels with the aim to investigate the influence of kaolin addition to these fuels. Softwood is the most common fuel used in residential and industrial combustion applications. This fuel shows an unproblematic combustion behavior, whereby a potential for reduction of PM emissions exists. The addition of kaolin could make this fuel also applicable under the constraints of tightened regulations regarding PM emissions in the future which is especially for small-scale applications (residential systems) of relevance where usually no dust precipitation devices are installed.

A more challenging fuel which has also been investigated is wheat straw. High yields of this fuel are available in many countries, which makes straw interesting for a broad usage. However, straw shows a rather problematic combustion behavior. Its ash melting temperatures

Table 1. Chemical Composition of the Spruce and Straw Utilized in Comparison with Database Values as Well as of Pure Kaolin^a

		softwood (spruce)				straw (wheat)				kaolin
		this study	database			this study	database			
			average	std dev	no.		average	std dev	no.	
ac 550 °C	wt % db	0.40	0.33	0.03	39	4.5	6.6	1.5	19	
ac corr	wt % db	0.35				4.2				
C	wt % db	50.2	50.2	0.8	24	46.6	44.9	2.7	15	
H	wt % db	6.2	6.3	0.34	24	6.0	5.6	0.36	15	
N	wt % db	0.05	0.08	0.03	27	0.40	0.6	0.16	15	
S	mg/kg db	72.0	53.6	2.4	36	913	1485	527	19	425.0
Cl	mg/kg db	59.0	37.6	11.6	38	2300	3046	1859	19	51.0
Ca	mg/kg	751	907	123.4	39	3010	3785	1614	19	132.0
Si	mg/kg db	420.0	158.7	2.4	33	11 100	17 618	4917	19	204 000
Mg	mg/kg db	140.0	120.9	8.8	39	688	945	662	19	22.7
K	mg/kg db	564	382.7	25.9	39	6970	6629	4149	19	857
Na	mg/kg db	21.7	10.9	4.7	39	201.0	282.9	228.0	19	1680
P	mg/kg db	43.9				385.0	442.0	148.2	19	224.0
Al	mg/kg db	34.2				217.0	237.9	244.9	18	223 000
Zn	mg/kg db	12.7	11.1	0.7	35	6.6	9.9	3.4	6	15.1
Pb	mg/kg db	0.21				0.23	0.32	0.20	6	47.3

^aDefinitions: ac 550°C, ash content determined by 550 °C under oxidizing conditions; ac corr, ash content carbonate corrected; db, dry basis; number, number of analysis considered in the database.

Table 2. Comparison of Theoretical Mixing Calculations with Results of Chemical Analysis for the Spruce/Kaolin Mixtures Investigated^a

		kaolin ratio (wt %)									
		0.0	0.2	0.2	0.2	1.0	1.0	1.0	3.0	3.0	3.0
			calc	meas	calc/meas (%)	calc	meas	calc/meas (%)	calc	meas	calc/meas (%)
ac 550 °C	wt % db	0.40	0.6	0.5	93	1.3	1.1	88	3.0	2.6	87
ac corr	wt % db	0.35		0.5			1.1			2.6	
C	wt % db	50.2	50.0	50.0	100	49.6	49.7	100	48.6	48.9	101
H	wt % db	6.2	6.2	6.3	101	6.2	6.3	101	6.0	6.1	101
N	wt % db	0.05	0.05	0.06	129	0.05	0.06	116	0.05	0.04	88
S	mg/kg db	72.0	72.7	60.7	83	75.5	52.1	69	82.6	66.8	81
Cl	mg/kg db	59.0	59.0	31.3	53	58.9	19.7	33	58.8	17.9	30
Ca	mg/kg	751	750	702	94	745	691	93	732	668	91
Si	mg/kg db	420.0	827	778	94	2456	2190	89	6527	5930	91
Mg	mg/kg db	140.0	139.8	129.0	92	138.8	126.0	91	136.5	125.0	92
K	mg/kg db	564	565	465.0	82	567	391.0	69	573	390.0	68
Na	mg/kg db	21.7	25.0	21.0	84	38.3	31.7	83	71.4	62.9	88
P	mg/kg db	43.9	44.3	36.4	82	45.7	36.7	80	49.3	38.7	78
Al	mg/kg db	34.2	480.1	662	138	2264	2240	99	6723	5820	87
Zn	mg/kg db	12.7	12.7	11.8	93	12.7	11.6	91	12.8	12.1	95
Pb	mg/kg db	0.21	0.31	0.21	67	0.7	0.9	133	1.6	0.6	36
Characteristic Ash Melting Temperatures (°C) (CEN/TS 15370-1)											
	shrinkage starting			1220		1260		1330			>1480
	deformation			n.o.		1290		1380			>1480
	hemisphere			1320		1320		1400			>1480
	flow			1340		1330		1420			>1480

^aDefinitions: calc, calculated; meas, measured; ac 550°C, ash content determined by 550 °C under oxidizing conditions; ac corr, ash content carbonate corrected; db, dry basis; n.o., not occurring.

are low compared to those of wood fuels. Moreover, straw combustion implies high temperature corrosion risks as well as high levels of PM emissions.¹⁸ The addition of kaolin opens up the possibility to reduce these problems regarding PM emissions and ash melting significantly and could thus make it possible or easier to utilize this fuel in the future in state-of-the-art combustion plants applied for wood fuels.

The softwood investigated originates from northern Sweden and is spruce stem wood without bark as usually used for pellet production.

The origin of the wheat straw is Denmark. The kaolin used was delivered from the company Thiele Nordic AB (Sweden), with a particle size of <2 μm.

Samples of the pure fuels and kaolin were analyzed. In Table 1, the chemical compositions of the pure biomass fuels and kaolin are summarized. Additionally, the compositions of the biomass fuels are compared with database values gained from the IEA Task 32 biomass fuel database¹⁹ as well as from an internal database from BIOS

Table 3. Comparison of Theoretical Mixing Calculations with Results of Chemical Analysis for the Straw/Kaolin Mixtures Investigated^a

		kaolin ratio (wt %)									
		0.0	1.0	1.0	1.0	4.0	4.0	4.0	7.0	7.0	7.0
			calc	meas	calc/meas (%)	calc	meas	calc/meas (%)	calc	meas	calc/meas (%)
ac 550 °C	wt % db	4.5	5.3	5.0	95	7.8	7.1	92	10.2	9.5	93
ac corr	wt % db	4.2		4.9			7.1			9.5	
C	wt % db	46.6	46.2	46.5	101	44.8	45.3	101	43.4	43.7	101
H	wt % db	6.0	5.9	6.0	101	5.7	5.9	103	5.6	5.8	104
N	wt % db	0.40	0.39	0.38	97	0.38	0.34	90	0.37	0.37	102
S	mg/kg db	913	908	849	93	893	857	96	879	874	99
Cl	mg/kg db	2300	2278	2210	97	2210	2240	101	2143	2240	105
Ca	mg/kg db	3010	2981	2820	95	2895	2790	96	2809	2800	100
Si	mg/kg db	11 100	13 029	12 000	92	18 816	17 000	90	24 603	22 400	91
Mg	mg/kg db	688	681	649	95%	661	636	96	641	651	101
K	mg/kg db	6970	6909	6430	93	6725	6430	96	6542	6370	97
Na	mg/kg db	201.0	215.8	204.0	95	260.2	244.0	94	304.5	287.0	94
P	mg/kg db	385.0	383.4	358.0	93	378.6	357.0	94	373.7	372.0	100
Al	mg/kg	217.0	2445	2010	82	9128	7160	78	15 812	12 600	80
Zn	mg/kg db	6.6	6.6	5.9	89	6.9	6.1	88	7.1	7.5	104
Pb	mg/kg db	0.23	0.7	0.37	53	2.1	0.7	34	3.5	1.2	33
Characteristic Ash Melting Temperatures (°C) (CEN/TS 15370-1)											
	shrinkage starting			780		1160			1330		1310
	deformation			1010		1220			1340		1330
	hemisphere			1070		1240			1370		1380
	flow			1130		n.o.			1440		1450

^aDefinitions: calc, calculated; meas, measured; ac 550°C, ash content determined by 550 °C under oxidizing conditions; ac corr, ash content carbonate corrected; db, dry basis; n.o., not occurring.

BIOENERGIESYSTEME GmbH, Graz, Austria. This has been done to check whether the fuel composition generally complies with typical ranges of element concentrations for these two fuel types and can thus be seen to be representative.

It can generally be said that the concentrations of the different elements in the fuels investigated are typical for the respective type of biomass.

Based on the analysis data, theoretical mixing calculations of promising kaolin addition ratios have been performed. The estimated mixtures were preevaluated with fuel indexes and TEC to prepare adequate kaolin mixtures for combustion purposes (see section 4.8). For spruce 0, 0.2, 1, and 3 wt % kaolin, whereas for straw 0, 1, 4, and 7 wt % kaolin, were selected, whereby for spruce 1 wt % kaolin and for straw 4 wt % kaolin have been evaluated as optimum kaolin addition ratios. The ratios of 0.2 wt % kaolin for spruce and 1 wt % kaolin for straw are expected to be too low to show a significant influence on the combustion behavior, whereas the ratios of 3 wt % kaolin for spruce and 7 wt % kaolin for straw have been chosen to investigate the overdosing of kaolin. The pure fuel samples were used as reference points. Generally, the preparation of the mixtures is related to dry basis regarding fuel and kaolin.

The pretreatment of the fuels as well as the pelletizing (Greenforze MZLP 400 series flat pellet die) was done by Teagasc (the Irish agriculture and food development authority) in cooperation with UmU (Umeå University Sweden Institute for Applied Physics and Electronics). The fuel raw materials were milled. In the next step kaolin was dosed to the fuel and mixed in a proper way to ensure an as homogeneous as possible kaolin distribution in the mixtures, and finally the fuel samples were pelletized. The pelletized fuels were then sent to BIOENERGY 2020+ for analysis and further studies.

3.2. Evaluation of the Quality of the Biomass Pellets Prepared. In order to check the quality of the fuel/kaolin mixtures prepared, the theoretically calculated concentrations of the mixtures were compared with the analysis results of the pellet samples. The results of chemical fuel analysis in comparison with theoretical mixing

calculations for spruce and the spruce/kaolin mixtures are summarized in Table 2.

For most elements a good agreement of measured and calculated concentrations can be observed. Deviations can be found for S, Cl, and Pb. This can be explained by the low concentrations of these elements in the fuel which are close to the detection limits of the measurement instruments. For the K concentrations in the mixtures of 1 and 3 wt % kaolin the result is also not satisfying. The reason for the strong deviation of measured in comparison with theoretically calculated values may be explained by an inhomogeneous distribution of K in the fuel. It has to be noted in this respect that the chemical analysis of the samples has been conducted for three subsamples and comparable results were obtained.

In Table 3, the comparison between the theoretically calculated concentrations of the mixtures and the results of chemical fuel analyses for straw and the straw/kaolin mixtures is presented.

From Table 3, it can be seen that very good agreement of measured and calculated values except for Pb exists. This can again be explained by the low concentration range of Pb in the fuel.

Concluding, it can be said that the mixing quality can be evaluated as good and that the samples produced can be seen as representative for the purpose of the work.

4. RESULTS

4.1. Evaluation of Fuel Indexes. As a first step of fuel characterization, an evaluation based on fuel indexes has been conducted. The calculated values are summarized in Table 4.

4.1.1. $(Si + P + K)/(Ca + Mg + Al)$ as Indicator for the Ash Melting Behavior. This index takes the elements Si (in combination with K), P, and K (which typically reduce the ash melting temperate) in relation to the elements Ca, Mg, and Al (which typically increase the ash melting temperature). Therefore, with decreasing value of this index the ash melting temperature increases.

Table 4. Values of Relevant Fuel Indexes for the Fuels and Fuel/Kaolin Mixtures Investigated

	$(\text{Si} + \text{P} + \text{K})/(\text{Ca} + \text{Mg} + \text{Al})$ (mol/mol)	2S/Cl (mol/mol)
spruce–0.0% kaolin	1.2	2.7
spruce–0.2% kaolin	0.9	2.7
spruce–1.0% kaolin	0.8	2.8
spruce–3.0% kaolin	0.9	3.1
straw–0.0% kaolin	5.3	0.9
straw–1.0% kaolin	3.5	0.8
straw–4.0% kaolin	2.2	0.8
straw–7.0% kaolin	1.7	0.9

The value for pure spruce is already on a low level (1.2), which indicates a high ash melting temperature. With kaolin addition the values slightly decrease (0.8–0.9). For spruce only a slight improvement of the ash melting tendency with kaolin addition is expected. For pure straw the value of the index amounts to 5.3, which indicates a low ash melting temperature. With increasing kaolin addition ratio the values of this index strongly decrease. Therefore, it is expected that the addition of kaolin to straw clearly improves the ash melting behavior, which reduces combustion related problems.

4.1.2. Molar 2S/Cl Ratio as Indicator for High Temperature Chlorine Corrosion Risk. It has been reported that with increasing Cl concentrations in the tube near deposit layers the high temperature corrosion risk rises, whereas only a minor corrosion risk has to be expected for 2S/Cl ratios in the fuel of >4 . To achieve negligible chlorine levels in the boiler deposits and thereby significantly reduce high temperature chlorine corrosion, it has been suggested that the molar 2S/Cl ratio should be at least 8.²⁰

For the evaluation of the molar 2S/Cl ratios for spruce the values gained from the theoretical mixing calculations have been used, since the results of the chemical analyses for S and Cl are problematic due to the low concentrations close to the detection limit. From Table 4, it can be determined that for spruce without kaolin an increased risk for high temperature chlorine corrosion exists (2.7). For kaolin addition to spruce the values of the 2S/Cl ratios slightly increase and reach 3.1 for an addition ratio of 3 wt % kaolin. Therefore, also for the

additive ratio of 3 wt % kaolin to spruce an increased risk of high temperature chlorine corrosion still exists.

For pure straw and the straw/kaolin mixtures a high corrosion risk (0.85–0.88) has to be expected. The kaolin addition does not influence the molar 2S/Cl ratio in a relevant way as the S concentration of kaolin is lower and the Cl concentration is significantly lower compared to the S and Cl concentrations of pure straw.

It can be summarized that for both fuels the kaolin addition has no significant influence on the molar 2S/Cl ratio. It is expected that the kaolin addition decreases the K release^{4,5} to the gas phase. In the gas phase the formation of KCl is probable. It is also shown in this work that with increasing kaolin addition the amount of KCl in aerosol emissions decreases (Figure 9). This indicates that with kaolin addition it is very likely that fewer KCl depositions are formed on the heat exchanger surfaces, which could also lead to a reduction of corrosion related problems.

4.2. Evaluation of the Ash Melting Behavior Predicted by TEC in Comparison with Experimental Results. The ash melting behavior has been investigated with the standard ash melting test (CEN/TS 15370-1) and TEC. The latter can provide more detailed insights into the ash melting behavior.

In Figure 2, results from TEC based on the chemical compositions of the ashed samples (ashed at 550 °C under oxidizing conditions) are presented, whereby Figure 2 (left) shows the results for the pure straw sample and Figure 2 (right) shows the results regarding straw with 7 wt % kaolin. For each temperature between 500 and 1600 °C the amount of molten fraction is specified. It is obvious that with increasing temperature the amount of molten fractions rises. Characteristic molten fractions indicated in the diagram as “30 wt % liquid phase” and “70 wt % liquid phase” have been calculated as the ratio between the mass of all molten phases at the specific temperature (T_{30} and T_{70}) and the total mass (solid and liquid). When taking T_{30} of pure straw (770 °C) (Figure 2, left), as an indicator for the SST (shrinkage starting temperature), good agreement with the standard ash melting test (SST 780 °C) is achieved. The calculated T_{70} temperature, which is 1250 °C, is a rather good indicator for the FT (flow temperature) (1130 °C). Moreover, useful information regarding the temperature dependent behavior of molten

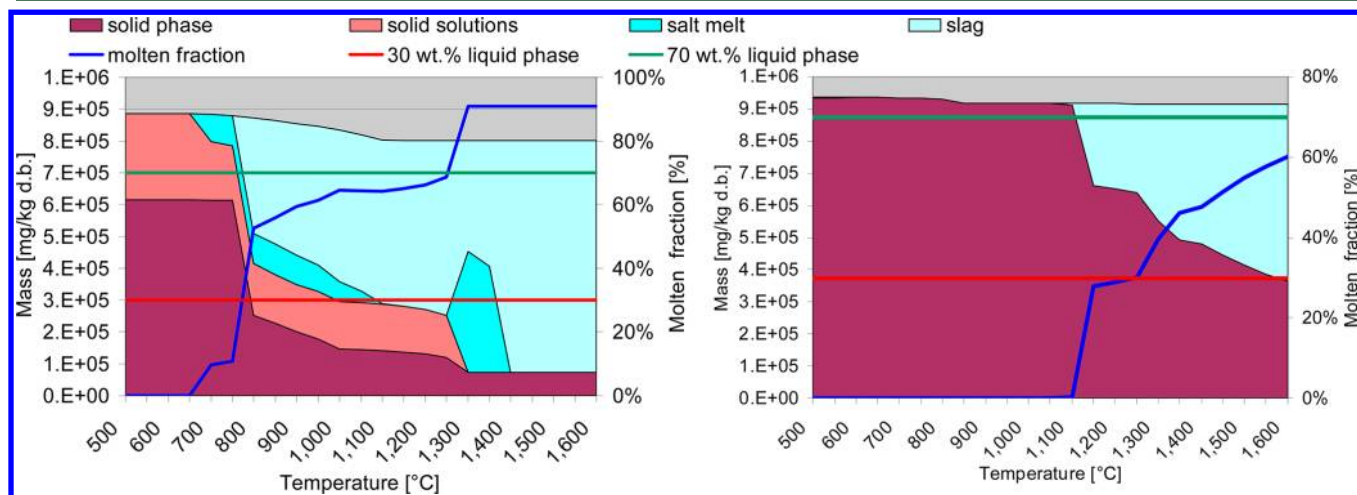


Figure 2. Ash melting behavior for pure straw (left) and straw with 7 wt % kaolin (right) determined by thermodynamic equilibrium calculations. d.b., dry basis.

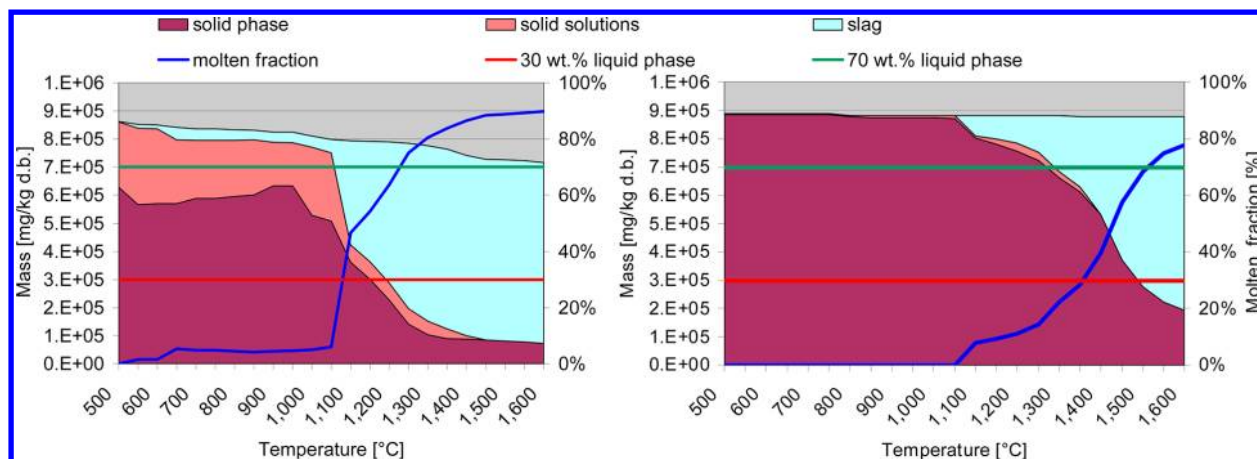


Figure 3. Ash melting behavior for pure spruce (left) and spruce with 1 wt % kaolin (right) determined by thermodynamic equilibrium calculations. d.b., dry basis.

phases as well as the molten compounds expected can be gained. From Figure 2 (right), where results of TEC for straw with 7 wt % kaolin are displayed, it can be seen that the T_{30} temperature amounts to 1240 °C, which is in good agreement with the SST of the standard ash melting test (1310 °C). A steep increase of the molten fraction can be observed between 1100 and 1150 °C. Between 1150 and 1250 °C the amount of molten fraction just slightly increases; above 1250 °C a steeper increase of molten fraction can be observed whereby TEC predicts a T_{70} temperature of >1600 °C, which is not in line with the FT (1450 °C) gained from the standard ash melting test.

In Figure 3, results of TEC concerning the evaluation of the ash melting temperature for spruce are displayed. Figure 3 shows the results for the pure spruce sample (left) and the results regarding spruce with 1 wt % kaolin (right). Comparing the T_{30} of pure spruce (1080 °C) with the SST, an acceptable agreement with the standard ash melting test (1220 °C) is achieved. The calculated T_{70} temperature, which is 1230 °C, is a rather good indicator for the FT (1340 °C). From Figure 3 (right), results of TEC for spruce with 1 wt % kaolin are displayed, where it can be seen that the T_{30} temperature (1360 °C) is in very good agreement with the SST of the standard ash melting test (1380 °C). The T_{70} temperature, 1510 °C, is also in good agreement with the FT (1420 °C).

In section 4.1 the index of the molar $(\text{Si} + \text{P} + \text{K})/(\text{Ca} + \text{Mg} + \text{Al})$ ratio was already discussed. In Figure 4, the molar $(\text{Si} + \text{P} + \text{K})/(\text{Ca} + \text{Mg} + \text{Al})$ ratio is plotted versus the SST. In addition, the results from TEC are displayed in the same diagram.

As seen in Figure 4, with increasing kaolin addition ratio the ash melting temperatures increase for straw and spruce. The SST of pure straw has been experimentally determined with 780 °C. With increasing kaolin addition SST increases and shows a maximum value (1330 °C) for a kaolin addition ratio of 4 wt %. As expected from the low values of the molar $(\text{Si} + \text{P} + \text{K})/(\text{Ca} + \text{Mg} + \text{Al})$ ratios for spruce and the spruce/kaolin mixtures, the SST values for these mixtures are on a high level. For pure spruce the SST exceeds 1200 °C. A kaolin addition to spruce further raises the SST, and for a kaolin addition of 3 wt % SST > 1480 °C has been determined. For straw as well as for spruce TEC predict lower ash SST compared to the experimental data with the exception of spruce with 1 wt % kaolin. The differences decrease with rising kaolin content.

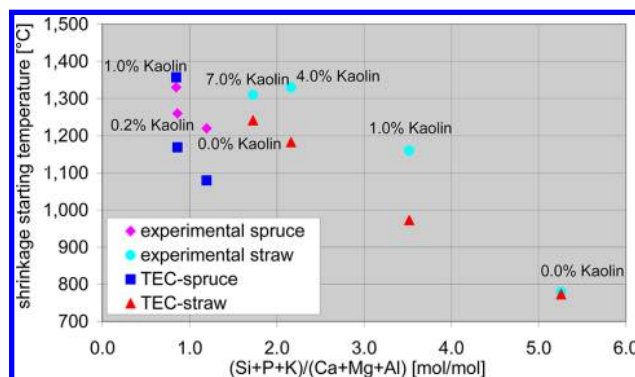


Figure 4. Molar $(\text{Si} + \text{P} + \text{K})/(\text{Ca} + \text{Mg} + \text{Al})$ ratio versus shrinkage starting temperature for pure spruce and spruce/kaolin mixtures as well as for pure straw and straw/kaolin mixtures in comparison with the results from thermodynamic equilibrium calculations. Experimental, shrinkage starting temperature according to the standard ash melting test (CEN/TS 15370-1); TEC, thermodynamic equilibrium calculations (temperature where 30 wt % liquid phase occurs).

TEC predictions are in good qualitative agreement with the experimental results.

4.3. Prediction of the Release Behavior of Ash Forming Elements with Thermodynamic Equilibrium Calculations. TEC have also been used to calculate the release behavior of ash forming elements for the biomass samples investigated. In Figure 5, the release rates of volatile and semivolatile elements for spruce and spruce/kaolin mixtures as well as for straw and straw/kaolin mixtures are summarized.

It can be seen from Figure 5 that TEC predict a complete release for S, Cl, and Pb for all fuels investigated regardless of the kaolin addition ratio. For pure spruce a K release of 22% is predicted, whereas with a kaolin addition of 0.2 wt % the K release decreases to 3.1%. For pure straw a K release of 16.8% is predicted, and for straw with 1 wt % kaolin the K release is reduced to 8.2%. For higher kaolin addition no K release is predicted. For K it can be concluded that with increasing kaolin addition the formation of K–Al–Si phases is preferred which are stable under reducing and oxidizing conditions up to 1250 °C.

Kaolin also seems to reduce the Zn release most likely due to incorporation of Zn in solid (e.g., ZnFe_2O_4 and ZnAl_2O_4) and liquid (e.g., ZnO) phases, but the release behavior of Zn is

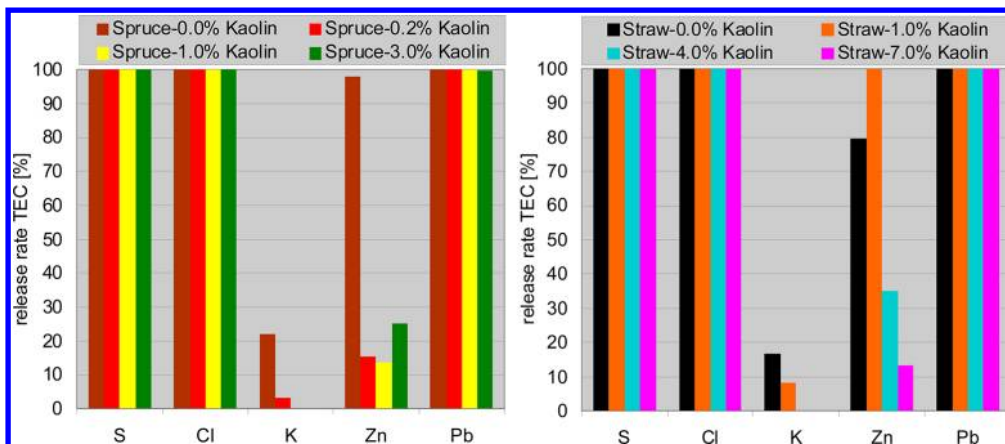


Figure 5. Release rates of volatile and semivolatile elements determined with thermodynamic equilibrium calculations.

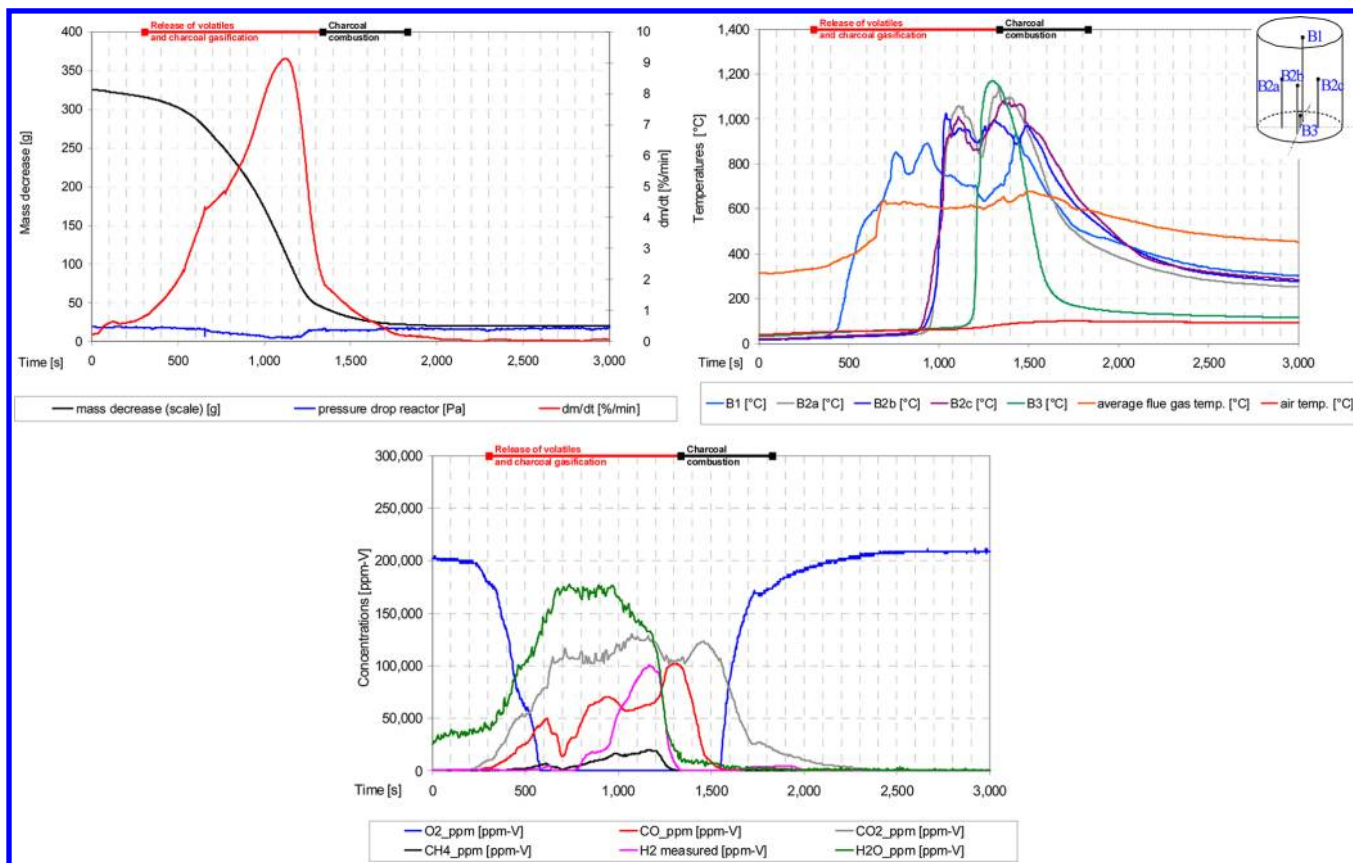


Figure 6. Measured trends regarding mass loss, fuel bed, and flue gas temperatures as well as main gas species concentrations over time for the test run with straw and 4 wt % kaolin.

difficult to determine correctly by TEC as a previous study¹³ shows.

The release behavior of Na has not been evaluated by TEC, due to very low concentrations in the fuels and mixtures. The P release also cannot be predicted by TEC, due to the insufficient quality of the thermodynamic data for P components.¹⁴

4.4. Thermal Decomposition Behavior Determined by Lab-Scale Reactor Experiments: Case Study Straw with 4 wt % Kaolin Addition. The test run with straw and 4 wt % kaolin is discussed in detail in order to present and explain the whole evaluation procedure of lab-scale reactor tests.

The chemical composition of the fuel can be taken from Table 3. Three test runs have been performed in repetition.

Since all three tests showed about the same results, here only test run one is discussed. Fuel masses of 325.3 g (wet basis, wb) and 275.8 g (db) were respectively used.

In Figure 6 the trends regarding mass loss, fuel bed temperatures, and flue gas temperatures as well as the concentrations of the main gas species over time are displayed.

As can be seen, the test run duration was about 1520 s. At the beginning, mainly drying takes place indicated by a moderate mass loss, low fuel bed temperatures, and the release of H₂O. After about 300 s, fuel decomposition starts indicated by decreasing O₂ concentrations and increasing CO₂ concentrations in the flue gas. The main decomposition phase starts with a rapid decrease of the O₂ concentration to

Table 5. Chemical Composition of Ash Residues from Lab-Scale Reactor Tests for Spruce and Spruce/Kaolin Mixtures as Well as for Straw and Straw/Kaolin Mixtures^a

		spruce–0.0% kaolin		spruce–0.2% kaolin		spruce–1.0% kaolin		spruce–3.0% kaolin	
		test 1	test 2						
Ca	mg/kg db	202 000	214 000	130 000	127 000	57 600	57 100	23 300	23 100
Si	mg/kg db	104 000	109 000	144 000	149 000	187 000	184 000	194 000	206 000
Mg	mg/kg db	35 300	37 800	23 000	22 700	10 900	10 800	4 700	4 500
Al	mg/kg db	11 200	9 880	118 000	122 000	189 000	185 000	216 000	203 000
K	mg/kg db	126 000	130 000	83 900	84 200	36 200	37 850	15 300	15 530
Na	mg/kg db	4440	4700	3870	3740	2670	2600	2180	2210
Zn	mg/kg db	108.0	93.9	107.0	78.7	69.1	83.0	61.3	53.6
Pb	mg/kg db	2.1	1.2	1.5	1.4	4.9	6.6	6.6	4.5
S	mg/kg db	3320	2890	1860	1550	417.0	404.0	196.0	137.0
Cl	mg/kg db	850	389.0	702	429.0	39.4	64.8	10.0	12.8
P	mg/kg db	12 300	12 700	6870	6720	3090	3030	1370	1360
TOC	mg/kg db	5000	5000	2300	6800	1000	1000	1000	1000
TIC	mg/kg db	4500	4500	4200	3600	1100	1100	1000	1000
		straw–0.0% kaolin		straw–1.0% kaolin		straw–4.0% kaolin		straw–7.0% kaolin	
		test 1	test 2						
Ca	mg/kg db	70 300	67 700	57 900	56 400	37 700	38 100	27 900	28 200
Si	mg/kg db	259 000	268 000	257 000	256 000	240 000	237 000	242 000	235 000
Mg	mg/kg db	16 900	17 400	14 300	14 300	9 590	9 500	7 160	7 210
Al	mg/kg db	4 900	4 840	46 200	46 200	104 000	104 000	137 000	136 000
K	mg/kg db	119 300	122 000	107 300	105 800	86 600	84 500	68 300	68 200
Na	mg/kg db	4170	4130	3760	3730	3290	3290	2970	2970
Zn	mg/kg db	43.7	43.2	23.6	29.3	48.7	32.4	37.9	25.8
Pb	mg/kg db	0.7	1.3	0.5	0.7	1.4	1.4	2.4	2.3
S	mg/kg db	2140	2350	1690	1880	1340	1320	493.0	465.0
Cl	mg/kg db	917	1320	299.0	324.0	531	124.0	59.6	30.4
P	mg/kg db	8750	8620	7170	7150	4730	4780	3550	3640
TOC	mg/kg db	11 800	12 900	4400	4400	6000	5900	4600	4800
TIC	mg/kg db	1000	1000	1000	1000	1000	1000	1000	1000

^aDefinitions: TOC, total organic carbon; TIC, total inorganic carbon; db, dry basis.

zero level after 600 s. Release of volatiles and parallel charcoal gasification then takes place until around 1350 s in the test run duration. Rapid mass losses, an increase of the bed temperatures, and combustion air ratios below 1 are typical indicators for this phase. Mainly CO₂, CO, H₂O, CH₄, and H₂ as well as minor amounts of other hydrocarbons are released to the gas phase. After 1350 s H₂ and CH₄ drop to zero, which is taken as an indicator for the end of the release of volatiles and the start of the charcoal combustion phase. This phase is characterized by smaller amounts of CO and increasing CO₂ concentrations in the flue gas as well as increasing O₂ concentrations (increasing excess air ratio). At the beginning of this phase typically the highest fuel bed temperatures (in this case 1168 °C) are measured.

After the end of the test run the amount of residues (ashes) amounted to 19.1 g (db). No sintered ash pieces or slag could be identified, which is not surprising since the maximum fuel bed temperature achieved was 1168 °C, significantly below the SST (1330 °C) according to CEN/TS 15370-1.

Element balances performed based on the fuel analysis data and the process data recorded showed good closures for C (88.6%), H (82.6%), O (99.0%), and the total ash after correction regarding TIC (97.2%). This good balance closure is a relevant aspect regarding the representativeness of the test runs.

The start of the release of volatiles and charcoal gasification, the start of the charcoal combustion, and the duration of each

phase were almost constant for spruce and the spruce/kaolin mixtures as well as for straw and the straw/kaolin mixtures. This shows that the addition of kaolin did not influence the thermal decomposition behavior of the fuels.

4.5. Evaluation of TEC in Comparison with Experimental Results Regarding the Release Behavior of Ash Forming Elements. Lab-scale reactor experiments can be used to quantitatively determine the release of inorganic elements from the fuel to the gas phase and therefore were applied in order to validate the results gained from TEC.

The release ratios, determined by lab-scale reactor experiments, are calculated by element balances, based on weight measurements and chemical analysis of the fuel and the ash obtained according to eq 1:

$$\text{release}_{y,\text{wt}\%} = \left(1 - \frac{c_{y,\text{output}(\text{db})} \cdot m_{\text{output}(\text{db})}}{c_{y,\text{input}(\text{db})} \cdot m_{\text{input}(\text{db})}}\right) \cdot 100 \quad (1)$$

where $m_{\text{input}(\text{db})}$ is the mass [g db] of the fuel sample fed to the reactor, $c_{y,\text{input}(\text{db})}$ is the concentration of element y in the fuel [mg/kg db], $m_{\text{output}(\text{db})}$ is the mass [g db] of the ash residual after the experiment, and $c_{y,\text{output}(\text{db})}$ is the concentration of element y in the ash residual [mg/kg db]. In Table 5, the concentrations of the ash residues of the test runs performed are summarized. For each fuel and fuel mixture the ashes from two test runs were chemically analyzed.

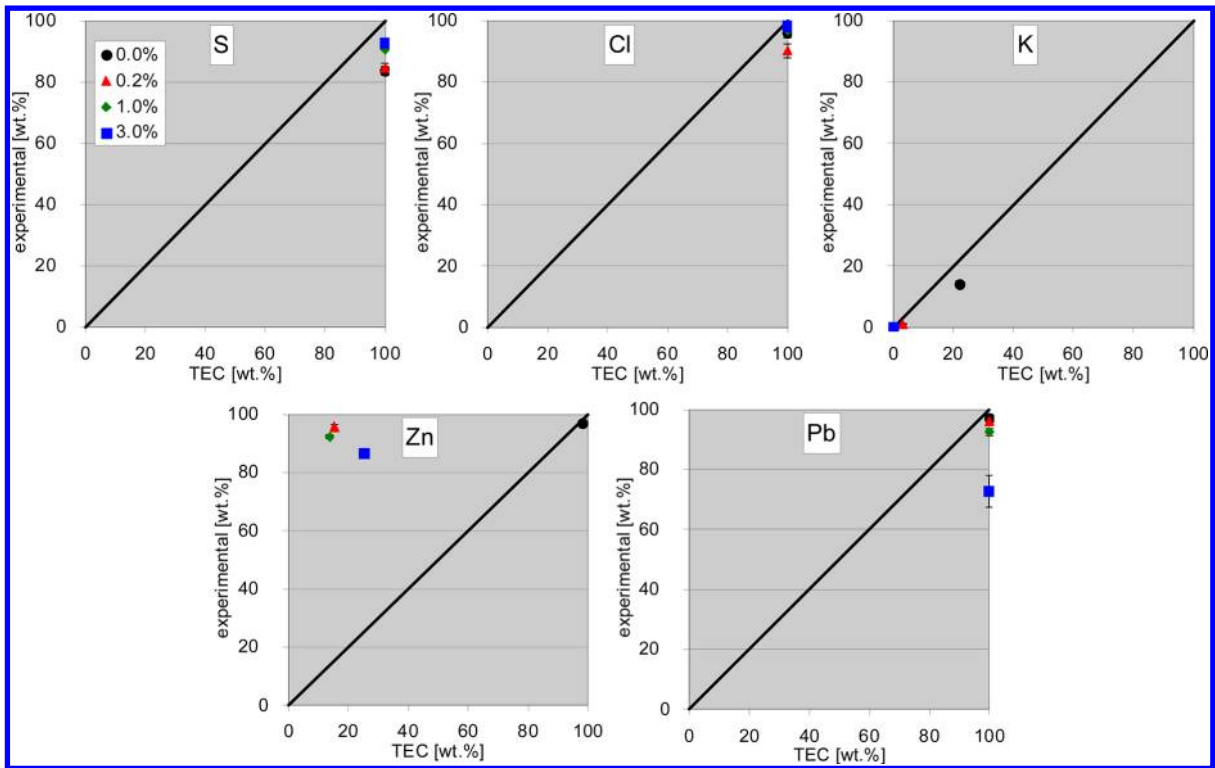


Figure 7. Experimentally determined element release from the fuel to the gas phase from lab-scale reactor experiments in comparison with thermodynamic equilibrium calculations for pure spruce and spruce/kaolin mixtures. TEC, thermodynamic equilibrium calculations (TEC release estimated at 1250 °C).

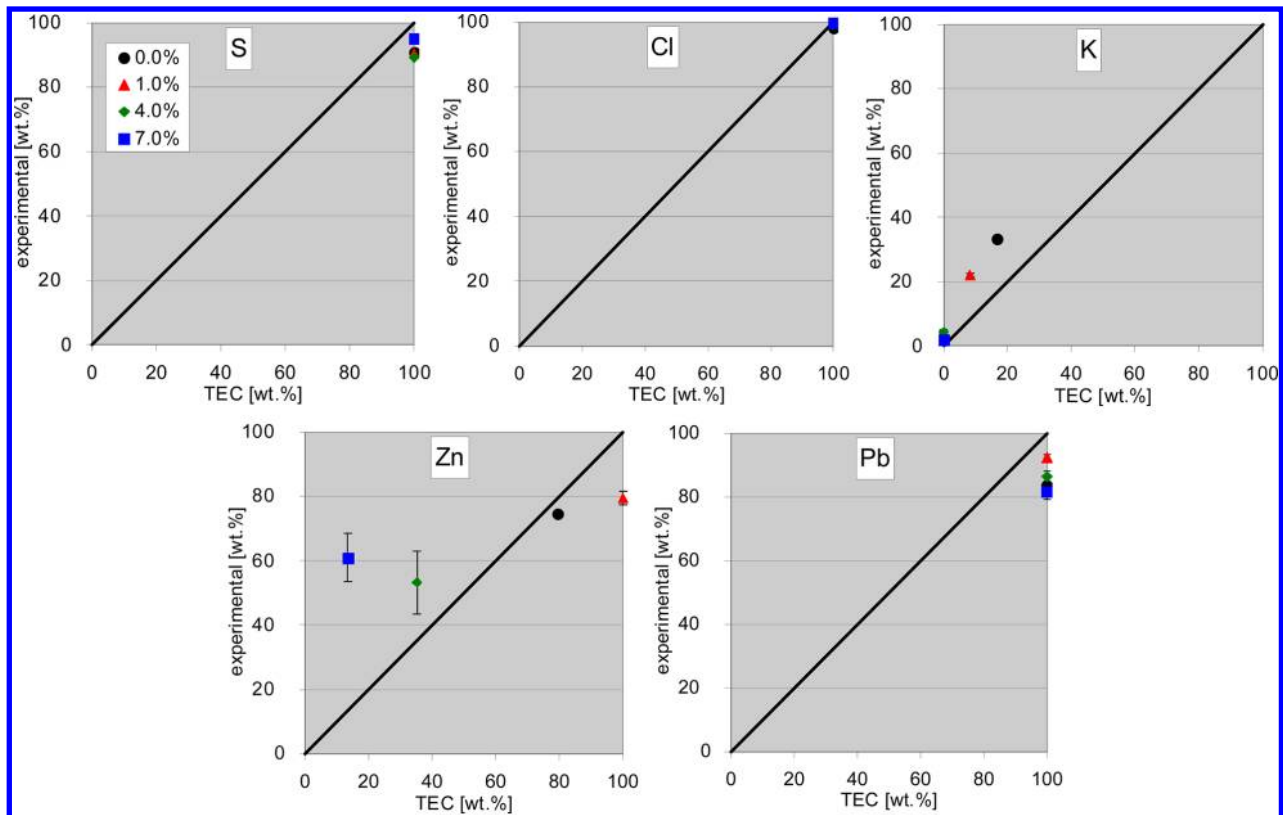


Figure 8. Experimentally determined element release from the fuel to the gas phase from lab-scale reactor experiments in comparison with TEC for pure straw and straw/kaolin mixtures. TEC, thermodynamic equilibrium calculations (TEC release estimated at 1250 °C).

In Figure 7, the experimentally determined inorganic element release ratios from the fuel to the gas phase from lab-scale

reactor experiments in comparison with results from TEC for pure spruce and spruce/kaolin mixtures are presented.

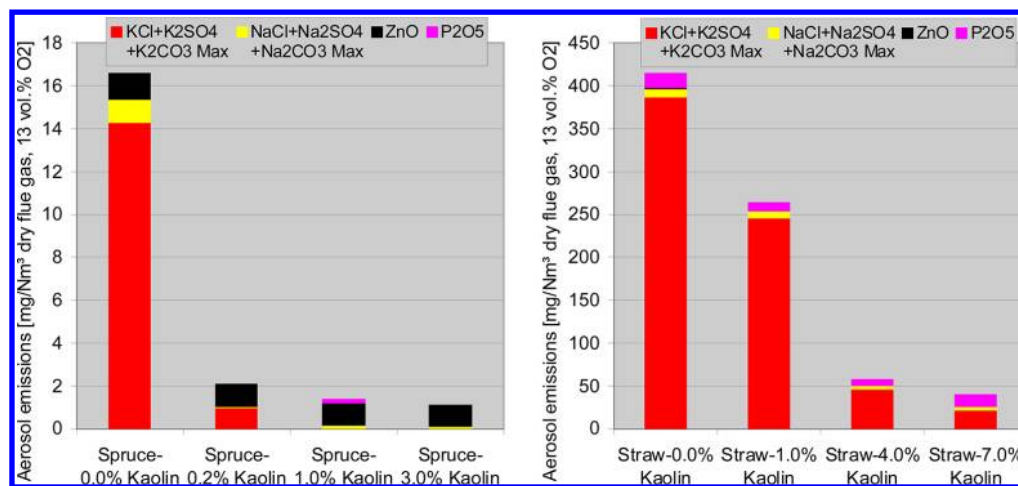


Figure 9. Estimated maximum aerosol emissions for pure spruce and spruce/kaolin mixtures as well as for straw and straw/kaolin mixtures.

From Figure 7, it can be determined that TEC predict slightly higher S, Cl, and Pb release ratios compared to the experimentally determined release. A complete release of these elements is predicted from TEC, whereas from lab-scale reactor experiments release ratios of 84–93 wt % for S, 90–98 wt % for Cl, and 73–97 wt % for Pb have been calculated. From a previous study²¹ release ratios for spruce wood chips have been determined for S of 82 wt % and for Cl of 99 wt %. It can be concluded that the addition of kaolin does not influence the release ratios of S and Cl to the gas phase. The low Pb release for the 3 wt % kaolin ratio might be explained with the low concentrations in the fuel sample (close to the detection limit) which increases the insecurity of results. This can also be seen from Table 2, where a poor agreement between theoretical mixing calculations and measurement results is shown. For the remaining fuels the Pb released from the fuel to the gas phase is on an almost constant level, and thus it can be stated that the addition of kaolin does not seem to influence the Pb release. Concerning K, it can be seen that with increasing kaolin addition ratio the K release to the gas phase decreases. The K release predicted by TEC is in good agreement with the determination by lab-scale reactor experiments. For Zn a good agreement between TEC and lab-scale experiments for pure spruce can be observed, whereas for the spruce/kaolin mixtures a strong deviation between TEC and the experimental determinations is obvious.

In Figure 8, a comparison between the experimentally determined element release from the fuel to the gas phase from lab-scale reactor experiments with TEC for pure straw and straw/kaolin mixtures is outlined.

From Figure 8, it can be determined that TEC predict S, Cl, and Pb release ratios of 100% for pure straw and the straw/kaolin mixtures. The experimentally determined release ratios for S (89–95 wt %), Cl (98–100 wt %), and Pb (82–92 wt %) are in good agreement with the results from TEC.

It can also be concluded that the addition of kaolin has no influence on the release ratios of S, Cl, and Pb. Concerning the K release, the same trend (as for spruce) of decreasing K release with increasing kaolin addition can be observed. The Zn release predicted by TEC is in rather good agreement with the experimental evaluation. No clear trend regarding the influence of kaolin on Zn release can be seen.

It has to be noted that TEC quite underestimate the K release in comparison with the lab-scale reactor experiments,

especially for pure spruce and straw as well as for straw with 1 wt % kaolin addition. For TEC the results from the wet chemical fuel analyses have been used as input data and the calculations have been evaluated at the maximum bed temperature occurring during the char combustion phase. The K release during the devolatilization phase is considered within the first calculation step of TEC. During lab-scale reactor experiments it is possible that a part of K is already released to the gas phase during the start of the char combustion phase. This part of K is not available for a possible inclusion in solid K–Al–Si phases. This behavior is a possible explanation for the overpredicted K release from TEC. In ref 22 a similar behavior has been found. This study reports an experimentally determined K release of 40.7 wt % for straw. The test runs were also performed in a lab-scale reactor^{23,24} and also TEC were performed whereby a K release of 28.5 wt % was predicted for a temperature of 1000 °C. This shows that process factors such as the temperature gradient inside the particle or a packed bed as well as diffusion most likely influence the K release.

In summary, TEC have proven to be a valuable tool to predict the trend of volatile and semivolatile element releases from the fuel to the gas phase for the fuel/kaolin mixtures evaluated, except for Zn. Furthermore, TEC support the interpretation of the experimentally determined release ratios. For validation of the predicted release ratios by TEC as well as to gain quantitative values, lab-scale reactor experiments have to be conducted.

4.6. Prediction of Aerosol as Well as HCl and SO₂ Emissions for Pure Biomass Fuels and Fuel/Kaolin Mixtures. Based on the release data gained from the lab-scale reactor experiments, an estimation of the potential for fine particulate emissions can be made. The aerosol forming elements K, Na, Zn, and P were considered as K₂SO₄, KCl, Na₂SO₄, NaCl, ZnO, and P₂O₅. In addition, the formation of carbonates (K₂CO₃ and Na₂CO₃) is probable if there is not enough S and Cl available in order to completely bind K and Na as chlorides and sulfates. For the calculation of the minimum aerosol emissions the formation of K and Na chlorides was preferred, whereas for the calculation of the maximum aerosol emissions a predominant formation of sulfates was assumed. The differences of the estimated amounts of aerosol emissions result from the differences in the molecular weights of sulfates and chlorides. These estimations do not consider particle losses caused by condensation of ash forming

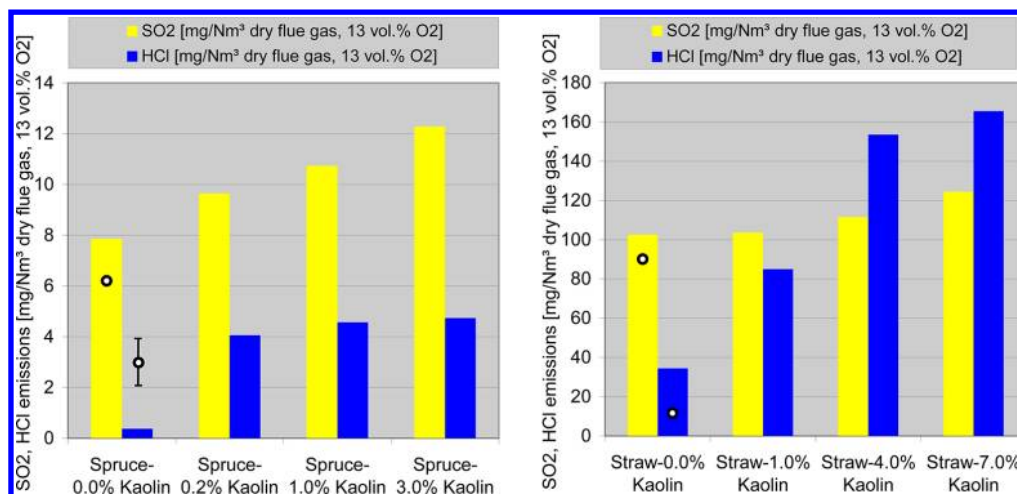


Figure 10. Estimated gaseous SO_2 and HCl emissions for pure spruce and spruce/kaolin mixtures as well as for straw and straw/kaolin mixtures. The black circles indicate SO_x as well as HCl emissions of comparable fuels taken from ref 3 as a basis for a validation of the calculated SO_2 and HCl emissions.

Table 6. Estimated Fuel Cost Increase for Kaolin Addition to Spruce and Straw

Spruce						
kaolin ratio (wt %)	fuel costs (€/MWh _(NCV))	kaolin amt (kg/MWh _(NCV))	kaolin costs (€/MWh _(NCV))	addnl disposal costs (€/MWh _(NCV))	fuel costs + addnl costs (€/MWh _(NCV))	cost increase (%)
0.2	34.3	0.39	0.09	0.04	34.4	0.37
1.0	34.3	2.0	0.43	0.20	34.9	1.8
3.0	34.3	5.9	1.3	0.6	36.1	5.5
Straw						
kaolin ratio (wt %)	fuel costs (€/MWh _(NCV))	kaolin amt (kg/MWh _(NCV))	kaolin costs (€/MWh _(NCV))	addnl disposal costs (€/MWh _(NCV))	fuel costs + addnl costs (€/MWh _(NCV))	cost increase (%)
1.0	24.8	2.1	0.46	0.21	25.5	2.7
4.0	24.8	8.4	1.9	0.8	27.5	10.9
7.0	24.8	14.8	3.3	1.5	29.6	19.0

vapors on walls and deposit formation in the furnace and the boiler sections, particle losses caused by reactions of ash forming vapors with coarse fly ash particles, or condensation on coarse fly ash particles as well as gaseous emissions of S (i.e., SO_x) and Cl (i.e., HCl).

The decreasing aerosol emission potential with increasing amount of kaolin addition can clearly be seen from Figure 9. It is also obvious that the main influence on aerosol emissions is given by the amount of K released from the fuel to the gas phase. For spruce it can be seen from Figure 9 (left) that already a ratio of 0.2 wt % kaolin is able to significantly reduce the aerosol emissions. Increases in the kaolin addition ratio to 1 and 3 wt % lead to a further slight decrease.

Concerning straw, a kaolin addition of 1 wt % reduces the estimated aerosol emissions from 416 to 264 mg/Nm³. Up to 4 wt % kaolin addition a strong decrease of the aerosol emissions can be seen; further kaolin addition than that shows only minor additional effects.

On the basis of the release data, also an estimation of the potential of gaseous SO_2 and HCl emissions can be made. In ref 3 a double logarithmic correlation between the 2S/Cl ratio in biomass fuels and the 2S/Cl ratio found in aerosols is given. It can then be estimated that the molar 2S/Cl ratios in aerosol emissions amount to about 1.1–1.2 and 0.38 if the molar 2S/Cl ratios in the fuel are about 2.7–3.1 and 0.8–0.9 (see section 4.1) for spruce and straw, respectively. With the release data for K, Na, S, and Cl and the estimated 2S/Cl ratios in the aerosols,

the gaseous emissions of SO_2 and HCl can be estimated (S and Cl which are not bound by K and Na). This estimation does not consider particle losses in boilers as well as S and Cl bound by Ca and Mg. In Figure 10, results of the estimation of gaseous SO_2 and HCl are displayed.

From Figure 10, it can be seen that for both fuels the SO_2 and HCl emissions increase with increasing kaolin addition. This is due to the fact that with increasing kaolin addition less K is released to the gas phase which is available for binding S and Cl to solid aerosol particles. It has to be noted that the estimated SO_2 and HCl emissions are unproblematic regarding emission limits for the spruce/kaolin mixtures. Regarding straw the kaolin addition may lead to significantly increased HCl emissions and therefore to the demand for dry sorption to keep the emission limits given.

4.7. Economic Aspects of Additive Utilization. The utilization of a fuel additive usually results in additional costs for the additive as well as higher ash disposal costs (due to the increasing ash content). For a complete techno-economic evaluation, the increase of fuel and ash disposal costs must be compared to the benefits and profits associated with the use of a specific fuel additive. For example, this can be the reduction of investment costs regarding advanced flue gas cleaning (fine particle precipitation), of operational/maintenance costs (e.g., slag, deposit, and corrosion related), and an increased availability/lifetime of the plant.

The direct costs for using kaolin are discussed and put in perspective to typical biomass fuel costs. For spruce the typical price of wood chips in Austria is 140 €/ton (P31.5, M20).²⁵ The net calorific value of wood chips is typically 14.7 MJ/kg wb (M20), which leads to a fuel cost of 34.3 €/MWh. For straw a price of 100 €/ton (based on typical straw prices in Austria) and a net calorific value of typically 14.5 MJ/kg wb (M15) (from former studies) results in a fuel price of 24.8 €/MWh. These prices do not consider the costs for pelletization. Furthermore, the kaolin price, (supplier, Thiele Nordic; grain size < 2 μm) was estimated to be 220 €/ton²⁶ (from factory excluding shipping). Depending on the kind of ash and respectively the type of disposal, ash disposal costs usually range from 60 to 100 €/ton²⁷ dry ash.

Table 6 shows the cost increase for different additive ratios based on the energy content (NCV) of the fuel for spruce and straw respectively under the realistic assumption that the additive is directly fed to the raw material during pelletization and thus does not cause additional fuel preparation costs. For the estimation of the ash disposal costs (additional ash due to kaolin addition) the value of 100 €/ton has been used for the calculations and the cost increase is also related to the energy content of the fuel.

The addition of kaolin leads to cost increases of 0.4–5.5% for spruce and 2.7–19% for straw. Then, moderate kaolin addition increases the fuel cost only to a small extent or in the case of wood even to a negligible extent.

4.8. Suggestion of an Appropriate Kaolin Addition Ratio. Regarding the definition of an optimum kaolin addition ratio the positive effects (reduction of K release and increased melting temperatures) have to be balanced with the slight disadvantages due to the additive and the additional ash disposal costs.

For spruce with 0.2 wt % kaolin a significant decrease of the aerosol emissions compared with pure spruce combustion has been determined, whereby further kaolin addition showed only minor additional effects. Since the SST of pure spruce is already at an unproblematic level, a kaolin addition of 0.2 wt % can be recommended. For straw a clear steep trend of decreasing K release and increasing ash melting temperatures can be observed for addition ratios up to 4 wt %. For higher kaolin addition this trend flattens for both parameters, and therefore 4 wt % kaolin additive can be recommended.

5. CONCLUSIONS

In previous studies experimental approaches were chosen for the determination of an appropriate fuel/additive ratio which improves the combustion properties of biomass fuels in terms of K release and ash melting. In this work an approach applying novel fuel characterization tools for a systematic evaluation of the effects of a certain additive on a biomass fuel is presented. This new strategy reduces the necessity of expensive and time-consuming testing campaigns.

For the investigations spruce and straw have been chosen as fuels and kaolin is used as the additive. An evaluation of fuel/additive mixtures based on fuel indexes and TEC proved to be a useful tool to access ash related problems (aerosol emissions, ash melting, high temperature corrosion). Fuel indexes and TEC are able to supply a good qualitative trend of the influence of the additive on the K release and the ash melting and are therefore also suitable to define meaningful additive ratios for a certain biomass fuel (range of additive ratio that seems of interest). In combination with lab-scale reactor tests, the effects

of an additive can also be quantitatively evaluated and meaningful additive ratios can be determined for a certain biomass fuel.

For spruce a kaolin addition of 0.2 wt % proved to be sufficient to reduce aerosol emissions by 87%. In addition, the ash melting temperature increased by 40 °C. The ash content for this mixture increases just slightly, the fuel cost increase is negligible (0.4%), and also the expected increase in SO₂ and HCl emissions is not problematic. The addition of kaolin seems especially interesting for small-scale (residential) applications using pellets to substantially reduce particulate emissions as these systems typically are not equipped with dust precipitators.

For straw about 4 wt % kaolin addition can be recommended to considerably reduce aerosol emissions and substantially improve the ash melting behavior. The ash content of this fuel/kaolin mixture increases by about 69%, and the fuel costs (including the higher ash disposal costs) increase by about 11%. The SO₂ emissions stay rather constant, but the HCl emissions are expected to increase considerably (by about 150%) in comparison with pure straw. This will most likely cause the need for dry sorption to maintain the emission limits. The addition of kaolin to straw is especially interesting in medium- and large-scale applications where an appropriate flue gas cleaning system is usual, whereas in small-scale plants the utilization is not interesting due to the elevated HCl emissions. The additional fuel and ash disposal costs seem moderate in comparison with the possible savings in investment costs and the expected higher plant availability.

Summing up, a new evaluation method for additive addition to biomass fuels is available regarding its impact on ash melting and fine particulate emissions. Moreover, a meaningful additive range for a certain biomass fuel can be predicted. By additional lab-scale reactor tests a quantitative evaluation of a certain additive is possible. With this approach the characterization of biomass/additive mixtures can be performed without time-consuming and expensive real-scale combustion tests.

■ ASSOCIATED CONTENT

📄 Supporting Information

Tables 1–6. This material is available free of charge via the Internet at <http://pubs.acs.org>.

■ AUTHOR INFORMATION

Corresponding Author

*E-mail: peter.sommersacher@bioenergy2020.eu. Tel.: + 43 (0) 316 873-9237. Fax: + 43 (0) 316 873-9202.

Notes

The authors declare no competing financial interest.

■ ACKNOWLEDGMENTS

The authors gratefully acknowledge the support of the FFG, Austrian Research Promotion Agency, within the ERANET-Bioenergy project FutureBioTec, future low emission biomass combustion systems.

■ REFERENCES

- (1) Lewandowski, L.; Scurlock, J. M. O.; Lindvall, E.; Christou, M. The development and current status of perennial rhizomatous grasses as energy crops in the US and Europe. *Biomass Bioenergy* **2002**, *25*, 335–361.
- (2) McKendry, P. Energy production from biomass (part 1): overview of biomass. *Bioresour. Technol.* **2002**, *83*, 37–46.

- (3) Sommersacher, P.; Brunner, T.; Obernberger, I. Fuel indexes: a novel method for the evaluation of relevant combustion properties of new biomass fuels. *Energy Fuels* **2012**, *26*, 380–390.
- (4) Bäfver, L.; Boman, C.; Rönnbäck, M. Reduction of particle emissions by using additives. Presented at the Central European Biomass Conference, Graz, Austria, Jan 26–29, 2011.
- (5) Boman, C.; Böström, D.; Öhman, M. Effect of fuel additive sorbent (kaolin and calcite) on aerosol particle emission and characteristics during combustion of pelletized woody biomass. *Proceedings of the 16th European Biomass Conference & Exhibition 2008, Valencia, Spain*; EU BC&E: Florence, Italy, June 2008; pp 1514–1517.
- (6) Öhman, M.; Boström, D.; Nordin, A. Effect of kaolin and limestone addition on slag formation during combustion of wood fuels. *Energy Fuels* **2004**, *18*, 1370–1376.
- (7) Xiong, S.; Burvall, J.; Örberg, H.; Kalen, G.; Thyrel, M.; Öhman, M.; Boström, D. Slagging characteristics during combustion of corn stovers with and without kaolin and calcite. *Energy Fuels* **2008**, *22*, 3465–3470.
- (8) Bäfver, L.; Rönnbäck, M.; Leckner, B.; Claesson, F.; Tullin, C. Particle emission from combustion of oat grain and its potential reduction by addition of limestone or kaolin. *Fuel Process. Technol.* **2009**, *90*, 353–359.
- (9) Boström, D.; Grimm, A.; Boman, C.; Björnbom, E.; Öhman, M. Influence of kaolin and calcite additives on ash transformations in small-scale combustion of oat. *Energy Fuels* **2009**, *23*, 5184–5190.
- (10) Davidsson, K. O.; Steenari, B.-M.; Eskilsson, D. Kaolin addition during biomass combustion in a 35 MW circulating fluidized-bed boiler. *Energy Fuels* **2007**, *21*, 1959–1966.
- (11) Bärenthaler, G.; Zischka, M.; Hanralsdsson, C.; Obernberger, I. Determination of major and minor ash-forming elements in solid biofuels. *Biomass Bioenergy* **2006**, 983–997.
- (12) Osborn, E. F.; Muan, A. *Phase Equilibrium Diagrams of Oxide Systems*; American Ceramic Society and the Edward Orton Jr. Ceramic Foundation: Columbus, OH, USA, 1960.
- (13) Evic, N.; Brunner, T.; Obernberger, I. Prediction of biomass ash melting behaviour—correlation between the data obtained from thermodynamic equilibrium calculations and simultaneous thermal analysis (STA). *Proceedings of the 20th European Biomass Conference & Exhibition, June 2012, Milan, Italy*; EU BC&E: Florence, Italy, 2012; pp 807–813. ISBN 978-88-89407-54-7.
- (14) Evic, N.; Brunner, T.; Obernberger, I. Prediction of characteristic melting temperatures of ten biomass ashes using thermodynamic equilibrium calculations. *Fuel* **2013**, submitted for publication.
- (15) Brunner, T.; Biedermann, F.; Evic, N.; Obernberger, I. Advanced biomass fuel characterisation based on tests with a specially designed lab-scale reactor. *Proceedings of the Conference Impacts of Fuel Quality on Power Production and Environment, Sept 23–27, 2012, Puchberg, Austria*; EPRI: Palo Alto, CA, USA, 2012.
- (16) Weissinger, A.; Fleckl, T.; Obernberger, I. Application of FT-IR in-situ absorption spectroscopy for the investigation of the release of gaseous compounds from biomass fuels in a laboratory scale reactor—Part II: Evaluation of the N-release as functions of combustion specific parameters. *Combust. Flame* **2004**, *137*, 403–417.
- (17) Stubenberger, G.; Scharler, R.; Obernberger, I. Nitrogen release behaviour of different biomass fuels under lab-scale and pilot-scale conditions. *Proceedings of the 15th European Biomass Conference & Exhibition, May 2007, Berlin, Germany*; EU BC&E: Florence, Italy, 2007; pp 1412–1420. ISBN 978-88-89407-59-X, ISBN 3-936338-21-3.
- (18) Obernberger, I. Novel characterization methods for biomass fuels and their application—case study straw. *Proceedings of the Conference Impacts of Fuel Quality on Power Production and Environment, Sept 23–27, 2012, Puchberg, Austria*; EPRI: Palo Alto, CA, USA, 2012.
- (19) <http://www.ieabcc.nl/database/biomass.php>.
- (20) Salmenoja K. *Field and Laboratory Studies on Chlorine-Induced Superheater Corrosion in Boilers Fired with Biofuels*. Ph.D. Thesis, Abo Akademi, Faculty of Chemical Engineering, Abo/Turku, Finland, 2000.
- (21) Sommersacher, P.; Brunner, T.; Obernberger, I. Fuel indexes—a novel method for the evaluation of relevant combustion properties of new biomass fuels. *Proceedings of the Conference Impacts of Fuel Quality on Power Production and Environment, Sept 23–27, 2012, Puchberg, Austria*; EPRI: Palo Alto, CA, USA, 2012.
- (22) Flemming, F.; van Lith, S. *Quantification of the Release of Inorganic Elements during Combustion of Biofuels and Coals—Comparison and Evaluation of Results from Different Techniques*; Final report for SES6-CT-2003-S0267: Ash and Aerosol Related Problems in Biomass Combustion and Co-Firing (BIOASH), Task 1.4; 2007.
- (23) Knudsen, J. N. *Volatilization of Inorganic Matter during Combustion of Annual Biomass*. Ph.D. Thesis, Technical University of Denmark, Lyngby, Denmark, 2004. ISBN 87-91435-11-0.
- (24) van Lith, S. C. *Release of Inorganic Elements during Wood-Firing on a Grate*. Ph.D. Thesis, Technical University of Denmark, Lyngby, Denmark, 2005. ISBN 87-91435-29-3.
- (25) Wood fuel prices (3rd report), year 2012 (2nd period). <http://www.biomassradecentre2.eu/wood-fuel-prices/>. Accessed Feb 25, 2013.
- (26) Boman, C. Fuel additives and blending as primary measures for reduction of fine ash particle emissions—state of the art; ERA-NET FutureBioTec, Sept 7, 2012. [http://futurebiotec.bioenergy2020.eu/files/FutureBioTec-Additives and fuel blending-state of the art report.pdf](http://futurebiotec.bioenergy2020.eu/files/FutureBioTec-Additives%20and%20fuel%20blending-state%20of%20the%20art%20report.pdf). Accessed Jan 22, 2013.
- (27) Supancic, K.; Obernberger, I. Wood ash utilisation as a stabiliser in road construction—results of large scale tests and evaluation. *Waste Manage.* **2013**, submitted for publication.

Paper III



Combustion related characterisation of Miscanthus peat blends applying novel fuel characterisation tools



Peter Sommersacher^{a,*}, Thomas Brunner^{b,c}, Ingwald Obernberger^{b,c}, Norbert Kienzl^a, Werner Kanzian^{b,c}

^a BIOENERGY 2020+ GmbH, Inffeldgasse 21b, 8010 Graz, Austria

^b Institute for Process and Particle Engineering, Graz University of Technology, Inffeldgasse 13, 8010 Graz, Austria

^c BIOS BIOENERGIESYSTEME GmbH, Inffeldgasse 21b, 8010 Graz, Austria

HIGHLIGHTS

- Laboratory methods presented regarding the combustion related characterisation.
- Peat addition to Miscanthus increases the ash melting temperatures.
- Decreased aerosol emissions with increasing peat shares.
- Increased NO_x and SO_x emissions can be expected with increasing peat shares.
- New evaluation method for the prediction of optimum fuel blends for biomass fuels.

ARTICLE INFO

Article history:

Received 4 March 2015

Received in revised form 15 May 2015

Accepted 18 May 2015

Available online 28 May 2015

Keywords:

Fuel blends

Miscanthus

Peat

Solid biomass characterisation

ABSTRACT

A continuously increasing demand for energy from biomass encourages utilisation of new biomass fuels which usually cause ash related problems in conventional wood combustion systems. One approach to make these biomass fuels applicable in such systems is to prepare blends with other fuels such as peat, which positively influence the behaviour of ash-forming elements. Usually the application of fuel blends has been evaluated experimentally, but in this study novel and advanced fuel characterisation tools (developed for fixed bed/grate combustion systems) are applied to Miscanthus/peat blends. In a first step the pure fuels and the Miscanthus/peat blends were chemically analysed. Fuel indexes provide primary information on ash-melting behaviour and a first estimation of the K release, indications of aerosol emissions, risk of high-temperature chlorine corrosion and the NO_x emission potential. Thermodynamic equilibrium calculations were used for a qualitative and semi-quantitative prediction of the release of volatile and semi-volatile elements (K, Na, S, Cl, Zn, Pb) and the ash-melting behaviour. To quantitatively determine the release behaviour of ash-forming elements, lab-scale reactor experiments for the pure fuels and blends were conducted and a comparison with the theoretical calculations was performed. This work shows that the new approach of applying novel and advanced fuel characterisation tools to characterise Miscanthus/peat blends works well and meaningful blends can be recommended. The advantage of this characterisation method is that the influence of varying peat compositions (since the composition of peat strongly depends on its origin) can be considered. Additionally this approach helps to significantly reduce time-consuming and expensive testing programs.

© 2015 Elsevier Ltd. All rights reserved.

1. Introduction and objectives

The relevance of biomass for energy production will most probably increase during the coming years. To cover the future demand for feedstocks besides traditional biomass fuels (e.g. wood chips, bark, etc.) also so-called new biomass fuels have to be introduced into the market. In this respect fast growing non-food crops which

are not competing with the food industry like perennial grasses such as Miscanthus and giant reed [1,2] and fast growing wood species (so-called short-rotation coppices (SRC) such as willow and poplar [3,4]) as well as herbaceous and agricultural residues (straw, press cake from oil production, kernels, etc.) show promising potential. Due to the high growth rates of these plants the nutrient uptake is increased which generally leads to higher N, S, Cl and ash contents in comparison to conventional wood fuels (wood pellets, wood chips, bark) [5]. Therefore, the combustion of these fuels is often associated to increased ash related problems

* Corresponding author. Tel.: +43 (0) 316 873 9237; fax: +43 (0) 316 873 9202.

E-mail address: peter.sommersacher@bioenergy2020.eu (P. Sommersacher).

(slagging, particulate matter emissions, corrosion) as well as, compared with conventional wood fuels, increased NO_x , SO_x and HCl emissions [6]. Consequently, an utilisation in conventional wood combustion systems is not meaningful, but for the broad introduction and utilisation of these new biomass fuels methods should be developed which make them applicable in such plants. One option therefore is to apply blends with fuels which positively influence the ash characteristics, especially the ash-melting behaviour and the K release. Peat is an often mentioned candidate for the preparation of such fuel blends.

Peat is an accumulation of partially decayed vegetation. One of the most common components is Sphagnum moss, although many other plants can contribute. Soils that contain mostly peat are known as a histosol. Peat forms in wetland conditions, where flooding obstructs flows of oxygen from the atmosphere, which reduces rates of decomposition [7].

The composition of peat [8] depends on the geological surroundings, historical topography as well as hydrology and meteorology, why peat lands give different peat compositions. For this reason it is important to consider the elemental composition, since it has a strong influence on the application of fuel blending.

From Ref. [8] it can also be concluded that peat usually contains higher amounts of N, S, Al and Ca and lower concentrations of K compared to virgin wood fuels without chemical treatments or coatings and painting. The Si concentration in peat may vary, depending on the type of peat, values of 0.55 ± 1.3 wt.% d.b. have been reported. Typically they are considerably higher than in wood fuels. For blending peat with new biomass fuels higher ash-melting temperatures are expected, since peat typically elevates the Ca and Al concentration of the blend, whereby Si in combination with K decreases the ash melting temperatures. A reduced K release may result due to better embedding of K in the ash due to K-alumo-silicate formation. In case of an elevated Si content in the peat a lower K release can also result from the formation of silica melts. A reduced K release may result mainly due to better embedding of K in the ash due to K-alumo-silicate formation. The increasing S content in the blend may lead to decreased high-temperature chlorine corrosion problems. On the other side gaseous NO_x and SO_x emissions may increase due to the increasing concentrations of S and N in the blend.

A few studies regarding biomass/peat blends have already been published. In Ref. [9] the effect of peat addition to wood pellets on slagging characteristics during combustion in residential pellet burners has been investigated. It has been reported that the addition of a Si rich peat increased the slagging tendency, whereas the slagging tendency was significantly lower when adding ash poor peat with a relatively high Ca/Si ratio. In Ref. [10] forest residues and wheat straw were co-combusted with peat (15 wt.% d.b.) in a small scale (15 kW) grate-fired boiler. Peat addition led to a reduction of the release of fine particle and deposit forming alkali metals of up to 74% for forest residues and to 45% for wheat straw. In Ref. [11] it is reported that the addition of peat prevented agglomeration in a fluidised bed, where bark from pine and spruce were used as fuels. This study reports that even 5% peat was found to have a significant effect on preventing bed agglomeration. Another study Ref. [12] investigated the combustion of forest residues and peat mixtures in controlled experiments in a bench-scale fluidised bed reactor. The main results are an increased bed agglomeration temperature, a decreased concentration of K and an increased concentration of Ca in the inner bed particle layers, a reduced amount of fine particle but an increased amount of coarse particle emissions. The mechanisms for the positive effects were the transfer and/or removal of K in the gas phase to a less reactive solid form via sorption and/or the reaction with the reactive peat ash (SiO_2 and CaO), which in most cases formed larger particles ($>1 \mu\text{m}$) containing Ca, Si and K.

All previous investigations were based on experimental (fixed bed and fluidised bed combustion) evaluations of biomass peat blends. Within this work however advanced fuel characterisation tools shall be used for an evaluation of the combustion related effects of peat blends during fixed bed/grate combustion. Advanced fuel characterisation tools such as fuel indexes, thermodynamic equilibrium calculations and lab-scale reactor experiments have already proven their general applicability for the evaluation of pure fuels [6,17] as well as fuel/additive mixtures [13]. Compared with combustion experiments they are rather quick, need significantly less amounts of fuel and are less cost intensive. The aim of this work was to investigate the influence of peat addition to Miscanthus and to identify a meaningful blending ratio.

2. Methods

For a combustion related characterisation of Miscanthus and peat blends the following methods were used. Wet chemical fuel analyses provide the chemical compositions of the pure fuels and the fuel blends. Fuel indexes were calculated which delivers first information about the ash-melting tendency and the K release (by using the molar $[\text{Si} + \text{P} + \text{K}]/[\text{Ca} + \text{Mg}]$ ratio), a first estimation of the aerosol emissions to be expected (by using the sum of K, Na, Zn and Pb) and an indicator for the high-temperature chlorine corrosion risk (by using the molar $2\text{S}/\text{Cl}$ ratio). Thermodynamic equilibrium calculations (TEC) were used for a prediction of the release of volatile and semi-volatile elements (K, Na, S, Cl, Zn, Pb) as well as of the ash-melting behaviour. Additionally lab-scale reactor combustion tests as well as ash-melting analysis according to CEN/TS 15370-1 have been conducted with selected Miscanthus/peat blends in order to gain experimental data and to compare the results to theoretical calculations.

2.1. Wet chemical analysis

Wet chemical fuel analyses form the basis for the fuel characterisation methods used in this study. Well proven fuel analysis methods were applied [6,14,15]. Fuel analysis have been performed according to ÖNORM CEN/TS 15104 (C, H, N), ÖNORM CEN/TS 15289 (Cl), ÖNORM EN 14775 (ash content). The concentrations of major and minor elements as well as of S have been determined by multi-step pressurised digestion of the fuel, followed by detection applying inductively coupled plasma-optical emission spectroscopy (ICP-OES) (Arcos, Spectro) or inductively coupled plasma-mass spectroscopy (ICP-MS) (Agiland 7500), depending on the detection limits.

2.2. Fuel indexes

Fuel indexes are calculated based on results of wet chemical fuel analysis and can be used to provide indications regarding relevant combustion related properties for biomass fuels. These are for instance the potentials for gaseous NO_x , SO_x and HCl emissions, the potentials for fine particulate emissions and deposit formation, high-temperature chlorine corrosion risks as well as the ash-melting behaviour. The indexes are derived under the consideration of the physical behaviour and chemical reactions of biomass fuels. Detailed background information regarding the definition and evaluation of fuel indexes can be found in Ref. [6].

Fuel indexes which were used within this study are the molar $(\text{Si} + \text{P} + \text{K})/(\text{Ca} + \text{Mg})$ ratio as indicator for the ash-melting tendency and for a first estimation of the K release. The sum of K, Na, Zn and Pb can be applied for an estimation of the aerosol emission potential, the molar $2\text{S}/\text{Cl}$ ratio as indicator for

high-temperature chlorine corrosion risks and the N content of the fuel as indicator for the NO_x emission potential.

2.3. Thermodynamic equilibrium calculations

Thermodynamic equilibrium calculations (TEC) provide the possibility to predict multi-phase equilibria, whereby gaseous, liquid and solid phases of interest can be identified and quantified. These calculations are conducted for a multi-component thermodynamic system in a pre-determined gas atmosphere, under the assumption that chemical equilibrium can be achieved for the system investigated. In this study TEC were used to qualitatively investigate the release behaviour of inorganic compounds (K, Na, S, Cl, Zn, Pb) and the ash-melting behaviour. The thermochemical software package FactSage 6.3 has been applied, which uses the image component method in Gibbs free energy minimisation concerning thermodynamic equilibrium. In FactSage a series of calculation modules as well as databases are included. The currently accessed databases are “solution databases” including the optimised parameters for a wide range of solution phases and “pure compound” databases containing the data for over 4500 stoichiometric compounds. For the work presented the component database Fact 53, the solution databases FToxid (slags and other oxide mixtures) and FTsalt (liquid and solid salt phases) have been applied. More than 1000 components and 9 solutions (which have been shown to be stable and thermodynamically relevant) were considered. The selection has been done application oriented for biomass fuels, peat and biomass/peat blends as well as their ashes.

Previous work showed that a realistic prediction of the characteristic ash-melting temperatures and the release behaviour primarily depends on a reliable quantification of the molten solution phases SLAGH and SALTf over the temperature range of interest. Experience shows that the assessment of these two phases was strongly influenced by the amounts of Al, Si and K. Therefore, based on empirically estimated limits for the characteristic molar ratios of $(Si + K + P)/(Ca + Mg)$, $K/(Si + P)$ and Al/Si , an optimisation method [16] for TEC has been developed which is briefly discussed in the following.

- (1) The fraction of reactive Si considered in the calculation is related to the molar ratio $(Si + K + P)/(Ca + Mg)$, whereby for fuels with a value lower than 0.94 a Si-reactivity of only 10% is assumed. Especially for pure wood ashes the inclusion of typically sand-like contaminants combined with the low ash content of the corresponding fuels causes a significant share of the Si to be less or almost not reactive. It can be assumed that this inert Si-fraction (approx. 90%) does not take place in the ash-melting processes and thus by limiting the reactive fraction an overestimation of slag formation can be avoided. For non-wood ashes the Si-reactivity is defined to be 100%, because the corresponding fuels usually contain high Si amounts in the ash, making the Si fraction coming from external contaminants (e.g. sand, stones) of minor relevance.
- (2) To avoid an unrealistic prediction of slag formation Al₂O₃ is excluded from SLAGH in calculation cases with a molar Al/Si ratio <0.1. Al₂O₃ has a strong influence on slag formation and the currently available thermodynamic data for Al in slag solutions seem inaccurate, therefore this reduction has been defined.
- (3) The molar ratio $K/(Si + P)$ determines whether the molten salt solution SALTf is used in the TEC model. SALTf is eliminated from the TEC model for molar ratios larger than 1, otherwise SALTf phases (mainly composed of K-carbonates/sulphates) are over-predicted which results in an unrealistic drop of the melting temperatures estimated.

To gain a better prediction of the inorganic element release from the fuel to the gas phase (especially regarding K and Na), the calculations have been performed following a 2 step procedure, which separately considers the devolatilisation and charcoal combustion phase. For the calculation step 1 the input data consist of the complete elemental fuel composition, under consideration of a sub-stoichiometric combustion air ratio (λ typically 0.7) and atmospheric pressure. The evaluation of step 1 has been performed for a temperature of 700 °C which is assumed to be a realistic fuel bed temperature during volatilisation. Furthermore, this evaluation temperature has proven its applicability in a previous study [13]. For calculation step 2 which simulates the charcoal combustion phase, the input consists of the solid residues from step 1 (ash forming matter and charcoal), whereby the charcoal is assumed to consist of pure C and amounts to 15 wt.% of the initial organic dry matter. For this step an oxidising atmosphere ($\lambda > 1$) and atmospheric pressure are applied, whereby the calculations are carried out in a temperature range from 700 to 1500 °C. The release resulting from this calculation stage has been evaluated for a temperature of 1250 °C, since this is a typical charcoal bed temperature for fixed bed combustion systems. The total release of the elements considered is calculated as the sum of the release from step 1 and step 2. The calculated release ratios are compared with experimentally determined release ratios from lab-scale experiments (see Section 4.3).

The calculations of the ash melting temperatures are performed in a 1-step approach using the results of chemical analysis of the laboratory ashed fuel (ashed at 550 °C) as input data. The ashed fuel has been used to gain a better comparability with the standard ash melting test according to CEN/TS 15370-1. The calculations have been performed under oxidising gas atmospheres as well as atmospheric pressure in a temperature range of 500–1600 °C. The calculated ash-melting temperatures have been compared with the results of the standard ash-melting test (see Section 4.2). In [13,16] additional information regarding the software, the applied models and the evaluation procedure can be found.

2.4. Lab-scale reactor experiments

Defined Miscanthus/peat blends (see Section 3.2) as well as the pure fuels have been investigated with a lab-scale reactor. The basic idea behind this reactor is to provide a tool which is capable for the simulation of the fuel decomposition behaviour in real-scale fixed-bed biomass combustion systems. The experiment delivers information regarding the release of NO_x precursor species, the release of ash-forming elements and a first indication regarding the ash melting behaviour. The setup, design and evaluation procedure of this reactor has already been described in Refs. [13,17–19].

3. Materials

3.1. Fuels investigated

Within the ERA-NET Bioenergy project FutureBioTec [20] different blends of Miscanthus and peat were prepared. Miscanthus was provided from Teagasc (the Irish agriculture and food development authority) from the research farm Oak Park Carlow and was harvested in March 2011. The peat used originated from Ireland and was a Spagnum type peat.

In Fig. 1, the chemical composition of the Miscanthus investigated is compared with Miscanthus samples from previous in-house investigations.

The database values shows a high standard deviations for the Si, Ca, K, Mg, S and Cl concentrations indicating the broad range of

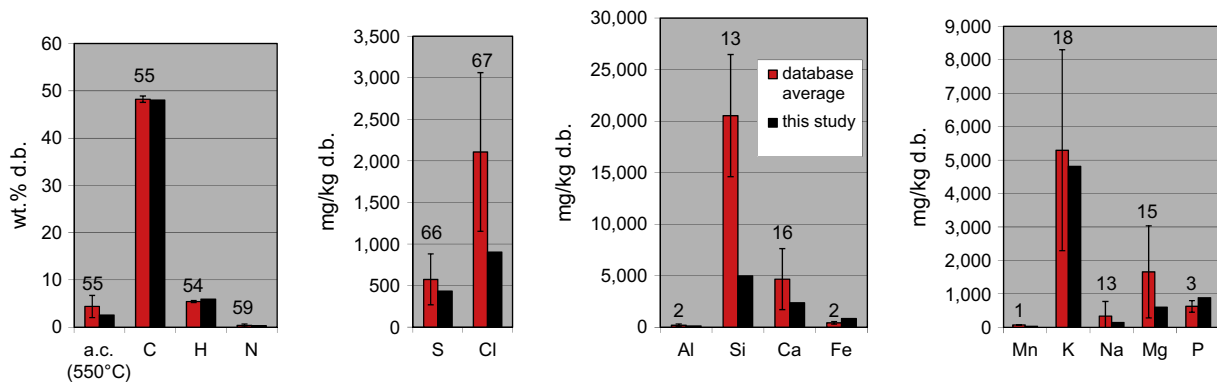


Fig. 1. Comparison of the chemical analysis of the Miscanthus sample investigated with results from previous investigations. Explanation: database average – average value from previous investigations (the number of samples investigated is indicated in the diagram); a.c. (550 °C) – ash content determined at 550 °C under oxidising conditions; d.b. – dry basis.

possible Miscanthus compositions. For C, H and N a good agreement between the database average values and the values of the Miscanthus sample investigated in this study can be observed. The same is true for S, whereas the Cl concentration of the sample investigated is below the lower end of the database range. The ash content of the Miscanthus sample investigated is at the lower end of the database range, which is mainly due to comparably low Ca and Si concentrations. For K and Na a good agreement between the database average values and the values of the sample investigated is given. The Fe and P contents of the Miscanthus sample investigated are above the upper end of the database range.

In Fig. 2, a comparison between the peat sample investigated with literature data is presented.

The main ash-forming elements of the peat investigated are Ca, Si and Mg (see Fig. 2). It can also be seen that the composition of a peat type strongly depends on the origin and its individual formation. For the C, H and N contents of the sample investigated a good agreement with literature data is given. Regarding S and Cl, higher amounts have been found compared to the average values from literature. Concerning the ash content the sample investigated shows typical values and also for Ca and Na a good agreement with literature data exists. The Mg concentration of the sample is considerably higher compared to literature values while for K, P, Al, Si and Fe lower values have been found compared to most of the average values of literature data.

3.2. Fuel blends prepared

For the investigations 3 different blends of Miscanthus and peat were prepared: 75 wt.% Miscanthus with 25 wt.% peat (P25), 50/50 (P50) and 25/75 (P75) related to dry basis. A pure Miscanthus sample (M100) and a pure peat sample (P100) have been used as

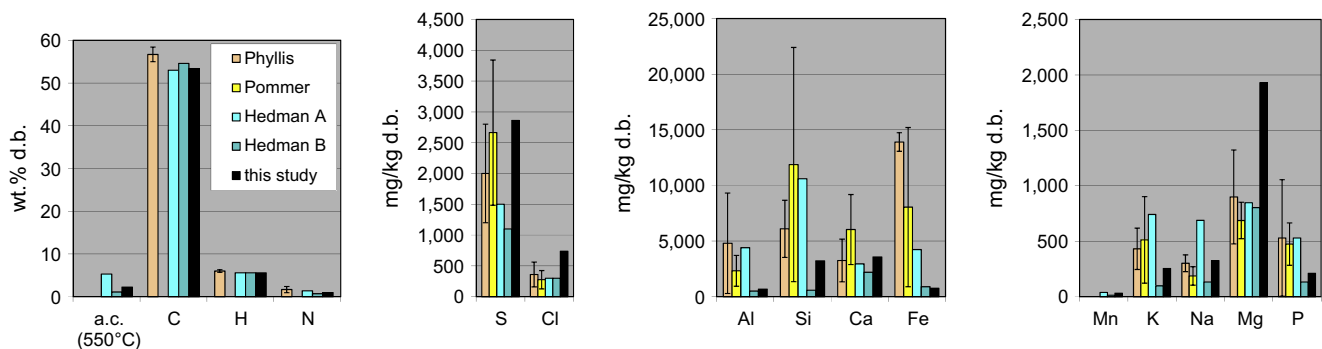


Fig. 2. Comparison of the chemical analysis of the peat sample investigated with literature data. Explanation: Pommer [12]; Hedman [21]; Phyllis [22]; Pommer and Phyllis: average and standard deviation of 9 respectively 2 samples; Hedman: 2 single values (A and B); a.c. (550 °C) – ash content determined at 550 °C under oxidising conditions.

reference points. The harvesting and the treatment of the fuels as well as the pelletising (Greenforze MZLP 400 series flat pellet die) was done by Teagasc (the Irish agriculture and food development authority) in cooperation with Umeå University Sweden, Institute for Applied Physics and Electronics.

Based on results of the chemical analysis of the pure fuels, mixing calculations were conducted. To check the quality of the blends these theoretically calculated concentrations were compared with results of analyses of the mixtures (see Table 1).

It can be seen from Table 1, that generally the results of chemical analyses are in good agreement with the calculated blend compositions indicating a good mixing quality. Only for P50 and P75 for Pb deviations exist which can be explained with the low concentrations of this element in the fuel, which are close to the detection limit of the analysis method applied.

It can also be seen from Table 1 that with increasing amounts of peat in the blend the concentrations of C and N increase whereas the H content decreases. The ash content remains rather constant for the blends whereby a lower value for P100 compared with M100 has been determined. An increase of S and a decrease of Cl in the blends with increasing peat ratio is also obvious. The concentrations of Si, K, P and Zn decrease with increasing amount of peat in the blend, whereas the concentrations of Ca, Mg, Na, Al and Pb increase. Regarding the ash-melting behaviour, peat shows a considerably higher shrinkage starting temperature in comparison to Miscanthus whereas the flow temperatures are rather similar.

4. Results and discussion

4.1. Evaluation of fuel indexes

In Table 2, the values of relevant fuel indexes are summarised.

Table 1

Comparison of theoretical mixing calculations with results of chemical analysis for the Miscanthus/peat blends investigated. Explanations: calc. – calculated; meas. – measured; a.c. 550 °C – ash content determined of 550 °C under oxidising conditions; a.c. corr. – ash content carbonate corrected; d.b. – dry basis; n.o. – did not occur.

% peat in blend		0	Calc.	Meas.	Calc./meas.	Calc.	Meas.	Calc./meas.	Calc.	Meas.	Calc./meas.	100
Notation		M100	25	25	25	50	50	50	75	75	75	P100
			P25	P25		P50	P50		P75	P75		P100
a.c.	wt.% d.b.	2.6	2.5	2.6	105%	2.4	2.6	106%	2.3	2.6	112%	2.3
a.c. corr.	wt.% d.b.	2.5		2.5		2.4			2.5			2.2
C	wt.% d.b.	48.0	49.4	49.1	100%	50.7	50.5	100%	52.0	51.9	100%	53.4
H	wt.% d.b.	6.0	5.9	5.8	99%	5.8	5.7	98%	5.7	5.5	97%	5.6
N	wt.% d.b.	0.33	0.49	0.48	97%	0.7	0.7	103%	0.8	0.9	104%	1.0
S	mg/kg d.b.	432.0	1039	889	86%	1646	1470	89%	2253	2090	93%	2860
Cl	mg/kg d.b.	902	861	854	99%	821	832	101%	780	831	107%	739
Ca	mg/kg d.b.	2380	2678	2640	99%	2975	2960	99%	3273	3350	102%	3570
Si	mg/kg d.b.	4970	4533	4390	97%	4095	4000	98%	3658	3740	102%	3220
Mg	mg/kg d.b.	601	933	858	92%	1266	1230	97%	1598	1520	95%	1930
K	mg/kg d.b.	4810	3671	3380	92%	2533	2260	89%	1394	1270	91%	255.0
Na	mg/kg d.b.	144.0	189.8	176.0	93%	235.5	226.0	96%	281.3	287.0	102%	327.0
P	mg/kg d.b.	886	717	681	95%	549	499.0	91%	379.8	348.0	92%	211.0
Al	mg/kg d.b.	130.0	265.5	251.0	95%	401.0	369.0	92%	537	385.0	72%	672
Zn	mg/kg d.b.	20.8	17.5	16.4	94%	14.1	14.3	101%	10.8	11.1	103%	7.5
Pb	mg/kg d.b.	0.49	1.8	2.1	114%	3.2	4.5	140%	4.6	6.2	135%	5.9
<i>Characteristic ash melting temperatures °C (CEN/TS 15370-1)</i>												
Shrinkage starting		870		1120			1140			1170		1210
Deformation		980		1150			n.o.			1210		n.o.
Hemisphere		1160		1170			n.o.			1220		1240
Flow		1190		1180			1210			1220		1240

Table 2

Values of relevant fuel indexes for the fuels and blends investigated. Explanation: d.b. – dry basis.

		M100	P25	P50	P75	P100
(Si + P + K)/(Ca + Mg)	mol/mol	3.9	2.6	1.81	1.21	0.76
K + Na + Zn + Pb	mg/kg d.b.	4975	3880	2785	1690	595
2S/Cl	mol/mol	1.1	2.7	4.4	6.4	8.6
N	wt.% d.b.	0.33	0.49	0.7	0.8	1.0

4.1.1. Ash-melting behaviour

This index $(Si + P + K)/(Ca + Mg)$ relates elements (Si in combination with K, P and K) which typically decrease the ash-melting temperature to the elements Ca and Mg which increase the ash-melting temperature. Therefore, a lower value of this index indicates a higher ash-melting temperature.

For pure Miscanthus (see Table 2) the value of the index amounts to 3.9, which can be assigned to a melting temperature below 1000 °C. With increasing amount of peat in the blend the values of the index decrease, whereby P100 is well comparable with wood fuels (softwood, hardwood, bark) [6]. Therefore, increasing ash-melting temperatures are expected with rising share of peat in the blend.

4.1.2. K release ratios

In Ref. [23] a correlation between the molar $(Si + P + K)/(Ca + Mg)$ ratio and the K release ratio has been presented, where increasing K release ratios have been obtained with decreasing molar $(Si + P + K)/(Ca + Mg)$ ratios. This behaviour results from a decreased formation of low melting K-silicates and phosphates.

From Table 2, decreasing values of this index with increasing amount of peat in the blend have been determined indicating increasing K release ratios for peat rich blends. This result of course has to be evaluated under consideration of the strongly decreasing K content with rising peat shares.

4.1.3. The sum of K + Na + Zn + Pb as an indicator concerning aerosol emissions and deposit build-up

A part of the semi-volatile and volatile ash-forming elements such as K, Na, S, Cl, Zn and Pb is released from the fuel to the gas

phase during combustion. In the gas phase they undergo homogeneous gas-phase reactions and later, due to supersaturation in the gas phase, they start to nucleate or condense on the surfaces of existing particles or of heat exchanger tubes [24,25].

From Table 2, a decreasing sum of K, Na, Zn and Pb with an increasing amount of peat can be seen, whereby for P100 a value which is comparable to the one of softwood Ref. [6] is reached. Therefore, with increasing amount of peat in the blend decreased aerosol emissions are expected, since the amount of K in the fuel decreases with an increasing amount of peat in the blend. It has to be mentioned that this index only works if comparable release ratios for the different blends prevail. Due to the trend of the molar $(Si + P + K)/(Ca + Mg)$ ratio the K release is supposed to increase with increasing peat shares and therefore a less pronounced decrease of aerosol emissions with increasing peat shares may be expected.

4.1.4. High-temperature chlorine corrosion risks

A comprehensive study has shown that with rising Cl concentrations in tube near deposit layers an increased risk regarding high-temperature chlorine corrosion prevails. Moreover, it has been observed that there is a correlation between the 2S/Cl ratio in the fuel and in fine particulate matter emissions, which are mainly responsible for S- and Cl-rich deposit build-up. Guiding values regarding the molar 2S/Cl ratios have been presented. A high corrosion risk for values <1 prevails, minor corrosion risks have to be expected for values >4 and for values over 8 negligible Cl levels in the boiler deposits can be achieved which eliminate corrosion from this source Ref. [26].

From Table 2, it can be revealed that for M100 and for P25 an increased high-temperature chlorine corrosion risk exists. With increasing share of peat in the blends the corrosion risk decreases, whereby according to the above classification P50 and P75 show minor and P100 almost negligible high-temperature chlorine corrosion risks.

4.1.5. NO_x emissions

In biomass combustion processes NO_x emissions mainly result from the fuel N, while their formation from combustion air (prompt and thermal NO_x formation) typically plays only a minor

role [27,28]. In Ref. [6] a correlation between the N content in the fuel and the NO_x emissions has been presented for fixed-bed biomass combustion, whereby with increasing fuel N content higher NO_x -emissions have to be expected.

It can be seen from Table 2, that with increasing share of peat also the N-content increases and consequently also higher NO_x emissions have to be expected.

4.2. Evaluation of the ash-melting behaviour predicted by TEC in comparison to experimental results

To investigate the ash-melting behaviour the standard ash-melting test (CEN/TS 15370-1) and TEC have been used. Based on TEC the amount of molten fractions can be calculated, whereby T_{30} is defined as the temperature at which 30 wt.% liquid phases occur. Previous work [13,16] has shown that this temperature is an appropriate indicator for the shrinkage starting temperature (SST) (according to CEN/TS 15370-1).

In Fig. 3, for comparison the SST and the T_{30} values are plotted against the molar $(\text{Si} + \text{P} + \text{K})/(\text{Ca} + \text{Mg})$ ratio (see Section 4.1.1).

An index of 3.9 for M100 indicates a very low SST which is confirmed by the ash melting test and the TEC results (see Fig. 3). With increasing amount of peat the index decreases and the SST increases, which is also confirmed by TEC.

4.2.1. Optical evaluation of selected ashes after lab-scale reactor experiments

Lab-scale reactor experiments (see Section 2.4) have also been used for an optical evaluation of the ash sintering tendencies. From the residual ashes of tests with M100 and P25 (see Fig. 4 middle) slightly sintered ash particles with a brittle structure have been obtained, whereby for P25 a decreasing amount of sintered particles compared to M100 has been observed. This is also in agreement with the SST determined for M100 (870 °C) and for P25 (1120 °C). For higher amounts of peat P50 (see Fig. 4 right), P75 as well as for P100 a loose ash residue has been noticed.

4.3. Comparison of the release behaviour of ash-forming elements calculated by thermodynamic equilibrium calculation with the experimentally determination by lab-scale reactor experiments

TEC has also been applied for the prediction of the release behaviour of ash-forming elements for the samples investigated. The calculated results have been compared with experimental results

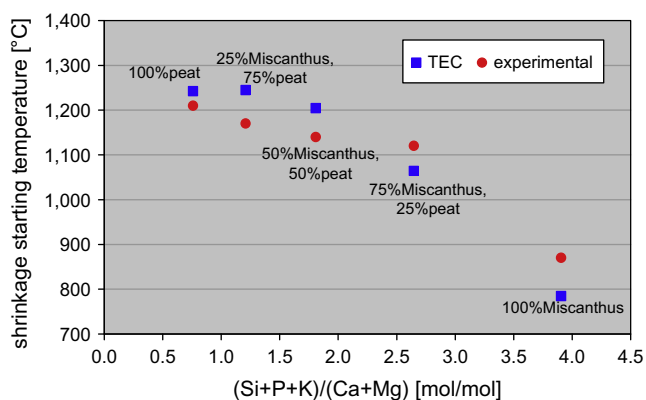


Fig. 3. Molar $(\text{Si} + \text{P} + \text{K})/(\text{Ca} + \text{Mg})$ ratio versus shrinkage starting temperature for pure Miscanthus/peat as well as for blends in comparison with thermodynamic equilibrium calculations. Explanations: experimental – shrinkage starting temperature according to standard ash-melting test (CEN/TS 15370-1); TEC – results of thermodynamic equilibrium calculations (temperature where 30 wt.% liquid phase occur).

from lab-scale reactor tests. From these tests release ratios are derived by mass and element balances based on analyses taken of the initial fuel as well as the residues (ashes) remains after the test runs. In Refs. [13,17] a detailed description of the release calculations and the evaluation of the lab-scale reactor experiments can be found.

The chemical compositions of the residual ashes of the test runs performed (in duplicate) are summarised in Table 3. In general it can be seen (Table 3) that with increasing peat share the ash chemistry shifts from a K–Si dominated system to a Ca–Si dominated system. Also the Al and Mg contents increase with increasing peat addition.

In Fig. 5, the experimentally determined inorganic element release ratios from the fuel to the gas phase from lab-scale reactor experiments are compared with results from TEC.

The release behaviour of S and Cl, which is of major relevance regarding the high temperature corrosion risk, is well predicted with TEC (see Fig. 5). For S TEC slightly overestimates the release ratios compared with lab-scale reactor experiments (84–89 wt.% respectively 95–99 wt.%). The release ratios determined for S are also in good agreement with a former work [23], where for a broad variety of fuels S release ratios between 72 and 93 wt.% with an average value of 87 wt.% were reported. The K release is the most relevant parameter regarding fine particulate matter emissions as well as deposit built-up. The trend of increasing K release with increasing peat shares, identified during the lab-scale reactor tests, is also predicted by TEC, whereby a detailed discussion regarding the K release is provided at the end of this chapter. The release prediction for Pb is in very good agreement with experimental results. For Na and Zn strong deviations between TEC and experimental results can be observed. While the lab-scale reactor experiments indicate an increased Na release with increasing peat content of the blend, TEC predicts a Na release <5% which results from an almost complete embedding in solid phases (Na–Ca–Si phases for M100 to P75; Na–Al–Si phases for P100) for calculation step 1 (devolatilisation phase) at 700 °C. Also the second calculation step predicts small amounts (<5%) of Na to be stable in the gas phase. Generally for Na the formation of solid phases is overestimated by TEC. For Zn TEC predicts a non-systematic variation of the release between 7 and 55 wt.% while the experimental results show release ratios of about 80–90 wt.%. Zn shows strongly differing release behaviours under oxidising and reducing conditions. Generally from TEC it can be revealed that the main part of Zn is released during calculation step 1 where reducing conditions prevail. A steep increase of the Zn release can be observed for calculation step 1 in the temperature window between 700 and 900 °C, whereas the release ratios for the remaining ash-forming elements (S, Cl, K, Na, Pb) stay rather constant. Reducing atmospheres inside char particles, which are not considered by TEC, are most probably responsible for the high Zn release ratios. Therefore, TEC-based release predictions for Zn have to be evaluated as problematic.

In Section 4.1.2 the molar $(\text{Si} + \text{P} + \text{K})/(\text{Ca} + \text{Mg})$ ratio has been used for a first prediction regarding the K release. In Ref. [23] a correlation between the molar $(\text{Si} + \text{P} + \text{K})/(\text{Ca} + \text{Mg})$ ratio and the K release has been presented where increasing K release ratios with decreasing values of this index have been found. In Fig. 6, the molar $(\text{Si} + \text{P} + \text{K})/(\text{Ca} + \text{Mg})$ ratio versus the experimentally determined K release and the predicted K release ratios from TEC as well as the correlation presented in Ref. [23] are plotted.

From Fig. 6, it can be revealed that with decreasing molar $(\text{Si} + \text{P} + \text{K})/(\text{Ca} + \text{Mg})$ ratio the K release increases. Also a qualitatively good agreement of the data presented in comparison with the correlation from Ref. [23] can be observed. For TEC an underestimation of the K release for M100, whereas for P100 an overestimation and a good agreement for the blends in comparison with experimental results exists. A detailed evaluation of TEC has



Fig. 4. Photos of the residual ash of M100 (left), P25 (middle) and P50 (right) gained from lab-scale tests.

Table 3

Chemical composition of the ash residues from lab-scale reactor tests for pure Miscanthus and peat as well as for the blends. Explanations: TOC – total organic carbon; TIC – total inorganic carbon; d.b. – dry basis.

		M100		P25		P50		P75		P100	
		Test 1	Test 2								
S	mg/kg d.b.	1740	2180	5730	5310	10,900	11,700	15,800	16,700	21,000	21,500
Cl	mg/kg d.b.	171	193	516	442	771	916	1270	1160	726	976
Ca	mg/kg d.b.	96,500	95,700	121,000	118,000	143,000	143,000	155,000	156,000	175,000	176,000
Si	mg/kg d.b.	204,000	200,000	203,000	200,000	188,000	184,000	183,000	179,000	153,000	163,000
Mg	mg/kg d.b.	25,500	25,600	40,400	39,700	59,600	58,900	72,600	74,900	95,300	94,700
K	mg/kg d.b.	165,000	167,000	134,000	128,000	88,900	90,200	48,300	48,600	10,200	9020
Na	mg/kg d.b.	5180	5350	7160	7160	8870	8780	10,100	10,000	10,400	10,300
P	mg/kg d.b.	35,100	34,800	30,500	30,100	23,700	23,500	16,300	16,800	10,200	9940
Al	mg/kg d.b.	5240	5380	11,100	11,200	17,400	17,000	24,600	24,000	30,700	30,500
Zn	mg/kg d.b.	108	138	132	128	92.1	101	59.3	60.6	29.5	26.7
Pb	mg/kg d.b.	0.94	1.25	3.5	3.0	3.9	4.2	2.7	3.4	4.6	5.3
TOC	mg/kg d.b.	<1000	<1000	<1000	<1000	<1000	<1000	<1000	<1000	<1000	<1000
TIC	mg/kg d.b.	1100	1200	1800	1400	1400	1200	1100	1000	500	<500

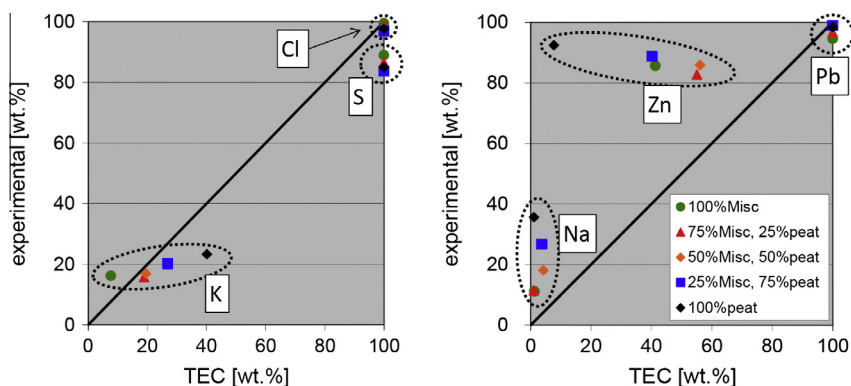


Fig. 5. Experimentally determined element release from the fuel to the gas phase from lab-scale reactor experiments in comparison with TEC – results for pure Miscanthus and peat as well as the blends. Explanation: TEC – thermodynamic equilibrium calculation, TEC release estimated at 1250 °C.

shown, that almost the complete release takes place during the devolatilisation phase (calculation step 1). Therefore, the evaluation temperature of this step influences the results of the release prediction. Furthermore, it has been shown that the gaseous atmosphere has a strong influence on the K release behaviour. In a fuel bed the conditions can switch between reducing and oxidising zones and thus equilibrium conditions might not be reached. This and the definition of the evaluation temperature of step 1 can be the reason for the quantitative differences observed regarding the K release. Generally, it can be concluded that TEC is able to describe the K release qualitatively but for quantitative evaluations lab-scale reactor tests are needed.

4.4. Aerosol as well as SO₂ and HCl emission potentials

Based on the release data gained from the lab-scale reactor experiments, the potential for aerosol formation can be estimated.

The released amounts of K, Na, Zn and P were considered to form K₂SO₄, KCl, Na₂SO₄, NaCl, ZnO and P₂O₅. Concerning the alkali metals K₂SO₄ and Na₂SO₄ also K₂Na(SO₄)₂ may be formed, whereby the formation of K₂Na(SO₄)₂ has almost no influence on the amount of aerosols. Regarding P it has been suggested in Ref. [29] that the release occurs in form of P₂O₅ to the gas phase and from Ref. [30] it can be concluded that P remains in its phosphate form in the aerosol fraction. It has to be noted that for P50, P75 and P100 the P release was rather low (<3%) and for M100 and P25 a P release of 4.2% and 3.2% has been determined. Since for P50, P75 and P100 the P concentration in the fuel is low, the contribution to the amount of aerosols is not significant, while for M100 and P25 P showed a considerable (~10%) contribution to the amount of aerosols due to higher P concentrations in the fuel. In Ref. [6] it is shown that data from test runs performed at real-scale grate fired combustion plants show a correlation between the 2S/Cl ratio in biomass fuels and the 2S/Cl ratio found in the aerosols sampled

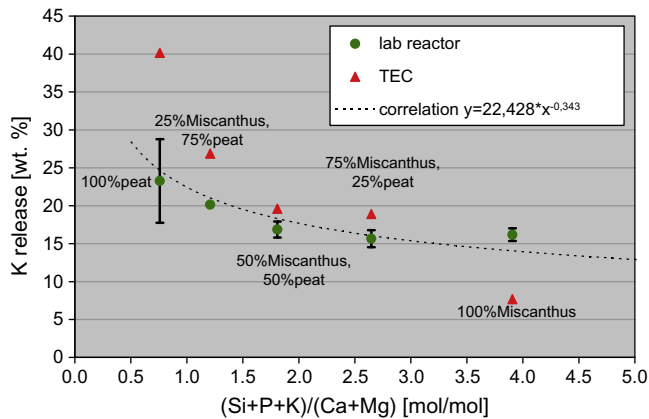


Fig. 6. Molar $(\text{Si} + \text{P} + \text{K})/(\text{Ca} + \text{Mg})$ ratio versus K release ratios. Explanations: lab reactor – experimentally determined K release by lab-scale reactor experiments; TEC – K release according to thermodynamic equilibrium calculations, TEC release estimated at 1250 °C, correlation – correlation presented in [23].

downstream the boiler. According to Ref. [6] a molar 2S/Cl ratio in aerosol emissions of about 0.43 in case of M100 and 2.9 in case of P100 can be estimated from the 2S/Cl ratios in the fuel (1.1 respectively 8.6) (see Section 4.1.4).

Based on the release data and the estimated distribution of S and Cl in the aerosols, an estimation of the aerosol emission potential ranges from 33 to 140 mg/Nm³ at 13 vol.% O₂ in the flue gas (Nm³ are m³ at 0 °C and 101325 Pa) for P100 and M100 respectively. Thereby, particle losses caused by condensation of ash-forming vapours on walls and deposit formation in the furnace and the boiler sections, by reactions of ash-forming vapours with coarse fly ash particles or condensation on coarse fly ash particles are not considered.

In Fig. 7, the sum of K, Na, Zn and Pb is plotted against the estimated aerosol emissions.

It can clearly be seen (Fig. 7) that with an increasing amount of the sum of K, Na, Zn and Pb the estimated aerosol emissions increase. A very good agreement between the trend of the sum of K, Na, Zn and Pb versus the aerosol emissions investigated in this study and the trend which has been investigated in Ref. [6] is given. It can also be concluded from Ref. [6] that for P100 a comparable behaviour like for softwood regarding the aerosol emissions can be expected. It has to be added that for M100 and the blends the main influencing factor on the estimated aerosol emissions is the amount of K released from the fuel to the gas phase, whereas for P100 the most relevant parameter is the amount of Na released.

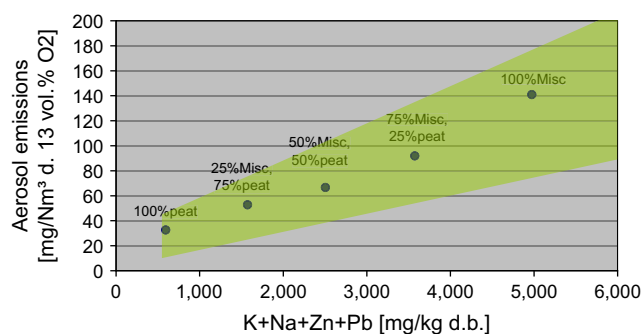


Fig. 7. Sum of K, Na, Zn and Pb versus estimated aerosol emissions for pure Miscanthus and peat as well as for the blends. Explanations: Misc – Miscanthus, green area – aerosol emission range according to Ref. [6]; Nm³ – m³ at 0 °C and 101325 Pa.

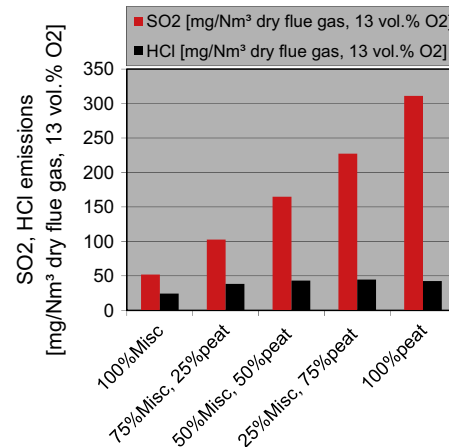


Fig. 8. Estimated gaseous SO₂ and HCl emissions for pure Miscanthus and peat as well as for the blends. Explanations: Misc – Miscanthus; Nm³ – m³ at 0 °C and 101325 Pa.

Based on the release data and the estimation of aerosol emissions (alkali sulphates and chlorides) also an estimation of the potential of gaseous SO₂ and HCl emissions can be made (S and Cl which are not bound by K and Na). This estimation does not consider S and Cl bound by Ca and Mg. In Fig. 8, results of the estimation of gaseous SO₂ and HCl are displayed.

It can be seen (Fig. 8) that the SO₂ emissions strongly increase with rising amounts of peat. This can be explained with the increasing S content and the decreasing K content in the fuel with increasing peat shares. HCl emissions slightly increase with increasing amount of peat in the blend and remain almost constant for >P50. This is due to the fact that the Cl concentrations in both fuels are almost the same, but with increasing amount of peat the K content in the blend decreases. Even if at the same time the K release ratio increases, the absolute K release (in mg/kg fuel) decreases. Therefore, less K is available in the gas phase to bind S and Cl which leads to increased SO₂ and HCl emissions. Consequently the blending of peat with Miscanthus may lead to strongly increased SO₂ emissions which has to be considered regarding the demand for (secondary) measures for SO₂ emission control.

5. Summary and conclusions

Blending of Miscanthus with peat represents a feasible option to reduce combustion related problems. While the usual approach for the investigation of fuel blends is based on pilot and full-scale combustion tests, in this study novel characterisation tools for a systematic evaluation of the effects of fuel blending on ash-related problems as well as particulate and gaseous emissions for fixed bed/grate combustion systems are presented, which reduce the necessity of expensive and time consuming testing programs.

Miscanthus and peat as well as 3 different blends (75/25, 50/50 and 25/75 wt.% d.b.) were investigated. With increasing shares of peat in the blends the content of K decreased, whereas the contents of N, S, Ca and Mg increased. Regarding the fuel composition, a lower K release, higher ash-melting temperatures and increasing gaseous SO₂ and NO_x emissions can be expected with increasing peat shares.

For the evaluation of the ash-melting temperatures fuel indexes (molar $[\text{Si} + \text{P} + \text{K}]/[\text{Ca} + \text{Mg}]$ ratio), TEC and the standard ash-melting test (according to CEN/TS 15370-1) have been used. It has been shown that TEC can predict the trend of the initial

ash-melting temperatures with acceptable accuracy. Evaluations of the ash-melting behaviour proof that M100 shows a low shrinkage starting temperature (SST) (870 °C), whereas for P100 a high SST (1210 °C) has been determined. An increase of the SST for P25 in comparison with M100 and further increasing melting temperatures for higher peat shares are observed.

Furthermore, TEC have been used for a qualitative and for some elements (e.g. S, Cl and Pb) also quantitative prediction of the element release ratios. For a quantitative determination of the release behaviour of volatile and semi-volatile ash-forming elements results from lab-scale reactor experiments were used. For the qualitative prediction of the K release additionally the fuel index (molar $[\text{Si} + \text{P} + \text{K}]/[\text{Ca} + \text{Mg}]$ ratio) can be applied. This index predicts increasing K release ratios with an increasing amount of peat in the blend, which is in line with results from TEC. Experimentally the highest K release ratio has also been determined for P100. With decreasing peat shares until P50 the K released also decreased, for lower peat shares (P25, M100) the K release was rather constant. The release ratios determined from lab-scale reactor experiments have been used for an estimation of the aerosol, HCl and SO₂ emissions to be expected. The aerosol emissions decrease with increasing shares of peat in the blend, which has also been predicted by the corresponding fuel index (sum of K, Na, Zn and Pb). This behaviour can mainly be explained with the decreasing amount of K in the fuel with increasing amount of peat in the blend. It has also been shown that the gaseous HCl and NO_x emissions slightly increase, whereas a steep increase of the SO₂ emissions with increasing shares of peat has to be considered. Concerning high-temperature chlorine corrosion, increased corrosion risks for M100 and P25 exist, whereby with rising shares of peat in the blend the corrosion risk decreases and reaches an almost negligible level for P100.

The amount of 25% of peat can be recommended for a preparation of a fuel blend with Miscanthus since the ash-melting temperatures are increased to a rather unproblematic level, the aerosol emissions decrease and the increase of gaseous HCl, SO₂ and NO_x emissions is still on a moderate level, whereas for this blend still an increased risk for high-temperature chlorine corrosion exists. Higher peat amounts decrease the corrosion risk and the aerosol emissions further, slightly rise the ash-melting temperatures, but also cause higher gaseous SO₂ and NO_x emissions. These trends have to be considered regarding the final selection of a suitable blend. Economic considerations as well as legal constraints (e.g. emission limits) will accompany the decision.

It has to be noted that the composition of peat strongly depends on its origin and formation. Therefore, the fuel characterisation methods presented in this study should be performed for the specific fuels used in a certain plant/region because the results may strongly differ depending on the chemical composition of the fuels used.

Summing up, a new evaluation method for the characterisation of fuel blends is available considering the influences on ash-melting, fine particulate, HCl, SO₂ and NO_x emissions. With this approach the characterisation of meaningful biomass blends can be performed and thus time-consuming and expensive pilot- and full-scale tests can be minimised.

Acknowledgements

The authors gratefully acknowledge the support of the FFG – Austrian Research Promotion Agency, within the ERANET-Bioenergy project FutureBioTec, future low emission biomass combustion systems. The work was also funded by the companies Andritz AG, Josef Bertsch GmbH & Co. KG, BIOS BIOENERGIESYSTEME GmbH, HET Heiz- und Energietechnik Entwicklung GmbH, KWB Kraft und Wärme aus Biomasse GmbH,

MAWERA Holzfeuerungsanlagen GmbH, Standardkessel GmbH and TIWAG Tiroler Wasserkraft AG.

References

- [1] Lewandowski I, Scurllock JMO, Lindvall E, Christou M. The development and current status of perennial rhizomatous grasses as energy crops in the US and Europe. *Biomass Bioenergy* 2002;25:335–61.
- [2] Brosse N, Dufour A, Meng X, Sun Q, Ragauskas A. Miscanthus: a fast-growing crop for biofuels and chemicals production. *Bioprod Bioref* 2012;6:580–98.
- [3] Mc Kendry P. Energy production from biomass (part I): overview of biomass. *Biorecour Technol* 2002;83:37–46.
- [4] Labrecque M, Teodorescu T. Field performance and biomass production of 12 willow and poplar clones in short-rotation coppice in southern Quebec (Canada). *Biomass Bioenergy* 2005;29:1–9.
- [5] Vassilev SV, Baxter D, Andersen LK, Vassileva CG. An overview of the chemical composition of biomass. *Fuel* 2010;89:913–33.
- [6] Sommersacher P, Brunner T, Obernberger I. Fuel indexes – a novel method for the evaluation of relevant combustion properties of new biomass fuels. *Energy Fuel* 2012;26:380–90.
- [7] Keddy PA. *Wetland Ecology: Principles and Conservation*. 2nd ed. Cambridge, UK: Cambridge University Press; 2010.
- [8] Nordin A. Chemical elemental characteristics of biomass fuels. *Biomass Bioenergy* 1994;6:339–47.
- [9] Nyström I, Boström D, Boman C, Öhman M. Effect of peat addition to woody biomass pellets on slagging characteristics during combustion in residential pellet burners. In: *Proceedings 17th European Biomass Conference & Exhibition 2009 June 2009, Hamburg, Germany, ETA-Renewable Energies (Ed.)*, Italy: 1400–05.
- [10] Fangerström J, Näzelius I, Boström D, Öhman M, Boman C. Reduction of fine particle- and deposit forming alkali by co-combustion of peat with wheat straw and forest residues. In: *Proceedings of the Conference Impacts of Fuel Quality on Power Production and Environment 2010, August 2010, Saariselkä, Finland, EPRI (Ed.)*, Palo Alto, CA, USA.
- [11] Lundholm K, Nordin A, Öhman M, Boström D. Reduced bed agglomeration by co-combustion biomass with peat fuels in a fluidized bed. *Energy Fuel* 2005;19:2273–8.
- [12] Pommer L, Öhman M, Boström D, Burvall J, Backman R, Olofsson I, et al. Mechanisms behind the positive effects on bed agglomeration and deposit formation combusting forest residue with peat additives in fluidized beds. *Energy Fuel* 2009;23:4245–53.
- [13] Sommersacher P, Brunner T, Obernberger I, Kienzl N, Kanzian W. Application of novel and advanced fuel characterization tools for the combustion related characterization of different wood/kaolin and straw/kaolin mixtures. *Energy Fuel* 2013;27(9):5192–206.
- [14] Bärenthaler G, Zischka M, Hanraldsson C, Obernberger I. Determination of major and minor ash-forming elements in solid biofuels. *Biomass Bioenergy* 2006;30:983–97.
- [15] Obernberger I. Strategy for the application of novel characterization methods for biomass fuels: case study of straw. *Energy Fuel* 2014;28:1041–52.
- [16] Evic N, Brunner T, Obernberger I. Prediction of biomass ash-melting behaviour – correlation between the data obtained from thermodynamic equilibrium calculations and simultaneous thermal analysis (STA). In: *Proceedings 20th European Biomass Conference & Exhibition 2012 June 2012, Milano, Italy, ETA-Renewable Energies (Ed.)*, Italy: 807–813.
- [17] Brunner T, Biedermann F, Evic N, Obernberger I. Advanced biomass fuel characterisation based on tests with a specially designed lab-scale reactor. *Energy Fuel* 2013;27:5691–8.
- [18] Weissinger A, Fleckl T, Obernberger I. Application of FT-IR in-situ absorption spectroscopy for the investigation of the release of gaseous compounds from biomass fuels in a laboratory scale reactor – Part II: Evaluation of the N-release as functions of combustion specific parameters. *Comb Flame* 2004;137:403–17.
- [19] Stubenberger G, Scharler R, Obernberger I. Nitrogen release behaviour of different biomass fuels under lab-scale and pilot-scale conditions. In: *Proc. of the 15th European Biomass Conference & Exhibition 2007 May 2007, Berlin, Germany*, 1412–20.
- [20] Boman C. Fuel additives and blending as primary measures for reduction of fine ash particle emissions – state of the art; ERA-NET FutureBioTec [07.09.2012, viewed on 28.02.20013] <[http://futurebiotec.bioenergy2020.eu/files/FutureBioTec-Additives and fuel blending-state of the art report.pdf](http://futurebiotec.bioenergy2020.eu/files/FutureBioTec-Additives%20and%20fuel%20blending-state%20of%20the%20art%20report.pdf)>.
- [21] Hedman H, Nyström I-L, Öhman M, Boström D, Boman C, Samuelsson R. Småskalig eldning av torv-effekter av torvinblandning i träpellets på förbränningsresultatet i pelletsbrännare. Rapport nr 9 i Torvforsks rapportserie; 2008. ISSN 1653–7955.
- [22] Phyllis Database of Energy Research Centre of the Netherlands (ECN – <http://www.ecn.nl/phyllis/>).
- [23] Sommersacher P, Brunner T, Obernberger I. Fuel Indexes – A novel method for the evaluation of relevant combustion properties of new biomass fuels. In: *Proceedings of the Conference Impacts of Fuel Quality on Power Production and Environment 2012, 23–27 September 2012, Puchberg, Austria, EPRI (Ed.)*, Palo Alto, CA, USA.
- [24] Brunner T. Aerosols and coarse fly ashes in fixed-bed biomass combustion. PhD-Thesis, Graz University of Technology, Austria; 2006.

- [25] Christensen K. The formation of submicron particles from the combustion of straw. PhD-Thesis 1995, ISBN 87-90142-04-7, Department of Chemical Engineering (Ed.), Technical University of Denmark, Lyngby, Denmark.
- [26] Salmenoja K. Field and laboratory studies on chlorine-induced superheater corrosion in boilers fired with Biofuels. PhD-Thesis, Abo Akademi, Faculty of Chemical Engineering, Abo/Turku, Finland; 2000.
- [27] Glarborg P, Jensen AD, Johnsson JE. Fuel nitrogen conversion in solid fuel fired systems. *Prog Energy Combust Sci* 2003;29:89–113.
- [28] Weissinger A. Experimentelle untersuchungen und reaktionskinetische simulationen zur NO_x -reduktion durch Primärmaßnahmen bei Biomasse-Rostfeuerungen. PhD-Thesis, Graz University of Technology, Graz, Austria; 2002.
- [29] Diaz-Ramirez M, Bohman C, Sebastian F, Royo J, Xiong S, Boström D. Ash characterization and transformation behavior of the fixed-bed combustion of novel crops: poplar, brassica, and cassava fuels. *Energy Fuel* 2012;26:3218–29.
- [30] Lindström E, Sandström M, Boström D, Öhman M. Slagging characteristics during combustion of cereal grains rich in phosphorus. *Energy Fuel* 2007;21:710–7.

Paper IV

Simultaneous Online Determination of S, Cl, K, Na, Zn, and Pb Release from a Single Particle during Biomass Combustion. Part 1: Experimental Setup—Implementation and Evaluation

Peter Sommersacher,^{*,†} Norbert Kienzl,[†] Thomas Brunner,[‡] and Ingwald Obernberger^{‡,§}

[†]BIOENERGY 2020+ GmbH, Inffeldgasse 21b, A-8010 Graz, Austria

[‡]BIOS BIOENERGIESYSTEME GmbH, Inffeldgasse 21b, A-8010 Graz, Austria

[§]Institute for Process and Particle Engineering, Graz University of Technology, Inffeldgasse 13, A-8010 Graz, Austria

ABSTRACT: The interest in experimental data regarding thermal fuel decomposition as well as the release behavior of ash-forming elements of biomass fuels for modeling and simulation purposes is continuously increasing. On the basis of combustion experiments with lab-scale reactors and single-particle reactors, integral release data regarding ash-forming vapors can be obtained, whereby the release is calculated on the basis of analysis data of the fuel and the ash residues. At the moment, almost no time-resolved release data of ash-forming elements from single particles exist. Therefore, a single-particle reactor was designed, which has been coupled to an inductively coupled plasma mass spectrometer (ICP-MS). This reactor can be used for targeted experiments in a temperature range of 250–1050 °C under inert, reducing, and oxidizing conditions. With this reactor, it is possible to simultaneously determine the surface and center temperatures of a biomass particle, weight loss of the particle, and flue gas composition. The reactor has been coupled to an ICP-MS through a gas stream that is sufficiently diluted with Ar. First performance tests with pure salts (KCl, NaCl, (NH₄)₂SO₄, ZnCl₂, and PbCl₂) proved that relevant volatile ash-forming elements can be detected with the ICP-MS. For a further validation of the received signals, combustion tests with *Miscanthus* pellets have been carried out, whereby the controlled interruption of the experiments has also been investigated. These tests prove that with this system the simultaneous time-resolved determination of S, Cl, K, Na, Zn, and Pb is possible whereby the Cl signal can only be used with restrictions. On the basis of the determined release of ash-forming elements for the entire combustion experiment, a quantification/calibration of the measured intensities has been carried out. The data gained from these tests will provide deeper insights into release processes as well as form a relevant basis for release model development.

1. INTRODUCTION AND OBJECTIVES

During recent years, the interest in experimental data regarding the thermal decomposition behavior of biomass fuels as well as the release of inorganic elements (e.g., S, Cl, K, Na, Zn, and Pb) during decomposition for modeling and simulation purposes is continuously increasing. For this reason, experiments with different reactor types have been carried out. In thermogravimetric analyzers (TGA), experiments are usually conducted under inert atmospheres with low^{1–3} or high^{4,5} heating rates and low sample masses in a kinetically controlled regime for the determination of kinetic fuel decomposition data. The data obtained have been used for modeling and simulation of the release of volatile organic fuel compounds. Moreover, lab-scale reactors are used whereby single particles or a small biomass bed is pyrolyzed, gasified, or combusted in a batch reactor. By chemical analyses of the input and output material, integral release data of ash-forming elements for the whole conversion experiment can be obtained.^{6–11} Furthermore, in refs 7 and 8, thermodynamic equilibrium calculations (TEC) are applied to study release processes, but this method can only be used for qualitative release predictions. However, presently almost no data regarding the time-resolved release of ash-forming elements from single particles exist. Especially regarding K and Na release, such data would be important because K and for some fuels also Na are responsible for deposit and aerosol formation. A fuel index exists, but it can

only be used as a first indication regarding the K release during combustion processes.¹² For the online detection of K, only scarce data is available, whereby mainly optical techniques have been used so far. In ref 13, tunable diode laser absorption spectroscopy has been used for the detection of gaseous elemental K, which is released from a single pellet. Energy wood and wheat straw were converted in air at a furnace temperature of 850 °C. In addition, tests have been carried out where the combustion process has been stopped at different times (mainly during char burnout). The residues after the stop of the combustion process have been chemically analyzed, and the release of ash-forming elements has been determined. During the devolatilisation phase, between 5 and 10% of the total K content in the original pellet has been released to the gas phase. During devolatilisation, about 1% of the total K release during this combustion phase occurs in the form of elemental K. Therefore, for only a very small fraction of the total K release time-dependent release data has been obtained. It has further been suggested that KCl and KOH are the dominant K release species for energy wood during devolatilisation; for wheat straw, the major K release species has been assigned to be KCl. For the experiments, a macro-

Received: March 24, 2015

Revised: September 15, 2015

Published: September 15, 2015



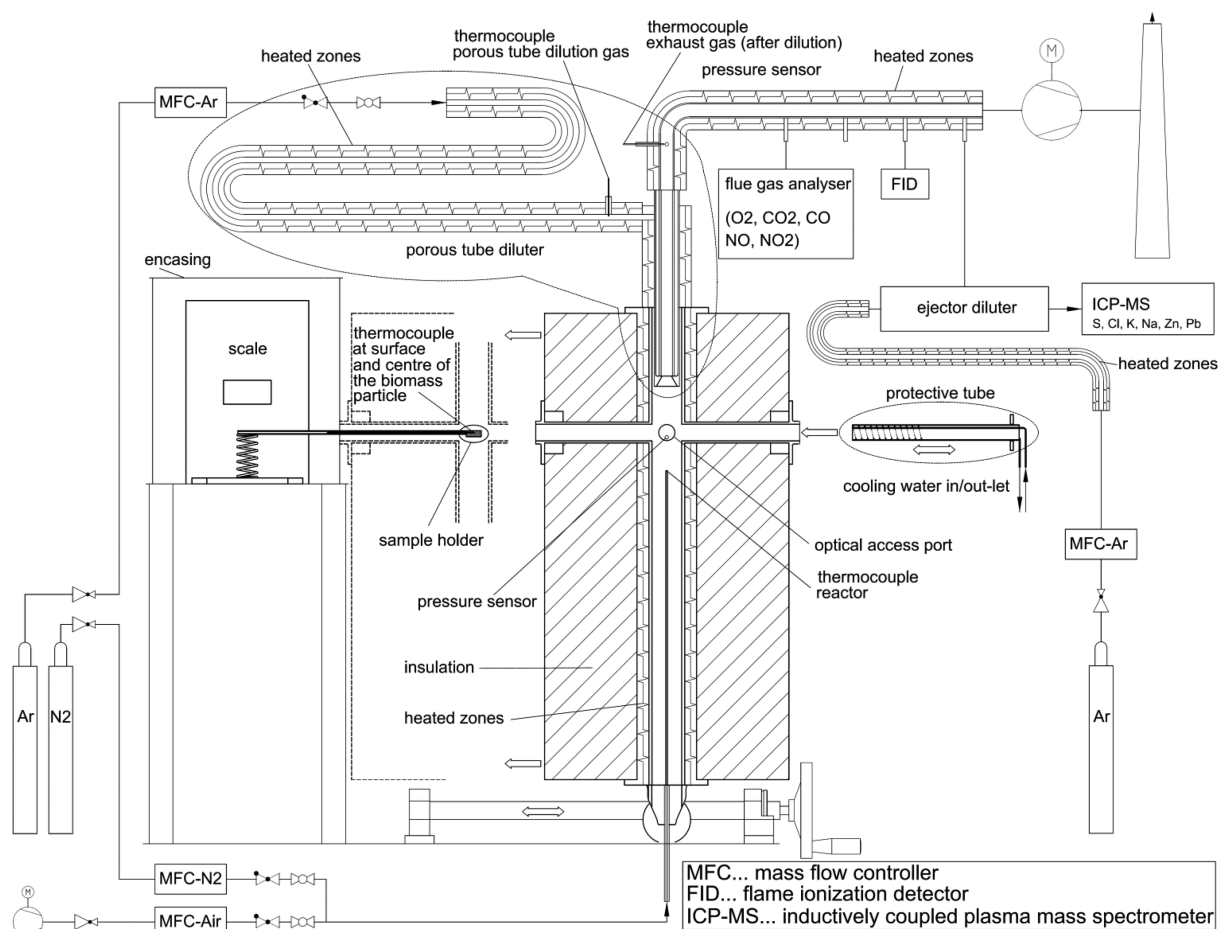


Figure 1. Scheme of the single particle reactor including measurement setup.

TGA has been used where no prompt sample introduction is possible. During the sample introduction, the sample is already exposed to the hot environment; therefore, release reactions already take place. Furthermore, it has been reported that some weaknesses regarding the experimental framework conditions in this reactor exist (e.g., cold air entering the furnace through the optical access holes). In another study,¹⁴ the simultaneous detection of K, KCl, and KOH has been carried out using colinear photofragmentation and atomic absorption spectroscopy from a 10 mg spruce bark sample. The reactor used in this study ensured a quick sample introduction and well-defined framework conditions. During the experiments, only the CO₂ concentration has been determined; no further data to characterize the combustion process has been recorded. The experiments show that at the beginning of devolatilisation small amounts of K are mainly released in its elemental form. During devolatilisation, K is mainly released as KCl, and small amounts are also released as KOH. During char burnout, the KOH release increases, and for reactor temperatures of 850 °C, only small amounts of KOH are evaporated, which increase with higher reactor temperatures (950 and 1050 °C). The same setup has been used for the investigation of torrefied wood and straw (samples mass of 10 mg).¹⁵ For torrefied wood, a K release behavior has been reported as similar to that for bark, whereas for straw it has been shown that the main K release consists of KCl and that the amount of KOH release is small. The share of KOH increases with higher temperatures, which has also been reported for bark and torrefied wood.

In previous studies, reactors have been used to show that experimental weaknesses or a full characterization of the combustion process was not possible or has not been carried out. Therefore, a new single-particle reactor, which has been coupled to an inductively plasma mass spectrometer (ICP-MS), was designed for a time-resolved characterization of the combustion process. The basic concept of the reactor is based on a macro-TGA operating under high heating rates whereby relevant combustion-related properties can be determined. The big advantage of this setup is the simultaneous online determination of the mass loss, temperatures, flue gas concentrations, and the release of S, Cl, K, Na, Zn, and Pb. The obtained time-resolved release data can support the understanding and knowledge of the release behavior of ash-forming compounds from biomass fuel particles in the future.

In the second part of this series, it is foreseen that we will present comprehensive results from combustion experiments with different biomass fuels. For this reason, tests runs under oxidizing atmospheres (5.6% O₂) have been carried out at reactor temperatures of 700, 850, and 1000 °C.

1.1. Motivation and Objectives. Presently, few data are available that allow an evaluation of inorganic element release along the different phases of thermal biomass conversion processes. Such data may provide valuable information regarding different release mechanisms that form a relevant basis for the development of release models and for understanding the ongoing chemical reactions and release processes. From this perspective, the experimental setup

described in this paper has been developed that shall facilitate a simultaneous online investigation of biomass decomposition and inorganic element release. To simulate the conversion behavior in real-scale applications, the setup should be designed as a single-particle reactor with high heating rates and variable atmospheres.

2. EXPERIMENTAL SECTION

2.1. Description of the Reactor. In Figure 1, the setup of the reactor and the ICP-MS coupling is presented.

The concept of the reactor (Figure 1) is based on a macro-TGA. The main part is an electrically heated oven, wherein a carrier gas (variable N_2 and air mixtures) is supplied from below. The biomass particle is placed on a sample holder that is connected to a scale for the determination of the mass loss during the thermal decomposition. The flue gases released during the experiment are diluted at the top of the reactor in a porous tube diluter. A part of the flue gas is drawn by an ejector diluter and is delivered after a further dilution step to an ICP-MS.

The reactor unit consists of an electrically heated (250–1050 °C) vertical main tube (height 755 mm, inner diameter 50 mm) and four horizontal side tubes (length 177 mm, inner diameter 28 mm) of which one port (two axial tubes on opposite sides) provides an optical access; the other ports are used for sample introduction and sample cooling. The material of the ceramic tubes is Alsint, a ceramic material mainly composed of Al_2O_3 (99.7%) which contains traces of MgO and SiO_2 . According to the manufacturer, diffusion of alkali metals into the material is negligible under reducing and oxidizing conditions. Comprehensive measurement and control devices are applied in order to control and monitor the conditions during the experiment. The carrier gas (N_2 /air mixtures), which is controlled with mass flow controllers (Sierra Smart Trak 2, Series 100), flows through the reactor from below and is heated up to a defined set temperature until it reaches the position of the sample holder. The sample (~1 g of biomass particle) is placed on a grid that is mounted on a horizontal sample holder. This sample holder is directly connected to a scale (Mettler Toledo XS105DU) for the determination of the mass loss during thermal decomposition. At the sample, two thermocouples Type N (NiCrSi-NiSiMg) are placed to measure the temperatures in the center and at the surface of the particle. The released flue gases (also containing inorganic vapors) enter a porous tube diluter at the top of the reactor, where Ar is used as dilution gas that is preheated to 500 °C. Precalculations have been carried out where the concentrations of inorganic vapors in the flue gas were estimated on the basis of TEC. The dilution ratio as well as the temperature of the diluted gas have been adjusted to avoid nucleation or condensation of these inorganic vapors. However, the formation of solid particles should only negligibly influence the ICP-MS measurement provided that solid particles are transported to the device and are not deposited in sampling lines. A check of possible deposit formation has been carried out for the heated sample line between the ejector diluter and the entrance of the ICP-MS, which indicated that deposit formation in this location is negligibly low (section 2.2). Furthermore, after 60 tests runs, the complete setup has been cleaned, whereby only a slight indications for depositions has been observed in the porous tube diluter and in the stainless-steel tube downstream the porous tube diluter. Because of the black color of these deposits, it was assumed that these depositions mainly result from soot particles and condensed tars. The dilution (in the porous tube diluter) further ensures that during pyrolysis the CO concentrations do not exceed the measurement range of the flue gas analyzer. A constant dilution ratio ratio of 1:3 is provided with a mass flow controller (Sierra Smart Trak 2, Series 100). The diluted flue gas passes further to a stainless-steel tube, to which different gas analyzers can be connected. Generally, a gas analyzer (Rosemount NGA 2000) that uses paramagnetism as measurement principle for O_2 detection and nondispersive infrared spectroscopy (NDIR) for CO and CO_2 detection has been used. A nitric oxide analyzer (ECO Physis CLD 700 El ht), which uses the principle of chemiluminescence, has been used for NO and NO_x

detection. The amount of C in organic hydrocarbons (OGC) is determined with a flame ionization detector (FID) (ErsaTec Smart FID). A side stream of the gas is provided to the ICP-MS, whereby a detailed description of the coupling to the ICP-MS is delivered in section 2.2. Generally, the flue gases are drawn through the reactor whereby a constant underpressure in the reactor is provided by a suction fan. The pressures close to the sample holder and in the flue gas tube after the ejector diluter are recorded using Kalinsky pressure transmitters (DS1-420).

The experiments were generally carried out according to the following procedure. Before the experiment, the reactor is preheated to the desired temperature. The carrier gas (typically 15 L/min; N_2 /air mixtures) is supplied to the reactor and an underpressure of 5 Pa (at the position of the sample holder) is adjusted. A reaction prevention tube is inserted in the reactor from the opposite side of the sample holder. The tube is water-cooled and can be flushed with N_2 . A hole to the center of the fuel particle in axial direction is drilled. A thermocouple is inserted in the fuel particle and records the center temperature during the experiment. A second thermocouple to measure the surface temperature is positioned between the sample holder grid and the particle. Because of the close contact between thermocouple and particle, especially at the start of the experiment, this thermocouple should provide a good indication regarding the surface temperature. However, different heat transfer processes (radiation and conduction) as well as the shrinkage of the particle may influence this measurement during particle conversion to a certain extent. In the next step, the reactor is moved until the sample holder reaches the center of the reactor. During this movement, the sample is cooled and flushed with N_2 by the protection tube. When the reactor reaches the encasing of the scale and is sealed against the environment, the valve of the N_2 supply for flushing the sample is closed. After the pressure in the reactor is stable (~20 s), the protection tube is removed, and the experiment starts immediately. After the experiment, the ash residues are collected from the sample holder, whereby the main part of the ashes typically remains on the thermocouple determining the center temperature. This is an indication that the gas flow applied in the reactor (0.5 m/s at 1000 °C) is low enough that almost no entrapment of ash particles takes place.

2.2. Coupling of the Reactor and the ICP-MS. To determine the release of S, Cl, K, Na, Zn, and Pb from the fuel into the gas phase online, the reactor has been coupled to an ICP-MS. ICP-MS is a well-proven technique for analysis of liquid solutions and a highly sensitive method in inorganic element analysis. In principle, this system is a liquid-phase analyzer, wherein the sample to be analyzed is injected as an aerosol into an Ar carrier gas stream. The sample gas passes through a high-frequency current and is heated to 5000–10 000 °C. Thereby, the ions which are generated in the plasma are accelerated by an electric field in the direction of the analyzer of the mass spectrometer, where the isotopes are determined.¹⁶

In our case, intensities from the ICP-MS result from the release of inorganic compounds in the hot zones of the reactor. These released vapors are diluted in a porous tube diluter to an extent that shall avoid condensation of inorganic vapors and keep the concentrations within the measurement ranges of the flue gas analyzer (section 2.1). A side stream of the diluted gas is further diluted in two steps and is provided to the ICP-MS. This gas flow (1 L/min) must be sufficiently diluted with Ar so that the molecules carried in the gas can be ionized in the Ar plasma. The dilution has been realized in a porous tube diluter (dilution ratio 1:3), which has already been explained. A second dilution is carried out with an ejector diluter, and a third dilution is realized prior the ionization in the ICP-MS.

The ejector diluter operates with Ar, where a continuous gas flow is ensured by a mass flow controller (Sierra Smart Trak 2, Series 100). To avoid also the condensation of vapor compounds during this dilution step, the dilution/transport gas is preheated to 500 °C before entering the ejector diluter. The dilution ratio in this ejector diluter is 1:10, which has been experimentally determined. Therefore, a N_2 – CO_2 mixture (33 vol % CO_2) has been fed into the reactor and was diluted with the ratio of 1:3 in the porous tube diluter, resulting in a CO_2 concentration of 11.1%. This concentration has been measured

after the porous tube diluter with a gas analyzer, ensuring a correct operation of the porous tube diluter. The CO₂ concentration at the outlet of the ejector diluter, which leads to the ICP-MS, can also be determined with a gas analyzer during operation of this device. On the basis of the measured CO₂ concentration, a dilution ratio of ~10 can be calculated in the ejector diluter, which results in an overall dilution of 1:30. We also checked if deposit formation in the heated sample line between the location on the ejector diluter and the unheated sample line that enters the ICP exists. Therefore, after the performance of the salt tests (section 3.2) and a series of pretests with biomass fuels (three tests with softwood and three tests with straw at 900 °C), the heated sample tubes were washed with an HNO₃ solution and subsequent analysis. No relevant mass fractions of volatile inorganic elements were found, which verifies that condensation and deposit formation in this sample line seems to be negligible.

Although no relevant indication of condensation and deposit formation in the heated sample line was noticeable, after the first tests with biomass fuels it was noticeable that the blank values for K, Na, Pb, and Zn were continuously rising. This was an indication that the concentration of volatile ash-forming elements was so high that the operation especially for nonwood fuels leads to contaminations of the ICP-MS. These contaminations can occur by possible condensation/deposition in the short, unheated sample line between the entrance of the ICP-MS and the sample cone. Furthermore, the cleaning of the short unheated sample line (from the entrance of the ICP-MS until the sample cone) and the sample cone itself resulted in a decrease of the blank values to a usual level. To minimize these contaminations and to decrease the cleaning intervals, an additional dilution step prior to the ICP-MS has been introduced. The ICP-MS also has the opportunity to additionally dilute the sample before ionization. A flow rate of 0.3 L/min of Ar has been chosen for this so-called make-up gas flow that results in a dilution of 1:5 in this last step. To determine the overall dilution of the carrier gas that enters the reactor, a tracer gas (100 ppm Xe in Ar) of 0.5 L/min is introduced at the reactor inlet. The ICP-MS is very sensitive with respect to Xe, and the intensity of Xe without the last dilution step and the last dilution has been determined. On the basis of this information, the dilution in the last step and the total dilution of 1:150 has been determined and validated.

2.3. ICP-MS Settings. An ICP-MS from Agilent Technologies series 7700x is used. The sample gas flow amounts to 1 L/min, and the makeup gas flow is 0.3 L/min. The radio frequency power to run the plasma is 1550 W; a standard lens setting and a Pt sample cone are used. Regarding the data acquisition, a time-resolved setting is selected. The isotopes ¹³C, ³⁴S, ²³Na, ³⁵Cl, ³⁹K, ⁶⁶Zn, ¹³²Xe, and ²⁰⁸Pb are recorded. An acquisition time of 900 s has been selected for the combustion experiments. The integration time for the detector amounts to 0.1 s/mass, which results in a data acquisition rate of about 1 s.

3. RESULTS AND DISCUSSION

First, several tests without ICP-MS coupling (section 3.1) were carried out to check the functionality of the reactor. Second, the reactor was coupled to the ICP-MS, and tests with pure salts were carried out (section 3.2). These tests showed that intensities of relevant ash-forming vapors can be measured with the system. In section 3.3, the interpretation of the measured signals of the ICP-MS, the time synchronization procedure, and calibration of the signals are discussed. This is essential for the understanding of data determined during the tests. After first tests with straw and Miscanthus pellets, the determined signals have been validated. Therefore, tests with S-doped straw pellets (section 3.4) and quench experiments (section 3.5) have been carried out with Miscanthus pellets and subsequently been discussed.

3.1. Launch of the Reactor without ICP-MS Coupling.

In a first phase, the reactor has been tested without the ICP-MS coupling. The recorded parameters as well as the definition of

prevailing combustion phases (release of volatiles and char burnout) will be discussed on the basis of a test run with a Miscanthus pellet. Generally, one single pellet with a particle diameter of ~8 mm and a length of ~20 mm is used per test run (sample mass ≈ 1 g). The chemical composition of the Miscanthus pellets used can be found in ref 8. The sample mass was 1142 mg of fresh substance (mg f.s.) with a corresponding ash-free mass of 1113 mg f.s. The test run has been carried out at a reactor temperature of 850 °C and O₂ content in the carrier gas of 5.6 vol % at a flow rate of 15 L/min. This O₂ content has been selected to achieve pyrolysis/gasification conditions during the devolatilisation phase (typical in real-scale combustion processes).

To define the prevailing combustion phase, an increase of the CO₂ concentration above 0.1 vol % has been used. It can be seen from Figure 2 (bottom) that in this case after 16 s the release of volatiles starts. The CO₂ concentration increases and reaches a plateau, after which the concentration decreases again. When the CO₂ trend reaches an inflection point, it is assumed that charcoal combustion starts to be the dominating process step. It is worth noting that devolatilisation and charcoal combustion overlap during particle conversion. Therefore, these processes cannot be exactly separated, but the phases when a certain process dominates can be defined. In this case, the inflection point occurs after 64 s. To identify the end of the char combustion phase and the end of the experiment, the drop of the CO concentration to the initial value before the start of the experiment has been used. The end of the experiment occurs after 1071 s, which is not displayed.

In Figure 2 (top), the gravimetric data as well as the pressure trends for the reactor and the flue gas are presented. To start the experiment, the protective tube is removed, and the sample is exposed to the hot carrier gas. It is obvious that after 5 s the mass starts to decrease and after 10 s a steep decrease of the mass during the release of volatile compounds occurs which is followed by a slower mass decrease during char burnout. It can be seen that about 78% of the mass is decomposed during the release of volatile compounds. The pressure in the reactor is adjusted to 5 Pa before the experiment. After 27 s, the pressure drops to zero because of released gases from the pellet. After the release of volatile compounds, the pressure in the reactor increases and reaches the initial value again.

The temperature curves are displayed in Figure 2 (middle). After the protective tube is removed, a steep increase of the surface temperature takes place, and after 95 s, a temperature of 900 °C is reached, which stays rather constant until the end of the test run (after 1071 s). The slope of the center temperature is characterized by a slow initial increase to 100 °C, attributed to the drying phase, followed by a quick increase until 70 s (pyrolysis) and a steeper increase to 850 °C during char burnout. After 100 s, the temperature in the core of the pellet reaches 900 °C and then stays rather constant until the end of the experiment. The differences of the surface and center temperatures especially during the devolatilisation phase indicate that the conversion takes place in different layers of the particle. It can also be seen that the flue gas temperature, which is measured after the porous tube diluter, increases during the devolatilisation phase and reaches the initial value during the charcoal combustion phase.

The flue gas concentrations are displayed in Figure 2 (bottom). Analogous to the surface temperature increase, the CO₂ and CO concentrations as well as OGC increase, and the O₂ concentrations decrease. During char burnout, the CO₂

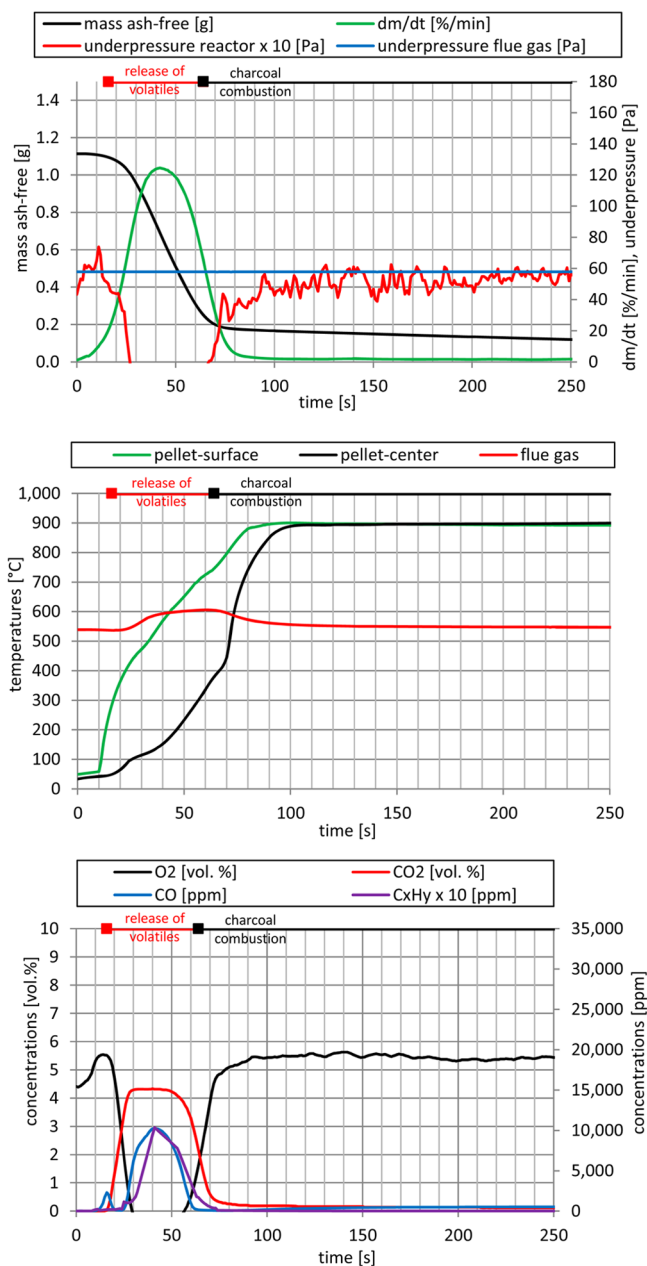


Figure 2. Experimental data for Miscanthus at 850 °C set temperature: gravimetric data and pressure trend (top), temperature curves (middle), and flue gas compositions (bottom).

concentrations decrease and the O_2 concentrations reach the initial value of 5.6 vol %. For the first 15 s of the test run, most probably the N_2 for cooling the sample dilutes the carrier gas; therefore, a concentration lower than 5.6 vol % is measured. Also the CO and the OGC concentration decrease at the end of the devolatilisation phase. During char combustion, the CO_2 and CO concentrations continuously decrease until the end of the experiment. For a validation of the test run, mass balances for C and the ashes have been calculated. For the fuel applied, a C content of 48 wt% dry basis (d.b.) has been determined, and under consideration of the moisture content of 8.2 wt % wet basis (w.b.) at the start of the experiment, an amount of 503.4 mg C can be calculated. For the calculation of the balance, the amounts of C released to the gas phase and C in the ashes has been considered. The amount of C in the gas phase has been

determined on the basis of the measured CO and CO_2 concentrations (gas analyzer) and the OGC (FID). Furthermore, the amount of C in the ash has been determined on the basis of analysis data of the total organic carbon (TOC) and the total inorganic carbon (TIC). For the test run described, a balance closure of 93% has been determined. A CO_2 free ash content of 2.5% d.b. has been determined for this fuel. For the calculation of the ash mass balance, the expected ash according to fuel analysis has been compared with the ash received after the experiment; for this test run, a balance closure of 88% has been determined. Only test runs that show reasonable C and ash balance closures in the range between 80 and 120% have further been evaluated. Experience has shown that possible ash losses mostly occur during ash sampling from the sample holder. To quantify these losses, the balance closure regarding refractory (nonvolatile) elements (e.g., Si, Ca, and Mg) has also been checked for each test run.

3.2. First ICP-MS Evaluations with Pure Salts. The coupling and dilution strategies were discussed in the previous sections. Next, salt solutions have been evaporated in the reactor, and the received signals of the ICP-MS have been interpreted. A 3 mg mass of pure salt (KCl) and 8–30 μg of $[NaCl, (NH_4)_2SO_4, ZnCl_2, \text{ and } PbCl_2]$ were applied in order to simulate the expected element release from a straw pellet and to simulate the gas concentrations of inorganic vapors occurring during such experiments. To handle these small amounts of salts, aqueous salt solutions of KCl, NaCl, $(NH_4)_2SO_4$, $ZnCl_2$, and $PbCl_2$ have been prepared. The salt solution is brought by a pipet to a 0.2 mm thin Inconel sheet that is placed on the original sample holder where the water evaporates and the salt remains. After the water is evaporated, the sample is introduced into the hot reactor; for these experiments, the protective tube and the N_2 cooling were not used. The tests were carried out at 850 °C under a carrier gas flow rate of 10 L/min of air, whereby the data recording of the ICP-MS starts already after the drying of the sample. An almost complete evaporation of the salts was observed for these tests.

In Figure 3, two examples for the measured counts are shown. For S, two clear peaks have been detected. Regarding

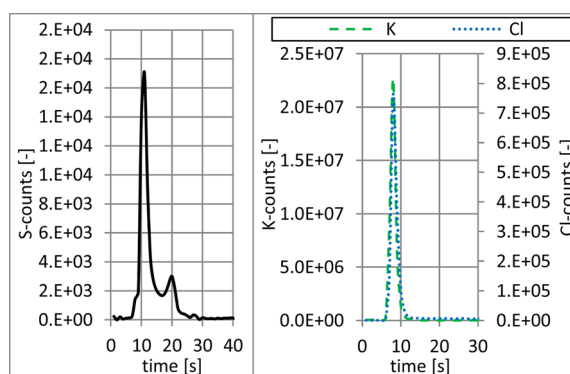


Figure 3. S counts for a test with $(NH_4)_2SO_4$ (left) and K and Cl counts for the salt test with KCl (right).

the K and Cl counts, a clear peak for each element can be detected. It can also be seen in the diagram that the peak maximum for Cl is 100 times smaller than that for K. This can be explained with differences in the ionizability of Cl in the Ar plasma. The ionizability for most metals in an ICP-MS, which operates under Ar, is lower than 90%. In comparison, ionization

rates of nonmetals of less than 50% are achieved. For Cl, ionization rates of only about 1% can be reached,¹⁷ which explains the low number of Cl counts compared to K counts. This already shows that the detection of Cl appears to be difficult with an ICP-MS.

Clear signals were detected for S, K, Na, Zn, and Pb. For Cl, only during the evaporation of KCl a clear signal was measured, whereby the amount of Cl during these tests is approximately equal to the amount of Cl that is expected to be released from a straw pellet. For the test with NaCl, ZnCl₂, and PbCl₂, no clear Cl signals were recognizable. During these tests, the Cl amounts were too low for a reasonable detection because the mass of salt at the start of the experiment was significantly lower compared to that in the tests with KCl.

3.3. Interpretation of the Measurement Signals of the ICP-MS, Time Synchronization, and Quantification. After the successful completion of test runs with salts, test runs with biomass fuels have been carried out. The interpretation and the quantification of the signals obtained during an experiment are discussed on the basis of a test run with a wheat straw pellet (chemical composition according to ref 7) regarding the signals for the isotope ³⁴S. The test run has been carried out at a reactor temperature of 850 °C and an O₂ content of 5.6 vol % at a carrier gas flow rate of 15 L/min.

A time-dependent signal (intensity/counts) for the given isotope (Figure 4 top) during the thermal decomposition process has been recorded with the ICP-MS. After 35 s, intensities for the ³⁴S isotope were recorded, and the main release for this isotope occurs between 40 and 100 s. It is obvious that the main release has been completed after 120 s and that further signal can be interpreted as noise. A signal will be interpreted as such when the intensity exceeds the blank value by at least threefold. Next, a time correction is carried out regarding the ICP-signals, the thermogravimetric data (mass loss and temperature profiles), and the gas analyzer data. For this purpose, the signal of the ¹³C isotope of the ICP-MS is compared with the calculated C signal on the basis of the CO, CO₂, and OGC measurements, and the recorded counts of ICP-MS for C were normalized accordingly. The response time determined has been used for the synchronization of all ICP-MS signals obtained. In Figure 4 (middle), the C signals based on the CO, CO₂, and OGC measurements and the normalized and synchronized C signals from the ICP-MS are displayed.

On the basis of fuel and ash analysis data, the element balances as well as the release rates of the elements considered can be determined. The time-dependent signal from the ICP-MS is normalized with a factor until the area under the curve corresponds to the released amount of S based on the element balance. Thereby, a quantification/calibration of the ICP-MS signal is possible (Figure 4 bottom). In Table 1, the closure of the ash and element balance (Si, Ca, and Mg) is presented. For both data sets, very good balance closures prevail, which is essential for the calculation of the release rates of volatile inorganic elements. For the presented test runs (three repetitions), 66.7% of S have been released to the gas phase on average. The mass of the pellet was 1.1 g d.b. with a S content of 913 mg/kg d.b. The mass of the ash was 51.3 mg d.b. with a S content of 6400 mg/kg d.b., resulting in a S release of 67.3% corresponding to a total S release of 677 μg. For Cl, K, Na, Zn, and Pb, the quantitation is based on the same principle.

3.4. In-Depth Validation of the S-Signals. For S and C, the ICP-MS data show rather similar trends. This may mean that the S release is coupled to the degradation of the organic

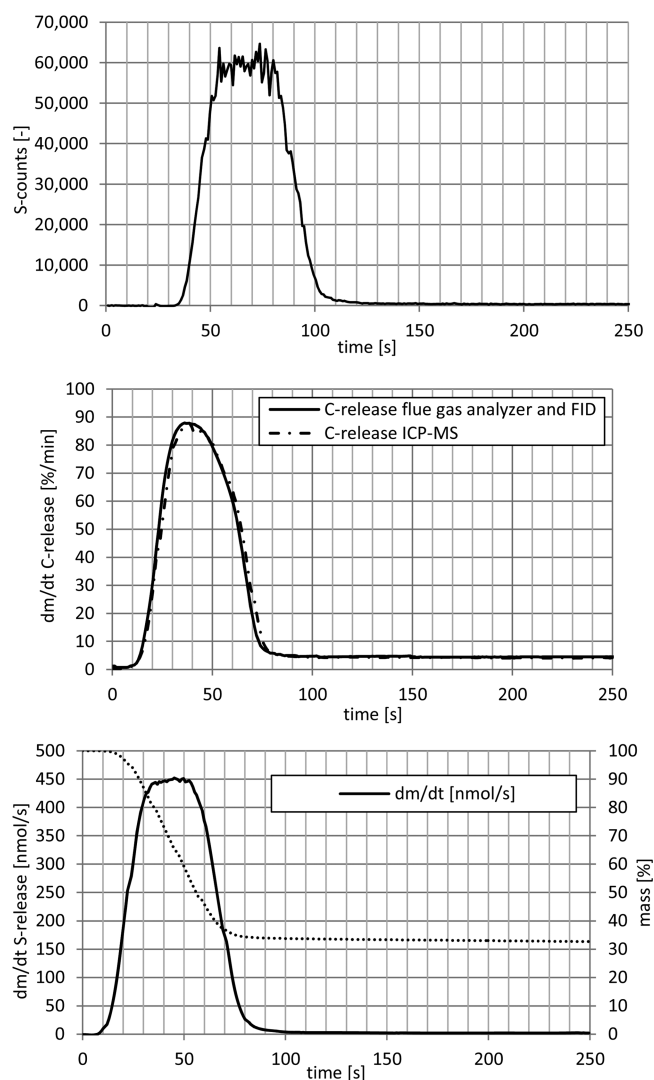


Figure 4. Quantification procedure for the ³⁴S isotope for wheat straw at 850 °C: time-dependent ICP-MS raw signal ³⁴S (top), comparison of C degradation data from the flue gas analysis and FID with the normalized signal of the ¹³C isotope from the ICP-MS (middle), and quantified S release for this test run (bottom).

Table 1. Ash and Element Balance Closures for Three Repetitions Performed with Wheat Straw

test run no.	ash balance closure (% d.b.) ^a	element balance closure (% d.b.)			
		Si	Ca	Mg	S
1	105.5	102.4	101.5	101.8	32.7
2	103.6	104.5	106.8	102.9	32.7
3	101.4	96.7	105.2	102.9	34.4

^ad.b., dry basis.

matrix, but it is also possible that this is an indifference of the ICP-MS. It is possible that the mass spectrometric separation of C and S is reaching its limit. An initial S release related to the degradation of organic sulfur compounds (proteins) has been proposed in literature.¹⁸ To verify if an indifference during ICP-MS measurements exists, experiments were carried out with straw pellets doped with (NH₄)₂SO₄.

The same wheat straw pellets used in ref 7 were used for these tests, which contained a S amount of about 1 mg. Using

an aqueous solution of 371 g/L $(\text{NH}_4)_2\text{SO}_4$, which was pipetted on the straw pellets, the S amount of the pellets was increased to 2 and 4 mg, respectively.

The test runs have been carried out at a reactor temperature of 850 °C, an O_2 content of 5.6 vol %, and a carrier gas flow rate of 15 L/min. For undoped straw pellets, two repetitions as well as three repetitions with two- and fourfold amounts of S have been carried out.

To characterize the combustion behavior, only a gas analyzer has been used. For the data of the flue gas analyzer, the temperature profiles, and the data of the mass loss curves, similar conditions for all experiments can be assumed. Regarding the ICP-MS signals, similar results have been obtained for the repetitions; therefore, only one test run for undoped straw and for the two- and fourfold amounts of S is displayed in the following discussion.

In Figure 5 (top), the counts for the ^{34}S and ^{13}C isotopes are displayed, whereby both signals show one plateau. For the S signal; after 70 s a drop to zero is obvious, whereas the C

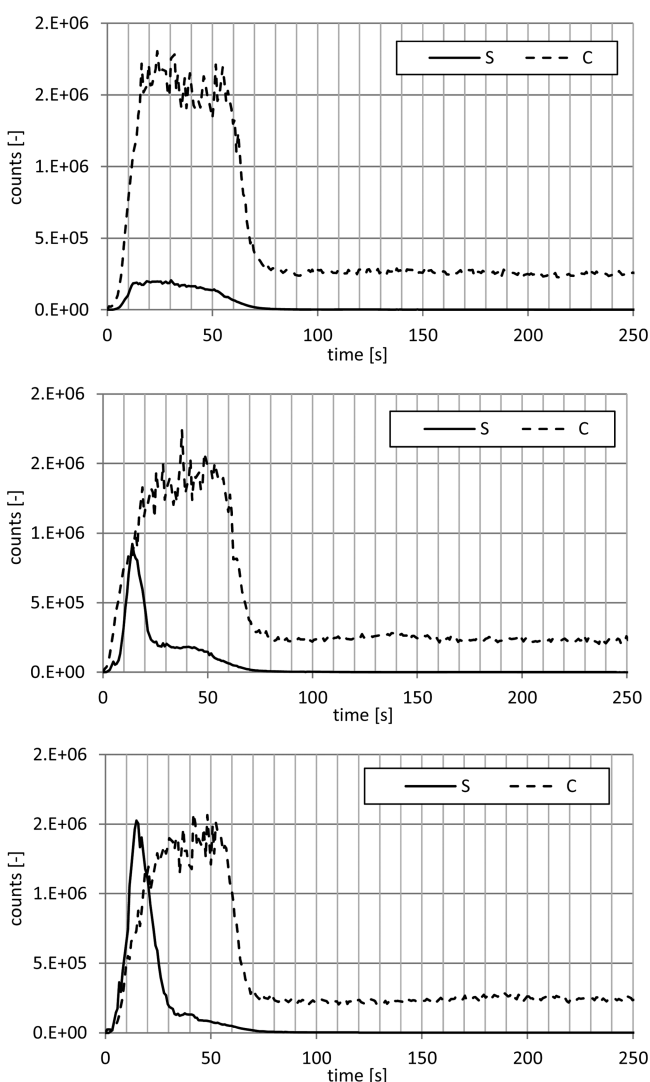


Figure 5. S and C counts recorded by ICP-MS for an undoped straw pellets (top), for a straw pellet with 2-fold S doping (middle), and for a straw pellet with fourfold S doping (doping with $[\text{NH}_4]_2\text{SO}_4$) (bottom).

release after 70 s is still ongoing. It can also be seen that the shape of the curve for the plateau of both signals is similar.

The counts of the ^{34}S and ^{13}C isotopes recorded via the ICP-MS for the doped straw pellets with two- and fourfold S amounts are displayed in Figure 5. From the results, it can clearly be seen that the trend of the curve for C is the same for doped and undoped pellets. Regarding the experiments with doped pellets, for the S signal a higher peak is clearly visible at the beginning of the main release. This higher peak corresponds to the evaporation of the $(\text{NH}_4)_2\text{SO}_4$ salt. After the evaporation of the salt is completed, the counts of the S signal reach about the same quantity which has been measured for undoped pellets. In the case of the fourfold S amount, the first S release peak is more distinct than that in the test run with twofold S amount. These experiments show that no indifferences between the S and C signals prevail and that the S signal can be interpreted as such. Furthermore, these experiments prove that the S release is coupled to the degradation of the organic matrix, which is derivable from the S and C signals of the ICP-MS.

3.5. Quench Tests with Miscanthus. In a quench test, the ongoing combustion reactions are abruptly stopped at a certain time. These tests have been used for a further validation of the ICP-MS signals obtained. When the experiment is stopped during the release of ash-forming elements, the signals immediately drop to 0 if care is taken that still-released flue gas (containing inorganic vapors) does not enter the sample line. This is realized by leading still-released flue gases and quench gases leaving the reactor into an exhaust pipe, thus avoiding their entering the sampling line to the ICP-MS. If condensation and deposit formation of ash-forming vapors occurs, then it is likely that this takes place in the section of the unheated sample line prior to the ionization in the ICP-MS (section 2.2). Condensates and deposits can be re-evaporated from the sample tube or the sample cone, which can cause intensities of ash-forming elements not resulting from the momentary release of inorganic vapors from the pellet, which seems likely for Cl.

The quench experiments were carried out with Miscanthus pellets (chemical composition given in ref 8) at a reactor temperature of 850 °C and an O_2 content of 5.6 vol % (carrier gas flow rate = 15 L/min). The point for quenching has been chosen to take place after the release of volatile compounds so that the quench time does not match with the maximum release of ash-forming elements. Quench times of 70 and 100 s after the start have been defined.

To start the experiment, the protective tube is removed, and the sample holder is exposed to the hot carrier gas. For quenching the sample, the protective tube must be moved back over the sample holder, and the N_2 purge gas is enabled for quenching the sample. At the same time as the activation of the N_2 purge gas, two valves are opened at the enclosure of the balance. This ensures that the sample is cooled and that the majority of the still-arising combustion gases are flowing toward the scale enclosure and subsequently the laboratory.

The sample was cooled after the N_2 purge gas activation for about 5 min, and the ICP-MS signals were recorded for the experiment as well as for the cooling period.

To compare the quenching experiments, test runs with unquenched Miscanthus pellets have also been carried out. Generally, the experiments have been carried out in triplicate, whereby similar results have been obtained; therefore, only one

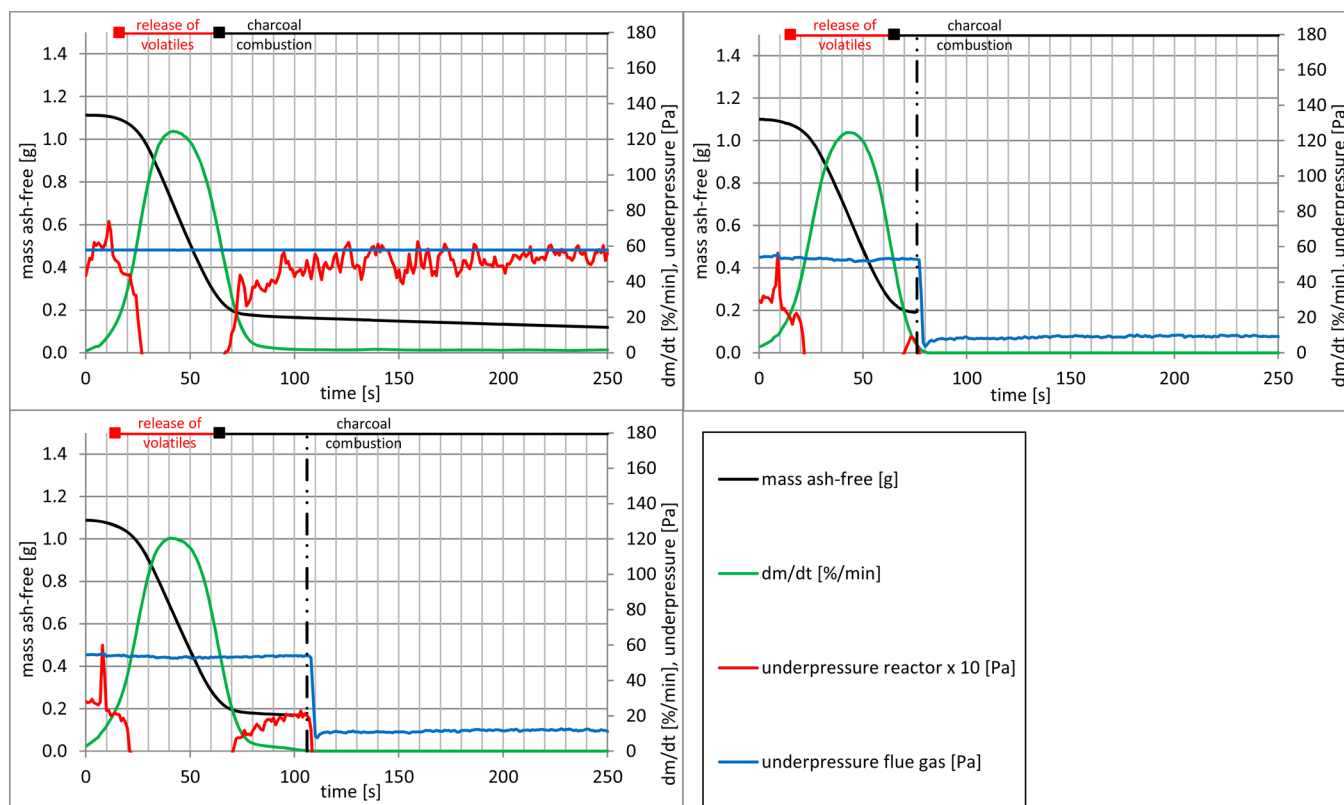


Figure 6. Gravimetric data and pressure trend for tests with Miscanthus at 850 °C: unquenched experiment (upper left) as well as those with quench times of 70 s (upper right) and 100 s (lower left). Explanation: The actual quench time is a few seconds higher than the planned quench times because it takes a few seconds to move the protective tube completely above the sample.

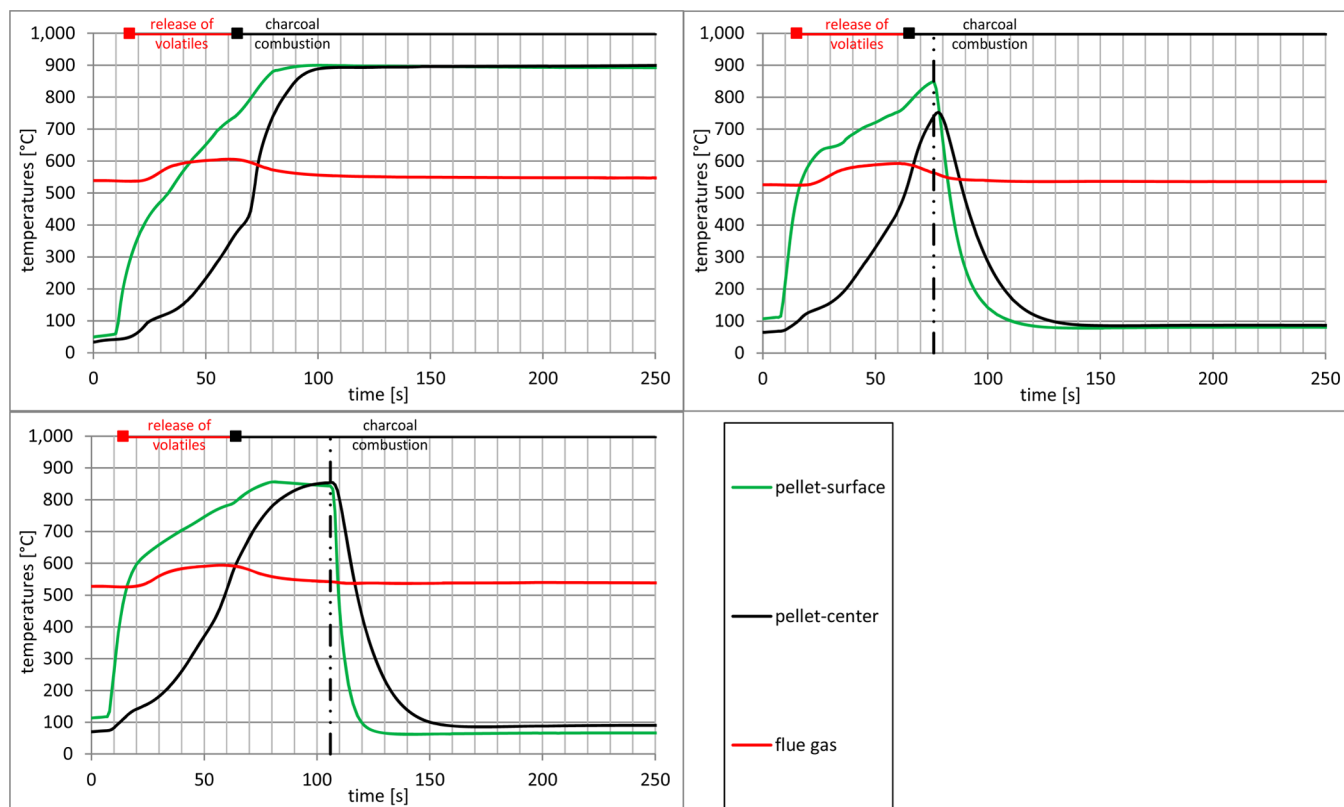


Figure 7. Temperature curves for tests with Miscanthus at 850 °C: unquenched experiment (upper left) as well as those with quench times of 70 s (upper right) and 100 s (lower left).

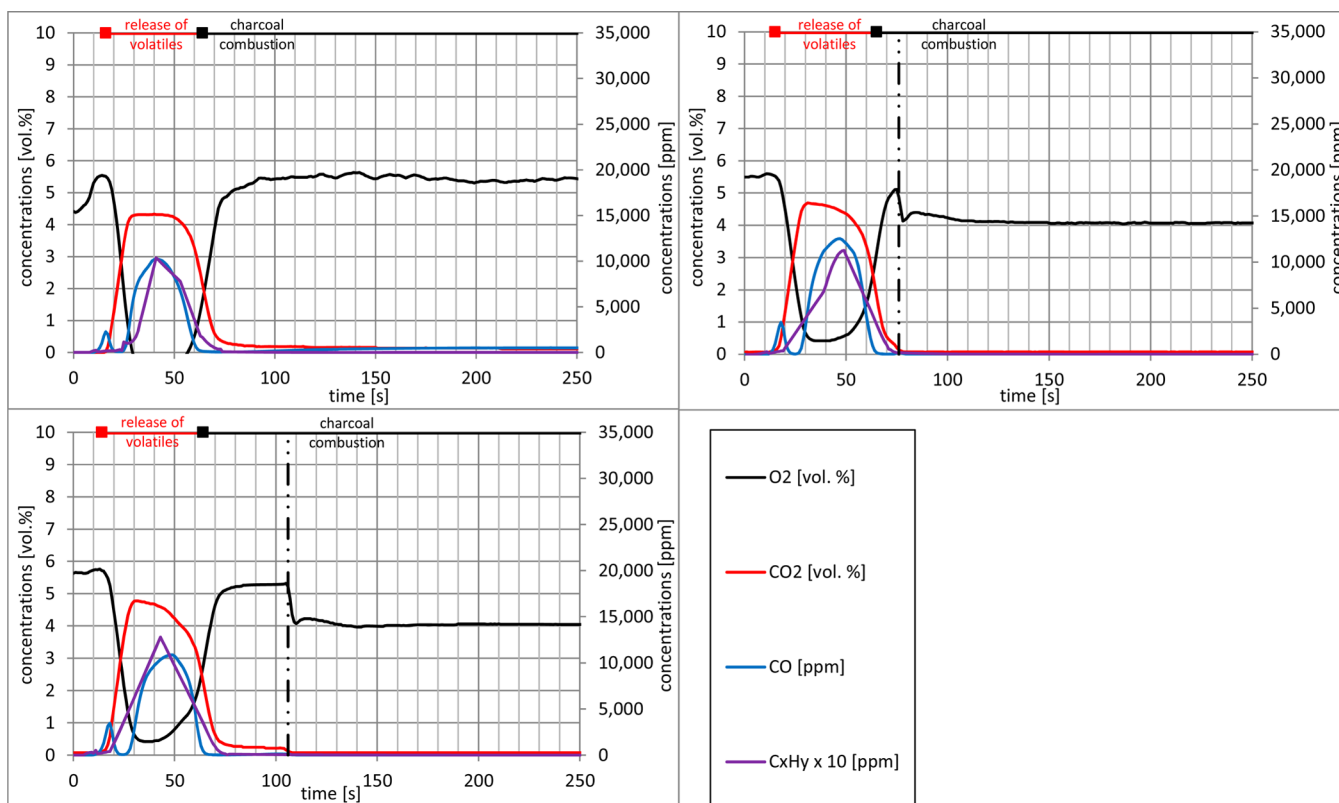


Figure 8. Flue gas compositions for tests with Miscanthus at 850 °C: unquenched experiment (upper left) as well as those with quench times of 70 s (upper right) and 100 s (lower left).

experiment is presented for the unquenched as well as for each quenched sample.

Figure 6 shows a comparison of gravimetric data and pressures for an unquenched experiment and quenching experiments after 70 and 100 s. The quench point is indicated by a dashed and dotted line. The mass loss after the quench is not displayed because the protective tube touches the sample holder; therefore, the mass loss cannot be determined during the quench. A clear pressure drop in the exhaust gas and the reactor after the quench can be seen. This is because the sample is flushed with N_2 , and the valves at the enclosure of the scale were opened.

Figure 7 shows the temperature profiles for an unquenched experiment and quenching experiments after 70 and 100 s. For the quenching experiments, a steep drop in temperature after quenching can be seen, where after 10 s the temperature in the center of the pellet is lower than 500 °C.

Figure 8 shows the flue gas compositions for an unquenched experiment and quenching experiments after 70 and 100 s. It can be seen that after the quench no CO_2 is measured and that a lower O_2 concentration than at the beginning of the experiment is reached. This is an indication that a small fraction of N_2 which is needed to quench the sample is sucked in the direction of the porous tube diluter. However, it can be assumed that the small amounts of flue gas entering the direction of the porous tube diluter after the quench do not affect the results of the quenching experiments because no concentrations of flue gas compounds are measured.

In Figures 9 – 11, signals from the ICP-MS for C, S, K, Na, Zn, Pb, and Cl for the quenching experiments (left, 70 s; right, 100 s) are shown in comparison to those of an unquenched experiment. The signals are time-corrected as described in

section 3.3 on the basis of the C signals of the ICP-MS as well as the data of the flue gas analyzer and FID. The comparison illustrates the influence of quenching for each recorded isotope.

In Figure 9, a clear drop of the C, S, K, and Na signals to 0 after the quench point can be observed. This is an indication for a proper dilution of the sample gas and for minimization of possible interactions (condensation and/or deposition of inorganic vapors as well as interactions on or close to the sample cone) prior to the ionization of the gas in the ICP-MS. For K and Na, the release for the unquenched experiments occurs in two stages. The main release takes place during devolatilisation, whereas the remaining K is released during char burnout.

Although Zn and Pb are trace elements in biomass fuels, usable signals on the ICP-MS can be obtained. For Zn and Pb (Figure 10), two release peaks were measured for the unquenched experiments. For the quench test after 100 s for Zn, the second peak of the release is not as strongly pronounced but is still present compared to that of the unquenched experiment.

The bimodal release behavior can be explained with the thermal history of the pellet as well as by consideration of a suggested release mechanism from literature. In refs 10 and 19, for fiber board combustion a mechanism similar to that for coal combustion has been proposed: The reduction of $ZnO_{(s)}$ in the reducing char environment of the particle causes a volatilization of $Zn_{(g)}$ at temperatures above 500 °C, which is also supported by TEC. The quantities of Si and Al in the fuel seem to be important for the partial retention of Zn in the ashes.¹⁹

The temperature development of the particle (Figure 7) indicates that the devolatilisation layer proceeds with the heat up of the particle toward the center. The temperature profile

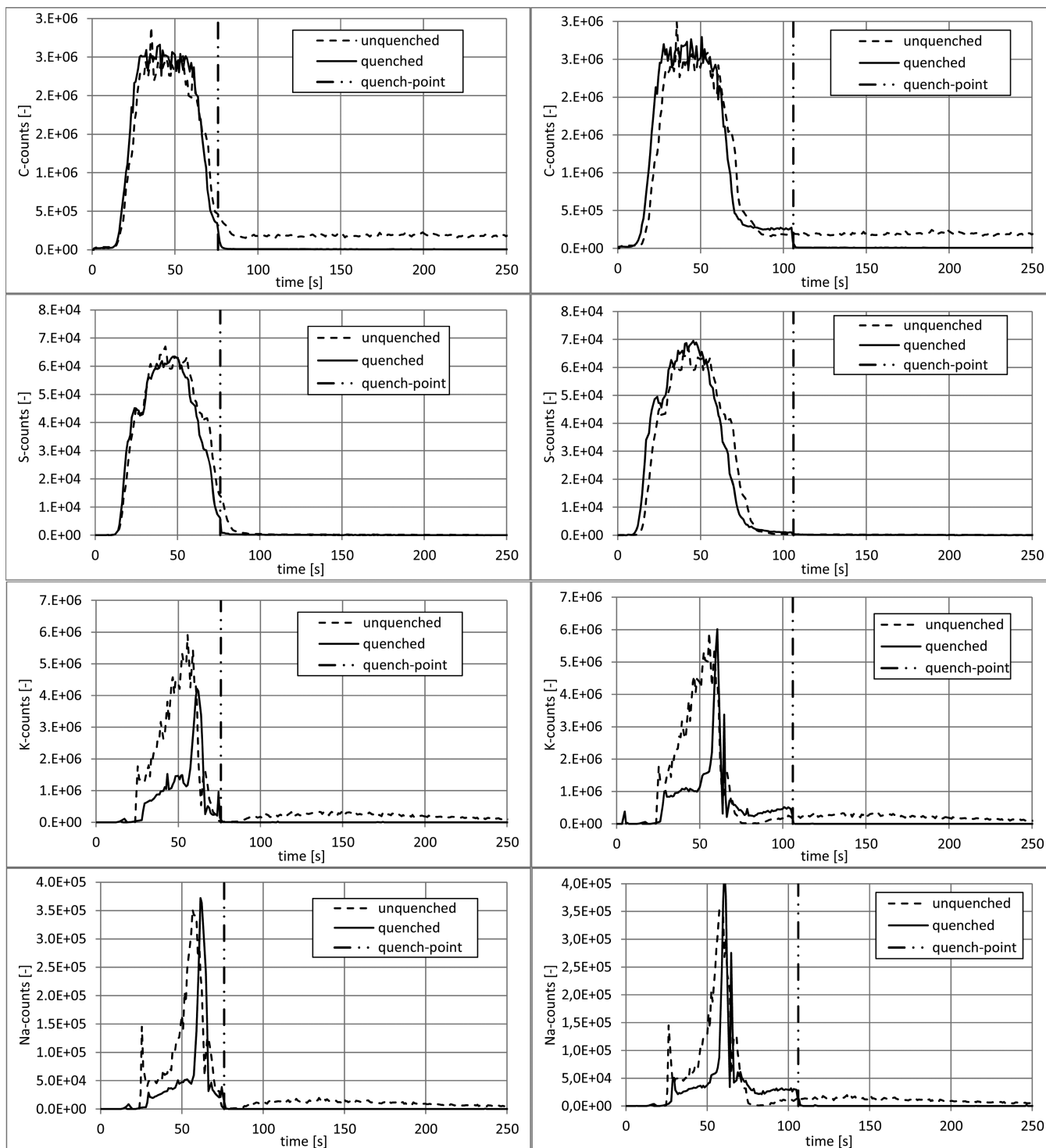


Figure 9. ICP-MS signals for (top to bottom, respectively) C, S, K, and Na of the quenching experiments 70 s (left) and 100 s (right) compared to those of an unquenched experiment for Miscanthus at 850 °C.

also indicates that in the outer layer charcoal combustion takes place at the same time when devolatilisation in the center starts which has to be considered regarding the release behavior. The Zn release starts when a surface temperature of about 500 °C is reached, and a distinct release takes place at surface temperatures of about 700 °C. This peak most likely originates from a $ZnO_{(s)}$ reduction to $Zn_{(g)}$ in near-surface regions of the particle, which seems to be not hindered by the char or ash matrix. The minimum between the two release peaks can be

caused by a possible capture of Zn compounds in the char or an embedding of Zn compounds in the ashes formed. Also, a possible occurrence of locally oxidizing conditions in the particle can cause a reduction of the Zn release. The second release peak occurs during char burnout at the particle center (center temperature around 900 °C). During this phase, Zn compounds most likely previously captured in the char or partly retained in the ashes are released to the gas phase. For Pb, only one clear peak can be seen for the quench experiments

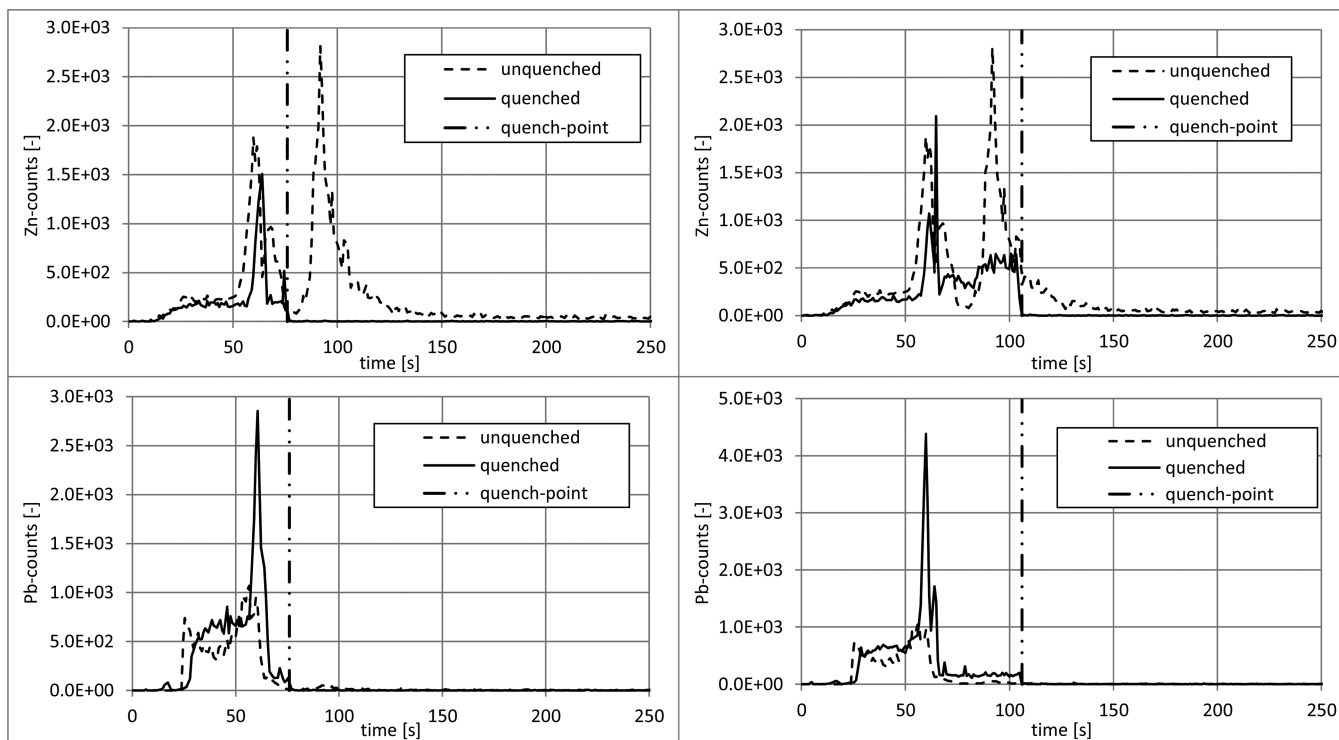


Figure 10. ICP-MS signals for Zn and Pb of the quenching experiments 70 s (left) and 100 s (right) compared to those of an unquenched experiment for Miscanthus at 850 °C.

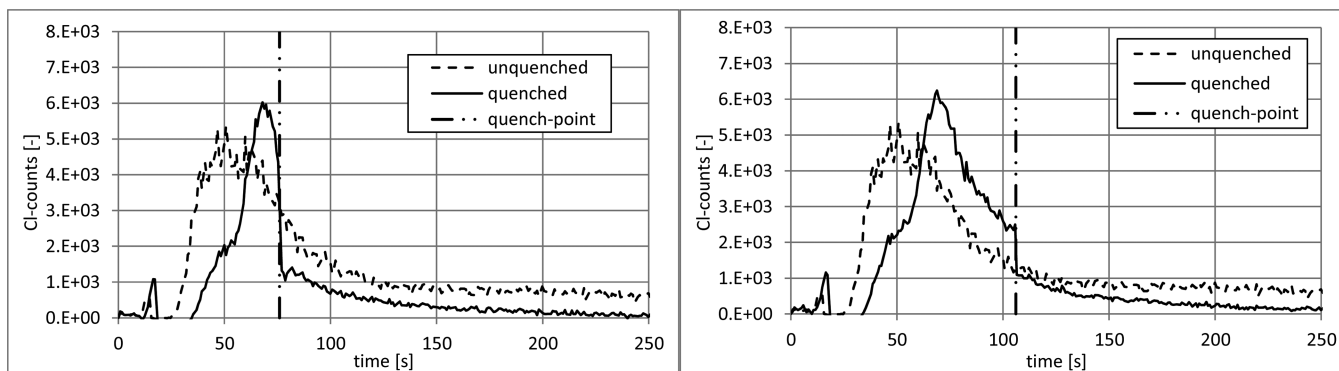


Figure 11. ICP-MS signals for Cl of the quenching experiments 70 s (left) and 100 s (right) compared to those of an unquenched experiment for Miscanthus at 850 °C.

compared to the data of the unquenched test run. Although these differences exist between unquenched and quenched experiments, it can clearly be seen that after the quench the release of Zn and Pb drops to zero. The drop of the ICP-MS signals after the quench for C, S, K, Na, Zn, and Pb indicates that the ICP-MS signals are not influenced by possible interactions of the gas prior the ionization in the ICP-MS. Therefore, the signals obtained can be interpreted as resulting from the release of inorganic compounds from the biomass pellet. For the signals obtained, the parts before the quench for the quenched and unquenched tests are slightly different. A good agreement of the start of the release and the occurrence of the maximum release exists for the unquenched and quenched experiments. A slight variation can be observed for K and Na regarding the release curves between the start and the maximum release. During this phase, different processes (pyrolysis, gasification, and char combustion) occur in parallel, which can also influence the release of inorganic compounds.

Furthermore, the temperature development of the particle for the unquenched and quenched experiment is slightly different (Figure 7), which also influences the release profiles.

Regarding Cl (Figure 11), it can be seen from the unquenched experiment that the main release takes place during the release of volatile compounds. In contrast to K (Figure 9), only a continuous decrease of the signal with ongoing test duration is determined. This long-tailing may originate from a Cl release of the pellet but also can result from deposition and release processes in the ICP-MS prior to the ionization of the gas. On the basis of the Cl signals of the quenching experiments, a drop of the Cl signals after the quench occurs, whereas after the drop, a continuously tailing Cl signal has been measured. Thus, deposition and release processes (interactions) of Cl compounds, most likely located in the unheated zone (between the entrance of the ICP-MS and the sample cone), cause this behavior. Ref reports that chlorine is released as $\text{CH}_3\text{Cl}_{(g)}$ in a temperature range of 250–350 °C

during torrefaction of wood and straw. A condensation of this component in the sample line prior to the ionization in the ICP-MS can be excluded because of the low boiling point ($-23.8\text{ }^{\circ}\text{C}$ at 101 300 Pa) as well as the high dilution (dilution ratio = 1:150) of the sample gas. However, interactions of Cl compounds can possibly also occur at the sample cone as a result of possible deposition and re-evaporation processes that cannot be avoided. However, this unexplainable behavior of the Cl signals means that only strong changes of the Cl signals may be qualitatively evaluated, whereas continuously decreasing Cl signals most likely result from interactions in the ICP-MS. It also has to be noted that the probability of ionization of Cl in an ICP-MS is about 1%.¹⁷ The low ionizability and possible interactions of Cl compounds indicate that the Cl signal can only be evaluated with restrictions.

The quench tests also have proven that the time synchronization regarding the recorded data works well which can directly be seen because the quench point occurs at the same time for the gravimetric data the temperature profiles, the measured flue gas compounds, and the ICP-MS data.

4. SUMMARY AND CONCLUSIONS

The general interest in experimental data regarding the decomposition and release behavior of biomass fuels for modeling and simulation purposes is continuously increasing. On the basis of combustion experiments with lab-scale reactors and single-particle reactors, integral release data regarding ash-forming vapors can be obtained. At the moment, almost no data regarding time-resolved release of ash-forming elements from single particles exists. Therefore, in this study the coupling between a new single-particle reactor with an ICP-MS is presented. On the basis of this setup, the online determination of the release of ash-forming elements is possible, and a characterization of the combustion process as well as of the formed flue gases based on measured thermogravimetric data can be carried out. The temperatures at the surface and the center of the particle, the weight loss of the particle, the pressures, and the formed flue gases have been recorded during the experiments. To couple the reactor to an ICP-MS, a part of the flue gas stream has to be delivered to the ICP-MS, whereby this gas stream needs to be sufficiently diluted with Ar to ensure that the gas as well as the containing molecules can be ionized in the Ar plasma. The ionized isotopes are subsequently detected in a mass spectrometer where intensities or counts are recorded for the respective isotope. To check if vapors that have been released in the reactor are received in the ICP-MS, tests with pure salts [KCl, NaCl, $(\text{NH}_4)_2\text{SO}_4$, ZnCl_2 , and PbCl_2] have been carried out. These tests have shown that intensities for S, K, Cl, Zn, and Pb can be measured with the system. During the validation of the signals, it was also shown that the S release is coupled with the degradation of the organic matrix. For further validation of the system, quench tests with *Miscanthus* pellets have been carried out. Here the combustion process has been stopped after the devolatilisation phase. It has been ensured that the sample is cooled and that the still-released flue gas species are not entering the sampling line passing to the ICP-MS. The isotopes ^{13}C , ^{34}S , ^{23}Na , ^{35}Cl , ^{39}K , ^{66}Zn , and ^{208}Pb were recorded during these tests. It has been shown that after the quench the signals for ^{13}C , ^{34}S , ^{23}Na , ^{39}K , ^{66}Zn , and ^{208}Pb abruptly drop to zero. This indicates that the carried out dilution of the sample gas minimizes interactions of inorganic vapors (possible condensation and or deposition and

later re-evaporation) for C, S, Na, K, Zn, and Pb. Regarding Cl, interactions of Cl compounds have been observed; thus, the interpretation of Cl signals is only possible with restrictions.

On the basis of element balances, the release of ash-forming elements over the whole combustion experiments can be calculated. These release data can be used for a quantification/calibration of the measured intensities of S, K, Na, Zn, and Pb. The system presented can be used for quick and targeted experiments in a temperature range of 250–1000 $^{\circ}\text{C}$ under inert, reducing, and oxidizing conditions. Furthermore, the time-resolved release data provide a deeper insight in ash transformation and release processes. For the case study of *Miscanthus*, a short discussion has been provided regarding Zn release, and a more detailed description of possible release processes for all ash-forming elements analyzed will be provided in the second part of the paper.

5. OUTLOOK

Experiments with different biomass fuels have been carried out under oxidizing conditions (5.6 vol % O_2) at temperatures of 700, 850, and 1000 $^{\circ}\text{C}$. For these experiments, the setup presented has been used. The most relevant findings of these experiments and a discussion of the results will be provided in part 2 of this paper. Furthermore, a review of relevant release processes that are essential for the understanding of the release data will be provided.

■ AUTHOR INFORMATION

Corresponding Author

*Telephone: + 43 (0) 316 873-9237. Fax: + 43 (0) 316 873-9202. E-mail: peter.sommersacher@bioenergy2020.eu.

Notes

The authors declare no competing financial interest.

■ ACKNOWLEDGMENTS

This article is the result of a project carried out within the framework of the Austrian COMET program, which is funded by the Republic of Austria as well as the federal provinces of Styria, Lower Austria, and Burgenland. The work was also funded by the companies Andritz AG, Josef Bertsch GmbH & Co. KG, BIOS BIOENERGIESYSTEME GmbH, HET Heiz und Energietechnik Entwicklung GmbH, KWB Kraft und Wärme aus Biomasse GmbH, Viessmann Holzfeuerungsanlagen GmbH, Standardkessel GmbH, and TIWAG Tiroler Wasserkraft AG.

■ REFERENCES

- (1) Branca, C.; Albano, A.; Di Blasi, C. Critical evaluation of global mechanisms of wood devolatilisation. *Thermochim. Acta* **2005**, *429*, 133–141.
- (2) Manyà, J.; Velo, E.; Puigjaner, L. Kinetics of Biomass Pyrolysis: a Reformulated Three-Parallel-Reactions Model. *Ind. Eng. Chem. Res.* **2003**, *42* (3), 434–441.
- (3) Anca-Couce, A.; Berger, A.; Zobel, N. How to determine consistent biomass pyrolysis kinetics in a parallel reaction scheme. *Fuel* **2014**, *123*, 230–240.
- (4) Saddawi, A.; Jones, J. M.; Williams, A.; Wojtowicz, M. A. Kinetics of the Thermal Decomposition of Biomass. *Energy Fuels* **2010**, *24*, 1274–1282.
- (5) Brown, A. L.; Dayton, D. C.; Daily, J. W. A Study of Cellulose Pyrolysis Chemistry and Global Kinetics at High Heating Rates. *Energy Fuels* **2001**, *15*, 1286–1294.

- (6) Brunner, T.; Biedermann, F.; Kanzian, W.; Evic, N.; Obernberger, I. Advanced biomass fuel characterization based on tests with a specially designed lab-reactor. *Energy Fuels* **2013**, *27* (10), 5691–5698.
- (7) Sommersacher, P.; Brunner, T.; Obernberger, I.; Kienzl, N.; Kanzian, W. Application of novel and advanced fuel characterization tools for the combustion related characterization of different wood/Kaolin and straw/Kaolin mixtures. *Energy Fuels* **2013**, *27* (9), 5192–5206.
- (8) Sommersacher, P.; Brunner, T.; Obernberger, I.; Kienzl, N.; Kanzian, W. Combustion related characterisation of Miscanthus peat blends applying novel fuel characterisation tools. *Fuel* **2015**, *158*, 253–262.
- (9) Knudsen, J.; Jensen, P.; Dam-Johansen, K. Transformation and Release to the Gas Phase of Cl, K, and S during Combustion of Annual Biomass. *Energy Fuels* **2004**, *18*, 1385–1399.
- (10) Van Lith, S.; Alonso-Ramirez, V.; Jensen, P.; Frandsen, F.; Glarborg, P. Release to the Gas Phase of Inorganic Elements during Wood Combustion. Part 1: Development and Evaluation of Quantification Methods. *Energy Fuels* **2006**, *20*, 964–978.
- (11) Fagerström, J.; Granholm, M.; Gardbro, G.; Steinvall, E.; Boström, D.; Boman, C. Potassium release in a single pellet macro-TGA using wood and straw. In *Proceedings: Impacts of Fuel Quality on Power Production and Environment*, September 23–27, 2012, Puchberg, Austria; EPRI: Palo Alto, CA, 2012.
- (12) Sommersacher, P.; Brunner, T.; Obernberger, I. Fuel indexes – a novel method for the evaluation of relevant combustion properties of new biomass fuels. In *Proceedings: Impacts of Fuel Quality on Power Production and Environment*, September 23–27, 2012, Puchberg, Austria; EPRI: Palo Alto, CA, 2012.
- (13) Qu, Z.; Fagerström, J.; Steinvall, E.; Broström, M.; Boman, C.; Schmidt, F. Real-time in-situ detection of potassium release during combustion of pelletized biomass using tunable diode laser absorption spectroscopy. In *Proceedings: Impacts of Fuel Quality on Power Production and Environment*, October 26–31, 2014, Snowbird, UT; EPRI: Palo Alto, CA, 2014.
- (14) Sorvajärvi, T.; DeMartini, N.; Rossi, J.; Toivonen, J. In situ measurement technique for simultaneous detection of K, KCl, and KOH vapors released during combustion of solid biomass fuels in a single particle reactor. *Appl. Spectrosc.* **2014**, *68*, 179–184.
- (15) Sorvajärvi, T.; Advanced Optical Diagnostic Techniques for Detection of Alkali Vapors in High-Temperature Gases. Ph.D. Thesis, Tampere University of Technology, Finland, 2013.
- (16) Skoog, D. A., Holler, F. J., Crouch, S. R. *Principles of Instrumental Analysis*; Thomson Brooks/Cole: Belmont, CA, 2007.
- (17) Monatser, A. *Inductively coupled plasma mass spectrometry*. Wiley-VCH: New York, 1998; p 811.
- (18) Knudsen, N. J.; Jensen, A. P.; Lin, W.; Frandsen, J. F.; Dam-Johansen, K. Sulfur Transformations during Thermal Conversion of Herbaceous Biomass. *Energy Fuels* **2004**, *18*, 810–819.
- (19) Van Lith, S. C. Release of Inorganic Elements during Wood-Firing on a Grate. Ph.D. Thesis, Technical University of Denmark, Lyngby, Denmark, 2005.
- (20) Saleh, S. B.; Flensburg, J. P.; Shoulaifar, T. K.; Sárossy, Z.; Hansen, B. B.; Egsgaard, H.; DeMartini, N.; Jensen, P. A.; Glarborg, P.; Dam-Johansen, K. Release of Chlorine and Sulfur during Biomass Torrefaction and Pyrolysis. *Energy Fuels* **2014**, *28* (6), 3738–3746.

Paper V

Simultaneous Online Determination of S, Cl, K, Na, Zn, and Pb Release from a Single Particle during Biomass Combustion. Part 2: Results from Test Runs with Spruce and Straw Pellets

Peter Sommersacher,^{*,†} Norbert Kienzl,[†] Thomas Brunner,[§] and Ingwald Obernberger^{‡,§}

[†]BIOENERGY 2020+ GmbH, Inffeldgasse 21b, A-8010 Graz, Austria

[‡]Institute for Process and Particle Engineering, Graz University of Technology, Inffeldgasse 13, A-8010 Graz, Austria

[§]BIOS BIOENERGIESYSTEME GmbH, Hedwig-Katschinka-Straße 4, A-8020 Graz, Austria

ABSTRACT: To gain better insight into inorganic element release processes, test runs with a specially designed single particle reactor connected with an inductively coupled plasma mass spectrometer (ICP-MS) have been performed. Relevant combustion related parameters such as mass loss during thermal degradation, temperature development of the particle (surface and center), and composition of released gases were recorded. By coupling the reactor to an ICP-MS, time-resolved release profiles of relevant aerosol forming elements (S, Cl, K, Na, Zn, and Pb) were determined. Targeted and controlled interruptions of the experiments (quenching) after a certain time were performed to validate reactor performance and reliability of the measurements. Test runs with softwood and straw pellets (8 mm in diameter and about 20 mm in length) were performed at reactor temperatures of 700, 850, and 1000 °C under oxidizing conditions (5.6 or 4.2 vol % O₂). These test runs have revealed that the release ratios of volatile and semivolatile ash forming elements (S, Cl, K, Na, Zn, and Pb) generally increase as reactor temperatures rise. Moreover, regarding straw, higher Si and Al contents influence the release behavior of K, Na, Zn, and Pb. For K, existing release mechanisms proposed in the literature have been confirmed, and for Na it has been suggested that release mechanisms similar to K prevail. Especially during the starting phase of the experiment, a distinct temperature gradient exists from the surface to the center of the particle. Thus, different conversion phases occur in parallel in different layers of the particle, which has to be considered during the interpretation of the time-resolved release profiles of the main inorganic elements. Furthermore, transport limitations due to the occurrence of molten phases (especially for straw at reactor temperatures of 1000 °C) were obvious and could be directly derived from the online recorded release profiles. The targeted interruption of the ongoing decomposition process (quenching) provided an indication of the validity of the release profiles for S, K, Na, Zn, and Pb. Additionally, these experiments delivered valuable information regarding possible release mechanisms.

1. INTRODUCTION AND OBJECTIVES

During thermal biomass conversion, volatile and semivolatile ash forming elements are partly released from the fuel to the gas phase. Reactions of these released ash forming elements lead to fine particle and deposit formation causing operational problems (fouling, slagging, etc.) which reduce the efficiency of the combustion system.^{1,2} For this reason, it is necessary to investigate inorganic element release behavior, especially of S, Cl, K, Na, Zn, and Pb. Previous related studies focused on the calculation of mass and element balances based on lab-scale batch combustion experiments.^{1,3–5}

However, not much online release data exist for inorganic elements, which are urgently needed for release model development. Therefore, in part 1 of this series,⁶ a setup was presented for the online determination of the inorganic element release from a single biomass particle. This single particle reactor, which is basically a macro TGA, operates at high sample heating rates, and a sample mass of about 1000 mg can be applied. The system works under reactor temperatures of up to 1000 °C, which are reached in the center of a single pellet in less than 1 min. The main gas species (CO, CO₂, and O₂) are determined downstream of the reactor. Moreover, the reactor is connected to an inductively plasma mass spectrometer (ICP-MS), enabling the online determination of inorganic com-

pounds (S, Cl, K, Na, Zn, and Pb) contained in the exhaust gas. Summing up, this setup provides thermogravimetric data, the main compound release as well as time-resolved release data of inorganic compounds.

The online release data of inorganic elements gained from this setup can be used as the basis for release model development. At the moment, there are models available for the description of the thermal decomposition behavior of single biomass particles.^{7,8} They have also been implemented in computational fluid dynamics (CFD) simulations.⁹ Combining these models with release models for inorganic elements would also make it possible to simulate subsequent processes such as particle and deposit formation more precisely.

The online release data of inorganic elements can also lead to an improved understanding of ongoing chemical reaction and release processes. For this reason, relevant release processes for the understanding of the results presented in this study are briefly summarized in the following.

1.1. Release Mechanism Regarding Relevant Inorganic Ash Forming Elements. (a). S Release. About 75% of

Received: November 24, 2015

Revised: March 9, 2016

the S contained in biomass fuels is organically bound in proteins.¹⁰ Therefore, the major part of the S-release occurs during the devolatilization of the organic matrix. Remaining inorganic bound S is retained in the ash or released at temperatures >900 °C.^{11–13}

(b). *Cl Release.* In ref 14 it has been shown that Cl is mainly released as $\text{CH}_3\text{Cl}(\text{g})$ during pyrolysis at temperatures up to 350 °C. This means that, for low-Cl wood fuels, almost 100% of the Cl is released, and, as Cl content increases, the release ratios decrease (e.g., straw 64%). Cl released at low temperatures (<700 °C) may partially be recaptured in the char by secondary reactions with available metals and forms, e.g., KCl. At temperatures above 700–800 °C, Cl is then released via KCl(s) sublimation.

(c). *K and Na Release.* K release at low temperatures (300 to 500 °C) can be explained by the release of alkaline carboxylates and phenol-associated K.¹² At 700–800 °C KCl(s) sublimation takes place. For temperatures above 800 °C, $\text{K}_2\text{CO}_3(\text{s})$ decomposition is supposed to occur and K(g) is released.¹² Depending on the availability of water vapor and HCl, KOH(g) or KCl(g) is formed. Na, which is of minor relevance for most biomass fuels, is supposed to show a release behavior comparable with K.

(iv). *Zn and Pb Release.* In the reducing environment of the char particles, Zn starts to volatilize above 500 °C^{5,11} or reacts with Si and Al.¹² Pb release also starts at around 500 °C and a mechanism similar to that of Zn has been suggested. Under the assumption that Pb is most likely present as carbonate, hydroxide, or oxide, a reducing atmosphere is needed to transform these species into volatile Pb species like Pb(g). Furthermore, interactions with solid TiO_2 , Al_2O_3 , and SiO_2 or a combination of these oxides in a temperature range of 700–1000 °C can cause a reduced Pb release to the gas phase.¹²

1.2. Objective of the Work Presented. The aim of this work is to investigate if the time-resolved release data for inorganic elements gained from single particle reactor tests can support the release mechanism proposed in the literature. A second aim is to reveal transport limited release processes by means of the experiments conducted. Furthermore, the time dependent release profiles should be validated by additional quench experiments. These experiments should also provide further insights regarding ongoing release processes.

2. EXPERIMENTAL SECTION

2.1. Single Particle Reactor. In part 1⁶ of this series, a new lab-scale reactor with ICP-MS coupling especially designed to investigate the S, Cl, K, Na, Zn, and Pb release of single biomass particles was presented.

The simplified diagram in Figure 1 shows the main parts of the reactor. The core element of the reactor is an Alsint tube (composed of 99.7% Al_2O_3) with a diameter of 50 mm, which is placed in an electrically heated oven. The tube is equipped with four lateral access boards, two for optical access and two for sample handling. Through one of the latter a sample holder is introduced which is connected to a balance (Mettler Toledo XS105DU).

A single biomass pellet or chip (sample mass 300–1200 mg) is placed on the sample holder and introduced into a protective tube mounted inside the preheated reactor tube (target temperatures up to 1000 °C are possible). Then the system is sealed and a reaction agent (N_2 /air mixtures) is injected from the bottom of the reactor tube. The protective tube is removed and the sample is exposed to the defined atmosphere and starts to decompose. The evolving gases are diluted with Ar in a porous tube diluter (heated to 500 °C, dilution ratio 1:3) placed at the reactor exit. Side streams are extracted from diluted gas and forwarded to online gas analyzers. Another side stream is

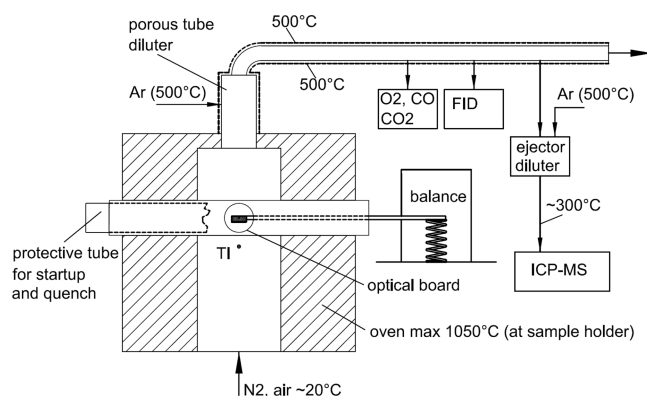


Figure 1. Simplified diagram of the single particle reactor including measurement setup. Explanation: FID, flame ionization detector; TI, thermocouple for temperature control; ICP-MS, inductively plasma mass spectrometer.

extracted, further diluted with Ar in an ejector diluter (dilution ratio 1:10), an additional dilution is realized prior to the entrance of the ICP-MS (dilution ratio 1:5) and supplied to an ICP-MS. The dilution steps are applied to avoid condensation of ash forming vapors in the sample lines and to keep the gas composition within the detection ranges of the analyzers applied.

Extensive measurement equipment is applied to control and monitor the whole process. The most relevant parameters and devices are briefly summarized. The mass loss of the sample is determined with a microbalance. The center and surface temperatures at the particle are determined with Type N thermocouples (NiCrSi-NiSiMg). The O_2 and CO and CO_2 concentration is detected with a gas analyzer (Rosemount NGA 2000) which uses paramagnetism as the measurement principle for O_2 and nondispersive infrared spectroscopy for CO and CO_2 detection. C in organic gaseous hydrocarbons (OGC) is determined with a flame ionization detector FID (ErsaTec Smart FID). An ICP-MS from Agilent Technologies series 7700x is used for the online determination of relevant inorganic elements (S, Cl, K, Na, Zn, and Pb). The gas streams entering the reactor or dilution system are controlled using mass flow controllers (Sierra Smart Trak 2, Series 100).

Data gained from the fuel and ash residues analysis are used to calculate the overall release of inorganic elements to the gas phase during one experiment.

2.2. Fuel and Ash Analysis. The fuel and ash analysis methods applied have already been described in ref 15–17. Sample preparation was carried out according to EN 14780, and the moisture content of biomass fuels was determined according to EN 14774-1. EN 15104 was used for C, H, and N contents, and EN 15289 was used for Cl contents. The ash content (loss of ignition at 550 °C) was determined according to EN 14775, and the TIC (total inorganic carbon) content of the ashed fuel was analyzed to calculate a carbonate free (only oxide based) ash content. The content of volatile matter was determined according to EN 15148, and the fixed carbon content was obtained by difference from the results of volatiles and the carbonate free ash content. The concentrations of major and minor elements as well as of S in the fuel and ash samples were determined by multistep pressurized digestion of the samples, followed by detection applying inductively coupled plasma-optical emission spectroscopy (ICP-OES) (Arcos, Spectro) or ICP-MS (Agilent 7700x), depending on the element contents and detection limits. Additionally, the samples of the residues (ashes) were analyzed regarding total organic carbon (TOC) and total inorganic carbon (TIC). The ash melting behavior was determined according to CEN/TS 15370-1. The determination of particle density was carried out according to EN 15150.

2.3. Evaluation of Single Particle Reactor Test Runs. The evaluation strategy is described in this section to aid understanding of the discussion of the test run results.

Table 1. Chemical Composition of the Spruce and Wheat Straw Utilized in Comparison with Database Values^a

		softwood (spruce)					straw (wheat)			
		this study		database			this study	database		
		batch A	batch B	average	std. dev.	number		average	std. dev.	number
m.c.	wt % w.b.	8.8	7.7				13.5			
a.c. 550 °C	wt % d.b.	0.40	0.34	0.33	0.03	39	4.5	6.6	1.5	19
a.c. corr.	wt % d.b.	0.35	0.26	n.a.			4.2	n.a.		
v.m.	wt % d.b.	85.0	84.8	n.a.			78.1	n.a.		
f.c.	wt % d.b.	14.7	14.9	n.a.			17.7	n.a.		
C	wt % d.b.	50.2	49.8	50.2	0.8	24	46.6	44.9	2.7	15
H	wt % d.b.	6.2	6.3	6.3	0.34	24	6.0	5.6	0.36	15
N	wt % d.b.	0.05	0.07	0.08	0.03	27	0.40	0.6	0.16	15
S	mg/kg d.b.	72.0	67.9	53.6	2.4	36	913	1,485	527	19
Cl	mg/kg d.b.	59.0	36.0	37.6	11.6	38	2,300	3,046	1,859	19
Ca	mg/kg d.b.	751	927	907	123.4	39	3,010	3,785	1,614	19
Si	mg/kg d.b.	420.0	93.8	158.7	2.4	33	11,100	17,618	4,917	19
Mg	mg/kg d.b.	140.0	130.0	120.9	8.8	39	688	945	662	19
K	mg/kg d.b.	564	412.0	382.7	25.9	39	6,970	6,629	4,149	19
Na	mg/kg d.b.	21.7	18.2	10.9	4.7	39	201.0	282.9	228.0	19
P	mg/kg d.b.	43.9	41.2	n.a.			385.0	442.0	148.2	19
Al	mg/kg d.b.	34.2	19.4	n.a.			217.0	237.9	244.9	18
Zn	mg/kg d.b.	12.7	11.4	11.1	0.7	35	6.6	9.9	3.4	6
Pb	mg/kg d.b.	0.21	0.21	n.a.			0.23	0.32	0.20	6
characteristic ash melting temperatures °C (CEN/TS 15370-1)										
shrinkage starting		1,220	n.a.	n.a.			780	n.a.		
deformation		n.o.	n.a.	n.a.			1,010	n.a.		
hemisphere		1,320	n.a.	n.a.			1,070	n.a.		
flow		1,340	n.a.	n.a.			1,130	n.a.		

^aExplanations: m.c., moisture content; a.c. 550°C, ash content determined at 550°C under oxidizing conditions; a.c. corr., ash content carbonate corrected; v.m., volatile matter; f.c., fixed carbon; w.b., wet basis; d.b., dry basis; number, number of analysis considered in the database; n.a., no data available; n.o., not occurred.

For the evaluation of a test run, the data gained from the balance, the temperatures at sample surface and center, the data gained from the gas analyzers and the ICP-MS, as well as the results of the fuel and ash analysis are considered.

At first, all signals recorded are time synchronized. Then, a validity check is performed, whereby mass and element balances are calculated. Regarding the C balance, the C introduced with the fuel, the C content of the ash, as well as the measurements of C containing species CO, CO₂, and OGC are considered. The ash balance is calculated from the carbonate free ash content of the fuel and the carbonate free mass of the residual ash. Only test runs which show reasonable C and ash balance closures between 80 and 120% are further evaluated, and experiments outside of this range are rejected. A total of 5% of the test runs performed were out of this range and needed to be repeated.

In a next step, characteristic data describing the thermal fuel decomposition are evaluated. These data include the duration of the experiment, the mass of the sample and of the ash residues, the cumulative mass loss curve, the first derivation of the cumulative mass loss curve over time (dm/dt), and the temperature evolution at sample surface and center. Then, on the basis of the trends of the main flue gas species contents, the experiment is divided into a devolatilization and a char combustion phase (the defined criteria are described in detail in section 3.1), and the durations and mass losses related to these phases are determined. Finally, the data gained from the chemical analyses of the ashes are evaluated, and the release of inorganic elements for the entire combustion experiment is calculated. These release ratios are used for a quantification or calibration of the online release profiles gained from the ICP-MS. A more detailed description of the quantification procedure of the ICP-MS signals as well as the synchronization procedure can be found in part 1 of this series.⁶

The release rates of inorganic elements were calculated following the same principle presented in refs 1, 16, and 17. In a first step,

element balances for the major ash forming species (Ca, Si, and Mg) are calculated as a plausibility check for the ash sampling and the analyses. It is important that these balances show a good closure, with recovery rates between 80 and 120%. As long as the chemical analyses are of good quality, the major sources of deviations are ash losses during ash sampling (especially when molten phases occur) and an entrainment of ash particles during the experiment, which cannot be avoided. Therefore, an additional correction can be performed according to reference elements. Reference elements in this context are elements such as Ca and Mg (for wood fuels) or Si (for herbaceous fuels) which show high concentrations in the respective ashes. The occurrence of high Ca concentrations in wood and increased Si contents in straws and grasses have also been reported in ref 18. According to ref 19, these elements are mainly present as oxides in the ashes which will stay solid in the combustion temperature range considered due to their low vapor pressure.²⁰ By using these reference elements as tracers, the mass balances are corrected for ash losses, assuming that the total mass of these elements in the fuel must be equal to their mass in the residual ash. The release rates for S, Cl, K, Na, Zn, and Pb are subsequently calculated from the corrected element balances.

2.4. Fuel Composition. Softwood (spruce SW) and wheat straw pellets were used in this study. In Table 1, the chemical compositions of the fuels are summarized and compared with database values taken from an internal database from BIOS BIOENERGIESYSTEME GmbH, Graz, Austria. The compositions of both fuels are comparable with the respective database values. The only exception is SW batch A, which shows an increased Si content, compared to the database average value. This is an indication for a slight contamination of this fuel. Such increased amounts of mineral contaminants due to the manufacturing process have also been reported in ref 18 for some wood fuels.

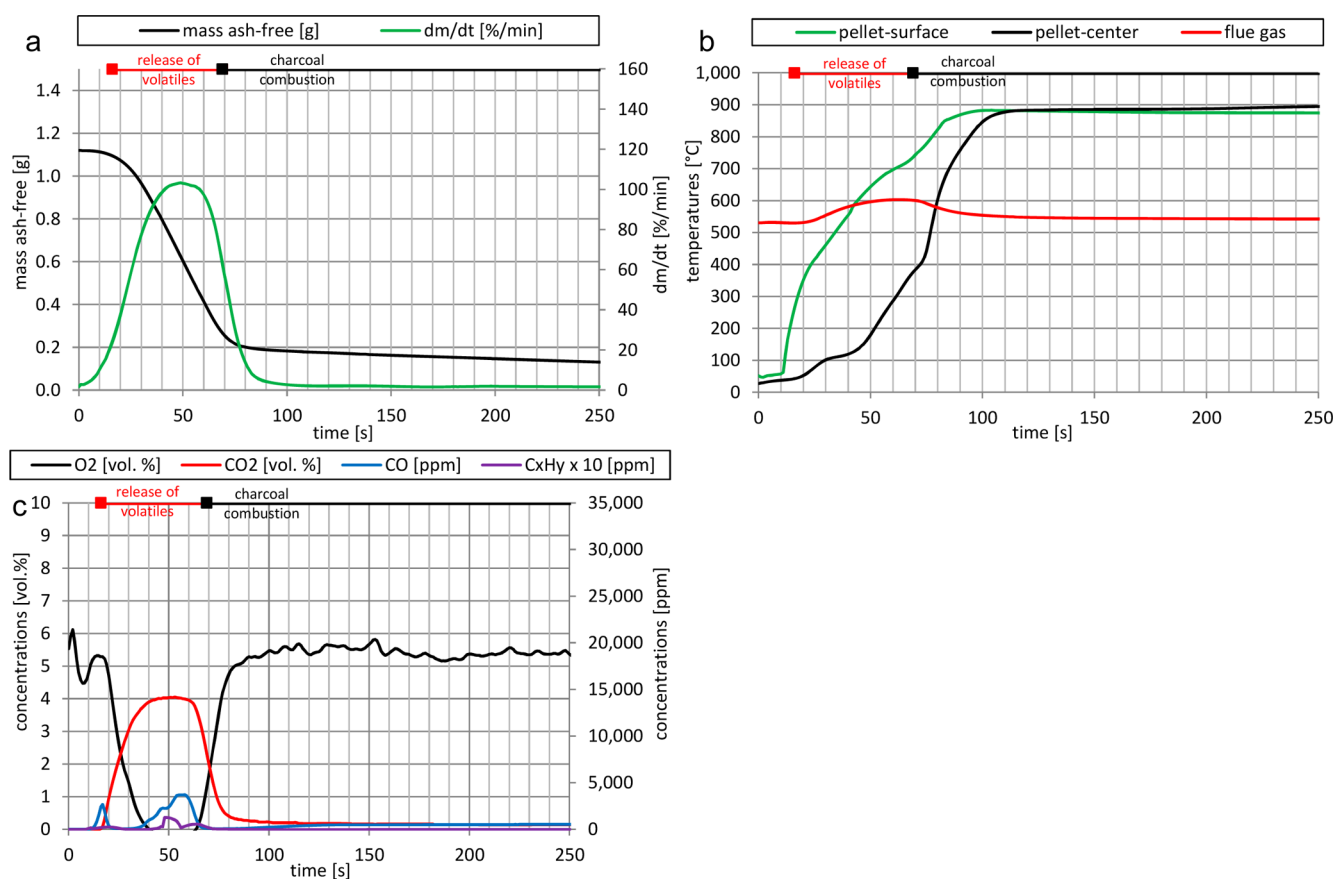


Figure 2. Experimental data for straw850: Gravimetric data (a), temperature curves (b), flue gas compositions (c).

2.5. Experimental Conditions during the Test Runs Performed. Test runs were performed with softwood (spruce SW) and wheat straw at reactor temperatures of 700, 850, and 1000 °C (in the following referred to as SW700, SW850, SW1000 and straw700, straw850, straw1000). Samples from batch B were used for SW700, and samples from batch A were used for SW850 and SW1000 (see Table 1). For the SW pellets (batch B) a density of 1150 kg/m³ and for the straw pellets a density of 1070 kg/m³ was determined. In ref 21, for wood pellets an average pellet density of 1180 kg/m³ with a standard deviation of 60 kg/m³ (21 different samples) have been presented. Since a very good agreement with the determined pellet density from batch B with the literature value exists, the same range of the pellet density for batch A can be expected. For straw pellets densities of 1080 kg/m³ and 950 kg/m³ have been reported,²¹ whereby the density determined in this study is in the range of the literature values.

For the test runs single biomass pellets were used, which were 8 mm in diameter and about 20 mm in length, resulting in a sample mass of about 1 g. A small hole was drilled into the center of the particles to mount them on the thermocouple for the particle center temperature measurement. Therefore, dense and not fragile pellets are essential for sample preparation and sample handling. The tests have been performed under oxidizing atmospheres (5.6 vol % O₂ in the reaction gas) at a total flow rate of the reaction gas of 15 l/min at 0 °C and 101325 Pa. The flow rate was selected to ensure a velocity in the reactor of below 0.5 m/s at 1000 °C to minimize entrainment of ash particles. O₂ content has been selected to achieve gasification or pyrolysis conditions during the devolatilization phase comparable with real-scale combustion processes. For the SW700 experiments, the O₂ content has been decreased to 4.2 vol % to gain a better stability of the decomposition process. The tests have generally been performed in triplicate to check the reproducibility of the method.

2.6. Performance of Quench Tests. Quench tests have been performed as a validity check for the online release profiles and to gain

further information about ash transformation and inorganic release processes. The controlled interruption (or quenching) of the ongoing decomposition process has been presented in detail in part 1 of these series⁶ and is therefore only briefly described in the following.

To quench the ongoing combustion reactions at a certain time, a water cooled protective tube is moved around the sample holder with the particle. Furthermore, the tube is purged with N₂ (at 25 °C) to quench the sample as quickly as possible. Special care has been taken that no ash particles are blown from the sample holder by the quench gas.

The quench tests (conducted for straw) were performed in triplicate at the same boundary conditions (see section 2.5) as was the case with complete burnout. After quenching, the residues were removed and chemically analyzed. On the basis of these data release ratios for the relevant inorganic ash, forming elements at the quench point were calculated.

3. RESULTS AND DISCUSSION

3.1. Case Study Straw850. As an example for the detailed evaluation of single particle reactor tests, the test run with straw at a reactor temperature of 850 °C is discussed in the following. Subsequently, a summary of relevant results from all performed test runs is provided. Since the three replications of each point of the test matrix provided very comparable results (see also section 3.2), a representative test is discussed.

The chemical composition of the wheat straw applied can be taken from Table 1. A single pellet (8 mm in diameter and about 20 mm in length) with a mass of 1168.4 mg wet basis (w.b.) with a corresponding ash free mass of 1119.4 mg w.b. was used. Figure 2 presents the gravimetric data, trends of the surface and the center temperatures of the particle, as well as of

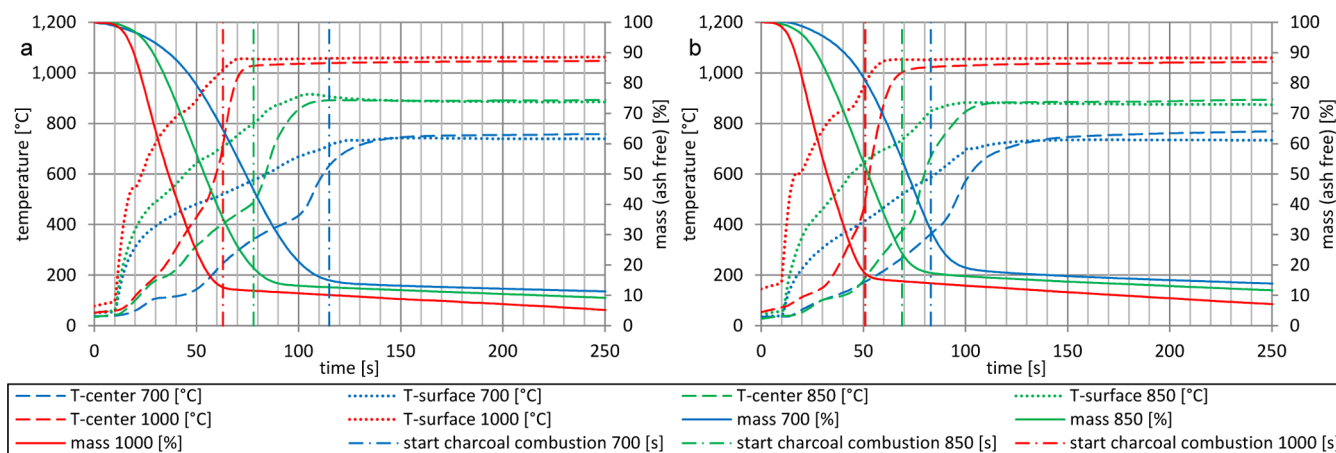


Figure 3. Temperature development of the particle (surface and center) and normalized mass loss for softwood (a) and straw (b) for the reactor temperatures of 700, 850, and 1000 °C. Explanation: The point where charcoal combustion becomes a more dominant process than devolatilization is indicated by a dash dot line for the respective reactor temperature.

the concentrations of the main gas species measured downstream of the reactor.

A CO₂ concentration of >0.1 vol % has been used as an indicator for the start of the devolatilization phase which was reached after 16 s (see Figure 2 c). After this point, the main fuel decomposition phase starts, indicated by increasing CO₂ concentrations and decreasing O₂ concentrations in the flue gas. After 40 s, the O₂ concentration drops to 0. Release of volatiles takes place until around 70 s. Typical indicators for this phase are a rapid mass loss, an increase of the surface and center temperatures to 740 and 380 °C respectively, as well as a drop of the O₂ concentration in the reaction gas to 0. Mainly CO₂, CO, as well as minor amounts of hydrocarbons are measured in the exhaust gas during this phase. After 62 s, the CO₂ concentration decreases, and at 69 s, the inflection point of the CO₂ trend is reached. Here devolatilization is almost completed, and charcoal combustion becomes the dominating process. The charcoal combustion is characterized by lower mass loss rates, smaller amounts of CO, a drop of the OGC concentrations to zero, higher CO₂ concentrations in the flue gas, and increasing O₂ concentrations. The end of the experiment is reached after 1005 s, indicated by the drop of the CO concentration to 0.

To measure the center and the surface temperature of the particle, the sample is placed on a thermocouple (see section 2.5), and a second thermocouple is placed below the particle. The center temperature measurement provides good indications of the actual center temperature of the particle, since this measurement is only negligibly influenced by heat transfer processes. Regarding the surface temperature, different heat transfer processes and shrinkage of the particle can influence the quality of the measurement. Especially during the first phase of the experiment, it is most likely that the measured temperatures provide a realistic picture of the actual surface temperatures; however, the data have to be interpreted with care.

After 11 s, a steep almost linear increase of the surface temperature can be noticed, reaching 400 °C after 23 s (see Figure 2 b). This temperature increase corresponds to a heating rate of about 30 K/s. A second flatter, almost linear temperature increase follows, until 700 °C is reached after 60 s (corresponding heating rate about 8 K/s). Finally, surface temperatures of 880 °C prevail, which is slightly above the

reactor target temperature of 850 °C. The center temperature increases only slightly to about 100 °C between 28 and 40 s, which indicates drying in the inner layer of the pellet. Two, almost linear temperature ramps can then be observed between 45 and 74 s as well as 74 and 85 s (150 to 420 °C and 420 to 700 °C), which correspond to heating rates of 9 and 25 K/s. Similar to the surface temperature trend, a temperature of 888 °C is reached after 110 s. The temperature trends for surface and center indicate overlapping processes in different layers of the particle. The devolatilization layer proceeds with heating up the particle into the inner layers. After, for example, 40 s, when charcoal combustion takes place at the outer layer, devolatilization starts in the center. After ~80 s the whole particle is in the charcoal combustion phase. Consequently, no clear distinction between the end of the devolatilization and the start of the charcoal combustion phase exists for the whole particle. Therefore, the above-defined criterion (start of the devolatilization for a CO concentration >0.1 vol %; inflection point of the decreasing CO₂ trend for the start of the charcoal combustion phase) divides the experiment into a phase dominated by devolatilization and a phase dominated by charcoal combustion.

3.2. Thermogravimetric Data. To compare the thermogravimetric data of all test runs performed, the trends regarding mass loss and particle surface and center temperatures as well as the start of the charcoal combustion (indicated with a dash dot line) are displayed in Figure 3.

The main mass loss takes place during the devolatilization phase, and lower decomposition rates occur during charcoal combustion. Higher reactor temperatures cause higher heating rates of the sample. During devolatilization at higher heating rates, an increased degradation of the sample took place which subsequently decreases the amount of char (residues at the beginning of the charcoal combustion phase). The temperature trends at the surface and the center of the particle are similar for the three applied reactor temperatures. For straw, the duration of the devolatilization phase is shorter than SW, which can result from a higher reactivity caused by catalytic effects due to the higher contents of inorganic components.^{22,23} SW700 has a longer devolatilization phase than straw700 due to the lower O₂ content (4.2 vol %) of the reaction gas for SW700 (O₂ content straw700: 5.6 vol % see section 2.5).

Relevant results from the test runs with SW and straw are presented and compared in Table 2. The initial sample masses

Table 2. Characteristic Data Gained from the Test Runs^a

	softwood (spruce)						straw (wheat)					
	700		850		1,000		700		850		1,000	
	average	std. dev.	average	std. dev.	average	std. dev.	average	std. dev.	average	std. dev.	average	std. dev.
sample mass (mg w.b.)	1,175	38.5	1,108	1.7	1,094	1.7	1,175	3.7	1,160	21.7	1,140	51.3
ash mass after test run (mg d.b.)	4.0	0.05	3.6	0.25	2.9	0.12	51.2	0.50	45.7	0.50	41.9	6.9
duration of devolatilization (s)	89	3	61	1	49	5	58	5	53	2	42	2
duration of char burnout (s)	1,739	155	843	60	517	41	1,157	29	900	45	674	64
mass loss during devolatilization (%)	82.8	2.3	81.0	1.0	85.9	1.8	71.4	5.1	76.9	1.0	81.6	1.4
mass loss during char burnout (%)	17.2	2.2	19.0	0.8	14.1	0.15	28.6	3.8	23.1	1.0	18.4	0.42
C element balance closure (%)	100.2	1.6	85.6	0.9	84.7	1.5	110.3	1.1	88.7	1.0	86.9	2.0
ash mass balance closure (%)	96.6	2.1	93.9	6.1	80.9	3.7	107.9	1.6	101.7	1.8	99.0	17.4

^aExplanations: average and standard deviation (std. dev.) have been determined for the three repetitions performed for each fuel at the respective reactor temperature; w.b., wet basis; d.b., dry basis.

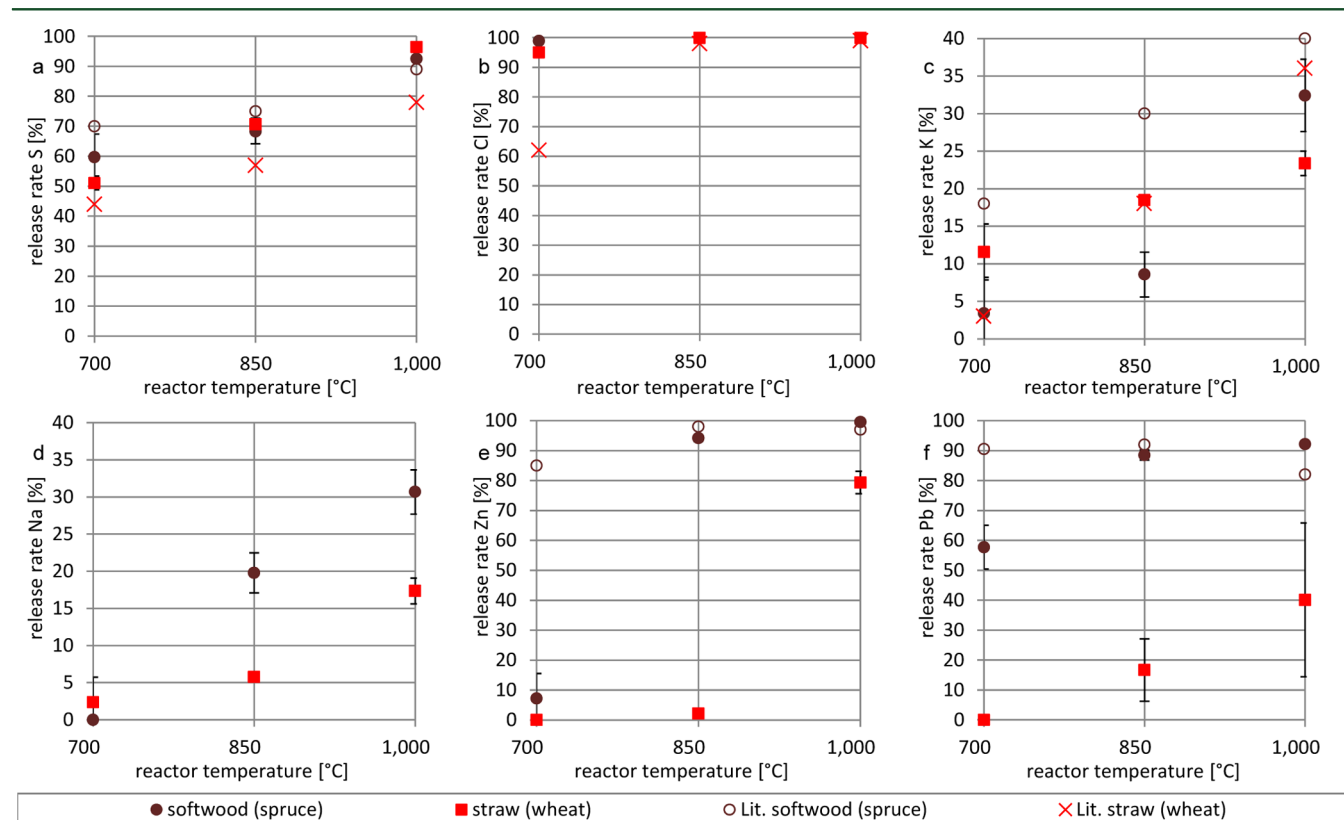


Figure 4. (a–f) Release of inorganic elements from the fuel to the gas phase at different reactor temperatures in comparison with literature data. Explanations: Lit. softwood (spruce), literature data¹² from laboratory combustion tests with softwood (spruce), Lit. straw (wheat), literature data¹³ from lab-scale combustion tests with wheat straw.

are in a narrow range (1108–1175 mg w.b.). The ash residue masses decrease slightly with higher reactor temperatures, due to ash losses (explained in context to the ash balance closure). This also affects the closure of the ash mass balance. The duration of the two main combustion phases decreases with increasing reactor temperatures. It has been determined that the two main combustion phases last longer with SW than with straw at 700 °C. This is due to a lower O₂ concentration in the reaction gas. The mass loss during devolatilization is quite similar for SW700 and SW850 but higher for SW1000.

The C mass balance and the ash balance closures are between 85 and 110% and 81–108% respectively, which are

acceptable values. For the determination of the C mass balance closure, the gaseous C containing species were considered. Only for SW700 and straw700 recovery rates above 100% have been determined, which may be caused by an overestimated C content by the FID especially for straw700. Regarding the ash mass balance closure particularly with SW, where low ash contents and high ash melting temperatures prevail, the higher thermal stress with rising reactor temperatures may lead to a breakup of ash particles from the ash matrix with subsequent entrainment of these particles. In the case of straw, possible inhomogeneities of the sample can cause recovery rates above 100%, which is most probably the case for reactor temperatures

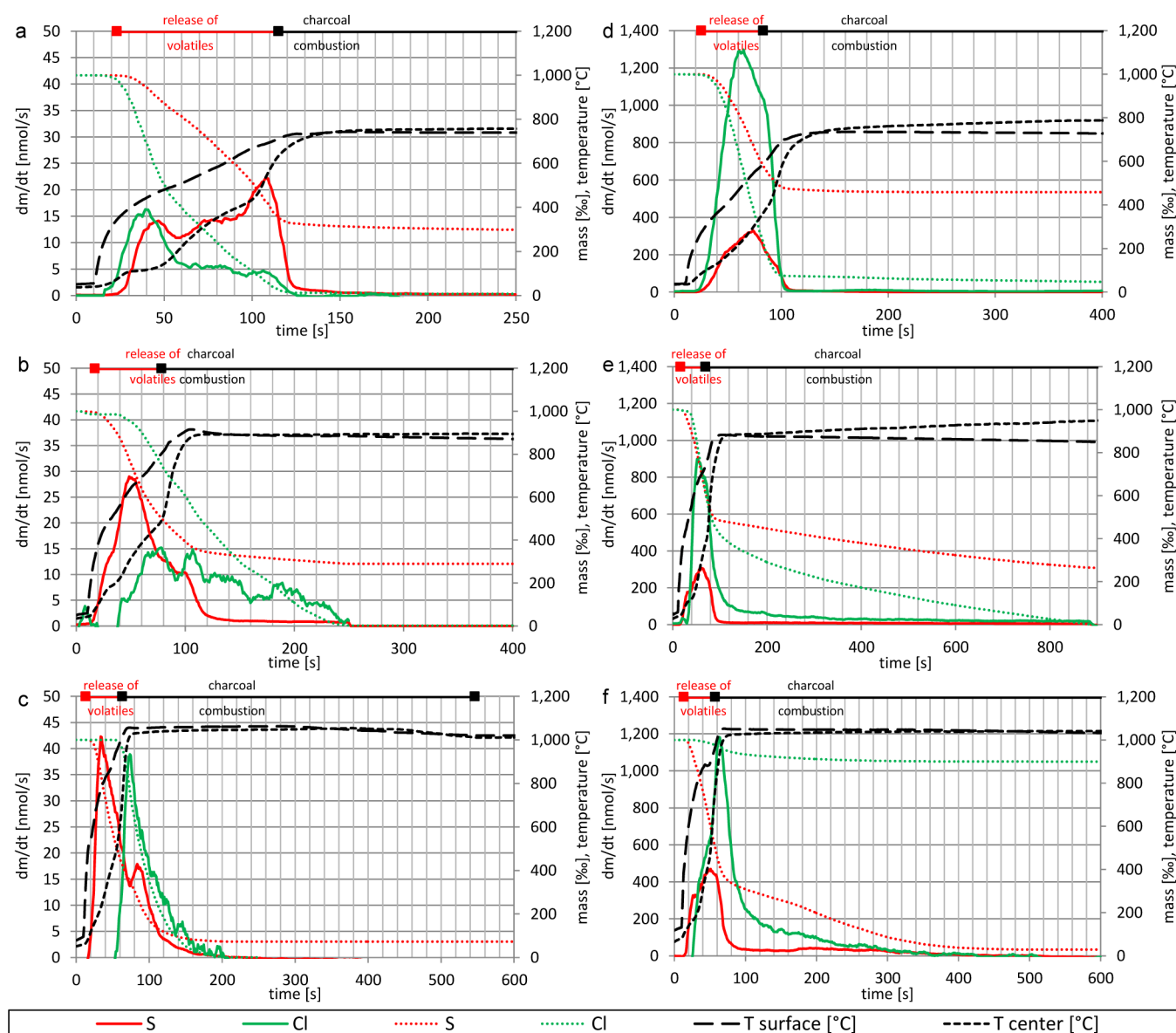


Figure 5. Time dependent release of S and Cl from softwood (a–c) and straw (d–f) for reactor temperatures of 700, 850, and 1000 °C (from top to bottom).

at 700 °C. In addition, ash melting also makes the ash sampling difficult, whereby first indications of melting have already been observed for straw850, where the temperatures rise above the shrinkage starting temperature (SST) (780 °C see Table 1). Completely fused ash has been obtained for straw1000, whereby the fused residues remained on the thermocouples and the sample holder and must be removed mechanically with some effort, which makes the ash sampling a potential source for ash losses. However, in the case of low ash recovery rates (e.g., SW850 and SW1000), a correction with reference elements (see section 2.3) was performed.

3.3. Release Behavior of Ash Forming Elements. On the basis of element balances (see section 2.3), the overall inorganic element release ratios from the fuel to the gas phase for the entire combustion experiment were calculated and summarized in Figure 4. The results obtained were also compared with literature data.^{12,13}

Generally, the release of inorganic elements increases with higher temperatures, which is in agreement with literature data.

The absolute values of the release ratios are, with some exceptions, also in good agreement with the literature data. For straw700, a 33% higher Cl release was achieved. While the K releases for straw are in good agreement with literature data, the resulting values for SW were on average 15% lower. In the case of Zn and Pb, major deviation occurs in the SW700 test. Generally, these differences most likely result from different experimental boundary conditions prevailing in refs 12 and 13 than in this work. In ref 12 a 30 g sample of spruce (milled) and in ref 13 a 4 g wheat straw sample (milled) were combusted with variable O₂ contents (0% during pyrolysis and 20% during later stages of char combustion) in the reaction gas. These variable O₂ contents have been applied to avoid a temperature overshoot in the reaction zone during char combustion, particularly when conducting experiments with spruce.¹¹ However, the absence of O₂ during the devolatilization might be the reason for the higher Zn and Pb release. Moreover, differences in the fuel compositions might have an influence on the release.¹²

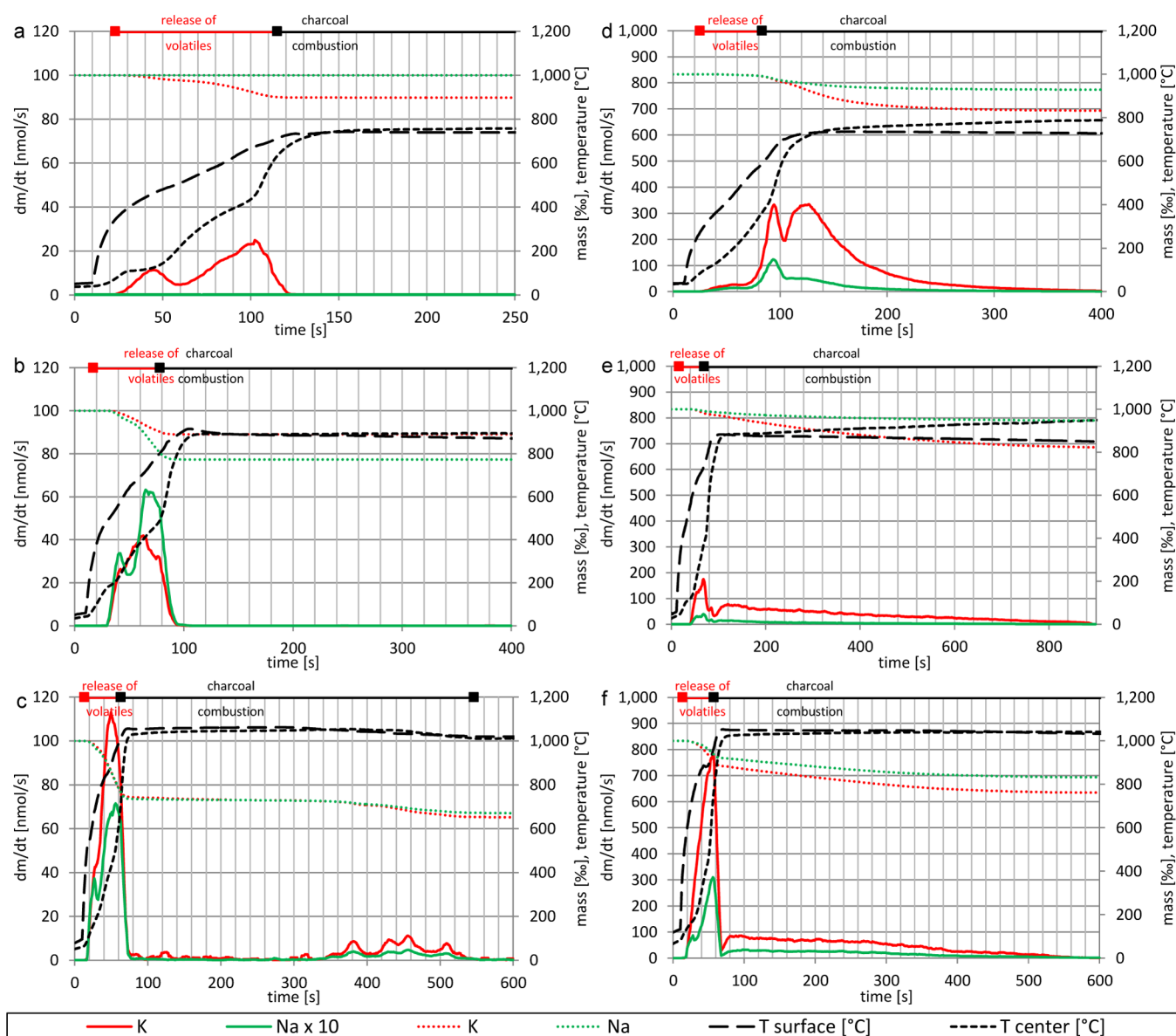


Figure 6. Time dependent release of K and Na from softwood (a–c) and straw (d–f) for reactor temperatures of 700, 850, and 1000 °C (from top to bottom).

The results are also in good agreement with the release mechanisms summarized in section 1.1. In the case of S, the release of mainly organically S can be assumed for the temperatures 700 and 850 °C. Typically, 75% S is organically bound and the remaining part is inorganically associated,¹⁰ which explains the high release rates (50–60%) seen as early as 700 °C. High Cl release ratios are also obtained for 700 °C, and, especially in the case of straw, the remaining Cl is most likely bound in alkali salts (e.g., KCl). Higher K release ratios have been determined for straw700 and straw850 than for SW at these temperatures. The higher K release for straw may result from the significantly higher Cl content in the fuel and therefore in an increased KCl(s) evaporation.^{4,5,13} The molar K/Cl ratios of the fuels (8.7 SW batch A, 10.4 SW batch B and 2.8 straw) support the proposed mechanism.

For straw1000, an inclusion of K in molten K–Si phases is most likely and reduces the K release, since the molar K/Si ratio amounts to 0.45 and 0.96 for straw and the SW used at this temperature (batch A see Table 1). Furthermore, a rather

low shrinkage starting temperature of 780 °C has been determined for straw, and with reactor temperatures of 1000 °C the ash was completely fused after the experiment.

Lower Na release rates were determined for SW700 than for K and, in the case of straw, lower Na release rates have been obtained for all temperatures. A low Na release below 800 °C has also been reported in refs 24 and 25, which is in line with results at 700 °C. In the case of higher reactor temperatures, sublimation of NaCl and Na-carbonate decomposition¹² can cause higher release ratios.

For Zn, a steep increase of the release ratios can be observed between 700 and 850 °C in the case of wood, whereas for straw the steep increase is shifted to the temperatures between 850 and 1000 °C. Lower release ratios of straw in comparison to SW can be explained by a possible interaction of Zn with Si and Al.¹² Thermodynamic equilibrium calculations, performed in a previous study,¹⁶ also showed the formation of solid Si–Zn phases below 500 °C.

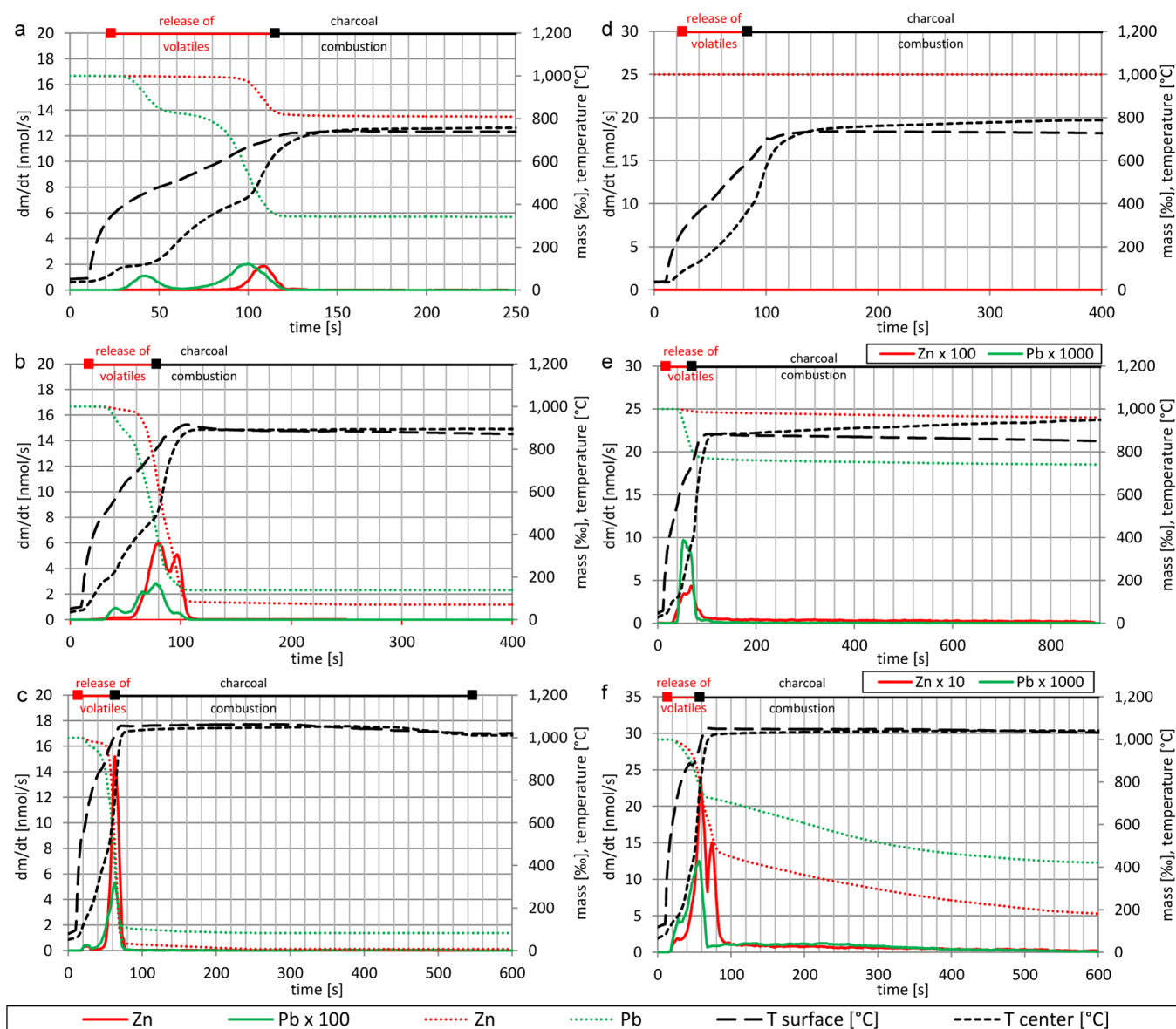


Figure 7. Time dependent release of Zn and Pb from softwood (a–c) and straw (d–f) for reactor temperatures of 700, 850, and 1000 °C (from top to bottom).

For Pb, lower release ratios have been determined for straw than for SW. Straw shows higher concentrations of Si and Al (see Table 1) than SW, whereby interactions of these elements with Pb¹² can reduce the Pb release. Furthermore, Pb compounds can be included in molten phases which can reduce the Pb release. The occurrence of these inclusions can vary for each experiment, and therefore higher standard deviations prevail for straw (for reactor temperatures above 700 °C) than for SW.

3.4. Time Resolved Release Behavior of Ash Forming Elements during Combustion Experiments. Trends regarding the release of S and Cl over time as well as the development of the particle temperatures (surface and center) during the experiments are displayed in Figure 5. Because of the good reproducibility of the repetitions, only one representative test is displayed per temperature and fuel.

In the case of reactor temperatures of 700 and 850 °C, mainly organically bound S is released, as was already mentioned in section 3.3. Furthermore, in refs 11–13 it has

been proposed that release of inorganic S begins at temperatures above 900 °C. On the basis of the release curves (see Figure 5), the release of S usually starts at surface temperatures between 300 and 400 °C for both fuels. At a reactor temperature of 850 °C, a release of mainly organic associated S is most likely, but inorganically associated S (e.g., alkali sulfate) can also contribute to the S release. For SW1000, the bimodal release profile might consist of an organic and inorganic part, which is supported by the temperature development of the particle. Straw1000 is seen to exhibit different behavior than SW1000. For straw, one release peak is clearly pronounced, whereas the remaining S is continuously released during char burnout. The low release during char burnout is most likely caused by transport limitation due to the occurrence of molten phases.

Part 1 of this series⁶ concluded that the ICP-MS determined Cl release can only be interpreted with restrictions. Possible deposition and release processes of Cl compounds, most likely located in the unheated zone of the sample line, can influence

the Cl signals. Strong changes to the Cl release profiles may be qualitatively evaluated, whereas continuously decreasing Cl release most likely results from condensation or deposition and release processes in the unheated part of the sample line and the ICP-MS. However, the determined release trends are displayed in the diagrams and have been validated for straw by additional quench experiments (see section 3.5).

For SW700 and straw700, the release starts at surface temperatures of about 300 °C, and the main release takes place during devolatilization, which most likely results from the release of CH_3Cl .¹⁴ During experiments with higher reactor set-temperatures (850 and 1000 °C), the main release starts at higher surface temperatures, which may result from transport limitations when the particle is being heated up. The section of the Cl trends after the release peak should, as already mentioned, not be evaluated.

In general, the release processes summarized in section 1.1 are in good agreement with time-resolved release profiles (see Figure 6). In the case of K, the release starts in the temperature range of 500 °C, independent of the fuel and heating rate, which can be explained by the release of alkaline carboxylates and phenol-associated K.¹² At temperatures above 700 KCl(s), sublimation and $\text{K}_2\text{CO}_3(\text{s})$ decomposition take place.¹² The main release (see Figure 6) takes place during devolatilization, and a lower K release occurs during char burnout. For SW700, low shares of K release as KCl(g) are probable, since the K release is almost finished when surface temperatures above 700 °C are reached. For reactor temperatures of 850 and 1000 °C, particle temperatures clearly above 700 °C are reached, and the evaporation of KCl(s) and a dissociation of K_2CO_3 take place. For straw, a bimodal K release trend (especially for straw700) has been determined. The first release peak (occurring during devolatilization and early stages of char combustion) may result from organically associated K as well as a possible sublimation of KCl. Quench experiments (see section 3.5) have been performed, which revealed that the second release peak mainly results from K_2CO_3 decomposition. For straw850 and straw1000, the occurrences of molten phases (mainly K–Si, further information also supported by thermodynamic equilibrium calculations can be found in ref 16) can cause the continuously decreasing K release during char burnout.

Since significantly less literature data is available for Na than for K, similar release behavior has been proposed under consideration of different characteristic temperatures regarding the Na release (melting points: NaCl 801 °C, carbonate decomposition above 850 °C).

The release starts at a surface temperature of about 500 °C (see Figure 6), which is in good agreement with^{24,25} where the start of the release has been proposed to be at around 400 °C during pyrolysis. This low temperature release can be observed for reactor temperatures of 700 and 850 °C and also partly for reactor temperatures of 1000 °C. Similar release trends can be observed for Na and K (see Figure 6) for straw850 and straw1000. The bimodal release profile in the case of SW850 most likely originates from the dissociation of organically associated Na (first peak), and the second release peak results from NaCl evaporation and possible Na_2CO_3 decomposition since surface temperatures around 800 °C prevail. For straw700, a different release profile to that of K can be observed at that temperature. Since a relatively high Na release ratio (7%) has been determined for the presented test and the particle surface temperatures in particular are close to 800 °C,

an evaporation of NaCl or carbonate decomposition can already take place at that reactor temperature.

In part 1 of this series,⁶ it has already been mentioned that the Zn release starts at temperatures above 500 °C and that particle temperatures above 700 °C are necessary for a distinct Zn release. For the conducted experiments (see Figure 7), Zn release starts at surface temperatures between 500 °C (SW850, straw850, and straw1000) and 700 °C (SW700 and SW1000). For SW, the main Zn release finishes when the maximum surface temperature is reached. Especially in the case of straw1000, a low and continuously decreasing release trend can be observed during char burnout. The occurrence of molten phases most likely hinders the Zn release during char burnout. For SW850, a bimodal release trend has been obtained. The release maxima can be explained by reaching a sufficient temperature at the surface and at the center of the particle for a distinct Zn release, whereby the minimum between the release maxima may result from a possible capture of Zn compounds in the char matrix. A possible retention of Zn compounds in ashes by Si and Al is very improbable for SW due to the low concentrations of these elements in the fuel (see Table 1). During the second release peak, surface temperatures above 900 °C prevail where Zn compounds previously captured in the char are released. For SW1000, one single release peak has been obtained, with the maximum at center temperatures about 900 °C. The higher reactor temperatures cause a faster decomposition of the particle, and a possible capture of Zn compounds in the char is not visible in the release profile. For straw, different Zn release profiles have been determined than for SW, most likely caused by interactions of Zn compounds in the ashes by Si and Al. For straw850, only a single Zn release peak occurs with an unclear maximum at surface temperatures between 700 and 800 °C. In the case of straw1000, a bimodal Zn release trend prevails, where maximum release peaks occur at surface and center temperatures of 1000 °C. It seems that, at temperatures below 1000 °C, Zn compounds are retained in the ashes, and a sudden release takes place when 1000 °C is reached. Generally, the peaks of the release profiles are shifted to higher particle temperatures with rising reactor temperatures (or heating rates of the particle) (see Figure 3), which are caused by transport limitations when the particle is heated up. This shift can be observed for Zn and Pb for both fuels.

Pb release starts at surface temperatures around 500 °C (see Figure 7), independent of the reactor temperature and the fuel. For SW, a bimodal release trend (SW700 and SW1000) and a multimodal release (SW850) can be observed. The minima of these release trends can be caused by Pb compounds being captured in the char. The captured Pb compounds are later released at higher particle temperatures. For SW, a low release takes place at surface temperatures above 500 °C. A second release peak occurs during the switch between devolatilization and char burnout, which is more pronounced with higher reactor temperatures. In contrast to SW, straw shows one distinct release peak during devolatilization and a continuous decreasing release trend during char burnout (transport limitations caused by ash melting). Straw has a significantly higher ash content than SW as well as a different ash composition (interactions of Pb with Si and Al; see also section 3.3), factors that explain the different release profiles for both fuels.

3.5. Results of Targeted Quench Experiments with Wheat Straw Pellets. The quench points have been adjusted

Table 3. Release Data for Complete Burnout in Comparison with Quench Experiments for Straw at Reactor Temperatures of 700, 850, and 1000 °C^a

reactor temperature [°C]			complete burnout	reference point	quench tests				
					1	2	3	average	std. dev.
700	T-quench	°C			574	612	564		
	S	wt %	54.1	51.5	47.6	46.3	45.8	46.6	0.7
	Cl	wt %	95.3	93.4	89.1	94.1	86.7	90.0	3.1
	K	wt %	16.7	3.3	4.2	3.5	2.0	3.2	0.9
	Na	wt %	7.1	2.8	1.4	3.6	2.2	2.4	0.9
	Zn	wt %	0.00	2.0	0.00	3.3	6.6	3.3	2.7
	Pb	wt %	0.00	0.00	0.00	0.00	0.00	0.00	0.00
850	T-quench				757	753	750		
	S	wt %	73.5	64.9	53.9	51.8	51.9	52.5	1.0
	Cl	wt %	99.9	54.0	88.3	70.7	74.3	77.8	7.6
	K	wt %	17.7	2.6	4.0	6.2	5.8	5.3	0.9
	Na	wt %	5.2	1.3	5.8	8.6	5.1	6.5	1.5
	Zn	wt %	4.0	1.5	6.0	5.5	2.5	4.6	1.5
	Pb	wt %	25.9	24.2	9.9	3.4	14.9	9.4	4.7
1000	T-quench				967	936	938		
	S	wt %	97.1	66.8	60.4	59.6	57.2	59.1	1.4
	Cl	wt %	100.0	34.3	81.8	79.7	78.0	79.8	1.6
	K	wt %	23.8	11.4	14.9	9.9	10.0	11.6	2.3
	Na	wt %	16.8	8.3	13.3	11.1	5.7	10.0	3.2
	Zn	wt %	81.9	39.9	53.3	46.8	33.7	44.6	8.2
	Pb	wt %	57.9	57.1	66.3	64.7	60.6	63.8	2.4

^aExplanation: T-quench, center temperature at the quench point; reference point, released amount derived from the time resolved release profiles at complete burnout determined at the averaged center temperature at the quench points.

to the K release profiles determined (see Figure 6). For straw700, the quench point was defined with the minimum between the peaks of the bimodal K release profile (105 s). For straw850 and straw1000, the quench has been chosen to occur after devolatilization and to start at char burnout, which is after 90 and 70 s, respectively. The release ratios at the reference point have been derived from the time-resolved release profiles at complete burnout (Figure 5, Figure 6, and Figure 7) determined at the averaged center temperature which occurred at the quench points. The determined center temperatures at the quench point (see Table 3) are in a range of 564–612 °C for the tests at 700 °C. For higher reactor temperatures they are in a more narrow range (750–753 °C and 938–967 °C for a reactor temperature of 850 and 1000 °C respectively). These data have been compared with the data gained from the quench experiments. On the basis of these framework conditions, quench tests as presented in section 2.6 have been performed with straw.

In Table 3, the results of the quench experiments, the release at the reference point and the release at complete burnout are summarized.

With the exception of Cl, a very good agreement between the reference point and the averaged release ratios for the quench tests prevails (see Table 3). Consequently, meaningful time dependent release profiles have been obtained for S, K, Na, Zn, and Pb.

For straw850, slightly lower Na and Zn release and a higher Pb release ratio were determined for the reference point in comparison with the quench test. The deviations regarding Na and Zn are most probably due to their low concentrations and an inhomogeneous distribution in the fuel. The deviations of Pb can be explained by the high standard deviation of the release ratios determined at complete burnout.

The results of the quench tests can also provide a rough estimation regarding the K release that may result from KCl evaporation and K₂CO₃ decomposition. The K release is not completed at the quench point in any quench experiments. Organically associated K is released before the quench point. Additionally, the high Cl release ratios at the quench points indicate (78–90%) that a part of K is released in the form of KCl. A decomposition of K₂CO₃ before the quench is only probable for straw1000, since the average center temperature of 947 °C at the quench point was above the temperature when K₂CO₃ decomposition starts (800 °C¹²). After the quench, the remaining KCl(s) is evaporated and K₂CO₃(s) decomposition mainly takes place.

In the case of Cl, an acceptable agreement between the reference point and the quench point only exists for straw700. For reactor temperatures of 850 and 1000 °C, the calculated reference point shows a significantly lower release than the quench test. This again confirms that the Cl release during charcoal combustion is overestimated during the tests at complete burnout.

4. SUMMARY AND CONCLUSION

At the moment, there is little time-resolved release data for ash forming elements from single fuel particles. Therefore, test runs were performed with a specially designed single particle reactor, connected to an inductively coupled plasma mass spectrometer (ICP-MS). During the experiments, relevant parameters such as the mass loss during thermal decomposition, the temperature development of particles (surface and center), flue gas composition, and the S, Cl, K, Na, Zn, and Pb release trends were recorded online. A validation of the time-resolved inorganic element release profiles for straw was performed by a targeted and controlled interruption (or quench experiment) of the ongoing decomposition process, which also supported

the interpretation of the release data. Test runs with softwood and straw have been performed at reactor temperatures of 700, 850, and 1000 °C under oxidizing conditions (5.6 or 4.2 vol % O₂).

The surface and center temperature developments of the particles clearly indicate overlapping processes (drying, devolatilization, and char combustion) in different layers of the particle. Increasing reactor temperatures lead to higher heat-up rates of the particle, higher thermal degradation rates and shorter test durations being needed to reach a complete particle burnout. Furthermore, as reactor temperatures rise, the release ratios of inorganic elements from fuel to gas phase increase. Results show S release ratios between 50 and 93%, an almost complete release for Cl, even at 700 °C, and K and Na release ratios below 33%. The Zn and Pb release ratios strongly depend on the reactor temperatures prevailing and on interactions with the ash matrix, where, in general, higher release ratios have been obtained for SW than for straw.

The time dependent release profiles of inorganic elements indicate that the S release is mainly coupled to the decomposition of the organic matrix and, in the case of SW, a distinction between the release of organically and inorganically associated S is possible. In the case of K, release mechanisms proposed by ref 12 (decomposition of organically dissociated K for T below 500, KCl and K₂CO₃ decomposition above 700 °C) have been confirmed by the tests performed. The same mechanism can also be applied to Na. For Zn and Pb, the release strongly depends on the particle temperature development during the thermal conversion process, whereby a particle temperature above 700 °C is necessary for a distinct release. The maximum peaks of the Zn and Pb release profiles are shifted to higher particle temperatures with rising reactor temperatures (higher heating rates), most probably caused by transport limitations while the particle is being heated up. A clear indication for transport limitations due to the occurrence of molten phases was obvious for straw850 and straw1000.

The quench tests performed are an effective method for validating the time dependent release profiles. Such tests confirm the results for S, K, Na, Zn, and Pb. They also show that the Cl release trends must be interpreted with caution since they are overestimated during char burnout. The quench tests additionally supported the interpretation of the time-resolved K release profiles with respect to KCl sublimation.

In the future, the online release data presented shall be used as a basis for inorganic element release modeling.

AUTHOR INFORMATION

Corresponding Author

*Telephone: + 43 (0) 316 873-9237. Fax: + 43 (0) 316 873-9202. E-mail: peter.sommersacher@bioenergy2020.eu.

Notes

The authors declare no competing financial interest.

ACKNOWLEDGMENTS

This article is the result of a project carried out within the framework of the Austrian COMET program, which is funded by the Republic of Austria as well as the federal provinces of Styria, Lower Austria and Burgenland. The work was also funded by the following companies: Andritz AG, Josef Bertsch GmbH & Co. KG, BIOS BIOENERGIESYSTEME GmbH, HET Heiz- und Energietechnik Entwicklung GmbH, KWB Kraft und Wärme aus Biomasse GmbH, Standardkessel GmbH,

TIWAG Tiroler Wasserkraft AG and Viessmann Holzfeuerungsanlagen GmbH.

REFERENCES

- (1) Sommersacher, P.; Brunner, T.; Obernberger, I. Fuel indexes – a novel method for the evaluation of relevant combustion properties of new biomass fuels. *Energy Fuels* **2012**, *26*, 380–390.
- (2) Gilbe, C.; Öhman, M.; Lindström, E.; Boström, D.; Backman, R.; Samuelsson, R.; Burvall, J. Slagging Characteristics during Residential Combustion of Biomass pellets. *Energy Fuels* **2008**, *22*, 3536–3543.
- (3) Brunner, T.; Biedermann, F.; Kanzian, W.; Evic, N.; Obernberger, I. Advanced biomass fuel characterization based on tests with a specially designed lab-reactor. *Energy Fuels* **2013**, *27* (10), 5691–5698.
- (4) Knudsen, J. N. Volatilization of Inorganic Matter during Combustion of Annual Biomass. Ph.D. thesis, Technical University Denmark, Lyngby, Denmark, 2004; ISBN: 87-91435-11-0.
- (5) Van Lith, S. C. Release of Inorganic Elements during Wood-Firing on a Grate. Ph.D. thesis 2005, Technical University of Denmark, Lyngby, Denmark; ISBN: 87-91435-29-3.
- (6) Sommersacher, P.; Kienzl, N.; Brunner, T.; Obernberger, I. Simultaneous online determination of S, Cl, K, Na Zn and Pb release from a single particle during biomass combustion Part 1: Experimental setup - implementation and evaluation. *Energy Fuels* **2015**, *29*, 6734–6746.
- (7) Mehrabian, R.; Zahirovic, S.; Scharler, R.; Obernberger, I.; Kleditzsch, S.; Wirtz, S.; Scherer, V.; Lu, H.; Baxter, L. A CFD model for thermal conversion of thermally thick biomass particles. *Fuel Process. Technol.* **2012**, *95*, 96–108.
- (8) Lu, H. Experimental and modeling investigations of biomass particle combustion. Ph.D. Thesis, Brigham Young University (Department Chemical Engineering), USA, 2006.
- (9) Mehrabian, R.; Shiehnejadhesar, A.; Scharler, R.; Obernberger, I. Multi-physics modelling of packed bed biomass combustion. *Fuel* **2014**, *122*, 164–178.
- (10) Werkelin, J. Ash forming matter and their chemical forms in woody biomass fuels. Ph.D. thesis, Abo Akademi University, Finland, 2008.
- (11) Van Lith, S.; Alonso-Ramirez, V.; Jensen, P. A.; Frandsen, F. J.; Glarborg, P. Release to the Gas Phase of Inorganic Elements during Wood Combustion. Part 1: Development and Evaluation of Quantification Methods. *Energy Fuels* **2006**, *20*, 964–978.
- (12) Van Lith, S.; Jensen, P. A.; Frandsen, F. J.; Glarborg, P. Release to the Gas Phase of Inorganic Elements during Wood Combustion. Part 2: Influence of Fuel Composition. *Energy Fuels* **2008**, *22*, 1598–1609.
- (13) Knudsen, J.; Jensen, P.; Dam-Johansen, K. Transformation and Release to the Gas Phase of Cl, K, and S during Combustion of Annual Biomass. *Energy Fuels* **2004**, *18*, 1385–1399.
- (14) Saleh, S. B.; Flensburg, J. P.; Shoulafar, T. K.; Sárossy, Z.; Hansen, B. B.; Egsgaard, H.; DeMartini, N.; Jensen, P. A.; Glarborg, P.; Dam-Johansen, K. Release of Chlorine and Sulfur during Biomass Torrefaction and Pyrolysis. *Energy Fuels* **2014**, *28* (6), 3738–3746.
- (15) Bärenthaler, G.; Zischka, M.; Haraldsson, C.; Obernberger, I. Determination of major and minor ash-forming elements in solid biofuels. *Biomass Bioenergy* **2006**, *30*, 983–997.
- (16) Sommersacher, P.; Brunner, T.; Obernberger, I.; Kienzl, N.; Kanzian, W. Application of novel and advanced fuel characterization tools for the combustion related characterization of different wood/Kaolin and straw/Kaolin mixtures. *Energy Fuels* **2013**, *27* (9), 5192–5206.
- (17) Sommersacher, P.; Brunner, T.; Obernberger, I.; Kienzl, N.; Kanzian, W. Combustion related characterisation of Miscanthus peat blends applying novel fuel characterisation tools. *Fuel* **2015**, *158*, 253–262.
- (18) Vassilev, S. V.; Baxter, D.; Andersen, L. K.; Vassileva, C. G. An overview of the chemical composition of biomass. *Fuel* **2010**, *89*, 913–933.

(19) Boström, D.; Skoglund, N.; Grimm, A.; Boman, C.; Öhman, M.; Broström, M.; Backman, R. Ash Transformation Chemistry during Combustion of Biomass. *Energy Fuels* **2012**, *26*, 85–93.

(20) Lamoreaux, R. H.; Hildenbrand, D. L.; Brewer, L. High-Temperature Vaporization Behavior Of Oxides II. Oxides of Be, Mg, Ca, Sr, Ba, B, Al, Ga, In, Tl, Si, Ge, Sn, Pb, Zn, Cd and Hg. *J. Phys. Chem. Ref. Data* **1987**, *16* (3), 419–443.

(21) Obernberger, I.; Thek, G. Physical characterisation and chemical composition of densified biomass fuels with regard to their combustion behavior. *Biomass Bioenergy* **2004**, *27*, 653–669.

(22) Jones, J. M.; Darvell, L. I.; Bridgeman, T. G.; Pourkashanian, M.; Williams, A. An investigation of the thermal and catalytic behaviour of potassium in biomass combustion. *Proc. Combust. Inst.* **2007**, *31*, 1955–1963.

(23) Jensen, A.; Dam-Johansen, K.; Wójtowicz, M. A.; Serio, M. A. TG-FTIR Study of the Influence of Potassium Chloride on Wheat Straw Pyrolysis. *Energy Fuels* **1998**, *12*, 929–938.

(24) Quyn, D. M.; Wu, H.; Li, C.-Z. Volatilization and catalytic effects of alkali and alkaline earth metallic species during the pyrolysis and gasification of Victorian brown coal. Part I. Volatilization of Na and Cl from a set of NaCl-loaded sample. *Fuel* **2002**, *81* (2), 143–149.

(25) Quyn, D. M.; Wu, H.; Bhattacharya, S. P.; Li, C.-Z. Volatilization and catalytic effects of alkali and alkaline earth metallic species during the pyrolysis and gasification of Victorian brown coal. Part II. Effects of chemical form and valence. *Fuel* **2002**, *81* (2), 151–158.